BEST AVAILABLE IMAGES

Defective images within this document are accurate representations of the original documents submitted by the applicant.

Defects in the images may include (but are not limited to):

- BLACK BORDERS
- TEXT CUT OFF AT TOP, BOTTOM OR SIDES
- FADED TEXT
- ILLEGIBLE TEXT
- SKEWED/SLANTED IMAGES
- COLORED PHOTOS
- BLACK OR VERY BLACK AND WHITE DARK PHOTOS
- GRAY SCALE DOCUMENTS

IMAGES ARE BEST AVAILABLE COPY.

As rescanning documents *will not* correct images, please do not report the images to the Image Problem Mailbox.

APPENDIX A

IN THE UNITED STATES PATENT AND TRADEMARK OFFICE

Appl. No.	:	10/613,374	Confirmation No. 7181
Applicants	:	S. Datta et al.	
Filed	:	July 3, 2003	
TC/A.U.	:	1711	
Examiner	:	Nathan M. Nutter	
Docket No.	:	1998B037A/2	
Customer No.	:	1473	

Hon. Commissioner for Patents
P.O. Box 1450
Alexandria, VA 22313-1450

New York, New York 10020
April 22, 2004

DECLARATION OF PROFESSOR RUFINA G. ALAMO

Sir:

I, RUFINA G. ALAMO, Ph.D., declare that:

1. I am a Professor in the Department of Chemical Engineering at Florida A&M University and Florida State University (FAMU-FSU). I make this declaration in support of Datta et al.'s U.S. patent application serial no. 10/613,374.

2. I have been a tenured Professor at FAMU-FSU since August 8, 2003. Prior to this, I held the position of Associate Professor (1995-2003) in the Chemical Engineering Department at FAMU-FSU.

3. I received my Bachelor of Science and Master of Science degrees in Chemistry from the University of Valladolid, Spain, in 1977 and 1978, respectively. I was awarded a Doctor of Philosophy in Chemistry from Complutense University of Madrid, Spain, in 1981. Further details of my educational and research career are set forth in my curriculum vitae, which is attached hereto as Exhibit 1.

4. My overall research interests focus on phase transitions in polymeric materials, including crystallization and melting processes in flexible and semi-rigid polymers, random copolymers, and polymer blends. My current research topics include crystallization and melting kinetics of polypropylenes, morphological and structural studies in polyolefins and blends of polyolefins.

5. Specifically, my research relates to crystallization kinetics and the effect of chain rigidity and molecular weight on the kinetic parameters controlling the nucleation process and the temperature coefficient of crystallization. My research also involves the study of random copolymers and the effects of the chemical or stereo type of defects, composition and distribution of defects on the crystallization kinetics. Furthermore, my research has included the investigation of linear polyethylenes, linear low density polyethylenes and long-chain branched high pressure polymerized polyethylenes, as well as Ziegler-Natta and metallocene-type polypropylenes, by a variety of techniques, including, but not limited to, optical and electron microscopies, Raman spectroscopy and small and wide angle X-Ray scattering.

6. The subject matter of this declaration relates to the gamma crystallographic form of polypropylene and random copolymers comprising propylene and ethylene studied by X-ray diffraction. By way of background, isotactic polypropylene exhibits three different, well-defined, crystallographic forms: 1) alpha or monoclinic form, 2) beta or hexagonal form, and 3) gamma or orthorhombic form. The chain conformation of each of these polymorphs is a classical 3_1 helix. Although the molecular mass (in a range of 40,000-300,000 g/mol) has only a minor effect on the formation of the gamma polymorph, the concentration of defects has a major effect, i.e., an increase in defects leads to short isotactic sequences and results in an increase in gamma polymorph content (Hosier, et al., *Macromolecules*, **2003**, *36*, 5623-5636, Exhibit 2).

7. I have considered the propylene-ethylene copolymers that are described in the above-identified application (hereinafter "Datta '374 application").

8. The maximum content of gamma polymorph that an ethylene-propylene copolymer can develop may be estimated by referring to systematic studies published in Hosier et al., *Macromolecules*, **2003**, *36*, 5623-5636 (Exhibit 2). This work analyzes the formation of the gamma polymorph in metallocene catalyzed propylene alpha-olefin copolymers and gives quantitative data for the fraction of gamma crystals developed as a function of the content of alpha-olefin in the copolymer. Copolymers with an ethylene content greater than 7 mole % under isothermal or very slow crystallizations develop greater than 90 % of the crystals in the gamma form. These crystallization conditions are commonly used in the analysis of crystallization behavior of these materials.

9. For example, I have considered the exemplary copolymer SPC2 that is discussed at page 44 of the Datta '374 application. SPC2 had an ethylene content of 5.8 weight percent (8.45 mole %). Based on the discussion above, I conclude that a slow crystallization of SPC2 would result in greater than 90% of the gamma polymorph for all crystals formed under the described conditions (see Datta '374 application, Example 1, pp. 35-36).

10. I would expect a propylene-ethylene copolymer synthesized with a Ziegler-Natta catalyst to develop a significantly lower content of crystals in the gamma polymorph than a comparable copolymer with the same ethylene content but made using a metallocene-type catalyst. The reasons were discussed in Alamo et al., *Macromolecules*, **1999**, *32*, 4050-4064 (Exhibit 3) and Hosier et al., *Macromolecules*, **2003**, *36*, 5623-5636 (Exhibit 2). The formation of gamma crystals is favored by the existence of short continuous isotactic sequences. The comonomer disrupts the continuity of isotactic propylene sequences in the polymer chain; hence, a higher content of comonomer favors the formation of the gamma

polymorph. The inter chain distribution of comonomer in the Ziegler-Natta copolymers is broad with a fraction of highly defected short molecules which likely do not participate in the crystallization (Zhang et al., *Polym. J.*, **2002**, *34*, 700-708, Exhibit 4). The intra chain distribution of defects of Ziegler-Natta copolymers deviates from random. Conversely, the comonomer distribution in a copolymer made with a metallocene catalyst is narrow among the polymer chains and random within the chains. Therefore, at similar comonomer contents, the crystalline chains of the Ziegler-Natta copolymer contain longer isotactic sequences and tend to produce less gamma polymorph than copolymers produced with a metallocene catalyst.

11. There is a significantly large number of published data that corroborate the above correlations. For example, Thomann et al., *Polymer*, **2001**, *42*, 4597-4603 (Exhibit 5), reported that the fraction of gamma crystals for a slowly cooled (0.2 °C/min) Ziegler-Natta propylene-ethylene copolymer with 5.8 wt% (8.45 mole %) ethylene was 60%. Perez et al., *Polymer*, **1999**, *40*, 675-681 (Exhibit 6), reported that the fraction of gamma crystals found in a metallocene propylene-1-hexene copolymer (2.6 mole % 1-hexene) was ~70%, wherein a comparative ZN propylene-1-hexene copolymer (4.7 mole % 1-hexene) develops less than 30% of the crystals in the gamma form. Foresta et al., *Polymer*, **2001**, *42*, 1167-1176 (Exhibit 7) reported that Ziegler-Natta propylene-ethylene copolymers with up to 3.1 % ethylene develop less than 30% of the crystal in the gamma phase. Metallocenes with similar contents of ethylene were found to develop maximum contents of gamma crystals between 40 and 85 % (Hosier et al., *Macromolecules*, **2003**, *36*, 5623-5636, Exhibit 2). The publication by Turner-Jones, *Polymer*, **1971**, *12*, 487-508 (Exhibit 8), reported that a Ziegler-Natta propylene-ethylene copolymer with 5 wt% (7.32 mole %) ethylene developed ~30 % of the crystals in the gamma phase. This percentage is significantly lower than the greater than 90% maximum fraction of gamma crystals found in a matched metallocene copolymer (Hosier et al., *Macromolecules*, **2003**, *36*, 5623-5636,

Exhibit 2). Finally, in a work published by Alamo, et al. in *Macromolecules*, **2003**, *36*, 1559-1571 (Exhibit 9), the crystallization behavior of a metallocene isotactic polypropylene (iPP) and a Ziegler-Natta iPP having matched weight average molecular weight and matched average defect composition was comparatively analyzed. While the maximum fraction of gamma crystals developed by the metallocene iPP was higher than 40%, the gamma fraction in the Ziegler-Natta iPP was significantly lower, i.e., ~10%.

12. Based upon the above discussion and references to published data, it is my opinion that propylene-ethylene copolymers with ethylene contents up to at least about 11.6 wt% (16.45 mole %) synthesized with a metallocene catalyst will develop higher contents of gamma crystals than those with comparable ethylene content and prepared with a Ziegler-Natta catalyst (see, e.g., SPC-3 listed in Table 1, p. 37, of the Datta '374 application).

13. I declare that all statements made herein of my own knowledge are true and that all statements made on information and belief are believed to be true; and further that these statements were made with knowledge that willful false statements and the like so made are punishable by fine or imprisonment, or both, under Section 1001 of Title 18 of the United States Code and that such willful false statements may jeopardize the validity of the Datta et al. '374 application or any patent issuing therefrom.

Dated: April 22 2004
Tallahassee, Florida

R. Alamo

Rufina G. Alamo, Ph.D.

EXHIBIT 1

Dr. RUFINA G. ALAMO

Curriculum Vitae

FAMU-FSU College of Engineering
Department of Chemical Engineering

Tallahassee, FL 32310
Phone: (850)410-6376
FAX : (850)410-6150
E-Mail: alamo@eng.fsu.edu

Index

Dr. RUFINA G. ALAMO

EDUCATION

- B.S. in Chemistry. University of Valladolid (Spain), 1977.

- M.S. in Chemistry. University of Valladolid (Spain), 1978.
  Title of Thesis: "Properties of poly(diethylene glycol terephtalate)"
  Director of Thesis: Prof. J.G. Fatou.

- Ph.D. in Chemistry. Complutense University of Madrid, 1981.
  Title of Thesis: "Mechanism of Polymerization and the Crystalline State of Poly(1,3-Dioxolane)".
  Directors of Thesis: Prof. J.G. Fatou and Dr. J. Guzman.

Postdoctoral.

1. Instituto de Plasticos y Caucho (The Rubber and Plastics Institute) of the Consejo Nacional de Investigaciones Cientificas (National Research Council of Science) in Madrid, Spain. Feb. 1981 - Nov. 1982. Work on "Mechanisms of Formation and the Solid State Properties of Polymers with Heteroatoms in the Main Chain".
   Director: J.G. Fatou

2. Institute of Molecular Biophysics. Florida State University. Tallahassee, Florida. Nov. 1982 - May 1985. Work on "Thermodynamic and Morphological Properties of Linear and Branched Polyethylenes".
   Director: Prof. L. Mandelkern

APPOINTMENTS.

- Research staff at the DOW Chemical Co. in Tarragona, Spain. 1985-1987.

- Advisor to the Committee for the Foundation of the Quincentenial Bilingual University in Central Spain, 1987.

- Assistant Scholar in Research. Florida State University. Tallahassee, Florida, 1988.

- Associate Scholar in Research. Florida State University. Tallahassee, Florida, 1991-August 7th, 1995.

- Research Advisor with the Polymer Section of the Department of Chemistry of the National University of Costa Rica at Heredia, Costa Rica, 1993-Present.

- Associate Professor. FAMU-FSU College of Engineering. Department of Chemical Engineering. Tallahassee, Florida. August 8th, 1995-2003

- Professor. FAMU-FSU College of Engineering. Department of Chemical Engineering. Tallahassee, Florida. August 8th, 2003-present

AWARDS, HONORS, RECOGNITIONS.

- Special Recognition Award for " Outstanding Contributions to Scholarship" from the Office of Graduate Studies, FAMU. September 2001.

- Recipient of the 2000 Engineering Research Award of the FAMU/FSU College of Engineering, Spring 2000.

- Scholarship to participate in the project "Configurational Analysis and Rheological Properties of Macromolecules" sponsored by the Comision Asesora de Investigacion Cientifica y Tecnica (CAICT) of the Spanish Research Council. The Rubber and Plastics Institute, Madrid (Spain), (1978 - 1979).

- Postgraduate scholarship from the Spanish National Research Council of Science. The Rubber and Plastics Institute, Madrid (Spain), (1979 - 1982).

- Postdoctoral scholarship from the U.S. -Spanish Joint Committee for Scientific and Technological Cooperation (equivalent to a Fulbright Scholarship). Institute of Molecular Biophysics, "Thermodynamic and Morphological Properties of Linear and Branched Polyethylenes", (1982 - 1983).

- Graduated with Honors (first in the graduate class) from the Rubber and Plastics Institute of the Spanish Research Council in Madrid, Spain 1978.

- Invited to participate in the FLORICA program at Florida State University, (Florida-Costa Rican Institute), 1992.

- Invited as plenary speaker at the Osaka University Macromolecular Symposium (OUMS98). May, 1998.

- Invited by Wiley to write a review article on Semicrystalline Polymers for the new edition of the Encyclopedia of Polymer Science and Technology. Fall 2000.

REVIEWER EXPERIENCE.

Macromolecules, ACS Pub., F.H. Winslow Ed.
Journal of Polymer Science, Polymer Physics Ed.
National Science Foundation (proposals)
Polymer Engineering and Science.
Journal of Rheology.
Journal of Thermal Analysis and Calorimetry.
Polymer.
Petroleum Research Fund.
Thermochimica Acta (Book Chapter)
NIST (Research Proposals)
Acta Polymerica, Germany

Books Reviews:

- Attenuated Total Reflectance Spectroscopy. Marek W. Urban. ACS Books, Washington, 1996. Review appeared in *Applied Spectroscopy,* 1998.

- Handbook of Fourier Transform Raman and Infrared spectra of Polymers. A.H. Kuptsov and G.N. Zhizhin. Elsevier *Physical Sciences Data 45*. New York 1998. Review appeared in *Applied Spectroscopy* 1999.

PROFESSIONAL ACTIVITIES.

Member of the following organizations:

- The American Chemical Society and of the Division of Polymer Chemistry. Also member of the Division of Polymeric Materials Science and Engineering.
- The American Physical Society and of the Division of High Polymer Physics
- The North American Thermal Analysis Society (NATAS)

- The American Institute of Chemical Engineers
- Grupo de Polimeros de la Real Sociedad Espanola de Fisica y Quimica
- ZONTA International

TEACHING EXPERIENCE

Summary of courses taught in the FAMU-FSU College of Engineering:

Undergraduate courses

Spring 1996	ECH 3023	Introduction to Chemical Engineering
	ECH 4905r	DIS
Fall 1996	ECH 3023	Introduction to Chemical Engineering
Spring 1997	ECH 3023	Introduction to Chemical Engineering
	ECH 3264L	Fluid Flow Through a Pipe (laboratory)
Fall 1997	ECH 3023	Introduction to Chemical Engineering
Spring 1997	ECH 3023	Introduction to Chemical Engineering
Fall 1997	ECH 3023	Introduction to Chemical Engineering
Spring 1998	ECH 4937	Introduction to Polymer Science and Engineering
Fall 1998	ECH 4504	Kinetics and Reactor Design
	ECH 4906	Honors in Chemical Engineering
Spring 1999	ECH 3023	Introduction to Chemical Engineering
	ECH 4937	Introduction to Polymer Science and Engineering
	ECH 4906	Honors in Chemical Engineering
Fall 1999	ECH 4504	Kinetics and Reactor Design
	ECH 4906	Honors in Chemical Engineering
	ECH 4905	DIS
Spring 2000	ECH 3023	Introduction to Chemical Engineering
	ECH 4906	Honors in Chemical Engineering
	ECH 4905	DIS
Fall 2000	ECH 3023	Introduction to Chemical Engineering
	ECH 4504	Kinetics and Reactor Design
Spring 2001	ECH 3023	Introduction to Chemical Engineering
	ECH 4823	Introduction to Polymer Science and Engineering

Fall 2001	ECH 4504	Kinetics and Reactor Design
Spring 2002	ECH 3023	Introduction to Chemical Engineering
Fall 2002	ECH 4504	Kinetics and Reactor Design
Spring 2003	ECH 4823	Introduction to Polymer Science and Engineering

Graduate courses

Spring 1997	ECH 5937	Advanced Polymer Science and Engineering
Spring 1998	ECH 5937	Advanced Polymer Science and Engineering
Spring 1999	ECH 5937	Advanced Polymer Science and Engineering
Spring 2000	ECH 5937	Crystallization and Melting of Polymers
Spring 2001	ECH 5937	Advanced Polymer Science and Engineering
Spring 2003	ECH 5937	High Resolution Microscopy
Spring 2003	ECH 5823	Introduction to Polymer Science and Engineering

RESEARCH EXPERIENCE

RESEARCH INTEREST

Physical chemistry and physical properties of macromolecules.
Kinetics of phase transitions, structure and morphology of the crystalline state, structure - properties relations in semicrystalline polymers.

PUBLICATIONS

A. *Journal Articles (Refereed Publications)*

1. Guzman J., R. Alamo, J.G. Fatou. "Glass Transitions and Solubility Parameter of Poly(Diethylene Glycol Terephtalate)". *An. Quim.*, **76**, 214, 1980.

2. Alamo R., J. Guzman, J.G. Fatou. "Kinetics of Polymerization of Tetrahydrofuran Initiated by Acetyl Perchlorate". *Makromol. Chem.*, **182**, 725, 1981.

3. Alamo R., J. Guzman, J.G. Fatou. "Polymerization of Tetrahydrofuran by Bifunctional Cationics Initiators: Terephtaloil Perchlorate". *Makromol. Chem.*, **182**, 731, 1981.

4. Alamo R., J. Guzman, J.G. Fatou. "Kinetics of Polymerization of 1,3-Dixolane Initiated by Acetyl Perchlorate and Terephthaloil Perchlorate". *An. Quim.*, **78**, 317, 1982.

5. Alamo R., J.G. Fatou, J. Guzman. "Crystallization of Polyformals. I. Crystallization Kinetics of Poly(1,3-Dioxolane)". *Polymer*, **23**, 374, 1982.

6. Alamo R., J.G. Fatou, J. Guzman. "Crystallization of Polyformals. II. Influence of Molecular Weight and Temperature on the Morphology and Growth Rate in Poly(1,3-Dioxolane)". *Polymer*, **23**, 379, 1982.

7. Alamo R., J. Guzman, J.G. Fatou. "Effect of Acetic Acid and Acetic Anhydride on the Cationic Polymerization of Tetrahydrofuran". *An. Quim. Ser. A*, **79**, 648, 1983.

8. Alamo R., J. Guzman, J.G. Fatou. "Influence of Water in the Polymerization of Tetrahydrofuran". *Makromol. Chem.*, **184**, 563, 1983.

9. Alamo R., J.G. Fatou, J. Guzman. "Dependence of the Molecular Weight on the Glass Transition Temperature of Poly(1,3-Dioxolane)". *An. Quim. Ser. A*, **79**, 652, 1983.

10. Alamo R., J.G. Fatou, A. Bello. "Solubility Parameter and Random-Coil Dimensions of Poly(1,3-Dioxolane)". *Polym. J.*, **15**, 491, 1983.

11. Alamo R., J. Guzman, J.G. Fatou. "Comments on G. Pruckmayr's Criticisms on our Paper, Influence of Water in the Polymerization of Tetrahydrofuran". *Makromol. Chem.*, **185**, 1233, 1984.

12. Domszy R.C., R. Alamo, P.J.M. Mathieu, L. Mandelkern. "The Structure of Copolymer Crystals Formed from Dilute Solution and in the Bulk". *J. Polym. Sci., Polym. Phys. Ed.*, **22**, 1727, 1984.

13. Alamo R., R.C. Domszy, L. Mandelkern. "Thermodynamic and Structural Properties of Copolymers of Ethylene". *J. Phys. Chem.*, **88**, 6587, 1984.

14. Domszy R.C., R. Alamo, C.O. Edwards, L. Mandelkern. "The Thermoreversible Gelation and Crystallization of Homopolymers and Copolymers". *Macromolecules*, **19**, 310, 1986.

15. Voigt- Martin I.G., R. Alamo, L. Mandelkern. "A Quantitative Electron Microscopic Study of the Crystalline Structure of Ethylene Copolymers". *J. Polym. Sci., Polym. Phys. Ed.*, **24**, 1283, 1986.

16. Snyder R.G., N.E. Schlotter, R. Alamo, L. Mandelkern. "Observation of a Conformationally Liquid-Like Component in Crystalline Polyethylene by Raman Spectroscopy". *Macromolecules*, **19**, 621, 1986.

17. Alamo R., L. Mandelkern. "Origins of Endothermic Peaks in Differential Scanning Calorimetry". *J. Polym. Sci., Polym. Phys. Ed.*, **24**, 2087, 1986.

18. Mandelkern L., R. Alamo, W.L. Mattice, R.G. Snyder. "Observation of the Raman D-LAM Band in Ethylene Copolymers: Hydrogenated Polybutadienes". *Macromolecules*, **19**, 2404, 1986.

19. Alamo R.G., R.H. Glaser, L. Mandelkern. "The Cocrystallization of Polymers: Polyethylene and Its Copolymers". *J. Polym. Sci., Polm. Phys. Ed.*, **26**, 2169, 1988.

20. Alamo R.G., L. Mandelkern. "Thermodynamic and Structural Properties of Ethylene Copolymers". *Macromolecules*, **22**, 1273, 1989.

21. Chiu G., R.G. Alamo, L. Mandelkern. "Formation of Ringed Spherulites in Polyethylenes". *J. Polym. Sci., Polym. Phys. Ed.*, **28**, 1207, 1990.

22. Alamo R.G., K.W. McLaughlin, L. Mandelkern. "Changes in the Phase Structure of the Polyethylenes After Long-Time Storage at Room Temperature". *Polymer Bulletin*, **22**, 299, 1989.

23. Mandelkern L., A. Prasad, R.G. Alamo, G.M. Stack. "The Melting Temperature of the n-Alkanes and the Linear Polyethylenes". *Macromolecules*, **23**, 3696, 1990.

24. Mandelkern L., R.G. Alamo, M.A. Kennedy. "Interphase Thickness of Linear Polyethylene". *Macromolecules*, **23**, 4721, 1990.

25. Alamo R.G., A. Bello, J.G. Fatou, C. Obrador. "Solution and Thermal Properties of Poly(1,3-Dioxocane)". *J. Polym. Sci., Polym. Phys. Ed.*, **28**, 907, 1990.

26. Alamo R.G., L. Mandelkern. "Crystallization Kinetics of Ethylene Copolymers". *Macromolecules*, **24**, 6480, 1991.

27. Mandelkern L., K.W. McLaughlin, R.G. Alamo. "The Phase and Supermolecular Structure of Binary Mixtures of Linear Polyethylene Fractions". *Macromolecules*, **25**, 1440, 1992.

28. Jarret W.L., L.J. Mathias, R.G. Alamo, L. Mandelkern, D.L. Dorset. "Thermally-Induced Molecular Motion and Premelting in Hexacontane". *Macromolecules*, **25**, 3468, 1992.

29. Failla M., R.G. Alamo, L. Mandelkern. "On the Analysis of the Raman Internal Modes of Crystalline Polyethylene". *Polymer Testing*, **11**, 151, 1992.

30. Shen C., A. Peacock, R.G. Alamo, T. Vickers, L. Mandelkern, C.K. Mann. "Structural Studies of Crystalline Linear Polyethylenes as Reveal by Factor Analysis of Their Raman Spectra". *Applied Spectroscopy*, **46**, 1226, 1992.

31. Bark M., H.G. Zachmann, R.G. Alamo, L. Mandelkern. "Investigations of the Crystallization of Poly(ethylene) by Means of Simultaneous Small Angle and Wide Angle X-Ray Scattering". *Makrom. Chem.*, **193**, 2363, 1992.

32. Alamo R.G., E.K.M. Chan, L. Mandelkern, I.G. Voigt-Martin. "The Influence of Molecular Weight on the Melting and Phase Structure of Random Copolymers of Ethylene". *Macromolecules*, **25**, 6381, 1992.

33. Dorset D.L., R.G. Alamo, L. Mandelken. "Premelting of Long Paraffins in Chain-Extended Lamellae - An Electron Diffraction Study". *Macromolecules*, **25**, 6284, 1992.

34. Dorset D.L., R.G. Alamo, L. Mandelkern. "Surface Order and the Sectorization of Polymethylene Lamellae". *Macromolecules*, **26**, 3143, 1993

35. Alamo R.G., L. Mandelkern, G.M. Stack, C. Kronke, G. Wegner. "Isothermal Thickening of Crystals of High Molecular Weight n-Alkanes ". *Macromolecules* **26**, 2743, 1993

36. Snyder R.G., H. L. Strauss, R.G. Alamo, L. Mandelkern. "Chain Length Dependence of Interlayer Interaction in Crystalline N-Alkanes from Raman LAM-n Measurements". *J. Chem. Phys*, **100**, 5422, 1994

37. Alamo R.G., B. D. Viers, L. Mandelkern. "Phase Structure of Random Ethylene Copolymers: A Study of the Counit Content and Molecular Weight as Independent Variables". *Macromolecules*, **26**, 5740, 1993

38. Alamo R.G., L. Mandelkern, G.M. Stack, C. Kronke, G. Wegner. "The Kinetics of Crystallization of Long-Chain n-Alkanes from the Melt and from Solution". *Macromolecules*, **27**, 147, 1994

39. Alamo R.G., J.D. Londono, L. Mandelkern, F.C. Stehling and G.D. Wignall. "The Phase Behavior of Blends of Linear and Branched Polyethylenes in the Molten and Solid States by Small-Angle Neutron Scattering". *Macromolecules*, **27**, 411, 1994

40. Mandelkern L., R. G. Alamo, E. L. Sokolov, J. Li, B. Chu. "Small-Angle X-ray Scattering of n-Hexacontane as a Function of Temperature". *Macromolecules*, **27**, 2324, 1994

41. Lu L., R. G. Alamo, L. Mandelkern. "Lamellar Thickness Distributions in Linear Polyethylene and Ethylene Copolymers". *Macromolecules*, **27**, 6571, 1994

42. Wignall G.D., J. D. Londono, R. G. Alamo, M. J. Galante, L. Mandelkern, F. C. Stehling. "The Morphology of Blends of Linear and High Pressure Polyethylene in the Solid State. A Study by SANS, SAXS and DSC". *Macromolecules*, **28**, 3156, 1995.

43. Stribeck N., R. G. Alamo, L. Mandelkern, H. G. Zachmann. "Study of the Morphological Structure of Polyethylene by Means of Small Angle X-Ray Scattering and Raman Spectroscopy". *Macromolecules*, **28**, 5029, 1995.

44. Alamo R.G., B.D. Viers, L. Mandelkern. "A Re-examination of the Relation Between the Melting Temperature and the Crystallization Temperature: Linear Polyethylene". *Macromolecules*, **28**, 3205, 1995.

45. Stewart M.J., W.L. Jarrett, L.J. Mathias, R.G. Alamo, L. Mandelkern. "Thermally Induced Molecular Motion and Premelting in the Solid State of n-Hexatriacontane". *Macromolecules*, **29**, 4963, 1996.

46. Mandelkern, L. and R. G. Alamo, "Comments on Paper `Raman Spectroscopy Employed for the Determination of the Intermediate Phase in Polyethylene'", *Macromolecules*, **28**, 2988, 1995.

47. Annis, B.K., J. Strizak, R. G. Alamo, L. Mandelkern, "A Small Angle Neutron Scattering Study of the Plastic Deformation of Linear Polyethylene", *Polymer*, **37**, 137, 1996.

48. Graham, J.T., R. G. Alamo, L. Mandelkern, "The Effect of Molecular Weight and Crystallite Structure on Yielding in Ethylene Copolymers", *J. Polym. Sci., Polym. Phys. Ed.*, **35**, 213,1997.

49. Kitamaru, R., T. Nakooki, R. G. Alamo, L. Mandelkern, "A Carbon-13 NMR Study of the Phase Structure of Semi-Crystalline Polymers: Hydrogenated Poly(butadiene)", *Macromolecules*, **29**, 6847, 1996.

50. Alamo, R.G., M. J. Galante, L. Mandelkern, A. Lehtinen, R. Paukkeri, "Crystallization Kinetics of Metallocene Type Polypropylenes. Influence of Molecular Weight and Comparison with Ziegler-Natta Type Systems". *J. Thermal Analysis*, **47**, 913, 1996.

51. Wignall, G.D., R.G. Alamo, J.D. Londono, L. Mandelkern, F.C. Stehling, "Small Angle Neutron Scattering investigation of Liquid-liquid Phase Separation in Heterogeneous Linear Low Density Polyethylene". *Macromolecules*, **29**, 5332, 1996.

52. Mandelkern, L., R.G. Alamo, G.D. Wignall, F.C. Stehling, "The Phase Structure of Blends of the Different Polyethylenes", *Trends in Polym. Sci.*, **4**, 377, 1996.

53. Alamo, R.G. R. Krishnamoorti, D.J. Lohse, J.D. Londono, L. Mandelkern, F.C. Stehling, G.D. Wignall, SANS Investigations of Melt-Miscibility and Phase Segregation in Blends of Linear and Branched Polyethylenes as a Function of the Branch Content. *Macromolecules*, **30**, 561, 1997.

54. Isasi, J.R., R.G. Alamo, L. Mandelkern, A Study of the Dilation of the Unit Cell of Metallocene Isotactic Poly(propylenes): The Monoclinic Form, *J. Polym. Sci., Polym. Phys. Ed.* **35**, 2511, 1997.

55. Isasi, J.R., R.G. Alamo, L. Mandelkern, The Thermal Expansion of the Monoclinic Unit Cell of Isotactic Poly(propylene), *J. Polym. Sci., Polym. Phys. Ed.* **35**, 2945, 1997.

56. Galante, M.J., L. Mandelkern, R.G. Alamo, "The Crystallization of Blends of Different Type Polyethylenes: The Role of Crystallization Conditions". *Polymer,* **39**, 5105, 1998.

57. Mandelkern, L., R.G. Alamo, J.A. Haigh, On the Crystallization Kinetics of High Molecular Weight n-Alkanes, *Macromolecules*, **31**, 765 1998.

58. Chowdhury, F., J.A. Haigh, L. Mandelkern, R. G. Alamo, The Supermolecular Structure of Ethylene-Vinyl Acetate Copolymers, *Polymer Bulletin*, **41**, 463, 1998.

59. Peacock, A.J., L. Mandelkern, R.G. Alamo, J.G. Fatou, The Influence of the Deformation Temperature on the Tensile Properties of the Polyethylenes *J. Materials Science*, **33**, 2255, 1998.

60. Isasi, J., L. Mandelkern, M.J. Galante, R. Alamo, The Degree of Crystallinity of Isotactic Poly(propylene) *J. Polym. Sci., Polym. Phys. Ed.* **37**, 323, 1999.

61. Alamo, R.G., G.M. Brown, L. Mandelkern, A. Lehtinen, R. Paukkeri, A Morphological Study of a Highly Structurally Regular Isotactic Poly(propylene Fraction) *Polymer, **40,*** 3933, 1999.

62. Agamelian, M., R.G. Alamo, M-H Kim, J.D. Londono, L. Mandelkern, G.D. Wignall, Phase Behavior of Blends of Linear and Branched Polyethylenes on Micron-Length-Scales Via Ultra-Small Angle Neutron Scattering, *Macromolecules*, **32**, 3093, 1999.

63. Alamo, R., M-H Kim, M.J. Galante, J.R. Isasi, L. Mandelkern, Structural and Kinetic Factors in the Formation of the Gamma Polymorph of Isotactic Poly(propylene) *Macromolecules **32,*** 4050, 1999.

64. Kim, M.H., R.G. Alamo, J.S. Lin, The Cocrystallization Behavior of Binary Blends of Isotactic Polypropylene and Propylene - Ethylene Random Copolymers, *Polym. Eng. Sci.* **39**, 2117, 1999.

65. Dai, P.S., P. Cebe, M. Capel, R.G. Alamo, L. Mandelkern, Simultaneous *in-situ* SAXS and WAXS Study of Crystallization and Melting Behavior of Metallocene Isotactic Poly(propylene) ACS Symposium Series, *Scattering from Polymers. Characterization by X-Rays, Neutrons and Light*, P. Cebe, B. Hsiao, D. Lohse Ed. Page 152, 2000.

66. Alamo, R.G., C. Chi, Crystallization Behavior and Properties of Polyolefins in *Molecular Interactions and Time-Space Organization in Macromoleculer Systems* Y. Morishima, T. Norisuye, K. Tashiro Ed. Springer, 1999.

67. Huang, T.W., R.G. Alamo, L. Mandelkern On the Fusion of Isotactic Poly(Propylene) *Macromolecules*, **32**, 6374, 1999.

68. Agamelian, M., R.G. Alamo, J.D. Londono, L. Mandelkern, G.D. Wignall, Phase Behavior of Blends of Linear and Branched Polyethylenes on Micron-Length-Scales Via Ultra-Small Angle Neutron Scattering (USANS), *Journal of Applied Crystallography*, **33**, 714, 2000.

69. Haigh, J.A., C. Nguyen, R.G. Alamo, L. Mandelkern, Crystallization and Melting of Model Polyethylenes with Different Chain Structure *J. Thermal Analysis* **59**, 435, 2000.

70. Wignall, G.D., R.G. Alamo, J.D. Londono, L. Mandelkern, M.H. Kim, J.S. Lin, The Morphology of Blends of Linear and Short-Chain Branched Polyethylenes in the Solid State by Neutron and X-Ray Scattering and Differential Scanning Calorimetry and Transmission Electron Microscopy *Macromolecules* **33**, 551, 2000.

71. Dai, P.S., P. Cebe, M. Capel, R.G. Alamo, L. Mandelkern, Small and Wide Angle X-Ray Scattering Study of Metallocene Isotactic Poly(propylene), *Journal of Applied Crystallography*, **33**, 714, 2000.

72. Isasi, J.R., Haigh, J.A., Graham, J.T., Mandelkern, L., Alamo. R.G. Some Aspects of the Crystallization of Ethylene Copolymers *Polymer*, **41**, 8813, 2000.

73. VanderHart, D.L., R.G. Alamo, M.R. Nyden, M.H. Kim, L. Mandelkern, Observation of Resonances Associated with stereo and Regio Defects in the Crystalline Regions of Isotactic Polypropylene: Towards a Determination of Morphological Partitioning *Macromolecules*, **33**, 6078, 2000.

74. Alamo, R.G., D.L. VanderHart, M.R. Nyden, L. Mandelkern, Morphological Partitioning of Ethylene Defects in Random Propylene-Ethylene Copolymers. *Macromolecules*, **33**, 6105, 2000.

75. Huang, W., R.G. Alamo, A Comparative Study of the Melting and Crystallization Behavior of a Metallocene and a Narrow Fraction of Ziegler-Natta Isotactic Polypropylene, *Soc.*

Plast. Eng. J. **3**, 3546, 2000.

76. Nyden, M.R., D.L. VanderHart, R.G. Alamo "The Conformational Structures of Defect-Containing Chains in the Crystalline Regions of Isotactic Polypropylenes" *J. Comp. Theor. Polym. Sci.*, **11**, 175, 2001.

77. Nakaoki,T., R. Kitamaru, R.G. Alamo, W.T. Huang. L. Mandelkern ,"The Conformational Change with Temperature of End Group Sequences of Low Molecular weight Polyethylenes" *Polymer J.* **32**, 876, 2000.

78. Li, D., , D., H. Garmestani, S.R. Kalidindi, R.G. Alamo "Crystallographic Evolution in High-Density Polyethylene during Uniaxial Deformation" *Polymer*, **42**, 4903, 2000.

79. Gelder, M., F. Beyer, S.P. Gido, R. Alamo, K. Schmidt-Rohr, "Polyethylene Crystallite Thickness Distribution from ^{1}H NMR Relaxation, Calibrated by Electron Microscopy and LAM", *Macromolecules* (submitted)

80. Annis, B.K., M.H. Kim, R.G. Alamo, M. Pyda, "Inelastic Neutron Scattering from Isotactic Polypropylene" *J. Polym. Sci., Polym. Phys. Ed.* **39**, 2852, 2001

81. Wignall, G.D., R.G. Alamo, E. Richtson, L. Mandelkern, D. Schwahn, "SANS Studies of Liquid-Liquid Phase Separation in Heterogeneous and Metallocene-Based Linear Low Density Polyethylenes" *Macromolecules*, **34**, 8160, 2001

82. Simanke, A.G., R.G. Alamo, G. B. Galland, R. S. Mauler, "Wide-Angle X-ray Scattering of Random Metallocene-Ethylene Copolymers with Different Types and Concentration of Comonomer" *Macromolecules*, **34**, 6959, 2001

83. Chatterjee, J., R.G. Alamo "Phase Behavior of Low Molecular Weight Polyethylenes Crystallized from Homogeneous and Heterogeneous Solutions" *J. Polym. Sci., Polym. Phys. Ed.* , **40**, 878, 2002

84. Alamo, R.G., J.A. Blanco, I. Carrilero, R. Fu, "Measurement of the 13C Spin-Lattice Relaxation Time of the Non-Crystalline Regions of Semicrystalline Polymers by a cp-MAS based Method" *Polymer*, **43**, 1857, 2002

85. Alamo, R.G., J.A. Blanco, P. Agarwal, J.C. Randall, "Crystallization Rates of Matched Fractions of $MgCl_2$-Supported Ziegler Natta and Metallocene Isotactic Poly(propylenes). I. The Role of Chain Microstructure" *Macromolecules*, **36**, 1559, 2003

86. Randall, J.C., R.G. Alamo, P. Agarwal, C. Ruff "Crystallization Rates of Matched Fractions of $MgCl_2$-Supported Ziegler Natta and Metallocene Isotactic Poly(propylenes). II. Chain Microstructures from a Super Critical Fluid Fractionation of a $MgCl_2$-Supported Ziegler

Natta Isotactic Poly(propylene)" *Macromolecules*, **36**, 1572, 2003

87. Li, D., H. Garmestani, R.G. Alamo S.R. Kalidindi, "The Role of Crystallinity in the Crystallographic Texture Evolution of Polyethylenes During Tensile Deformation" *Polymer*, **44**, 5355, 2003

88. Dai, P.S., P. Cebe, M. Capel, R.G. Alamo, L. Mandelkern, "In-Situ Wide and Small Angle X-Ray Scattering Study of Melting Kinetics of Isotactic Poly(Propylene)" *Macromolecules*, **36**, 4042, 2003

89. Hosier, I.L., R.G. Alamo, P. Esteso, J.R. Isasi, L. Mandelkern "Formation of the Alpha and Gamma Polymorphs in Random Metallocene Copolymers. Effect of Concentration and Type of Comonomer". *Macromolecules*, **36**, 5623, 2003

90. Alamo, R.G. "Defects Distribution of Metallocene and $MgCl_2$-Supported Ziegler-Natta Isotactic Poly(propylenes) as Revealed by Fractionation and Crystallization Behaviors" *Macromol. Polymer Symp.* (in press)

91. Alamo, R.G. "The Role of Defect Microstructure in the Crystallization Behavior of Metallocene and $MgCl_2$-Supported Ziegler-Natta Isotactic Poly(propylenes)" *Polimeros, Ciência e Tecnologia*, **13**, 270, 2003

92. Hosier, I.L., R.G. Alamo, J.S. Lin, "Lamellar Morphology of Metallocene Random Propylene Copolymers Studied by Atomic Force Microscopy (Polymer, in press)

OTHERS.

Articles in the DOW CHEMICAL Co. -
Five Internal Confidential Publications, 1986-1987.

B. *Articles in Preparation*

1. Alamo R.G., L. Mandelkern, J.G. Fatou, C. Marco. "The Molecular Weight Dependence on the Rate of Crystallization of Polymeric Chains".

2. Alamo, R.G., L. Lu, L. Mandelkern. "A Study of the Branch Type on the Crystallization Kinetics of Random Ethylene Copolymers".

3. Alamo, R.G., T.W. Huang "Study of the Melting Kinetics of Isotactic Polypropylenes as a Function of Concentration of Defects"

4. Alamo, R.G., A. Simanke. Structure of Annealed Metallocene Ethylene Copolymers with Different Type of Comonomers

5. Alamo, R.G., J.A. Blanco, P. Agarwal, "The Molecular Weight Dependence on the Rate of Crystallization and Morphology of iPP fractions"

C. *Books and Book Chapters*

1. Alamo, R.G. "Propiedades del Poli(tereftalato de dietilenglicol)". Edited by the University of Valladolid. Valladolid. Spain, 1978

2. Alamo, R.G. "Mecanismos de Polimerizacion y el Estado Cristalino en Poli(1,3-dioxolano)". Edited by the University of Madrid. Madrid, Spain. 1981

3. Mandelkern L., R.G. Alamo. "Use of Raman Spectroscopy in Characterizing the Structure and Properties of Crystalline Polymers" in *Structure-Property Relations in Polymers: Spectroscopy and Performance.* Advances in Chemistry Series, No. 236, Pag. 157-190, M.W. Urban and C.D. Craver Eds., Washington D.C., 1993.

4. Yang Y., N. Ichise, Z. Li, Q. Yuan, J.E. Mark, E.K.M. Chan, R.G. Alamo, L. Mandelkern. "The Use of Mechanical Property Measurements to Characterize Gel and Gelation Processes". *Mat. Res. Soc. Symp. Proc.* Vol. 248, 325, 1992.

5. Yang Y., N. Ichise, Z. Li, Q. Yuan, J. Mark, E.K.M. Chan, R. G. Alamo, L. Mandelkern. "Investigation of Gelation Processes and Gel Structures by Means of Mechanical Property Measurements" in *Synthesis, Characterization and Theory of Polymeric Networks and Gels*, S.M. Aharoni Ed., Pag. 217. Plenum Press, New York 1992.

6. Mandelkern L., R.G. Alamo, D.L. Dorset. "Pre-Melting in the n-Alkanes: A Review". *Acta Chimica Hungarica, 'Models in Chemistry'.* Andras P. Schubert Ed. Budapest. **130**, (3-4), 415, 1993.

7. Alamo, R.G. "The Crystallization Behavior of Long Chain N-Alkanes and Low Molecular Weight Polyethylenes" in *NATO ASI-C Series, 'Mathematical and Physical Sciences Vol. 405: Crystallization of Polymers'.* M. Dosiere Ed. Klumer Academic Pub, Boston 1993.

8. Alamo, R.G. and L. Mandelkern. "The Crystallization Behavior of Random

Copolymers of Ethylene" in *"Thermal Analysis and Calorimetry in Polymer Physics", Thermochimica Acta*, **238**, 155, 1994.

9. Mandelkern L., R.G. Alamo. "Thermodynamic Quantities Governing Melting". in *"American Institute of Physics Handbook of Polymer Properties"*, J. Mark Ed.; AIP Press: New York, 1996.

10. Londono, J. D., G. D. Wignall, R. G. Alamo, L. Mandelkern, F. C. Stehling, J. S. Lin, "The Morphology of Blends of Linear and Branched Polyethylenes by Small-Angle Neutron and X-Ray Scattering" *Mat. Res. Soc. Sym. Proc.* Vol. 376, p. 281, 1995.

11. Agamalian, M.M., R.G. Alamo, J.D. Londono, L. Mandelkern, S. Spooner, F.C. Stehling, G.D. Wignall, "Ultra-High Resolution Small-Angle Neutron Scattering Investigations of Liquid-Liquid Phase Separation in Linear Low Density Polyethylene". *Mat. Res. Soc. Sym. Proc.* Vol. 461, p. 205, 1997.

12. Mandelkern, L., R.G. Alamo, "Polymer Data Handbook", Polyethylene, linear high-density. Ed. J.E. Mark. Oxford University Press, 1999, pp. 493 - 507.

PRESENTATION OF PAPERS IN PROFESSIONAL MEETINGS

A. *Meetings (Regular Presentations)*
(Speaker: *)

1. Alamo R.*, J.Guzman, J.G. Fatou. "Transfer effects in the Polymerization of Tetrahydrofurane". XVIII Bienal Meeting of the Spanish Society of Physics and Chemistry. Burgos. Spain, Oct. 1980.

2. Alamo R.*, J.G. Fatou, J. Guzman. "A Study of the Dependence Glass Transition Temperature/Molecular Weight in Poly(1,3-Dioxolane)". XIX Bienal Meeting of the Spanish Society of Physics and Chemistry. Santander. Spain, Oct. 1982.

3. Mandelkern L., R.C. Domszy, R. Alamo*, M. Davidson. "Crystallization Behavior and Transitions in Copolymers". 35th Southeastern Regional Meeting of the American Chemical Society. Charlotte, North Carolina, November 9-11, 1983.

4. Schlotter N.E.*, L. Mandelkern, R. Alamo, R.G. Snyder. "Detection of the Raman DLAM Mode in the Solid Phase". American Physical Society. Detroit, Michigan. March 26-30, 1984.

5. Alamo R.*, R.C. Domszy, L. Mandelkern. "Thermally Reversible Gels of Polyethylene Copolymers". 37th Annual Meeting of the American Chemical Society (Florida Section). Florida Southern College, Lakeland, Florida. May 9-12, 1984.

6. Anandakumaran K.*, R. Alamo, L. Mandelkern. "The Properties and Structure of Ethylene-Methacrylic Acid Copolymers". 37th Annual Meeting of the American Chemical Society (Florida Section). Florida Southern College, Lakeland, Florida. May 9-12, 1984.

7. Mandelkern L.*, R. Alamo. "Thermal Analysis and Polymer Crystallization". American Chemical Society. Symposium on Thermoanalysis . Miami, Florida, April 1985.

8. Mandelkern L.*, R. Alamo, R.G. Snyder, W.L. Mattice. "The Raman Low Frequency D-LAM Band in Random Ethylene Copolymers". Meeting of the Americal Physical Society, March 31- April 4, 1986.

9. Mandelkern L.*, R. Alamo, R. Glaser. "Crystallization and Properties of Blends of Homopolymers and Copolymers of Polyethylene". Meeting of the NATAS. Cincinnati. September 1986.

10. Alamo R.G.*, L. Mandelkern. "Thermodynamic and Structural Properties of Ethylene Copolymers". American Physical Society. New Orleans. Lousiana. March 21-25, 1988.

11. Alamo R.G.*, L. Mandelkern. "Crystallization Kinetics of Ethylene Copolymers: Hydrogenated Polybutadiene". FLACS, Vol.XLI, No. 2. March 1988. 39th Annual Meeting of Florida Division ACS. Tampa, Florida, April 13-16, 1988.

12. Alamo R.G., L. Mandelkern*. "The Melting and Crystallization Kinetics of Hydrogenated Polybutadiene". NATAS Meeting. Orlando, October 1988.

13. Alamo R.G.*, E.K. Chang, L. Mandelkern. "The Molecular Weight Dependence of the Thermodynamic and Structural Properties of Ethylene Copolymers". 198th ACS National Meeting. Miami Beach, Florida, September 10-15, 1989.

14. Vickers T.J.*, R. Alamo, C.K. Mann, L. Mandelkern. "Polymer Topics in Undergraduate Analytical Chemistry". 198th ACS National Meeting, Section on Teaching Polymer Chemistry, Miami Beach, Florida, September 10-15, 1989.

15. Alamo R.G.*, L. Mandelkern, G.M. Stack. "From the n-Alkanes to Polyethylene: The Crystallization of Chain Molecules". 33rd IUPAC Symposium of Macromolecules, Montreal, Quebec. Canada, July 8-13, 1990.

16. Vickers T.J.*, R. Alamo, C.K. Mann, L. Mandelkern. "Polymer Topics in Undergraduate Analytical Chemistry". 200th ACS National Meeting. Washington DC. August 26-30, 1990.

17. Alamo R.G.*, G.M. Stack, L. Mandelkern. "The Isothermal Thickening of Normal Alkanes and Low Molecular Weight Polyethylene Fractions". 19th NATAS Meeting. Boston.

September, 1990.

18. Alamo R.G.*, L. Mandelkern, R.G. Snyder. "An Analysis of the LAM of Long Chain N-Alkanes". American Physical Society, Cincinnati, Ohio. March 18-22, 1991.

19. Mandelkern L.*, R.G. Alamo. "Use of Raman Spectroscopy in Characterizing the Structures and Properties of Crystalline Polymers". 201th ACS National Meeting. Atlanta, Georgia, April 1991.

20. Alamo R.G.*, L. Mandelkern. "Crystallization Kinetics of Random Ethylene Copolymers". 202th ACS National Meeting. New York, New York. August 1991.

21. Li Z., Y. Yang, N. Ichise, J.E. Mark*, E.K.M. Chan, R.G. Alamo, L. Mandelkern."The Use of Mechanical Properties Measurements to Characterize Gels and Gelation Process". 1991 Fall Meeting of the Materials Research Society (Symposium on Complex Fluids). Boston, December 1991.

22. Alamo R.G.*, L. Mandelkern. "The Crystallization of Polyethylene Mixtures: Linear Polyethylene/High Pressure Polymerized Long Chain Branched Polyethylenes". 203rd ACS National Meeting. San Francisco, California. April 1992.

23. Yang Y., N. Ichise, Z. Li, W. Yuan, J. E. Mark*, E.K.M. Chan, R. G. Alamo, L. Mandelkern."Use of Mechanical Property Measurements to Characterize Gels and Gelation Processes". 203rd ACS National Meeting. San Francisco, California, April 1992.

24. Alamo R.G.*, L. Mandelkern. "The Phase Structure of Random Ethylene Copolymers". 204th ACS National Meeting. Washington D.C., August 1992.

25. Stribeck N.*, H.G. Zachmann, R.G. Alamo, L. Mandelkern. "Narrow-Molecular-Weight-Distribution Polyethylene (PE). Comparison of the Results from SAXS and LAM-Raman Spectroscopy Concerning the Thickness Distribution of the Crystalline Lamellae". 13th General Conference of the Condensed Matter Division. European Physical Society. Regensburg. Germany, March 1993.

26. Alamo R.G.*, B.D. Viers, L. Mandelkern. "Relation Between Melting Temperature and Crystallization Temperature in Linear Polyethylene and Ethylene Copolymers". ACS National Meeting. Chicago, Illinois, August, 1993.

27. Alamo R.G.*, L. Mandelkern. "Structure Properties Relation of Random Ethylene Copolymers". 22nd NATAS Meeting, Denver, Colorado, September 1993.

28. Alamo R.G.*, L. Mandelkern, J.G. Fatou, C. Marcos. "The Molecular Weight Dependence on the Rate of Crystallization of Polymeric Chains". 1993 Fall Meeting of the Materials

Research Society. Boston, Massachusetts, November 29, 1993.

29. Alamo R.G.*, L. Lu, L. Mandelkern. "Isothermal Crystallization of Random Ethylene Copolymers". 207th ACS National Meeting. San Diego, California, March 13-17. 1994.

30. Alamo R.G.*, J.C. Lucas, L. Mandelkern. "The Crystallization Behavior of Isotactic Polypropylenes from the Melt. I. Crystallographic Forms". 207th ACS Meeting. San Diego, California, March 13-17. 1994.

31. Lucas J.C.*, R.G. Alamo, L. Mandelkern. "The Crystallization Behavior of Isotactic Polypropylenes from the Melt. II. Melting Process". 207th ACS Meeting. San Diego, California, March 13-17. 1994.

32. Wignall G.D.*, J.D. Londono, R.G. Alamo, L. Mandelkern, F. C. Stehling. "The Phase Behavior of Blends of Linear and Branched Polyethylenes in the Molten and Solid States by Small Angle Neutron Scattering". March Meeting of the American Physical Society. Pittsburg, Pennsylvania, March 21-25, 1994.

33. Alamo R.G.*, L. Mandelkern, F.C. Stehling, G.D. Wignall, J.D. Londono. "The Morphology of Blends of Linear and Branched Polyethylenes in the Solid State". March Meeting of the American Physical Society. Pittsburg, Pennsylvania, March 21-25, 1994.

34. Mandelkern L.*, R.G. Alamo. "The Nucleation and Crystallization of Chain Molecules of Low Molecular Weight". 68th Annual Colloid and Surface Science Symposium, Stanford, June 19-22, 1994.

35. Wignall G.D.*, J.D. Londono, R.G. Alamo, L. Mandelkern, F.C. Stehling. "The Morphology of Blends of Linear and Branched Polyethylenes in Solid State by SANS". 208th ACS Meeting. Washington D.C. August 1994.

36. Stewart M.J.*, W.L. Jarrett, L.J. Mathias, R.G. Alamo, L. Mandelkern. "A CRAMPS and ^{13}C CP/MAS NMR Examination of Solid-Solid Transitions in n-Hexatriacontane ($C_{36}H_{74}$)". 208th ACS Meeting. Washington D.C. August, 1994.

37. Wignall G.D.*, J. D. Londono, R. G. Alamo, L. Mandelkern, F. C. Stehling. "The Morphology of Blends of Linear and Branched Polyethylenes by Small-Angle Neutron and X-Ray Scattering (SANS and SAXS)". Fall Meeting of the Materials Research Society. Boston, November 28, 1994.

38. Wignall G.D.*, J. D. Londono, R. G. Alamo, L. Mandelkern, F. C. Stehling, "The Phase Behavior of Blends of Linear and Branched Polyethylenes in the Molten and Solid States by Small-Angle Neutron Scattering" March Meeting of the American Physical Society, San José, California, March 20-23, 1995.

39. Galante M.J.*, R.G. Alamo, L. Mandelkern. "The Crystallization and Melting of Binary Mixtures of Polyethylenes". Symposium on Advances in Crystalline Polymers. Polymer Chemistry Division of the ACS. ACS National Meeting. Anaheim, California, April, 1995.

40. Wignall G.D.*, J.D. Londono, R.G. Alamo, L. Mandelkern. The Morphology of Blends of Linear and Branched Polyethylenes in Solid State by SANS". Symposium on Advances in Crystalline Polymers. Chemistry Division of the ACS. ACS National Meeting. Anaheim, California, April, 1995.

41. Alamo R.G.* "Analysis of the Crystallization and Melting Behavior of Polypropylenes from Different Catalyst Systems". Annual Meeting of the American Chemical Society (Florida Section), Orlando, Florida, May 5-6, 1995.

42. Galante M.J.*, R. G. Alamo*, L. Mandelkern "An Analysis of the Crystallographic Forms of Isotactic Polypropylenes with Narrow Molecular Weight Distributions". Annual Meeting of the American Chemical Society (Florida Section), Orlando, Florida, May 5-6, 1995.

43. Alamo R.G.*, M. J. Galante, A. Lehtinen, R. Paukkeri "The Dependence of the Molecular Structure on the Crystallization and Melting Behavior of Polypropylenes from Different Catalyst System". 1995 Meeting of the American Institute of Chemical Engineers, Miami Beach, November 1995.

44. Alamo R.G.*, M.J. Galante, L. Mandelkern, A. Lehtinen, R. Paukkeri. "Crystallization Kinetics of Metallocene Type Polypropylenes and Comparison with Ziegler-Natta Type Systems". March Meeting of the American Physical Society. St. Louis, Missouri, March 18-22, 1996.

45. Mandelkern, L., J.T. Graham*, R.G. Alamo, "The Effect of Molecular Weight and Crystallite Structure on Yielding in Ethylene Copolymers. March Meeting of the Ameriacn Physical Society. St. Louis, Missouri, March 18-22, 1996.

46. Graham J.T.*, L. Mandelkern, R.G. Alamo, "An Analysis of the 1060 cm^{-1} band of the Raman Spectrum of Polyethylene". March Meeting of the Ameriacn Physical Society. St. Louis, Missouri, March 18-22, 1996.

47. Wignall G.D.*, J.D. Londono, F.C. Stehling, R.G. Alamo, L. Mandelkern. "Small Angle Neutron Scattering Investigations of Liquid-Liquid Phase Separation in Heterogeneous Linear-Low Density Polyethylene". March Meeting of the Ameriacn Physical Society. St. Louis, Missouri, March 18-22, 1996.

48. Alamo R.G.*, J.A. Haigh, L. Mandelkern, "Crystallization and Melting of Model Polyethylenes of Different Chain Structures". 11th International Congress on Thermal

Analysis and Calorimetry (ICTAC). Philadelphia, PA. August 1996.

49. Haigh J.A.*, R.G. Alamo, L. Mandelkern, "Crystallization Behavior and Properties of Model Polyethylenes of Different Chain Structures". ACS National Meeting. Division of Polymer Chemistry. Orlando. August, 1996.

50. Isasi J.R*., L. Mandelkern, R.G. Alamo, "Crystallization Kinetics of Metallocene Type Isotactic Polypropylenes. II. Influence of Defect Concentration". ACS National Meeting. Division of Polymer Chemistry. Orlando. August, 1996.

51. Alamo R.G.*, G. Brown, L. Mandelkern, R. Paukkeri, A. Lehtinen, "A Morphological Study of a Higly Isotactic Polypropylene Fraction". Symposium *New Concepts of Polymeric Materials: Science and Engineering*. ACS National Meeting. Division of Polymeric Materials Science and Engineering. Orlando. August, 1996.

52. Ebube*, N.K., G. Owusu-Ababio, R.G. Alamo, Non-Destructive Characterization of the Phisicochemical Properties of Amorphous Polymers Using the Artificial Neural Networks. Annual meeting of the American Association of Pharmaceutical Scientists. Seattle. October 1996.

53. Agamalian*, M.M., G.D. Wignall, R.G. Alamo, J.D. Londono, L. Mandelkern, F.C. Stehling, Ultra-High Resolution Small Angle Neutron Scattering (USANS) Investigations of Phase Separations in Linear Low-Density Polyethylene (LLDPE). Materials Research Society 1996 Fall Meeting. Symposium BB, Morphological Control in Multiphase Polymer Mixtures. Boston, December 1996.

54. Galante*, M.J., Alamo R.G., L. Mandelkern, R. Paukkeri, A. Lehtinen, Crystallization Kinetics of Isotactic Polypropylenes. 5th. Latin American Polymer Symposium/3rd Ibero American Polymer Symposium. Mar del Plata, Argentina. 2-5 December, 1996.

55. Alamo*, R.G., L. Mandelkern, Morphology and Melting Behavior of Polypropylenes March Meeting of the American Physical Society. Kansas City, Kansas, March 17-21, 1997.

56. Isasi*, J.R., L. Mandelkern, R.G. Alamo, Unit Cell Dilation in Metallocene Monoclinic Polyprolynes March Meeting of the American Physical Society. Kansas City, Kansas, March 17-21, 1997.

57. Alamo*, R.G., C. Chi, Linear Growth Rates and Morphology of Metallocenes and Ziegler-Type Polypropylenes March Meeting of the American Physical Society. Kansas City, Kansas, March 17-21, 1997.

58. Wignall*, G.D., M.M. Agamalian, J.D. Londono, R.G. Alamo, L. Mandelkern, Ultra-High Resolution Small Angle Neutron Scattering (USANS) Investigations of Phase Separations in

Linear Low-Density Polyethylene (LLDPE). March Meeting of the American Physical Society. Kansas City, Kansas, March 17-21, 1997.

59. Yasurek*, L.R., R.G. Alamo, "Crystallization and Melting of Bacterial Poly(3-Hydroxy Butyrate) and its Random Copolymers with 3-Hydroxy Valerate" Regional Undergraduate AICHE Meeting. Charlote. South Caroline, April, 1997.

60. Alamo*, R.G., L. Mandelkern, G. Brown, "Melting Behavior of Isotactic Polypropylenes". 25th NATAS (North American Thermal Analysis Society National Meeting), McLean, Virginia, September 1997.

61. Isasi*, J.R., L. Mandelkern, R.G. Alamo, "Structural and Thermal Characterization of Metallocene Catalyzed Isotactic Copolymers of Poly(Propylene)". March Meeting of the American Physical Society. Los Angeles, CA, March 16-20, 1998.

62. Kim*, M-H., R.G. Alamo, L. Mandelkern, "The Crystallite Structure of Isotactic Polypropylenes and Propylene Copolymers by SAXS". March Meeting of the American Physical Society. Los Angeles, CA, March 16-20, 1998.

63. Dai*, S.P., C. Peggy, R. Alamo, L. Mandelkern, M. Capel. "Real Time Small Angle X-Ray Scattering and Differential Scanning Calorimetry Study of Metallocene Poly(propylene)" March Meeting of the American Physical Society. Los Angeles, CA, March 16-20, 1998.

64. VanderHar*t D.L., R.G. Alamo, M.H. Kim, L. Mandelkern, E. Perez, S. Mansel, "Partitioning of Various Chain Defects within the Semicrystalline Morphology of Isotactic Polypropylene". March Meeting of the American Physical Society. Los Angeles, CA, March 16-20, 1998

65. Agamalian, M.M., R.G. Alamo, J.D. Londono, L. Mandelkern, F.C. Stehling, G.D. Wignall*. "Phase Behavior of Blends of Linear and Branched Polyethylenes Via Small- and Ultra-Small Angle Neutron Scattering". ACS National Meeting. Division of Polymeric Materials Science and Engineering. Symposium on Thermodynamics of Polymer Blends. Dallas, TX. March, 1998.

66. Dai, S.P., C. Peggy*, R. Alamo, L. Mandelkern, "Crystallization and Melting of Narrow Molecular Weight Distribution Poly(propylene) prepared by Partial Melting", ACS National Meeting. Division of Polymeric Materials Science and Engineering. Symposium on Newer Methods in Thermal Analysis. Dallas, TX. March, 1998.

67. Alamo*, R.G, Kim, M-H., L. Mandelkern, M.J. Galante, G.D. Wignall, J.D. Londono, F.C. Stehling, "The Cocrystallization of Mixtures of Homopolymers and Copolymers: Polyolefins" ACS National Meeting. Division of Polymeric Materials Science and Engineering. Symposium on Newer Methods in Thermal Analysis. Dallas, TX. March, 1998.

68. Putcha*, S., R.G. Alamo, "Effects of Stereo and Regio Defects on the Crystallization Kinetics of Isotactic Polypropylene" Annual Meeting of the Florida Section of the American Chemical Society. Orlando May 8, 1998.

69. Alamo*, R.G., "Crystallization Behavior and Properties of Polypropylenes" Osaka University Macromolecular Symposium (OUMS'98). Molecular Interactions and Time-Space Organization in Macromolecular Systems". June 3-6,1998. Osaka. Japan.

70. VanderHart* D.L., H. Feng, M.R. Nyden, R.G. Alamo, M.H. Kim, L. Mandelkern, E. Perez, S. Mansel, C-13 NMR Study of the Inclusion of Stereo and Regio Defects in the Crystalline Regions of Isotactic Polypropylene. Rocky Mountains Conference in Analytical Chemistry, Denver, CO, July, 1998.

71. Dai, P.S., P. Cebe*, R.G. Alamo, L. Mandelkern, M. Capel, "Real-Time SAXS Study of the Crystallization of Metallocene Poly(Propylene)" ACS National Meeting. Division of Polymeric Materials Science and Engineering. Symposium on Scattering from Polymers. Boston, MA, August, 1998.

72. Wignall*, G.D., M.M. Agamelian, R.G. Alamo, L. Mandelkern, "Phase Behavior of Blends of Linear and Branched Polyethylenes via SANS and USANS" Annual meeting of the American Institute of Chemical Engineers (AIChE), Miami Beach, November 1998.

73. VanderHart*, D. R.G. Alamo, M. Nyden, L. Mandelkern. "Ethylene Defects in Isotactic Poly(propylene): Partitioning, Conformation and Chemical Shift Calculations" Experimental NMR Conference, Orlando, Fl, Feb. 28-March 5, 1999.

74. Mandelkern, L., G.D. Wignall*, J.D. Londono, R.G. Alamo, M.H. Kim, "The Morphology of Blends of Linear and Short Chain Branched Polyethylenes in the Solid State by Neutron Scattering and Differential Scanning Calorimetry". March Meeting of the American Physical Society. Atlanta, GA, March 20 - 26, 1999.

75. Alamo*, R.G., M.H. Kim, M.J. Galante, J.R. Isasi, L. Mandelkern, "The Structural and Kinetic Factors Governing the Formation of the Gamma Polymorph of Isotactic Polypropylene at Atmospheric Pressure". March Meeting of the American Physical Society. Atlanta, GA, March 20 - 26, 1999.

76. Huang*, T.W., R.G. Alamo, L. Mandelkern, "A Study of Melting Kinetics of Isotactic Polypropylene Crystals". March Meeting of the American Physical Society. Atlanta, GA, March 20 - 26, 1999.

77. VanderHart*, D. L., R.G. Alamo, M.R. Nyden, L. Mandelkern, "A Study of Ethyl Residues in Isotactic Polypropylene-co-Ethylene Copolymers: Morphological Partitioning by NMR

and Conformational Verification Via Chemical Shift Calculations" March Meeting of the American Physical Society. Atlanta, GA, March 20 - 26, 1999.

78. Sripada, L.S., R.G. Alamo "Properties of High Pressure Polymerized Ethylene Copolymers: Effect of the Type of Comonomer in their Phase Structure and Crystallization Behavior". Annual Meeting of the Florida Section of the American Chemical Society. Orlando May 7, 1999.

79. Agamelian, M.M., R.G. Alamo, J.D. Londono, L. Mandelkern, G.D. Wignall, "Phase Behavior of Blends of Linear and Branched Polyethylenes on Micron-Length-Scales Via Ultra-Small Angle Neutron Scattering", SAS99. Brookhaven National Laboratory. New York. May, 1999.

80. R.G. Alamo, J.R. Isasi, M.H. Kim, L. Mandelkern, D.L. VanderHart, "Thermal and Structural Behavior of Metallocene-Type Random Propylene Copolymers", ACS National Meeting. Division of Polymeric Materials Science and Engineering. Symposium on Semicrystalline Polymers. New Orleans, LA, August, 1999.

81. Dai, P.S., P. Cebe, M. Capel, R.G. Alamo, L. Mandelkern, "Self-Nucleation Study of Metallocene Isotactic Polypropylene", ACS National Meeting. Division of Polymeric Materials Science and Engineering. Symposium on Semicrystalline Polymers. New Orleans, LA, August, 1999.

82. Little, A.L., R.G. Alamo, "Linear Growth Rates of Random Propylene Copolymers: A Kinetic and Morphological Analysis" Annual meeting of the American Institute of Chemical Engineers (AIChE), Dallas, TX, November 5, 1999.

83. VanderHart, D.L., M.R. Nyden, R.G. Alamo, L. Mandelkern, "Incorporation of Stereo, Regio and Comonomer Defects into the Crystalline Regions of Isotactic Polypropylene: Results from NMR, Molecular Dynamics and Chemical Shift Calculations", ACS National Meeting. Division of Polymeric Materials Science and Engineering. Symposium on the Structure, Dynamics and Organization of Polymers in the Solid State by Magnetic Resonance. San Francisco, CA. March 26-31, 2000.

84. Alamo, R.G., T.W. Huang, L. Mandelkern, M.H. Kim, "A Comparative Study of the Melting and Crystallization Behavior of a Metallocene and a Ziegler Fraction of iPP with the Same Overall Defect Content". March Meeting of the American Physical Society. Symposium on Polymer Crystallization: New Perspectives on an Old Problem, Minneapolis, Minnesota, March 20 - 24, 2000.

85. Wignall, G.D., R.G. Alamo, J.D. Londono, L. Mandelkern, M.H. Kim, J.S. Lin, G.M. Brown, "The Morphology of Blends of Linear and Short-Chain Branched Polyethylenes in the Solid State by Small Angle Neutron and X-Ray Scattering, Differential Scanning

Calorimetry and Transmission Electron Microscopy. Materials Research Society. 2000 Spring Meeting. San Francisco, CA. April 24-28, 2000.

86. Little, A.L., R.G. Alamo, Linear Growth Rates of Random Propylene Copolymers: A Kinetic and Morphological Analysis Regional Meeting of the American Institute of Chemical Engineers (AIChE), Lexington, KY, April 6-8, 2000.

87. Huang*, W., R.G. Alamo, "A Comparative Study of the Melting and Crystallization Behavior For a Metallocene and a Narrow Fraction of Ziegler-Natta Isotactic Polypropylene", ANTEC, Orlando, FL May 5, 2000.

88. Dai, P.S., P. Cebe*, M. Capel, R.G. Alamo, L. Mandelkern, "Wide and Small Angle X-Ray Scattering Study of Melting Kinetics of Isotactic Polypropylene" ACS National Meeting. Division of Polymeric Materials Science and Engineering. Washington D.C., August 19, 2000.

89. Alamo*, R.G., W.T. Huang, L. Mandelkern, " Kinetics of Isothermal Melting of Isotactic Polypropylenes with Different Degrees of Isotacticity" ACS National Meeting. Division of Polymer Chemistry. Washington D.C., August 19, 2000.

90. Simanke*, A.G., R.G. Alamo, "The Thermodynamic and Structural Properties of Metallocene Type Random Ethylene Copolymers" 28th NATAS (North American Thermal Analysis Society) Meeting, Orlando, Florida, October 4, 2000

91. Chatterjee* J., A. Little, R.G. Alamo, "Kinetic and Morphological Studies of a Series of Narrow Propylene-Ethylene Copolymers" 28th NATAS (North American Thermal Analysis Society) Meeting, Orlando, Florida, October 4, 2000.

92. VanderHart*, D.L., R.G. Alamo, M.R. Nyden, L. Mandelkern, "NMR Study of Various Defects in Isotactic Polypropylene: Morphological Partitioning and Chain Conformation in the Crystalline Regions" International Chemical Congress of Pacific Basin Societies. Honolulu, Dec. 14, 2000.

93. Wignall G.D., R.G. Alamo*, L. Mandelkern, D. Schwahn "SANS Studies of Liquid-Liquid Phase Separation in Heterogeneous and Metallocene-Based Linear Low-Density Polyethylenes" March Meeting of the American Physical Society. Seattle, Washington, March 12 - 16, 2001.

94. Li, D.*, H. Garmestani, S. Kalidindi, R.G. Alamo "Crystallographic Texture Evolution in High Density Polyethylene During Uniaxial Tension" March Meeting of the American Physical Society. Seattle, Washington, March 12 - 16, 2001.

95. Alamo*, R.G., A. Simanke, G. Galland, R. Mauler " Study of the Effect of Comonomer Type

on the Properties of Rapidly Crystallized and Annealed Random Ethylene Copolymer" March Meeting of the American Physical Society. Seattle, Washington, March 12 - 16, 2001.

96. Simanke*, A.G., Alamo. R.G.,G. Galland, R. Mauler. "The Thermodynamic and Structural Properties of Metallocene Type Random Ethylene Copolymers" IX International Macromolecular Colloquium, November, 10- 15. Porto Alegre, Brazil, 2001.

97. Alamo*, R.G. "Crystallization and Melting Kinetics of Poly(Propylenes): Effect of Concentration and Type of Defects" POLYOLEFINS III Symposium. October 7 – 10. Sonoma, California, 2001.

98. Ritchson, E., J.A. Blanco, R.G. Alamo. "Crystallization Rates and Spherulitic Morphology of Fractions from Metallocene and Ziegler type Isotactic Poly(propylene)" AIChE Annual Conference, Reno, NV, November 3 –7, 2001

99. Alamo, R.G. "Molecular and Crystalline Characterization of Polyolefins, their Blends and Composites" NSF/Industry Cooperative Research Center Workshop on Affordable Composites Materials. Tallahassee, December 4-5, 2001

100. Alamo, R.G, J.A. Blanco, E. J. Ritchson, P. Agarwal "Crystallization Rates and Molecular Microstructure of Fractions from Metallocene and Ziegler type Isotactic Poly(propylenes)" ACS National Meeting. Division of Polymer Chemistry. Orlando, FL, April 8, 2002

101. Alamo, R.G., W.T. Huang, I. Hosier "Morphological Studies of Isotactic Poly(propylenes) Subject to Isothermal Melting Kinetics" 30th NATAS (North American Thermal Analysis Society) Meeting, Pittsburgh, Pennsylvania, September 23 – 25, 2002

102. I. L. Hosier, R.G. Alamo, P. Esteso "Crystallographic Polymorphs and Lamellar Morphology of Metallocene Random Propylene Copolymers". ACS National Meeting. Division of Polymeric Materials Science and Engineering. New Orleans, LO, March 23 - 27, 2003

103. D. M. Mowery, I. Carrilero, R.G. Alamo "Structural Studies of Ethylene 1-Octene and Ethylene Norbornene Random Copolymers by NMR and WAXS" March meeting of the American Physical Society. Austin, Texas, March 3 - 7, 2003

104. I. L. Hosier, R.G. Alamo, "Lamellar Morphology of Metallocene Random Propylene Copolymers Studied by Atomic Force Microscopy" March meeting of the American Physical Society. Austin, Texas, March 3 - 7, 2003

105. D. VanderHart, C. Snyder, R. Alamo " Proton NMR Study of Room Temperature Aging in Isotactic PolyPropylene and Ethylene Octene Copolymers" March meeting of the

American Physical Society. Austin, Texas, March 3 - 7, 2003.

106. R.G. Alamo, J.C. Randall, J.A. Blanco, P.K. Agarwal, C.J. Ruff "Crystallization Rates and Defects Distribution in Matched Metallocene and MgCl2 Supported Ziegler Natta Isotactic Polypropylenes. European Polymer Conference on Stereospecific Polymerization and Stereoregular Polymers. Milan, Italy June 8, 2003

107. R.G. Alamo "Melt and Nano-Scale Crystalline Properties of Industrial Poly(Propylenes) of the Ziegler-Natta and Metallocene Types. The Role of Defect Microstructure" CAPCE-ARC Second Rheology Workshop. Seoul, Korea. September 4-5, 2003

108. R.G. Alamo "Crystallization and Morphology of Matched Fractions of MgCl2-Supported Ziegler Natta and Metallocene Isotactic Polypropylene. The Role of Chain Microstructure" Brazilian Polymer Congress. Bello Horizonte, Brazil, November 2003

109. R.G. Alamo, I.L. Hosier, A. Ghosan "Structural and Thermal Properties of Random Propylene Copolymers" IUPAC, Macro 2004. Paris, July 4 – 9, 2004

110. R.G. Alamo, I.L. Hosier, J. Chaterjee, "Polymorphism and Crystallization Kinetics of Random Propylene Copolymers" ACS National Meeting. Division of Polymeric Materials Science and Engineering. Philadelphia, August 2004

111. R. G. Alamo, I.L. Hosier, A, Ghosan "Structural and Thermal Properties of Metallocene Random Propylene Copolymers" North American Thermal Analysis Conference (NATAS) . Symposium on Semicrystalline Polymers. Williamsburg, VA. October 4 – 6, 2004

B. *Invited Presentations*

1. Alamo R.G.* "The Use of Raman Spectroscopy in the Characterization of the Structure and Properties of Semicrystalline Polymers". Primer Simposio Iberoamericano de Polimeros. Vigo. Spain, 1992.

2. Alamo R.G.* "The Crystallization Behavior of Long-Chain n-Alkanes and Low Molecular Weight Polyethylenes". NATO Advanced Research Workshop on Polymer Crystallization. Mons, Belgium, 1992.

3. Alamo R.G.*, L. Mandelkern. "Crystallization Kinetics of Long Chain N-Alkanes". Annual Meeting of the American Chemical Society (Florida Section). Orlando, Florida. May 5 - 8, 1993.

4. Alamo R.G.*, L. Mandelkern, H. G. Zachmann, N. Stribeck. "The Use of Raman Spectroscopy and Small Angle X-ray Scattering in Characterizing the Phase Structure of Polyethylene and Random Ethylene Copolymers". Symposium on Hyphenated Techniques in Polymer Characterization. ACS National Meeting. Division of Polymeric Materials, Chicago, August, 1993.

5. Alamo R.G.* "The Crystallization Behavior of Random Copolymers of Ethylene" Cooperative Research Award Sympossium. Polymeric Materials: Science and Engineering Division of the ACS. ACS National Meeting. Anaheim, April, 1995.

6. Alamo R.G.*, M.J. Galante, J.C. Lucas, L. Mandelkern. "The Crystallization and Melting Behavior of Polypropylenes from Different Catalyst Systems". Symposium on Advances in Crystalline Polymers. Polymer Chemistry Division. ACS National Meeting. Anaheim, April, 1995.

7. Mandelkern* L., R.G. Alamo, "Raman Spectroscopy and Crystalline Polymers: The Polyethylenes". ACS National Meeting. Division of Polymeric Materials Science and Engineering. Orlando. August, 1996.

8. Alamo*, R.G, M.H. Kim., L. Mandelkern, M.J. Galante. G.D. Wignall, J.D. Londono, F.C. Stehling. The Cocrystallization of Mixtures of Homopolymers and Copolymers: Polyolefins. ACS National Meeting. Division of Polymeric Materials Science and Engineering. Symposium on Newer Methods in Thermal Analysis. Dallas, TX: March, 1998.

9. R.G. Alamo*. Crystallization Behavior and Properties of Polypropylenes International Macromolecular Symposium on Molecular Interactions and Time-Space Organization in Macromolecular Systems. Osaka, Japan. June, 1998.

10. R.G. Alamo*. The Co-Crystallization Behavior of Binary Blends of Isotactic Poly(propylene) and Propylene-Ethylene Random Copolymers and its Relevance to the Analysis of the CCD by TREF Workshop on Advances in Polyolefins II. October 24-27, 1999. Napa California.

11. Alamo*, R.G., W.T. Huang, L. Mandelkern, " Kinetics of Isothermal Melting of Isotactic Polypropylenes with Different Degrees of Isotacticity" ACS National Meeting. Division of Polymer Chemistry. Washington D.C., August 19, 2000.

12. Simanke*, A.G., Alamo. R.G.,G. Galland, R. Mauler. "The Thermodynamic and Structural Properties of Metallocene Type Random Ethylene Copolymers" IX International Macromolecular Colloquium, November, 10- 15. Porto Alegre, Brazil, 2001.

13. Alamo*, R.G. "Crystallization and Melting Kinetics of Poly(Propylenes): Effect of Concentration and Type of Defects" POLYOLEFINS III Symposium. October 7 – 10.

Sonoma, California, 2001.

14. Alamo*, R.G. "The Role of Defect Microstructure in the Crystallization Behavior of Metallocene and $MgCL_2$-Supported Ziegler-Natta Isotactic Poly(propylenes)" 7th Brazilian Polymer Congress. November 9, 2003

C. *Invited Seminars and Lectures*

1. Physical Chemistry Seminar Series. Institute of Molecular Biophysics. Florida State University. Tallahassee, Fl. April, 1984.
"Properties of Solution-Formed Crystals of Ethylene Copolymers" .

2. Lecturer at the Instituto de Plasticos y Caucho of the National Research Council in Madrid, Spain. December, 1990.
"Desde los n-Alkanos al Polietileno. La Cristalizacion de Moleculas de Cadena Larga"

3. Physical Chemistry Seminar Series. Institute of Molecular Biophysics. Florida State University. Tallahassee, Florida. February, 1991.
"From the n-Alkanes to the Polyethylene. The Crystallization of Long Chain Molecules"

4. Lecturer at the Seminar, "New Methods of Characterization of Polymers" of the First Iberoamerican Symposium of Polymers. Vigo. Spain, June 1992.
"The Use of Raman Spectroscopy in Characterizing the Structure and Properties of Crystalline Polymers"

5. Chemical Engineering Seminar Series. FAMU-FSU College of Engineering. Tallahassee, Florida. March, 1993.
"Structure and Properties of Random Ethylene Copolymers"

6. Chemistry Seminars. Florida Agricultural and Mechanical University (FAMU). "Crystallization of Long Chain Molecules". Tallahassee, Florida. June, 1993.

7. Lecturer at the National University of Costa Rica. Department of Chemistry, Polymer Section. June, 1993.
"Structure - Properties Relations in Polyethylenes".

8. Chemistry Seminars. University of South Florida (USF). Tampa, Florida. October, 1995.
"Crystallization of Chain Molecules".

9. Tallahassee Section of the AICHE. August, 1995.
"Crystallization and Properties of Polyolefins".

10. The Baytown Polymer Center Lecture Series. The EXXON Chemical Co. Baytown, TX. September, 1996.
"The Dependence on the Molecular Structure of the Morphology and the Crystallization and Melting Behavior of Polypropylenes".

11. University of Florida. Physical Chemistry Seminar. Gainesville, FL. December 2, 1996.
"The Crystallization of Long Chain Molecules".

12. The DOW Chemical CO. Lecture Series. Freeport, TX. July 29, 1997.
"Morphology, Crystallization and Melting Behavior of Polypropylenes".

13. The Baytown Polymer Center Lecture Series. The EXXON Chemical Co. Baytown, TX. February, 1998.
"The Co-Crystallization of blends of Polypropylene and Random Propylene Ethylene Copolymers".

14. Polymer Engineering and Science Department. Graduate Seminars. University of Massachussetts at Amherst. April 23, 1999.
"The Relation Between Molecular Structure and Morphology, Crystallization and Melting Behavior of Metallocene and Ziegler-Natta Polypropylenes".

15. Invited seminar at he Exxon-Mobil Corporate and Strategic Research Center. Annandale, NJ. January 26, 2001.
"Crystallization and Melting Kinetics of Poly(propylenes) Effect of Concentration and Type of Defects"

16. Florida State University Chemistry Department, Physical-Chemistry Seminars, Tallahassee, FL. October 1st, 2001.
"Poly(Propylenes). Crystallization and Melting Kinetics".

ORGANIZATION OF SYMPOSIA AND CHAIR ACTIVITIES.

1. Chairperson of the "Polymer Science Symposium Honoring Prof. L. Mandelkern on Occasion of his 65th Birthday". Tallahassee, Florida, August 1987.

2. Organization of the Symposium "TA in Polymer Phase Transitions" of the 24th NATAS (North American Thermal Analysis Society) Annual Conference. San Francisco, September 1995.

3. Invited to chair a technical session of the Symposium:" Advances on Crystalline

Polymers" at the National American Society Meeting to be held in Anaheim, March 1995.

4. Chair of the Symposium "Semicrystalline Polymers" NATAS, Williamsburg, VA 2004

SERVICE EXPERIENCE

Department

- 2001-2002 . Served in the Promotion and Tenure Committee

- 2000-2001. AICHE student chapter advisor.

- 1995 - Present. Served in the graduate committee of the Chemical Engineering Department of the FAMU-FSU College of Engineering. Sort applications of students from India. Helped the committee in the selection of prospective graduate students. In charge of recruiting American and European students. In charge of the annual evaluation of the graduate student□s progress.

- 1998-Present. Director of the Undergraduate Research Program (URP) of the Chemical Engineering Department and coordinator of Honors in the Major. In charge of reviewing students applications, and students reports from first and second semesters. In charge of keeping students and reports under schedule.

- 1998-Present. Departmental coordinator of Honors Program in the Chemical Engineering Major.

- 1997-Present. Served in the Undergraduate Committee. Participated in the Departmental Program Review and in the Abet 2000 implementation. Participated in the evaluation of folders for the hiring of a Laboratory Instructor. International students coordinator.

- Coordinator of Graduate Seminars. Organized 12 seminars during the 1996 Spring semester and 10 seminars during the Spring 1997 semester.

College

- 1995 - 1998. Chair, FAMU-FSU College Library committee. The Journals of the FSU library assigned to the College of Engineering were identified for the first time by engineering departments. A percentage of expenditures of each department in the FSU library is now available.

- Member of the College Associate Dean Search Committee. Reviewed 45 folders of prospective candidates. Identified and interviewed the four top candidates.

- Member of the 1996-1997 Faculty Search Committee for Industrial Engineering. Reviewed 57 folders of prospective applicants. Selected 9 top candidates. Interviewed a few of them.

- Active participation in the Annual College Industry Day since 1996. Faculty Ambassador for Industry Day, FAMU-FSU College of Engineering. Tallahassee, April 15-16, 1996. Presented talk on Research in Polyolefins, March 2000.

University

- 1995- 1999 College of Engineering representative on the Florida State University *Faculty Senate Library Committee* and member of the Electronic/Mechanical Access Subcommittee.

- Spring 1999. Member of the Sabbaticals Committee. Florida Agricultural and Mechanical University.

- Spring 2000. Reviewer of COFRS program (Internal Research awards of the Council of Research and Creativity of Florida State University)

- Participated in the Florida State University Honors in the Major Symposium organized by Phi Kappa Phi. March 28, 2000.

- Fall 2001 – Present. Served in the Advisory Council Board for the "Women' Studies Program, Women in Math, Science & Engineering Program"

Community

- Fall 2002. Member of the NSF Advisory Review Panel in selecting applicants for the International Research Fellowship Program MPS Sub-Panel and MPS Distinguished Research Fellowship Program.

- Fall 2000- present. Member of the Advisory Board for the Chemistry Department of the University of West Florida. Pensacola, Florida.

- Capital Regional Science and Engineering Fair. Judge of Physical Sciences Division. Tallahassee, March, 1996-2001.

- Member of the Service and Z-Club Commitees of Zonta International in Tallahassee. (Paralegal Spanish translator for Migrant workers in Quincy, Florida), 1993.

- Girls Science Club in Lincoln High School, organizing member. Tallahassee, Florida, 1992

-1995.

EXHIBIT 2

Formation of the α and γ Polymorphs in Random Metallocene−Propylene Copolymers. Effect of Concentration and Type of Comonomer

I. L. Hosier,[†] R. G. Alamo,*[,†] P. Esteso,[†] J. R. Isasi,[§] and L. Mandelkern[‡]

Department of Chemical Engineering, Florida Agricultural and Mechanical University and Florida State University, 2525 Pottsdamer Street, Tallahassee, Florida 32310, and Department of Chemistry and Biochemistry, Florida State University, Tallahassee, Florida 32306

Received March 5, 2003; Revised Manuscript Received May 19, 2003

ABSTRACT: Four sets of random propylene-based copolymers with 1−10 mol % of ethylene, 1-butene, 1-hexene, or 1-octene as co-units, synthesized with the same metallocene catalyst, were investigated by differential scanning calorimetry and wide-angle X-ray scattering following rapid and isothermal crystallization. Parameters related to defect concentration, defect type, and microstructure and thermodynamic and kinetic factors were evaluated as to their role in developing the γ polymorph. The effect of the comonomer in enhancing the fractional content of the γ polymorph is akin to the role of defects in the homo-poly(propylene) chain. However, differences in the partitioning of the comonomer between the crystalline and noncrystalline regions leads to contents of the γ phase that differ among the copolymers at any given crystallization temperature. Qualitatively, these differences can be used to assess the degree to which a counit participates in the crystallite. The experimental results suggest that there is no discrimination of the defects that enter the crystal lattice (stereo, regio, ethylene, or butylene units) between the α or γ crystallites. The results with copolymers establish that the bases that lead to the formation of the γ polymorph are the same for homo-poly(propylene) and its copolymers.

Introduction

Isotactic poly(propylenes) are important materials from both commercial and technical standpoints and have interesting and, in some aspects, not yet well-known crystallographic features. The properties of these materials can be varied from strong and rigid to elastomeric behavior by virtue of copolymerization. Understanding the effect of chain microstructure on the morphology and crystallization behavior of poly(propylene) and its copolymers is the key to applying these materials to an ever-diversifying range of applications from household articles to engineering materials. Ethylene- and 1-butene-based propylene copolymers are widely used for film applications, often as one of the components of multilayered co-extruded films. A major advance in expanding the properties of poly(propylenes) and their range of applications was the advent of metallocene catalysts,[1,2] which afforded incorporation of large contents of comonomer,[2,3] copolymerization of cyclic and other comonomer types that are not easily incorporated with classical Ziegler−Natta (ZN) catalysts, and excellent control of stereoregularity. In addition, metallocene catalysts may yield copolymers with a truly random comonomer distribution, uniform intermolecular distribution of the comonomer content, and narrow molecular weight distribution, leading to a new class of random polyolefins, which are inaccessible through conventional heterogeneous Ziegler−Natta catalysts.[4] To date, metallocene-based propylene copolymers have been synthesized with a variety of comonomers of the linear 1-alkene type, from ethylene to 1-hexadecane,[5−12] and comonomers leading to branched side chains such as 4-methyl-1-pentene,[13] giving a wide range of interesting materials. Despite this success, many of the studies reported in the literature concentrate on ZN-based copolymers,[14−26] the large majority with ethylene as comonomer.[16,18,19,21−26] The properties of metallocene-catalyzed propylene copolymers are only recently surfacing.[5−12]

Inherent to the isotactic poly(propylene) chain, formed either with a ZN or a metallocene catalyst, is the presence of structural irregularities of the chemical (regio defects or comonomer units) or stereo type. Previous detailed studies of homopolymers have found a close correlation between the concentration of these irregularities and the maximum content of γ polymorph that the chain develops.[27] Concentrations of the γ polymorph exceeding 80% can be developed in metallocene-type polypropylenes at conditions approaching those used in industrial processes, lending new significance to the properties conferred by this crystallographic form beyond the laboratory and scientific interest. The orthorhombic unit cell of the γ polymorph, made of nonparallel bilayers, is unprecedented for polymeric systems. There has been some interest in understanding the role of chain defects in enhancing the formation of this uncommon crystallographic phase.[27−33] In the γ polymorph each bilayer is made of parallel chains with opposite hand helices, and adjacent bilayers are tilted at 81° with respect to each other.[34−37] The α polymorph has a more classical chain packing with parallel chains of alternating right- and left-hand 3/1 helices also arranged in bilayers. A series of metallocene poly(propylenes) with a random distribution of defects crystallized from the isotropic melt enabled the effects of both molecular mass and defects on the formation of these polymorphs to be systematically investigated. While molecular mass (in a range of 40 000−300 000

* Corresponding author: e-mail alamo@eng.fsu.edu.
† Florida Agricultural and Mechanical University and Florida State University.
‡ Florida State University.
§ Present address: Universidad de Navarra. Dpto. De Química y Edafología. C/ Irunlarrea s/n 31080 Pamplona, Spain.

10.1021/ma030157m CCC: $25.00
Published on Web 07/04/2003

g/mol) has only a minor effect on the formation of the γ polymorph, the concentration of defects has a major effect, increasing the content of this polymorph.[27] The γ phase is also favored with increasing crystallization temperature (T_{cryst}) up to a point where the kinetics of the crystallization of this phase, based on structural requirements, become very slow, and this leads to a local maximum in the γ content. It was found that the T_{cryst} at which the maximum content of γ phase is obtained increases from 120 to 150 °C for defect content decreasing from 4.4 to 0.41 mol %, respectively.[27] Local maxima were confirmed in subsequent works with similar metallocene type homo-poly(propylenes).[30,31] The presence of the maxima suggests that two competing factors affect the formation of this polymorph. On one hand, packing energy calculations suggest that the γ form would be slightly more stable than the α phase.[38] Hence, it is favored over the α phase with increasing temperature. On the other hand, defects, and therefore short isotactic sequences, favor the γ polymorph. However, the concentration of short sequences available for crystallization decreases with increasing T_{cryst}. The result is a maximum in the concentration of the γ form with T_{cryst}. Stereo (mrrm) and regio defects predominantly of the head-to-head type were found to lead to the same content of γ phase.[27,30]

Polypropylenes produced with a ZN-type catalyst have a broad distribution of defects from chain to chain and a distribution of defects intramolecularly that deviates strongly from the random behavior. The defects are more concentrated in the molecules with the lowest molar mass.[36] Since the presence of short isotactic sequences is a requirement for the formation of the γ polymorph, it is not surprising that ZN poly(propylenes), homopolymers, or copolymers, unfractionated or fractions, lead to insignificant[17,19,27,30,39,40] or much lower contents of crystallites of the γ form than those synthesized with a metallocene catalyst with the same overall concentration of defects.

Central to the present study is to investigate if the irregularity conferred by the comonomer to the polypropylene chain affects the formation of the γ polymorph in a manner akin to that given by stereo and regio defects and to what extent the type of comonomer influences the crystallographic polymorphs. Crystallographic, thermodynamic, and structural studies of propylene copolymers have been carried out previously in broad copolymers of the Ziegler–Natta type[21,22] or on fractions obtained from heterogeneous propylene–ethylene[23–25] and propylene–1-hexene copolymers.[17] Only a few reports on crystallization, melting, and some physical properties of metallocene-type propylene copolymers are available.[5–12] It is also difficult to extract from these works the effect of the comonomer type on properties because different catalysts were used in each study. Different catalysts may lead to significantly different concentrations of stereo and regio types of defects, which were not determined in these previous studies and may affect in different degrees the formation of the polymorphs.

This work presents a systematic study of the effect of type and concentration of comonomer on the formation of the α and γ polymorph of series of metallocene-type random propylene copolymers synthesized with the same type of catalyst. This ensures uniformity in the content and distribution of stereo and regio defects, which are also present in the chain and are known to affect the ratio of the crystallographic polymorphs, in addition to the comonomer effect. Two structural variables are studied independently of each other, comonomer content (up to ~10 mol %) and type of comonomer including ethylene, 1-butene, 1-hexene, and 1-octene under rapid and isothermal crystallization. The role of the "punctual" defects found in the homopolymer vs comonomer units, in the formation of the γ polymorph, is evaluated from an analysis of the experimental data. These fundamental studies serve as background properties that can be used in ascertaining the degree to which any other propylene copolymer deviates from the random behavior. For example, in two recent studies, the concentration of the γ polymorph was used as an indirect measure to determine the stereoblock character of polypropylenes catalyzed with ZN[39] and with unbridged metallocene systems.[41]

Studies of the crystalline regions by solid-state ^{13}C NMR of the same copolymers have shown direct evidence of the inclusion of ethylene and 1-butene units in this region.[10,11] These results were recently confirmed by acid etching followed by solution NMR.[7] Moreover, similar spectra of propylene-1–hexene and propylene–1-octene copolymers showed no evidence of inclusion in the crystal of butyl and longer branches.[42] The crystallographic parameters measured by Turner-Jones[14] and more recently by Marega et al.[20] also suggest that a significant proportion of 1-butene can be incorporated into the crystal lattice. As will be shown in this and forthcoming works, the differences in comonomer partitioning between the crystalline and noncrystalline regions are reflected in the concentration of the γ polymorph and the spherulitic lamellar morphology developed by these copolymers.

Experimental Section

Materials. The copolymers studied are experimental samples obtained with a bridged Exxpol metallocene catalyst.[1,2] Their molecular characterization is given in Table 1. The designation encodes the type of comonomer and the total defect content. Also listed in the table is a homopolymer (M170K1.70) synthesized with the same catalyst under the same experimental conditions. This sample, previously studied,[27] is included to ascertain the effect of stereo and regio irregularities in the formation of the γ polymorph independent from the comonomer effect. The molecular mass and concentration of stereo- and regio-type defects are very similar for all the copolymers studied and can be considered constants. Properties within the series can be analyzed as a function of comonomer concentration and type as the only variables. Listed in separate columns in Table 1 are molar concentrations of the comonomer, head-to-head misinsertions of the erythro type and concentration of stereo defects. Defects caused by hydrogen abstraction (1,3 type) were absent in these samples. The total concentration of all types of defects added to the concentration of comonomer is also listed in this table. The analysis of experimental data throughout the text is referred to this value.

A range of comonomer content was available in both the ethylene and 1-hexene series, which allows a systematic study of the effect of increasing comonomer, for fixed stereo and regio defects, on the formation of the crystallographic polymorphs. In addition, propylene copolymers with ethylene, 1-butene, 1-hexene, or 1-octene as comonomer are available containing approximately 3.3 mol % total defects. Data from this series allowed the study of the effect of comonomer type on the properties of these copolymers. The molecular mass and its distribution were determined by standard gel permeation chromatography.[43] Calibration was performed with polystyrene standards. The type and fractional content of all the defects was obtained from the solution-state ^{13}C NMR spectra.[44–47]

Table 1. Molecular Characterization of Metallocene Homopolymer and Metallocene Propylene Copolymers

sample	comonomer type	comonomer (mol %)	regio (mol %)	stereo (mol %)	total defects (mol %)	M_w (g/mol)	M_w/M_n
M170K1.70		0.0	0.8	0.9	1.7	169 800	1.80
PE1.8	ethylene	0.8	0.4	0.6	1.8	233 100	1.98
PE2.8	ethylene	1.7	0.4	0.7	2.8	221 300	1.81
PE3.3	ethylene	2.1	0.5	0.7	3.3	210 000	1.77
PE3.4	ethylene	2.2	0.5	0.7	3.4	214 800	1.75
PE5.8	ethylene	4.6	0.4	0.8	5.8	251 000	2.12
PE8.2	ethylene	7.0	0.5	0.7	8.2	185 300	1.86
PE8.7	ethylene	7.5	0.4	0.8	8.7	188 000	1.71
PB3.4	1-butene	1.7	0.8	0.9	3.4	216 500	1.70
PB4.8	1-butene	3.2	0.7	0.9	4.8	~210 000	1.85
PH2.0	1-hexene	0.3	0.7	1.0	2.0	245 000	1.83
PH2.2	1-hexene	0.6	0.7	0.9	2.2	~230 000	
PH3.2	1-hexene	1.6	0.7	0.9	3.2	~210 000	
PH3.5	1-hexene	1.8	0.7	1.0	3.5	206 800	1.71
PH4.3	1-hexene	2.7	0.7	0.9	4.3	217 000	2.53
PO2.9	1-octene	1.3	0.7	0.9	2.9	202 300	1.76

Crystallization Procedures. All samples were either isothermally crystallized from the melt at temperatures between 60 and 138 °C or quenched from the melt directly into tap water at 25 ± 1 °C. The following crystallization times at the isothermal temperatures were used: T_c = 100 °C (24 h), T_c = 110 °C (3 days), T_c = 120 °C (1 week), T_c = 125 °C (2 weeks), T_c = 130 °C (3–4 weeks), T_c = 138 °C (> 4 weeks). These times were sufficiently long so that all but the highest defect content copolymers crystallized to completion. Complete extent of transformation was verified by the absence of a low-temperature melting peak corresponding to crystallites formed subsequently on quenching.

Plaques approximately 20 mm long, 13 mm wide, and 0.5 mm thick were initially sandwiched between thin aluminum plates and molded in a laboratory Carver press. All isothermal crystallizations were carried out in two oil baths, one held at 180 °C (±1 °C) for melting the specimens (20 min) and the other at the required crystallization temperature. The typical accuracy of the crystallization bath was better than ±0.2 °C. To prevent degradation and contamination of the samples with the silicone oil used in the baths, melting and crystallizations were carried out in evacuated glass tubes, which were suspended in the oil baths. Following crystallization the tubes were quenched in tap water and the samples removed when the temperature reached ambient conditions. Selected samples were melted in the press between aluminum foils to provide a seal and then inserted directly into the oil bath for crystallization. Following crystallization, these samples were quenched in tap water and then washed in a strong detergent solution to remove the silicone oil prior to their removal from the mold. No discrepancies were observed in the melting behavior between the two methods of crystallization.

Wide-Angle X-ray Scattering (WAXS). Room temperature WAXS diffractograms were obtained using a slit collimated Siemens D-500 diffractometer in a 2θ range between 5° and 45° with a step size of 0.02°. The instrument was calibrated for d spacing with a standard polished piece of polycrystalline quartz, and the film thickness was offset using shims. Filtered Cu Kα radiation was used as source. Diffraction patterns obtained above room temperature were recorded using a Siemens D500 $\theta-\theta$ diffractometer with an attached Anton Paar HTK high-temperature head. Temperature calibration was carried out with benzil (diphenylethanedione, mp 95 °C). Both diffractometers operated at 30 mA and 40 kV.

Peak assignments for the γ and α phases followed previous designations by Brückner and Meille[34] and Turner-Jones.[48] The fraction of crystals in the γ polymorph was obtained following the method of Turner-Jones[14] from the height of the (117) reflection at 2θ = 20.1°, characteristic of the γ form, and the (130) reflection at 2θ = 18.8°, typical of the α polymorph,[27] as Hγ/(Hγ + Hα).

Differential Scanning Calorimetry. Melting and crystallization behavior were followed using a Perkin-Elmer differential scanning calorimeter DSC-7 under nitrogen flow. Melting was carried out at a scanning rate of 10 K/min. When dual endotherms were present, the peaks were manually deconvoluted and the areas correlated with the γ and α polymorphs. Temperature calibration was carried out with indium as a standard.

The crystallization kinetics of each polymorph was followed by the variation of the heat of melting of the γ and α peaks with crystallization time. Each sample was initially melted at 180 °C for 3 min and cooled at 40 K/min to the required crystallization temperature. After the required crystallization time had elapsed, the specimens were melted at 10 K/min, starting from the crystallization temperature. This procedure was used to avoid any additional contributions of crystallites that may be formed during cooling or quenching the samples prior to scanning. A sequence of increasing times and temperatures was used for each material, up to a maximum crystallization time determined by that required for no further increase in melting enthalpy.

Results and Discussion

Polymorphs and Melting Behavior. Isotactic poly(propylenes) crystallized in a mixture of the γ and α phases usually melt in two peaks; the lower melting peak is associated with the γ form and the higher with the α.[27,30,49] Both α and γ polymorphs have characteristic WAXS reflections, and it was shown that those corresponding to the γ form disappear in the diffractograms obtained at temperatures between both endotherms, whereas only reflections of the α form are generally present at temperatures at the peak of the highest melting endotherm.[27,30] Thus, the content of each phase can be obtained either from X-ray diffractograms or from the thermal data. Previous works in homo-poly(propylenes) have established a good correspondence between the content of the γ polymorph obtained by WAXS and the content calculated from differential scanning calorimetry by deconvolution of the melting peaks.[27,30,49] The same features are observed in the copolymers studied in this work.

The homopolymer and all the copolymers listed in Table 1 yielded either broad endotherms (for quenched materials) or double melting when isothermally crystallized. One example is shown in Figure 1a for PE1.8 crystallized at 120 °C. At this temperature the copolymer develops 55% of crystallites in the γ polymorph. Correspondingly, two well-defined endotherms with very similar heat of fusion are observed. As discussed in other works,[30] crystallites formed isothermally do not reorganize to any significant extent on heating, and both meltings are associated with two types of crystallites with different thermal behavior. Figure 1b shows WAXS diffractograms of the same sample obtained at temper-

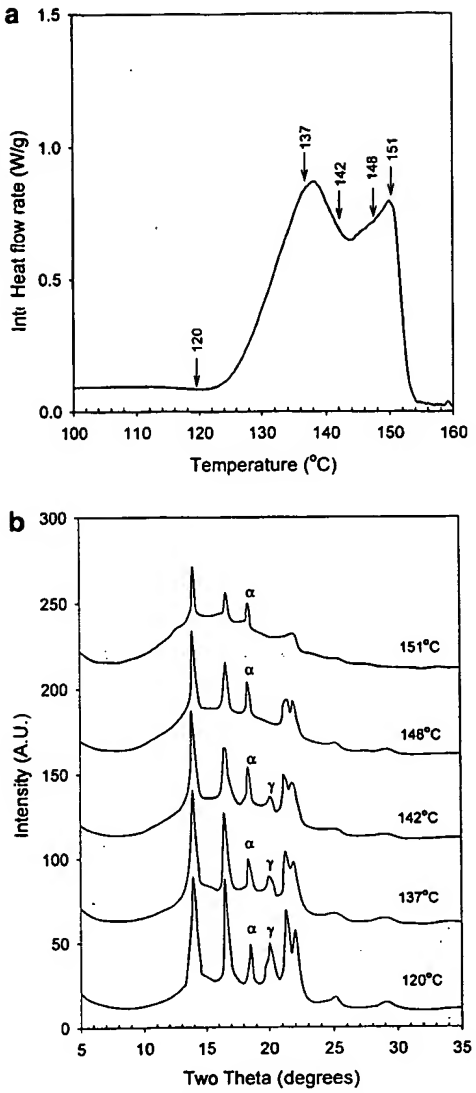

Figure 1. (a) DSC melting of sample PE1.8 crystallized at 120 °C. (b) Diffractograms taken at the temperatures indicated by the arrows in the thermogram. Reflections corresponding to the α and γ polymorphs are indicated.

atures indicated by the arrows in the thermogram of Figure 1a. There are no significant differences between the WAXS pattern obtained at room temperature and the pattern obtained at 120 °C, i.e., before any significant melting occurs. The content of γ phase up to this temperature is 55%, the same as that measured at room temperature. As the temperature is raised to 137 °C, near the peak of the lowest endotherm, the 117 reflection (2θ = 20.1 °C) characteristic of the γ polymorph starts to decrease while the reflection corresponding to the α phase (2θ = 18.8 °C) remains unchanged. Clearly only γ crystallites are melting in this temperature range. At 142 °C, a temperature between both endotherms, the γ peak is still observed albeit with low intensity and disappears at 148 °C, just below the highest temperature endotherm peak. It is therefore evident that, in agreement with the behavior of the homopolymer, the crystallites formed in the α and γ polymorphs from the copolymer melt at significantly different temperatures. The low melting endotherm is associated with melting of γ crystallites, and the high

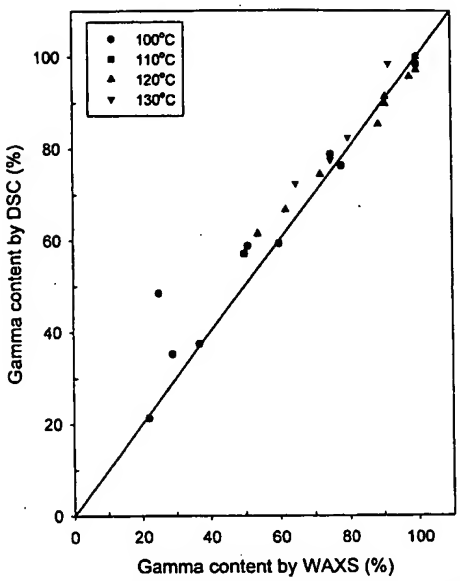

Figure 2. Content of γ phase calculated by DSC against γ phase obtained from WAXS. Solid line corresponds to line of slope one.

temperature corresponds to the α polymorph. As seen in Figure 1b, at temperatures just above the high-temperature melting peak (151 °C), only a small content of α crystallites remained unmelted. Thus, in addition to determining the γ content of the copolymers by WAXS, the fraction of this polymorph was also obtained from the DSC endotherms after peak deconvolution and analysis of the area of both peaks. The data from both methods are compared in Figure 2. A good correlation between the WAXS and DSC data was obtained for the homopolymer and copolymers crystallized in a range of temperatures between 100 and 130 °C, as seen by their proximity to the straight line with slope one drawn in the figure. The data for quenched samples is not included because the γ content in most of these samples was negligible, and the small crystallites formed on quenching reorganize to some extent during melting.[50] In addition, lower temperature maxima of copolymers with < 40% γ are poorly defined, leading to a greater scattering of the data in this region.

γ Content as a Function of Crystallization Temperature and Concentration of Comonomer. The effect of increasing comonomer concentration on the formation of the γ polymorph was studied in the series of propylene–ethylene and propylene–1-hexene copolymers crystallized in a range of temperatures between 25 and 138 °C. Representative diffractograms and meltings after isothermal crystallization in the temperature range between 25 and 120 °C are given in Figure 3a,b for PE2.8 and in Figure 4a,b for PH3.5. All the copolymers develop γ phase whose content increases with crystallization temperature. At the highest crystallization temperatures, propylene copolymers with total defect content higher than ~3 mol % crystallize almost exclusively in the γ form, as shown in the WAXS patterns of PH3.5 crystallized at temperatures ≥120 °C. In this diffractogram the α reflection is negligible. For a constant crystallization temperature the concentration of the γ polymorph increases with increasing comonomer concentration. Rapid crystallization at 25 °C of all the copolymers, except the ones with the highest defect contents, led to the formation of α crystallites. Under

these quenching conditions propylene copolymers with ~7 mol % ethylene develop 34% of the crystallinity in the γ phase. The smectic phase, which develops under rapid quenching in films whose thicknesses are less than about 25 μm,[27] did not form in the thicker films used in the present study. Slower heat transfer in these films led to primarily α crystallites even after rapid crystallizations. As the temperature is raised above 50 °C, the reflection at 20.1° corresponding to the γ phase begins to develop and increases with temperature in any copolymer at the expense of the α.

The relative changes in the low- and high-temperature endotherms with increasing crystallization temperature (Figures 3b and 4b) parallel the changes in the WAXS reflections associated with the α and γ phases. As the concentration of the γ phase increases with increasing temperature, the magnitude of the low-temperature endotherm also increases at the expense of the high-temperature one. This feature is general for any of the copolymers in each series as shown in the examples provided in Figures 3b and 4b. The good correlation between the double melting and the content of each polymorph is indicated by the proximity of the experimental data to the straight line with a slope of one in Figure 2. All copolymers melt over a broad temperature range; this feature is characteristic of semicrystalline random copolymers in which the concentration of the counit is not uniform between the crystalline and noncrystalline regions and follows from basic thermodynamic equilibrium theory.[51] During melting the defect concentration in the melt decreases, and the remaining crystals melt at increasingly higher temperatures. Hence, the observed broad melting of the propylene copolymers in Figures 3b and 4b is a natural consequence of their copolymeric nature.

The variation of the γ content with temperature is given in Figure 5 for the propylene–ethylene series and in Figure 6 for propylene–1-hexenes. In Figure 5 data for PE8.2 have been removed for clarity and because its behavior is identical to that of PE8.7 (shown). Both series display similar behavior. Up to ~130 °C the content of γ phase increases rapidly with temperature in any copolymer. At a fixed crystallization temperature the content of γ phase increases with increasing total defect content. It reaches values close to 100% at the highest concentration of defects even for relatively low crystallization temperatures, as seen by the data of PE8.7 crystallized at 100 °C. The form of these figures is very similar to that adopted for homo-poly(propylenes) with increasing concentration of stereo and regio defects.[27,30] A local maximum in the content of γ phase with temperature is also observed for the propylene–ethylene copolymer with the lowest defect content. Before describing the maximum in more detail and its implications on the mechanism of formation of the γ polymorph, experiments were carried out to ensure that the data plotted in Figures 5 and 6 correspond to the concentration of the γ polymorph developed at the crystallization temperature. In the high-temperature range the crystallization rate is slow, and the copolymers developed additional crystallinity when transferred to room temperature. Therefore, it is important to determine the crystal form of the quenched crystallites for a correct determination of the concentration of the γ polymorph. As also found in homopolymers, WAXS experiments indicated that the copolymer crystallites formed on quenching, after high isothermal T_{cryst}, are

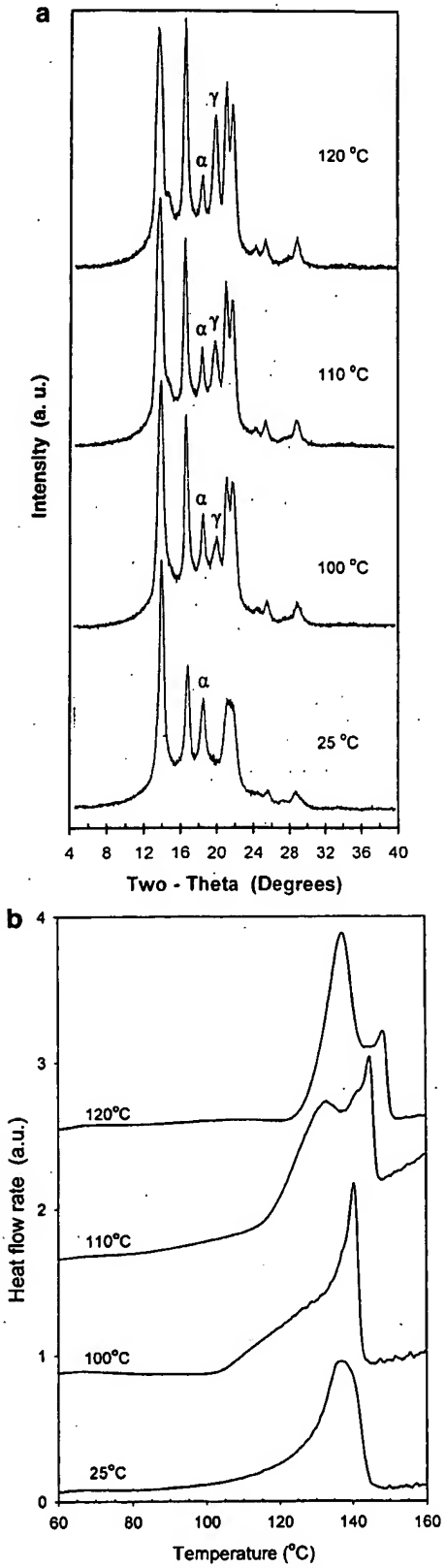

Figure 3. (a) Room temperature WAXS diffractograms and (b) DSC meltings of PE2.8 crystallized at the temperatures indicated.

of the γ phase, confirming the local maximum displayed in Figure 5. When a quenching peak was found in the

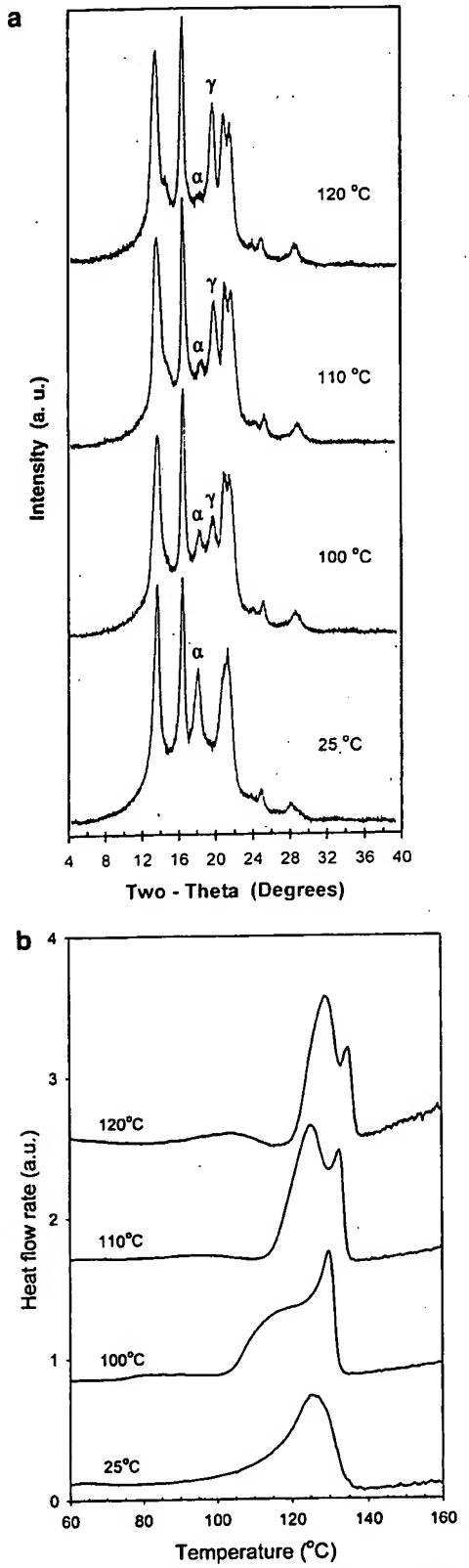

Figure 4. (a) Room temperature WAXS diffractograms and (b) DSC meltings of PH3.5 crystallized at the temperatures indicated.

melting data, its heat of fusion was used to correct the fractional content of γ calculated from WAXS. A maximum is not observed in the least defective propylene–1-hexene copolymer (2.0 mol %) or in any of the other copolymers analyzed here due to the unduly long crystallization kinetics at temperatures above 130 °C and depletion of long crystallizable sequences that form the α phase. This aspect will be analyzed in more detail in the Kinetics section.

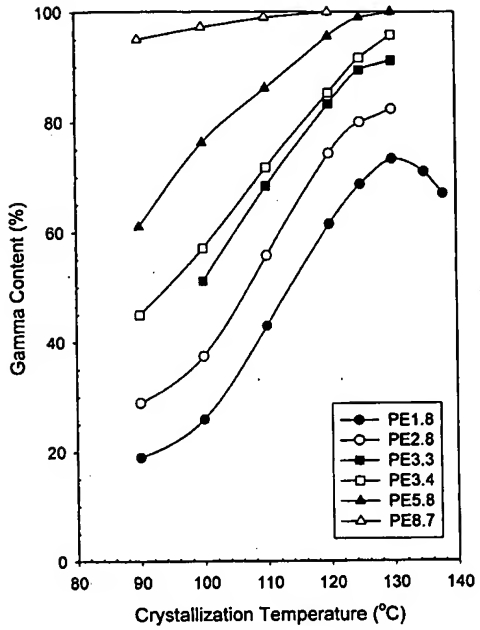

Figure 5. Percentage of γ phase as a function of crystallization temperature for propylene–ethylene copolymers with ethylene content increasing from 0.8 to 7.5 mol %.

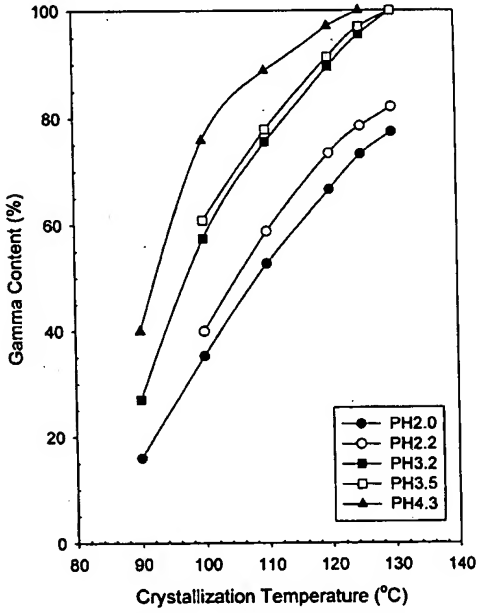

Figure 6. Percentage of γ phase as a function of crystallization temperature for propylene–1-hexene copolymers with 1-hexene content increasing from 0.3 to 2.7 mol %.

The similarity of behavior between homopolymers and copolymers when the comonomer is added as an additional structural irregularity in the iPP chain, suggests that the mechanism of formation of the γ polymorph in the homo-poly(propylene) is also operative for

its random copolymers. The requirements for the formation of this polymorph were described in detail in our previous work.[27] They involve the need of molecules with short or relatively short crystallizable sequences, such as those with randomly distributed structural irregularities (comonomers and other types of defects), and a structure in the crystal–amorphous interfacial region that prevents folding and requires tilted ordered chains to propagate a lamellar crystallite. While the formation of the γ phase is favored with increasing T_{cryst}, the number of short crystallizable sequences is depleted at the highest T_{cryst}, leading to the observed local maximum as a function of temperature. Regarding the formation of the γ phase, the data of Figures 5 and 6 suggest that the comonomer acts as any other defect would in the poly(propylene) chain.

A more detailed analysis of Figures 5 and 6 reveals that, for any given total defect content, the propylene–1-hexene series develop a concentration of the γ phase about 10% higher than their propylene–ethylene analogues. This point will be discussed in the next section where four different comonomers are analyzed for the same total defect concentration.

γ Content as a Function of Comonomer Type. Diffractograms and melting thermograms for propylene–ethylene (PE3.4), propylene–1-butene (PB3.4), propylene–1-hexene (PH3.5), and propylene–1-octene (PO2.9), all with ~3.3 mol % total defects and crystallized at 120 °C, are given in parts a and b of Figure 7, respectively. Both WAXS patterns and melting behavior show significant differences between the four copolymers. The 1-butene units lead to a more prominent reflection and melting peak corresponding to the α phase, followed by the ethylene units and then by the 1-hexene and 1-octene units. The ability of crystallization of each copolymer type in the γ form is evaluated in Figure 8, where the content of this polymorph is plotted as a function of T_{cryst} for the four copolymers. As expected from the reasonably high defect content, these copolymers developed a content of γ phase in excess of 50% in the range of T_{cryst} between 100 and 130 °C. The data for propylene–1-hexene and propylene–1-octene share a common curve and have the highest concentration of γ phase with values changing from ~60% to 100% with increasing T_{cryst}. Propylene–ethylene develops slightly lower contents of γ phase at most temperatures. Propylene–1-butene is the copolymer with the lowest concentration of γ phase at any temperature; the values change from ~45% to 80% in the same T_{cryst} range.

Differences in the content of γ phase for homo-poly(propylenes) with the same average concentration of defects were attributed to differences in the intramolecular distribution of defects.[39,41] A more blocky distribution of defects leads to significantly lower contents of this polymorph. This, however, is not the case for the copolymers studied. The use of the same type of metallocene catalyst led to the same random distribution in the comonomer and same content of regio and stereo defects.[2,39] The concentration of diads or triads of the comonomer, calculated from the solution ^{13}C NMR spectra of these copolymers, was very close to the predicted Bernoullian distribution.[52] Differences in the observed concentration of the γ phase at any T_{cryst} are consistent with a different ability of cocrystallization of each type of comonomer with the propylene units.

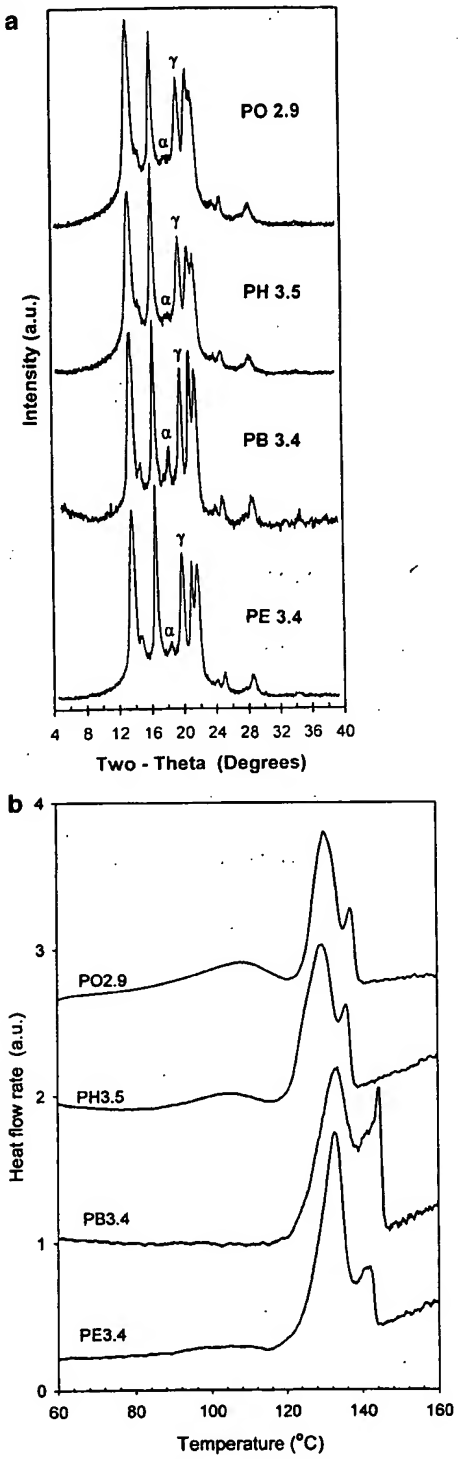

Figure 7. (a) Room temperature WAXS diffractograms and (b) DSC meltings of propylene–ethylene (PE3.4), propylene–1-butene (PB3.4), propylene–1-hexene (PH3.5), and propylene–1-octene (PO2.9) crystallized at 120 °C. All copolymers with ~3.3 mol % defects.

It was shown by direct analysis of the crystalline regions by solid-state ^{13}C NMR of the same copolymers that ethylene and 1-butene units are partially included in the crystalline phase. However, spectra of the crystalline regions of propylene–1-hexenes and propylene–1-octenes showed no evidence of resonances associated with the methyl or methylene groups of the branch of

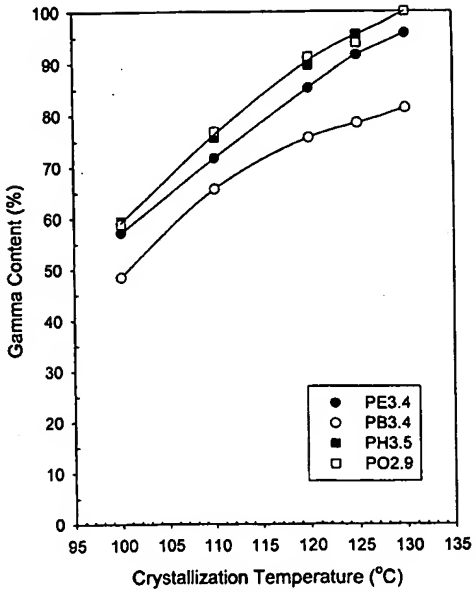

Figure 8. Percentage of γ phase as a function of crystallization temperature for propylene copolymers with ~3.3 mol % defects.

these comonomers.[10,11,42] At the same average concentration of comonomer in the chain, the concentration of 1-butene units in the crystalline regions, calculated from the NMR data, was higher than the concentration of ethylene units. The data suggest that the 1-butene units are better incorporated into the poly(propylene) lattice than the smaller ethylene units. This difference in partitioning of the counits also explains the melting behavior. As recently reported[7] and shown in Figure 7b, propylene–1-butene has the highest final melting temperature followed by propylene–ethylene. Copolymers with 1-hexene and 1-octene units show negligible melting differences. With a higher probability of 1-butene units to enter the crystalline lattice, the average crystallizable sequence length in this copolymer is longer than in the propylene–1-hexene or propylene–1-octene chains and may account for the observed higher melting temperature.

The results of Figure 7 are also consistent with the differences in partitioning of the counit (ethylene, 1-butene, 1-hexene, or 1-octene) between the crystalline and noncrystalline regions, in regards to chain structural requirements to form the γ polymorph. Described in previous works in homopolymers[27] was the premise that short sequences of crystallizable units favor the formation of this polymorph. At the same total concentration of defects, the average crystallizable sequence length of propylene–1-hexenes and propylene–1-octenes is shorter than for propylene–ethylenes and propylene–1-butenes; hence, higher contents of the γ polymorph are predicted in the former copolymers. The experimental data from Figures 5, 6, and 8 follow these predictions. They suggest that the concentration of the γ polymorph developed by a given propylene copolymer could be used as a qualitative assessment of the degree of partitioning of the comonomer unit upon crystallization. The higher the concentration of the γ phase, the more excluded the comonomer unit is from the crystalline lattice. Note that the last statement only applies to a series of copolymers with the same content of stereo and regio defects and the same content and distribution of comonomer units.

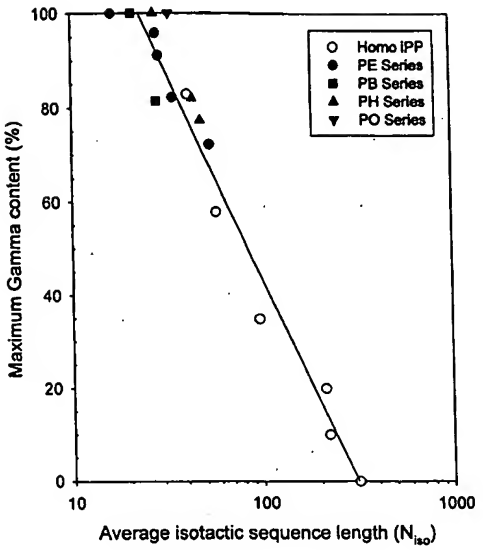

Figure 9. Maximum percentage of γ phase as a function of the average length of isotactic sequences. Open circles are data for homopolymers from ref 27.

The average length of isotactic sequences, N_{iso} (calculated as $1/\Sigma$fractional content of all defects), was found to scale with the maximum fractional content of the γ polymorph developed in homo-poly(propylenes).[27] The maximum fraction of the γ polymorph obtained for all copolymers at the optimum temperature (or at the highest temperature at which crystallization was experimentally feasible) is plotted against N_{iso} in Figure 9. Following suggestions by De Rosa et al.,[41] a semilogarithmic plot is presented. The open symbols are data previously reported for homopolymers obtained with a metallocene catalyst,[27] and the continuous line is a linear regression over these data. The data for propylene–ethylenes fall on the homopolymer line while the γ content of the two propylene–1-butenes is shifted to lower values. To develop the same 80% of γ crystallites requires a higher concentration of 1-butene than of ethylene or than a combined stereo (of the mrrm type) and 2,1 regio defects in a homopolymer. The data for propylene–1-octene and propylene–1-hexene (closed triangles in the figure) are slightly shifted to the right of the homopolymer reference line, in agreement with an enhanced ability to crystallize in the γ form. We find from this figure that average sequence lengths of 33 units would yield pure γ crystallites in propylene–1-hexene and propylene–1-octene copolymers while this number is reduced to 25 for homopolymers and propylene–ethylenes and to ~20 for propylene–1-butene copolymers.

A subject of interest concerning defects, such as isolated rr triads, regio 2,1 erythro defects, and ethyl and 1-butene comonomers, all found to enter the crystalline lattice at different levels,[7,10,11,42,53] is the possibility of a preferential partitioning of these defects in one of the polymorphs. In this context it was recently suggested that isolated rr triads are more easily accommodated in the γ than in the α crystallites.[30] In this latter work the diffractogram of homo-poly(propylenes) that crystallize in a mixture of the α and γ polymorphs was modeled by mixtures of a purely α diffraction pattern and a disordered γ pattern. The assumption of equal thickness for α and γ crystallites was made. The degree of disorder needed to account for the experimen-

tal pattern was found to increase with decreasing T_{cryst}, and it was associated with the experimental lower melting temperatures and broader endotherms of the γ crystallites formed at progressively lower T_{cryst}. Following this model of α/γ structural disorder, the conclusion was made that stereo mrrm defects are preferentially included in the γ polymorph while the α phase remains basically free of defects. While the presence of α/γ structural disorder of the type described by Auriemma et al.[30] may be found to some extent in poly(propylene) crystallites, the correlation with a preferential segregation of these mrrm stereo and possibly other "punctual" defects in the γ crystallites is not supported by previous NMR observations or by the data from the present work. For example, a homo-poly(propylene) with only stereo defects (predominantly of the mrrm type) that was slowly cooled or isothermally crystallized led to pure α crystallites.[53] However, analysis of the ^{13}C NMR spectrum of the crystalline regions indicated that a fraction of the stereo defects were included in the α crystallites. In an additional experiment, copolymer PE3.4 crystallized at 1 °C/min developed ~40% of the γ phase and negligible contents after rapid cooling in air. Solid-state NMR analysis gave the same concentration of ethylene units in the crystal in both samples.[10] If the defects were preferentially segregated to the γ form as speculated by Auriemma et al.,[30] poly(propylenes) crystallized in the α phase would have shown insignificant fractions or an absence of resonances associated with these types of defects in the spectra corresponding to the crystalline phase. It is, thus, concluded that the defects, stereo, regio, or ethylene units, must enter both polymorphs with roughly the same probability. Lower meltings of γ crystals are observed whether or not the chain structural irregularities enter the crystalline lattice, suggesting that γ crystals are thinner than α and not necessarily more defected.

The content of the γ phase developed by a homopolymer and two of the copolymers all with approximately the same total defect content (~1.8 mol %) is plotted against T_{cryst} in Figure 10. The γ contents of the homopolymer, M170K1.70 in Table 1, are extracted from the previous work,[27] and the data of the copolymers correspond to PE1.8 and PH2.0. Up to temperatures of ~130 °C, the homopolymer with defects of the stereo (mrrm) and regio (2,1) type and the propylene–ethylene copolymer with about half of the total defect content as ethylene units develop very similar concentrations of the γ polymorph. These data suggest a similar average defect partitioning in both polymers. The level at which ethylene units enter the crystalline lattice was found to be very similar to the average level at which stereo and regio defects enter the crystal;[54] hence, a similar behavior of these units is expected with regards to the formation of the γ polymorph.

At the highest T_{cryst}, the propylene–ethylene copolymer develops higher contents of the γ phase and shows significantly reduced crystallization rates than the homopolymer. For example, while complete crystallization of the homopolymer at 135 °C took ~24 h, it required over 2 weeks in the propylene–ethylene copolymer. These data suggest differences in the rate of partitioning of the ethylene and stereo groups as a function of T_{cryst}. Following the experimental data of Figure 10, one could predict slower kinetics for the accommodation in the crystalline regions of the ethylene units than those required to accommodate the stereo

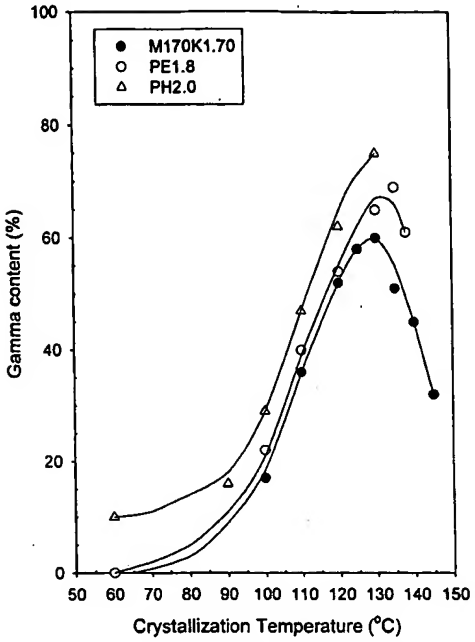

Figure 10. Percentage of γ phase as a function of isothermal crystallization temperature for homo-poly(propylene), propylene–ethylene PE1.8, and propylene–1-hexene PH2.0. The total concentration of defects is about the same in the three polymers.

defect groups. One consequence of a partitioning of stereo and ethylene units subject to thermal history would be a significant difference in crystallization rates, as observed between the homopolymer and the copolymer for T_{cryst} above 130 °C.

As seen in Figure 10, the content of γ phase developed by propylene–1-hexene is, in the whole range of T_{cryst}, ~10% higher than the data obtained in the homopolymer and propylene–ethylene copolymer with about the same concentration of defects. These results follow the pattern of the 3.3 mol % series shown in Figure 8 and reinforce the NMR results obtained in propylene–1-hexene copolymers, which were consistent with the rejection of this comonomer from the lattice.[42]

Previous extensive data in homopolymers and the present data in copolymers all reveal that the main structural requirement in the formation of the γ polymorph is the presence in the chain of short crystallizable sequences. Units that can cocrystallize with the propylene units increase the average length of crystallizable sequences and, thus, reduce the ability to develop the γ polymorph. The degree of cocrystallizability of stereo regio, ethylene, butene, hexene, and octene units with propylene, obtained by NMR is in excellent qualitative agreement with the fractions of the γ phase obtained in a series with a matched content of defects.

Kinetics of the Formation of the γ Polymorph in Random Propylene Copolymers. In this section we first describe the general features for the formation of the γ and α polymorphs with time. This leads to a universal behavior in homo-poly(propylenes) and their copolymers. An independent analysis of the effect of concentration and type of defect on the kinetics follows.

The development, with time, of the α and γ polymorphs of selected copolymers was followed by WAXS at fixed T_{cryst}. In addition, the heat of fusion of the low- and high-temperature endotherms was monitored as a

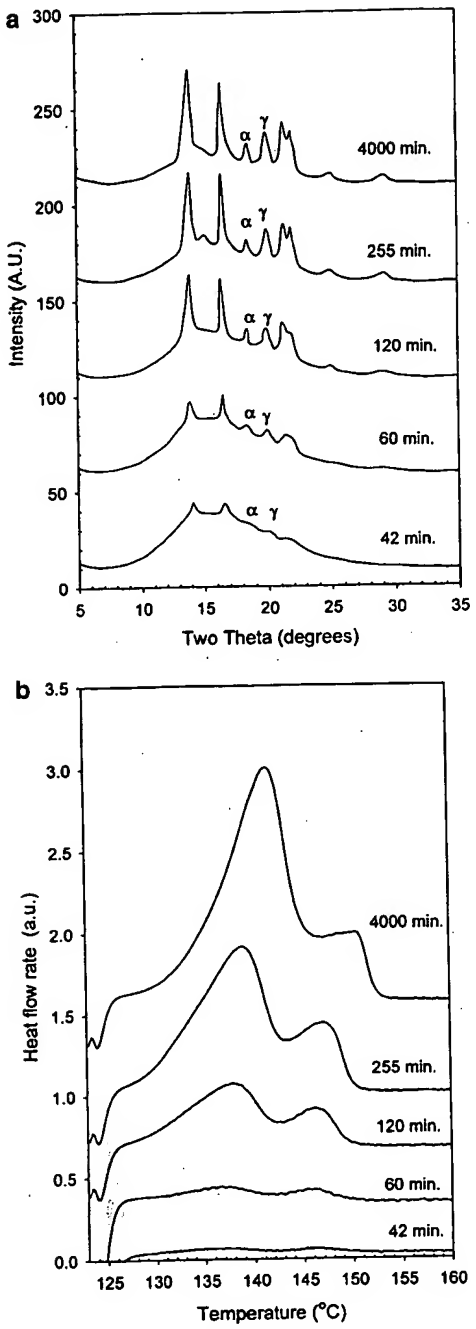

Figure 11. (a) WAXS diffractograms of PE2.8 obtained during crystallization at 123 °C at the times indicated. (b) DSC meltings started from the crystallization temperature.

function of crystallization time. Of interest is assessing whether the independent temporal development of the α and γ phases in copolymers follows that of the homopolymers.[27] If so, it would be suggestive of the same formation mechanisms.

Representative WAXS patterns of copolymer PE2.8 during crystallization at 123 °C are given in Figure 11a as a function of time. As was found during crystallization of homopolymers,[27,49] both polymorphs are observed at the very earliest detection of crystallinity. The (117)γ and (130)α reflections show the same increase in intensity during the initial 60 min of the crystallization. With further time the intensity of the α reflection remains constant while the γ reflection increases continuously. The relative variation of the intensities of both polymorphs depends on the specific copolymer and the crystallization temperature. However, the simultaneous appearance of both polymorphs in the initial stages of the crystallization is a common feature of the copolymers and homopolymers studied. Corresponding meltings are shown in Figure 11b, which corroborates the simultaneous formation of both polymorphs observed by WAXS. Two small endotherms with a similar area are obtained after crystallization for ~60 min. As crystallization proceeds, the area of the high-temperature melting, corresponding to the α phase, remains constant while the lower melting peak associated with the γ crystallites continues to increase. The sigmoidal variation of both endotherms with time is shown in Figure 12a for the same copolymer crystallized at T_{cryst} between 115 and 127 °C. These plots allow independent analysis of the development of both polymorphs. The α crystallinity quickly reaches a constant value that decreases with increasing T_{cryst}. On the other hand, the γ crystallinity continues to increase with time at any T_{cryst}. The highest value of the γ crystallinity first increases with T_{cryst}, reaches a maximum value, and then decreases with further increase in T_{cryst}.

The effect of increasing concentration of comonomer in the development of both polymorphs is shown in Figure 12b–d for three propylene–1-hexene copolymers. Independent of the type and concentration of comonomer, all of the copolymers display kinetics with similar characteristics. The development of both the α and γ polymorphs with time follows a sigmoidal function typical of the nucleation and growth processes in the crystallization of polymers. A large negative temperature coefficient of the crystallization, which is observed for all of the copolymers, is consistent with the importance of nucleation and, thus, undercooling to the crystallization process. At any fixed T_{cryst}, crystallization takes place at lower undercoolings with increasing concentration of 1-hexene. Thus, the crystallization kinetics become slower, and the range of T_{cryst} for experimental observation shifts to lower values, as is shown in Figure 12b–d. Data in Figure 12, and similar studies in homopolymers, make it evident that, independent of the type of defect in the poly(propylene) chain, the α and γ polymorphs appear simultaneously, suggesting that both have the same initial crystallization rates. Thus, WAXS and DSC kinetic data for the copolymers confirm that this behavior is universal for the crystallization of this polymorph in any type of homo-poly(propylene) or random propylene copolymer.

The kinetics of the combined heat of fusion of the α and γ peaks for copolymers with ~3.3 mol % of defects crystallized at 115 °C are given in Figure 13. These data allow evaluation of the effect of a different partitioning of the comonomer, between crystal and amorphous phases, on the crystallization rate at a fixed T_{cryst}. For example, to obtain an enthalpy of melting of 20 J/g, only 15 min of crystallization is needed for propylene–1-butene, while this time increases to 25 min for propylene–ethylene and to ~70 min for both propylene–1-hexene and propylene–1-octene. These times are directly related to the overall crystallization rates. They can be correlated with the NMR results that described the partitioning of the comonomer between the crystalline and amorphous phases. Comonomers that are excluded from the crystalline lattice, such as 1-hexene and 1-

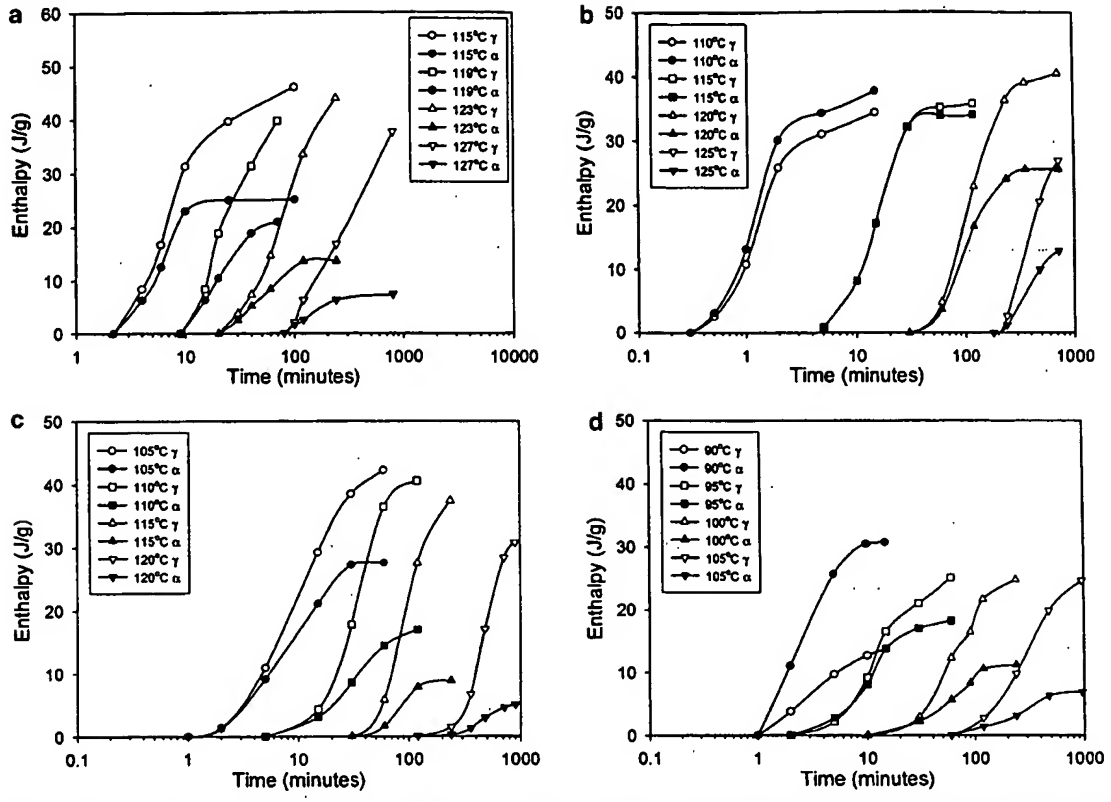

Figure 12. Sigmoidal development of α (filled symbols) and γ (open symbols) crystallinities with time at the indicated temperatures for the following copolymers: (a) PE2.8, (b) PH2.0, (c) PH3.5, and (d) PH4.3.

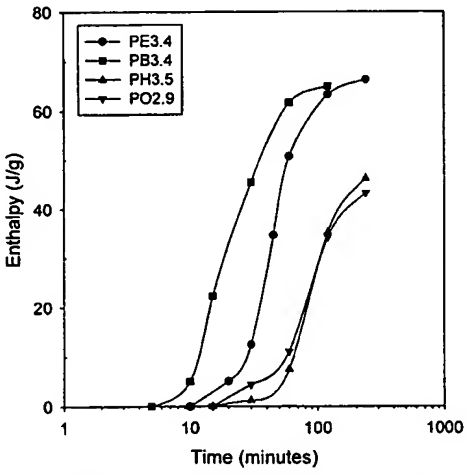

Figure 13. Sigmoidal variation of the total crystallinity for propylene–ethylene (PE3.4), propylene–1-butene (PB3.4), propylene–1-hexene (PH3.5), and propylene–1-octene (PO2.9) crystallized at 115 °C. All copolymers with ~3.3 mol % defects.

octene, have lower values for the sequence propagation probability of the crystallizable units, and, thus, slower crystallization than copolymers with counits that participate in the crystallization such as the 1-butene and ethylene groups. In the latter group the 1-butene copolymer crystallizes faster than the ethylene one, reflecting the greater partitioning of the 1-butene comonomer. Differences in crystallization rates affect the relative values of α and γ crystallinities and, thus, the observed fractional content of the γ form.

For any given copolymer with a total defect content higher than 2 mol % the concentration of γ phase increases systematically with increasing T_{cryst} (see data in Figures 5 and 6). Thus, it would be desirable to compare the crystallization kinetics of each copolymer crystallized at 115 °C in Figure 13, at constant undercooling and γ content. This can only be properly accomplished if the equilibrium melting temperature for each copolymer with 3.3 mol % defects is known. At the present time these values are unknown.

It is instructive to evaluate the total heat of fusion obtained at high levels of transformation, as well as the independent heat of fusion for the γ and α crystallites, with increasing crystallization temperatures as was done with the homopolymers.[27] Representative examples are given in Figure 14 for three propylene–ethylenes copolymers with increasing ethylene content. The series of propylene–1-hexenes, –1-butenes, and –1-octene copolymers display similar characteristics. The data of Figure 14 are for crystallites formed at the T_{cryst}; i.e., the melting was started at the T_{cryst} without previous cooling. Typical for crystallization of random copolymers, we find that the total heat of fusion decreases with increasing T_{cryst}. This result is a consequence of the decrease in the number of crystallizable sequences of sufficient length to form a stable crystallite with decreasing undercooling in any random copolymer.[55] At a fixed T_{cryst} the heat of fusion decreases with increasing concentration of comonomer and reflects the overall inhibition of the crystallization process imposed by the ethylene units despite their partial inclusion in the lattice. For example, based on a heat of fusion of the pure crystallite of 209 J/g,[56] crystallization at 130 °C leads to crystallinity levels of 43%, 24%, and ~2.5% as the concentration of ethylene increases from 0.8 to 4.6 mol % in Figure 14.

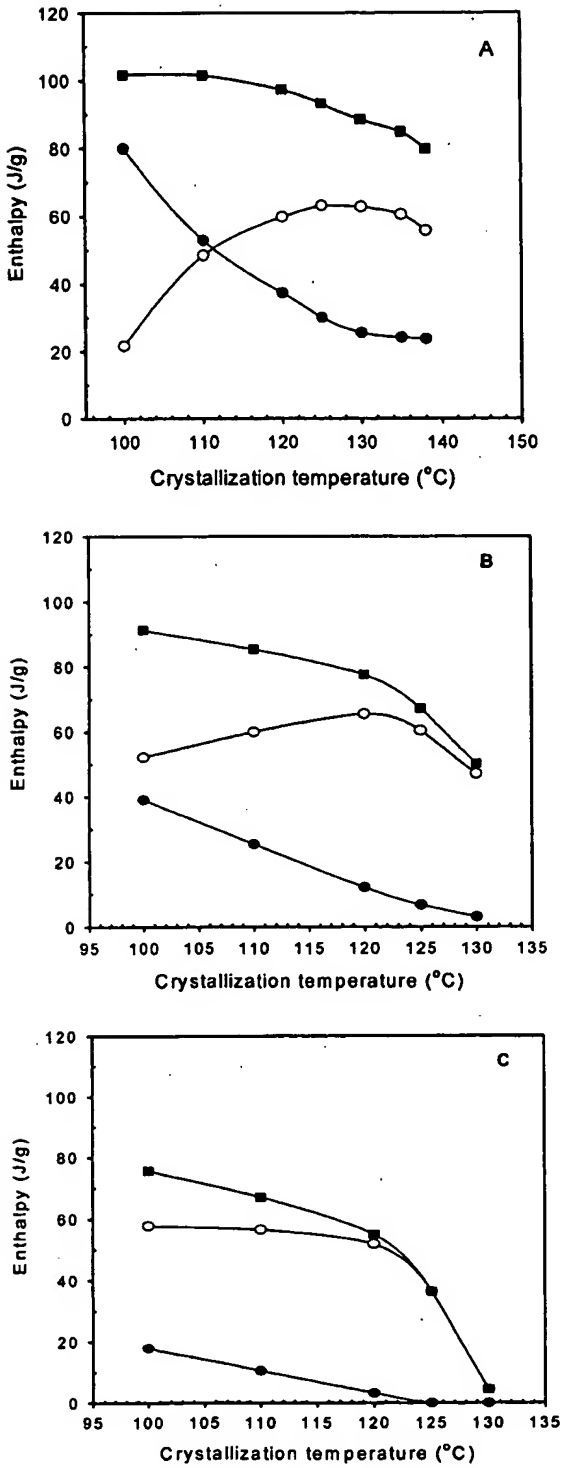

Figure 14. Variation of the independent heat of fusion of α (closed circles) and γ (open circles) crystallites, as well as the combined heat of fusion (closed squares), as a function of crystallization temperature for the following propylene copolymers: (A) PE1.8, (B) PE3.4, and (C) PE5.8.

The heat of fusion corresponding to the α crystallites decreases continuously with T_{cryst} following the expected trend for random copolymers. The heat of fusion of the γ crystallites first increases with temperature, reaches a maximum value, and then decreases with further increase in T_{cryst}. This behavior is universal for the crystallization of homo-poly(propylenes)[27] or for all random propylene copolymers. A maximum in γ crystallinity with T_{cryst} reflects that two competing mechanisms are involved in the formation of this polymorph. Hence, it is the relative variation in α and γ crystallinities with T_{cryst} which accounts for the observed maximum of the concentration of γ with T_{cryst} (Figure 5). For ethylene and (presumably) 1-butene copolymers with less than ~2 mol % defects, the relative fraction of the γ polymorph, calculated from heat of fusion, leads to a local maximum with temperature in agreement with the data of Figure 5. The maximum is not observed in propylene–1-hexenes with matched concentration of defects because of the slower kinetics. The temperatures at which α crystallites are no longer formed can be estimated from data such as those of Figure 14. These temperatures are experimentally attained at total defect concentrations >~3.5 mol % for propylene–ethylenes and at >~3 mol % for propylene–1-hexenes. For the copolymers studied they can be as low as 110 °C for the most defective propylene–ethylene (PE8.7) or above 130 °C. Crystallization at these and higher temperatures take place only in the γ polymorph.

Role of Structural Irregularities and Crystallization Kinetics in the Mechanism of Formation of the γ Polymorph. The experimental data of the formation of the γ polymorph in homopolymers were mechanistically reconciled from two major considerations:[27] (1) the partitioning by sequence length that isolated structural irregularities randomly introduced in a chain impose on the molecular structure[32,48] and (2) the role of very different crystal–amorphous interphases propagating either an α or γ type lamellar crystallite.[57]

Within any given series of copolymers of the same comonomer type, the fraction of γ polymorph that is obtained as a function of increasing comonomer content or increasing T_{cryst} follows an identical behavior to that observed by increasing defects in the homopolymer chain. The γ content increases with increasing the fractional content of any type of defects or comonomer as illustrated by the data in Figures 5 and 6. Thus, mechanistically, both homopolymers and copolymers follow the same initial requirement, the need of chains whose microstructure leads to thin crystallites, i.e., the presence of short crystallizable sequences in the chain.

The role of a different interface was reconciled with the experimental observation that the γ polymorph is favored in molecules with shorter average continuous isotactic sequences and at higher crystallization temperatures. It was suggested that the α polymorph is formed from the longest sequences through some type of folding while the molecular tilt, required to dissipate the ordered chain flux emanating from the crystalline regions, allows the propagation of γ crystallites from the short sequences without the need of folding.[27,32,34,57–59] This situation is a special case for polypropylene and of this particular polymorph because tilted chains in the unit cell represent a low-energy structure.

The maximum in the γ crystallinity with temperature is associated with two competing processes based on the availability of crystallizable sequences. The copolymer behavior sets a random sequence distribution, which combined with nucleation theory can be used to estimate the change in concentration of crystallizable sequences with T_{cryst} and mol % defects in the chain. This concentration is directly related to the isotactic sequence length required to form a nucleus of critical size, given

in Figure 17 of ref 27. At the lowest T_{cryst} the required length to form a stable nucleus (as primary step in the crystallization) is very small; thus, most crystallizable sequences may fold and lead to α crystallites. With increasing temperature, a larger number of crystallizable sequences approach in exact length the nucleation requirements. These sequences can crystallize in γ crystallites without folding. However, at higher temperatures the length requirements to form a stable crystallite become much higher. The availability of long sequences for crystallization is reduced; thus, the fraction of units that crystallize in the γ phase decreases at these high temperatures, in agreement with the experimental variation of the heat of fusion with temperature given in Figure 14.

Packing energy calculations suggested a slightly higher stability of the γ phase.[38] On this basis, one would have expected higher melting temperatures for γ crystallites. The observed melting points are, however, lower than those for the α phase, suggesting thinner γ crystallites, as also pointed out in a previous work.[58] As indicated earlier, the present experimental data do not suggest that a higher concentration of defects is included in the γ crystallites.

The formation of the γ phase in each series of random copolymers is adequately explained using the same qualitative arguments used in homopolymers with randomly distributed defects. However, when comparing the behavior for different comonomer types, important and systematic differences are identified in relation with differences in comonomer partitioning between the crystalline and noncrystalline regions. Propylene–1-butenes crystallize with lower concentrations of the γ polymorph than any of the other copolymers studied. This experimental observation confirms the NMR findings that the 1-butene units are included in the crystal at the highest level.[7,54] The 1-hexene and 1-octene units, rejected from the crystal, lead to the highest contents of the γ polymorph at any temperature. Qualitatively, the concentration of the γ polymorph gives a measure of the degree of incorporation of the comonomer in the crystalline regions of propylene random copolymers.

Acknowledgment. Funding of this work by the National Science Foundation, Grant DMR-0094485, is gratefully acknowledged. The assistance of Dr. J. Chatterjee and Mr. S. Doyle with collection of DSC data is also acknowledged.

References and Notes

(1) Kaminsky, W.; Hähnsen, H.; Külper, K.; Woldt, R. *US Patent* **1985**, *4*, 542, 199.
(2) Brintzinger, H. H.; Fischer, D.; Mülhaupt, R.; Rieger, B.; Waymouth, R. M. *Angew. Chem., Int. Ed. Engl.* **1995**, *34*, 1143.
(3) Busico, V.; Cipullo, R. *Prog. Polym. Sci.* **2001**, *26*, 443.
(4) Fink, G.; Mülhaupt, R.; Brintzinger, H. H. *Ziegler Catalysts: Recent Scientific Innovations and Technological Improvements*; Springer-Verlag: New York, 1995.
(5) Arnold, M.; Henschke, O.; Knorr, J. *Macromol. Chem. Phys.* **1996**, *197*, 563.
(6) Perez, E.; Zucchi, D.; Sacchi, M. C.; Forlini, F.; Bello, A. *Polymer* **1999**, *40*, 675.
(7) Hosoda, S.; Hori, H.; Yada, K.; Nakahara, S.; Tsuji, M. *Polymer* **2002**, *43*, 7451.
(8) Fujiyama, M.; Inata, H. J. *Appl. Polym. Sci.* **2002**, *85*, 1851.
(9) Lovisi, H.; Inês, M.; Tavares, B.; da Silva, N. M.; de Menezes, S. M. C.; de Santa Maria, L. C.; Coutinho, F. M. B. *Polymer* **2001**, *42*, 9791.
(10) Alamo, R. G.; Vanderhart, D. L.; Nyden, M. R.; Mandelkern, L. *Macromolecules* **2000**, *33*, 6094.
(11) Nyden, M. R.; Vanderhart, D. L.; Alamo, R. G. *Comput. Theor. Comput. Sci.* **2001**, *11*, 175.
(12) Shiu, Y.-W.; Uozumi, T.; Terano, M.; Nitta, K.-H. *Polymer* **2001**, *42*, 9611.
(13) Arnold, M.; Bornemann, S.; Köller, F.; Menke, T. J.; Kressler, J. *Macromol. Chem. Phys.* **1998**, *199*, 2647.
(14) Turner-Jones, A. *Polymer* **1966**, *7*, 23; **1971**, *12*, 487.
(15) Marega, C. Marigo, A.; Saini, R.; Ferrari, P. *Polym. Int.* **2001**, *50*, 4, 442.
(16) Mezghani, K.; Phillips, P. J. *Polymer* **1995**, *36*, 2407.
(17) Perez, E.; Benavente, R.; Bello, A.; Pereña, J. M.; Zucchi, D.; Sacchi, M. C. *Polymer* **1997**, *38*, 5411.
(18) Zhao, Y.; Vaughan, A. S.; Sutton, S. J.; Swingler, S. G. *Polymer* **2001**, *42*, 6599.
(19) Foresta, T.; Picarolo, S.; Goldbeck-Wood, G. *Polymer* **2001**, *42*, 1167.
(20) Marega, C.; Marigo, A.; Saini, R.; Ferrani, P. *Polym. Int.* **2001**, *50*, 442.
(21) Busico, V.; Corradini, P.; DeRosa, C.; Dibenedetto, E. *Eur. Polym. J.* **1985**, *21*, 239.
(22) Zimmermann, H. J. *J. Macromol. Sci., Phys.* **1993**, *B32-2*, 141.
(23) Feng, Y.; Hay, J. N. *Polymer* **1998**, *39*, 6589.
(24) Laihonen, S.; Gedde, U. W.; Werner, P. E.; Westdahl, M.; Jaaskelainen, P.; Martinez-Salazar, J. *Polymer* **1997**, *38*, 371.
(25) Laihonen, S.; Gedde, U. W.; Werner, P. E.; Martinez-Salazar, J. *Polymer* **1997**, *38*, 361.
(26) Monasse, B.; Haudin, J. M. *Colloid Polym. Sci.* **1988**, *266*, 679.
(27) Alamo, R. G.; Kim, M.-H.; Galante, M. J.; Isasi, J. R.; Mandelkern, L. *Macromolecules* **1999**, *32*, 4050.
(28) Marigo, A.; Marega, C.; Zannetti, R.; Paganetto, G.; Canossa, E. *Makromol. Chem.* **1989**, *190*, 2805.
(29) Thomann, R.; Wang, C.; Kressler, J.; Mülhaupt, R. *Macromolecules* **1996**, *29*, 8425.
(30) Auriemma, F.; De Rosa, C. *Macromolecules* **2002**, *35*, 9057. Auriemma, F.; De Rosa, C.; Boscato, T.; Corradini, P. *Macromolecules* **2001**, *34*, 4815.
(31) Thomann, R.; Semke, H.; Maier, R. D.; Thomann, Y.; Scherbe, J.; Mülhaupt, R.; Kressler, J. *Polymer* **2001**, *42*, 4597.
(32) Brückner, S.; Meille, S. U.; Petraccone, U.; Pirozzi, B. *Prog. Polym. Sci.* **1991**, *16*, 361.
(33) Rieger, B.; Mu, X.; Mallin, D. T.; Rausch, M. D.; Chien, J. C. W. *Macromolecules* **1990**, *23*, 3559.
(34) Brückner, S.; Meille, S. V. *Nature (London)* **1989**, *340*, 455.
(35) Meille, S. V.; Brückner, S.; Porzio, W. *Macromolecules* **1990**, *23*, 4114.
(36) Lotz, B.; Graff, S.; Straupe, S.; Wittman, J. C. *Polymer* **1991**, *32*, 2902.
(37) Lotz, B.; Wittman, J. C.; Lovinger, A. J. *Polymer* **1996**, *37*, 4979.
(38) Ferro, D. R.; Brückner, S.; Meille, S. V. Ragazzi, M. *Macromolecules* **1992**, *25*, 5231.
(39) Alamo, R. G.; Blanco, J. A.; Agarwal, P. K.; Randall, J. C. *Macromolecules* **2003**, *36*, 1559.
(40) Bond, E. B.; Spruiell, J. E.; Lin, J. S. *J. Polym. Sci., Part B: Polym. Phys.* **1999**, *37*, 3050.
(41) De Rosa, C.; Auriemma, F.; Circelli, T. Waymouth, R. M. *Macromolecules* **2002**, *35*, 3622.
(42) Alamo, R. G.; Isasi, J. R.; Kim, M.-H.; Mandelkern, L.; VanderHart, D. L. *Polym. Mater. Sci. Eng. Proc.* **1999**, *81*, 346.
(43) Westerman, L.; Clark, J. C. *J. Polym. Sci., Polym. Phys. Ed.* **1973**, *11*, 559.
(44) Tritto, I.; Fan, Z.-Q.; Locatelli, P.; Sacchi, M. C.; Camurati, I.; Galimberti, M. *Macromolecules* **1995**, *28*, 3342.
(45) Randall, R. C. *Macromolecules* **1978**, *11*, 592.
(46) Busico, V.; Cipullo, R.; Monaco, G.; Vacatello, M.; Segre, A. L. *Macromolecules* **1997**, *30*, 6251.
(47) Kakugo, M.; Naito, Y.; Mizunama, K.; Miyakate, T. *Macromolecules* **1982**, *15*, 1150.
(48) Turner-Jones, A.; Aizlewood, J. M.; Beckett, D. R. *Makromol. Chem.* **1964**, *75*, 134.
(49) Dai, P. S.; Cebe, P.; Capel, M.; Alamo, R. G.; Mandelkern, L. In *Scattering from Polymers. Characterization by X-Rays, Neutrons and Light*; ACS Symposium Series; Cebe, P., Hsiao, B., Lohse, D., Eds.; American Chemical Society: Washington, DC, 2000; p 152.
(50) Alamo, R. G.; Brown, G. M.; Mandelkern, L.; Lehtinen, A.; Paukkeri, R. *Polymer* **1999**, *40*, 3933.
(51) Flory, P. J. *Trans. Faraday Soc.* **1955**, *51*, 848.
(52) We thank J. C. Randall for this analysis.

(53) VanderHart, D. L.; Alamo, R. G.; Nyden, M. R.; Kim, M. H.; Mandelkern, L. *Macromolecules* **2000**, *33*, 6078.
(54) VanderHart, D. L.; Nyden, M. R.; Alamo, R. G.; Mandelkern, L. *Polym. Prepr.* **2000**, *82*, 140.
(55) Alamo, R. G.; Mandelkern, L. *Macromolecules* **1991**, *24*, 6480.
(56) Isasi, J.; Mandelkern, L.; Galante, M. J.; Alamo, R. G. *J. Polym. Sci., Polym. Phys. Ed.* **1999**, *37*, 323.
(57) Brückner, S.; Phillips, P. J.; Mezghani, K.; Meille, S. V. *Macromol. Rapid Commun.* **1997**, *18*, 1.
(58) Lotz, B.; Graff, S.; Wittman, J. C. *J. Polym. Sci., Polym. Phys. Ed.* **1986**, *24*, 2017.
(59) Morrow, D. R. *J. Macromol. Sci.* **1969**, *B3*, 53.

MA030157M

EXHIBIT 3

Macromolecules **1999**, *32*, 4050−4064

Structural and Kinetic Factors Governing the Formation of the γ Polymorph of Isotactic Polypropylene

Rufina G. Alamo* and Man-Ho Kim

Department of Chemical Engineering, Florida Agricultural and Mechanical University, and Florida State University College of Engineering, 2525 Pottsdamer St., Tallahassee, Florida 32310-6046

Maria J. Galante,† José R. Isasi, and Leo Mandelkern*

Department of Chemistry and Institute of Molecular Biophysics, Florida State University, Tallahassee, Florida 32306-4380

Received November 30, 1998; Revised Manuscript Received March 29, 1999

ABSTRACT: The molecular, thermodynamic, and kinetic factors that govern the formation and concentration of the α and γ polymorphs in metallocene-catalyzed isotactic poly(propylenes) have been studied with a set of polymers that have a wide range in molecular weight and defect contents. With these polymers it was possible to investigate the influence of molecular weight on γ formation at a fixed defect concentration, as well as the role of the defect concentration at constant molecular weight. The major experimental techniques used were wide-angle X-ray scattering and differential scanning calorimetry complemented by microscopy. From these studies the role of chain microstructure, the crystallization temperature, and the thermodynamic and kinetic requirement for the formation of the γ form could be established in more quantitative detail than heretofore. A particular important finding was the fact that at fixed defect concentration the fractional content of the γ polymorph goes through a maximum with crystallization temperature. The results that were obtained establish a quantitative framework within which the underlying bases that lead to formation of the γ form, and its unique crystalline structure, are discussed.

Introduction

Isotactic poly(propylene) possesses some features that are unique to a semicrystalline polymer. This polymer exhibits three different, well-defined, crystallographic forms. The chain conformation of each is in the classical 3_1 helix. The difference in the crystallography is the manner in which the chains are packed in the unit cell. The crystallographic habits of the three polymorphs have recently been reviewed in detail.[1] The most commonly observed crystal form is the monoclinic or α form. The lamellar morphology associated with this crystallographic form is unusual. Transversal lamellae grow epitaxially from those initially formed, giving a mesh-type crosshatched morphology.[2] Details of this lamellar structure and its influence on thermodynamic properties have been reported in detail.[3] The β or hexagonal form is found either after crystallization under stress or by adding specific nucleating agents to quiescent melts. The β form transforms to the α form on heating. Early X-ray diffraction studies of the third polymorph, the γ form, concluded that this crystallographic form was triclinic.[4,5] However, more recent work has determined that this polymorph is in fact orthorhombic.[6-8] The structure of the orthorhombic unit cell of the γ form is unprecedented for polymeric systems. It represents the first, if not the only, one to date, wherein the chain axes are nonparallel to one another. In this structure parallel helices, two chains wide, are tilted 80° with respect to another in an adjacent bilayer. The present work focuses attention on the conditions for the formation of the γ polymorph and its properties. Of particular interest is the role played by the chain microstructure and the crystallization temperature.

In early work, using Ziegler−Natta catalysts, the γ form was obtained by either crystallization of high molecular weight species at elevated pressures,[9-13] crystallization at atmospheric pressure of very low molecular weight chains,[14-17] or crystallizing propylene copolymers.[18-21] It is difficult, however, to develop meaningful correlations between molecular structure and properties of the isotactic poly(propylenes) prepared with this catalyst. The reason is that chain length and stereo defect composition are inversely related to one another.[22-25] The low molecular weights contain a high concentration of chain defects while the microstructures of the high molecular weights approach that of the stereoregular chain. The low molecular weight fractions that were used to obtain the γ form thus contained a high concentration of defects.[6,7] It has been speculated that interruptions in the regular sequences of isotactic poly(propylene) favored the development of the γ form.[1]

Metallocene-catalyzed isotactic poly(propylene) yields polymers that have most probable molecular weight distributions ($M_w/M_n \simeq 2$) and narrow composition distributions. The study of this type polymer allows for the molecular length and defect concentration to be varied independently. Thus, the relation between chain length, defect concentration, and the formation of the γ polymorph can be studied. In addition to the conventional stereo-type defect, metallocene-catalyzed isotactic poly(propylene) chains also contain regio defects. Several studies of γ formation in this type of isotactic poly(propylene) have been reported.[6,26-29a,b] In one, the fraction of the γ structure that develops in a relatively low molecular weight polymer, $M_w = 18\,000$ g/mol, with a high defect concentration was studied as a function

† Present address: INTEMA, Juan B. Justo 4302, Mar del Plata (7600), Argentina.

* To whom correspondence should be addressed.

10.1021/ma981849r CCC: $18.00
Published on Web 05/18/1999

Table 1. Molecular Characterization of Metallocene Poly(propylenes) with Constant Concentration of Defects

samples	M_w	M_w/M_n	isotactic[a] [mmmm]	stereo defects (%)	regio[b] defects (%)	total defects (mol %)	n_{iso}[d]
M41K	41 260	2.1					
M68K 1.57	68 480	2.1	0.940	0.97	0.60	1.57	58
M69K 1.70	69 190	2.1	~0.95	~0.90	~0.80	~1.70	54
M142K 1.70	142 000[c]	~2	~0.95	~0.90	~0.80	~1.70	56
M170K 1.70	169 800	1.8	~0.95	~0.90	~0.80	~1.70	56
M288K 1.69	288 430	1.8	0.954	0.83	0.86	1.69	57

[a] Fraction of isotactic pentads measured from ^{13}C NMR. [b] 2, 1 additions (erythro). [c] Interpolated from intrinsic viscosity/M_w relation. [d] From eq 1.

Table 2. Molecular Characterization of Metallocene Poly(propylenes) with a Constant Low Content of Mainly 2,1 Additions

sample	M_w	M_w/M_n	[mmmm]	stereo (%)	regio[a] 2,1 (%)	total defects (mol %)	n_{iso}
M102K 0.42	102 500	2.3	0.9959	0.06	0.36	0.42	194
M182K 0.40	182 000	2.0	0.9960	0	0.40	0.40	223
M200K 0.41	200 500	2.0	0.9925	0.01	0.40	0.41	220
M327K 0.41	327 000	2.2	0.9959	0	0.41	0.41	227
M403K 0.41	403 500	2.3	0.9959	0	0.41	0.41	230
M439K 0.39	439 000	2.1	0.9961	0.06	0.33	0.39	243

[a] 2,1 additions (erythro type).

Table 3. Molecular Characterization of Metallocene Poly(propylenes) with Different Concentration of Defects

sample	M_w	M_w/M_n	[mmmm]	stereo defects (%)	regio 2−1 (%)	regio 1−3 (%)	total defects (mol %)	n_{iso}
M575K 0.30	575 500	2.4	0.995	0.08	0.22	0	0.30	314
M200K 0.41	200 500	2.0	0.9925	0.01	0.40	0	0.41	220
M349K 0.44	349 500	2.5	0.991	0.09	0.35	0	0.44	212
M346K 1.00	346 500	2.3	0.954	0.84	0.16	0	1.00	96
M236K 1.17	236 400	~2		0.22	0.95	0	1.17	82
M288K 1.69	288 430	1.8	0.954	0.83	0.86	0	1.69	57
M335K 2.35	335 500	2.3	0.908	1.68	0.53	0.14	2.35	41

of the crystallization temperature.[28] In the other, the molecular weight of the samples ranged from 10 000 to 62 000 with a wide range in stereo and regio defects.[29] However, slow cooling from the melt was the only crystallization condition used. These works, although significant, do not allow for an analysis of the wide range of molecular weights, microstructure, and crystallization temperatures that are available.

In the present work, studies were carried out under atmospheric pressure, with metallocene-catalyzed isotactic poly(propylenes) that encompassed a range in molecular weights and defect content that were much greater than previously reported. With this set of polymers it was possible to investigate in a systematic manner the effect of molecular weight on γ formation at fixed defect concentration as well as the role of defect concentration when the molecular weight is held constant. By studying isothermal crystallization kinetics, the relative rates of the formation of the α and γ polymorphs could be determined as well as the amounts that are formed under specified conditions. From this work the role of chain microstructure and the thermodynamic and kinetic requirements for the formation of the γ form could be established in more quantitative detail than heretofore. The extensive results that are reported establish a framework within which to discuss the underlying basis for the development of this polymorph. It enables one to address the fundamental question as to the driving force(s) that lead to the unique crystalline structure. We limit consideration here to chains that only contain regio and stereo defects. The role of comonomers, when inserted in the chain, will be discussed in a subsequent paper.

Experimental Section

Materials. Three different series of metallocene poly(propylenes) were studied. The effect of the molecular weight and crystallization temperature on the formation of the γ phase was examined with the two sets of polymers listed in Tables 1 and 2. The samples are designated by molecular weight and defect concentration. Thus, in Table 1, M68K 1.57 represents a metallocene poly(propylene) with $M_w = 68\,000$ and 1.57% defects. The polymers listed in Table 1 have a constant defect concentration of about 1.7 mol of defects per 100 monomeric units, while the molecular weights vary from $M_w \sim 40\,000$ to ~300 000 g/mol. The molecular weight distribution is narrow, characteristic of this type of poly(propylene), $M_w/M_n \simeq 2.0$. Of the total defects, about half are of the stereo type while the remainder are of the 2,1 type of addition. The total defect content is also constant for the series of polymers listed in Table 2. However, the concentration is much lower than for the series listed in Table 1. All of the polymers in this series contain about 0.4 defects per 100 monomeric units. The defects in this series are mainly of the 2,1 type of additions. In some of these polymers the stereo defect content was below the detectable level (about 0.02%). The molecular weights vary from about 100 000 to 439 000 g/mol. The polymers listed in Table 3 were used to study the effect of defect concentration on the formation of the γ phase. Thus, in this series, the molecular weight and molecular weight distribution are approximately constant, and the total amount of structural irregularities (listed as total defect content in the table) varied from 0.3 to 2.34 mol %. The different types of stereo and/or regio defects are also listed. We thus have available a much wider range in molecular weights of metallocene-type isotactic poly(propylenes) that have been studied, heretofore, as well as a significant concentration range in both stereo and regio defects.

Although the major focus of this work is with the metallocene isotactic poly(propylenes) we have, for comparative purposes, also studied two unfractionated Ziegler−Natta catalyzed polymers. Their molecular characteristics are given in Table 4. These polymers only contain stereo defects that are broadly distributed.

In addition to the amount and type of defect, the molecular weight, the polydispersity, and the fraction of isotactic pentads, measured by ^{13}C NMR, are also listed in the tables.

Table 4. Molecular Characteristics of Ziegler–Natta Poly(propylenes)

sample	M_w	M_w/M_n	mmmm	mmmr/2	n_{iso}
A[a]	271 500	6.10	0.9457	0.0086	116
B[a]	312 300	4.5	0.9395	0.0102	98

[a] After removal of atactic fraction (see text).

Crystallizations from the melt at temperatures higher than about 80 °C were carried out in thermostated oil baths. In these experiments, films approximately 20 mm long, 13 mm wide, and 0.5 mm thick were used. The samples were sandwiched between thin aluminum plates and melted in an oil bath at 200 °C for 15 min and then rapidly transferred to another oil bath set at the required crystallization temperature. To prevent degradation during crystallizations that required over 1000 min, the molded plates were placed in vacuum-sealed tubes. After the required crystallization time elapsed, the tubes were quenched in an ice/water bath. Quenching to ice/water or rapid crystallization of the samples from the melt was carried out directly from the hot press to the quenching bath.

Techniques. The chain structure was characterized by high-resolution ^{13}C NMR following assignments previously reported.[30-32] The concentration of stereo defects was calculated from the mmmr pentads as mmmr/2. The fractional content of 2,1 or 1,3 additions was computed from their respective assigned resonances.[33-38] The ^{13}C NMR spectra were obtained in polypropylenes free of atactic fraction to avoid complications in analyzing the spectra from overlapping peaks. To separate the atactic fraction, the polymer was dissolved in tetrachlorobenzene (2% w/v) and allowed to crystallize by slowly cooling the solution to room temperature. The average length of isotactic sequences between any two structural irregularities in the chain, n_{iso}, is a quantity of strong interest. It is defined as the number of isotactic monomeric units divided by the number of isotactic sequences. By assuming a random distribution of defects it can be approximated by

$$n_{iso} = \frac{DP - DP\left[\frac{mmmr}{2} + regio(2,1) + regio(1,3)\right]}{1 + DP\left[\frac{mmmr}{2} + regio(2,1) + regio(1,3)\right]} \quad (1)$$

where DP is the degree of polymerization and mmmr/2, regio(2,1), and regio(1,3) are the fractional contents of stereo, 2,1, and 1,3 additions. The isotacticity content and molecular weight of the polymers studied here are high. Therefore, the n_{iso} values calculated according to eq 1 are basically identical to the average meso run length calculated from the fraction of triads, tetrads, or pentads as derived by Randall.[39] Under these conditions $\bar{n} = n_{iso} = 1/\text{fractional content of defects}$. The n_{iso} values for the polymers studied here are listed in Tables 1–4.

The melting behavior was studied with a Perkin-Elmer DSC-2B differential scanning calorimeter operated at a heating rate of 10 °C/min. The enthalpies of fusion were converted to degrees of crystallinity ($(1 - \lambda)_{\Delta H}$) by taking the enthalpy of fusion of a perfectly crystalline poly(propylene) as 50 cal/g[40] and using indium as standard. The crystallization kinetics were also studied by DSC following the increase in the endothermic peak areas with time.[41]

The wide-angle X-ray scattering patterns (WAXS) were obtained using a slit-collimated Siemens D-500 diffractometer operating in a 2θ range between 4° and 40°. The instrument is equipped with a removable high-temperature stage. Filtered Cu Kα radiation was used as source. The peak assignments of the γ phase, given by Brückner and Meille,[6] were followed. The Miller index assignments given by Turner-Jones[5] were used for the α phase. As an example, a diffractogram of an isotactic poly(propylene) that contains approximately equal amounts of α and γ phases is shown in Figure 1. The most characteristic reflection of the γ form is the (117) that appears at a 2θ of 20.05°. The characteristic peak of the α form is the

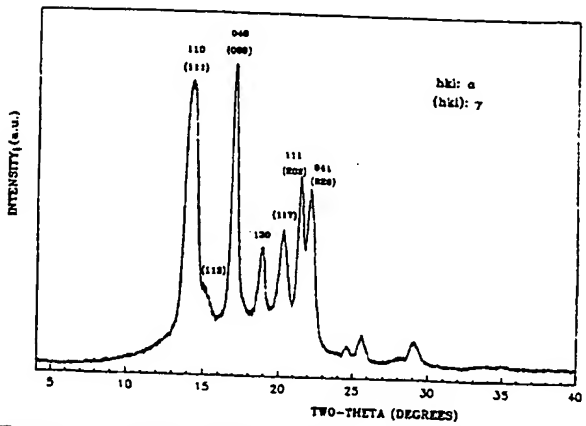

Figure 1. WAXS diffractogram of sample M142 K1.70 crystallized at 125 °C. The Miller indexes of the γ phase[6] given in parentheses and of the α phase[5] are indicated.

(130) index that appears at 2θ equals 18.8°. The fraction of the γ phase in the crystalline region was obtained from the diffractograms following the method given by Turner-Jones.[18] It was calculated from the heights of the peaks at 18.8° (H_α) and 20.05° (H_γ) as $(H_\gamma/(H_\gamma + H_\alpha))$.

Results and Discussion

Effect of Varying Molecular Weight for a Fixed Content of Defects. The effect of molecular weight on the formation of the γ form, at a fixed chain (stereo or regio) defect content, is analyzed with the set of isotactic poly(propylenes) listed in Table 1. Each of the polymers was isothermally crystallized in the temperature interval between 100 and 150 °C and then rapidly transferred to room temperature. The time required to obtain complete transformation at the highest crystallization temperatures was estimated from a previous study of the crystallization kinetics of the same samples.[41] The WAXS measurements were made at room temperature.

The percentage of crystals that develop as the γ polymorph as a function of crystallization temperature for these polymers, after complete crystallization, is given in Figure 2. As the crystallization temperature is raised above 90 °C, the γ form begins to develop at the expense of the α. In the crystallization temperature interval from 60 to 130 °C the γ fraction increases from 0 to about 60%. Crystallization at 100 °C yielded a relatively small amount of γ content, between 16% and 28%. An extrapolation of the low-temperature side of Figure 2 indicates that at a crystallization temperature of about 90 °C, and below, the γ form will not develop in this molecular weight range for polymers having about 1.7 mol % defects. Experiments show that after rapid crystallization from the melt, to either 23 or 60 °C, only the α form is observed. A maximum in the γ concentration is reached at about 130 °C, with a continuous decrease being observed above this crystallization temperature. No definitive trend in the γ content could be discerned with molecular weight.

An increase in the γ content with increasing temperature has also been reported for another metallocene-type isotactic poly(propylene).[28] This polymer had a relatively low molecular weight (M_w = 18 000 g/mol) and a defect content greater than 4.4 mol % and was crystallized under atmospheric pressure.[42] At crystallization temperatures between 115 and 125 °C, this sample crystallized almost completely in the γ form. Crystallizations were not carried out at higher temperatures with this polymer.

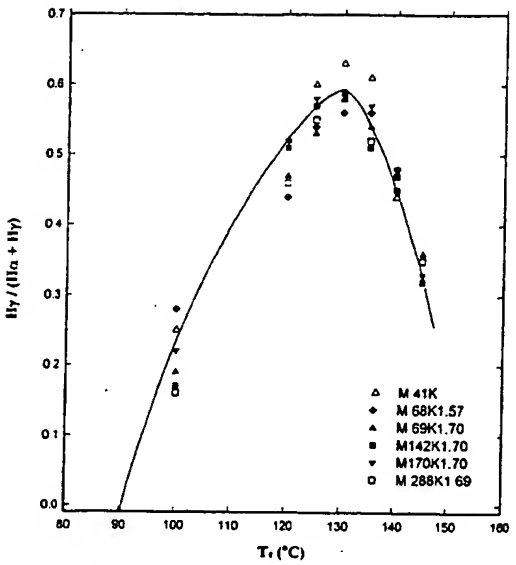

Figure 2. Fractional content of the γ polymorph in the crystalline region as a function of crystallization temperature for metallocene poly(propylenes) with the indicated molecular weights.

The observation of a maximum in the plot shown in Figure 2 is both unique and important. Therefore, its validity needs to be carefully examined and substantiated. In general, the crystallization rate of all polymers decrease markedly with increasing temperature at the right side of the maximum of the crystallization rate/temperature plot. Although the time scale of the crystallization was established from earlier crystallization kinetic studies,[41] there could be concern that the decrease in the concentration of the γ polymorph at the higher crystallization temperatures could be the result of an incomplete transformation. Any potential crystallizable material would crystallize upon quenching and contribute to the WAXS pattern. Quenching peaks do not appear in the DSC thermograms for samples crystallized at 130 °C and below. However, after crystallization at temperatures at the right side of the maximum, >130 °C, in addition to the main endotherm, which corresponds to the melting of the crystallites formed isothermally, a small peak with about 6% crystallinity is also observed at much lower temperatures, about 135 °C. Attempts to eliminate the quenching peak by prolonged crystallization at 135 °C were unsuccessful. Since the WAXS determination of the γ fraction was carried out at room temperature, it is important to determine the crystal form of the quenched crystallites because these crystallites contribute to the WAXS pattern. Our interest, however, is the γ fraction in the crystalline region developed at the crystallization temperature. If the material that crystallized upon quenching did so as α crystals, then the fractional content of the γ polymorph at the crystallization temperature would increase when these crystals are melted. In this case the maximum observed in Figure 2 would not be meaningful. On the other hand, if the quenched material were composed of γ crystals, then the maximum would be correct. Therefore, these possibilities were examined in more detail.

Figure 3a shows the DSC thermogram of sample M142K 1.70 that was crystallized at 145 °C for about 1 week and then quenched to 23 °C. A broad quenching

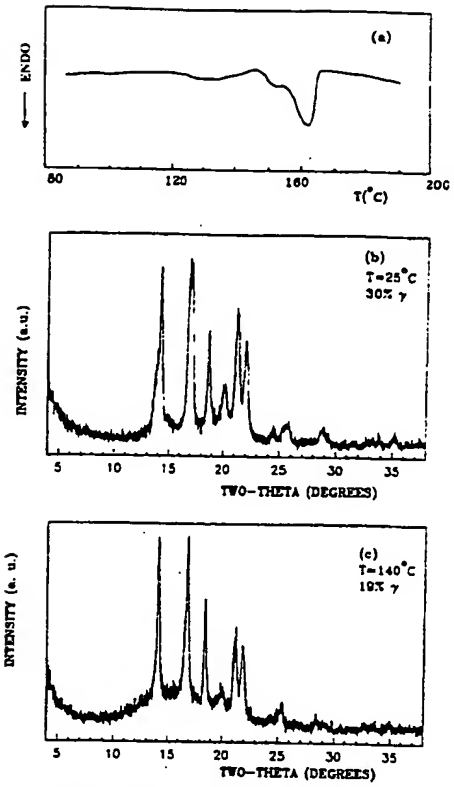

Figure 3. (a) DSC melting of sample M142 K1.70 crystallized at 145 °C. The broad melting peak at ~135 °C is due to crystallites formed on quenching. (b, c) WAXS diffractograms of the same sample obtained at 25 °C (b) and at 140 °C (c). Note the decrease of the γ reflection at $2\theta = 20.05°$ in the lower diffractogram.

peak (130–140 °C) appears in the thermogram together with the two melting peaks of the crystals formed isothermally. Parts b and c of Figure 3 give the WAXS diffractograms of this sample at room temperature and at 140 °C, respectively. The 140 °C temperature is above the melting of the crystals formed on quenching but below those formed isothermally. The intensity of the reflection assigned to the α polymorph is the same at 140 °C as at room temperature. However, the intensity of the reflection corresponding to the γ form decreases from room temperature to 140 °C. This result indicates that crystals of the γ polymorph are formed on quenching and, therefore, do not have a negative effect in the calculation of the γ content of the samples crystallized at high temperatures. A similar experiment with sample M170K 1.70 crystallized at 140 °C gave identical results; i.e., the crystals formed on quenching are of the γ polymorph. Thus, the decrease in the relative content of the γ phase formed in this series of poly(propylenes) at crystallization temperatures above 130 °C is confirmed.

Support for the maximum in Figure 2 is also found in the following observations derived from the melting behavior. As mentioned previously, all of the polymers in this series that were crystallized above 130 °C give a small quenching peak of approximately the same area that correspond to 5–10% crystallinity. An example is shown in Figure 4 of two thermograms of sample M41K that was crystallized at 135 and 140 °C. The degrees of crystallinity of about 42% are similar for both of the major endotherms. The crystallinity levels of small

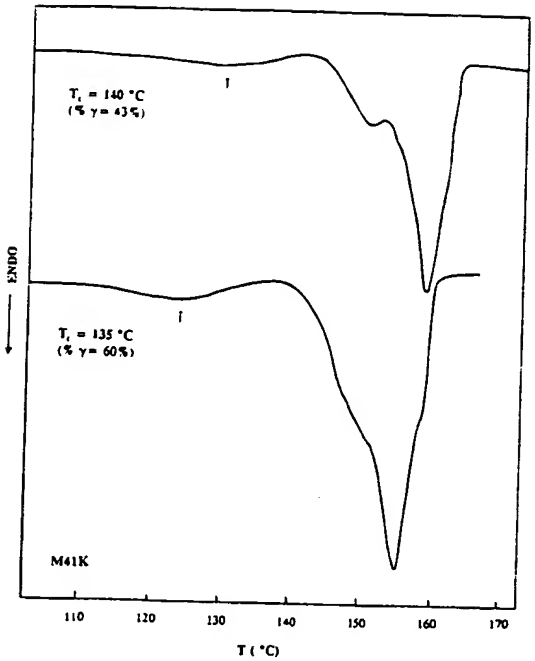

Figure 4. DSC endotherms of sample M41K crystallized at 140 °C (top) and 135 °C (lower). These temperatures are in the right side of the maximum of Figure 2. The fractional content of γ crystals formed is significantly different although the broad endotherm formed from quenching is similar.

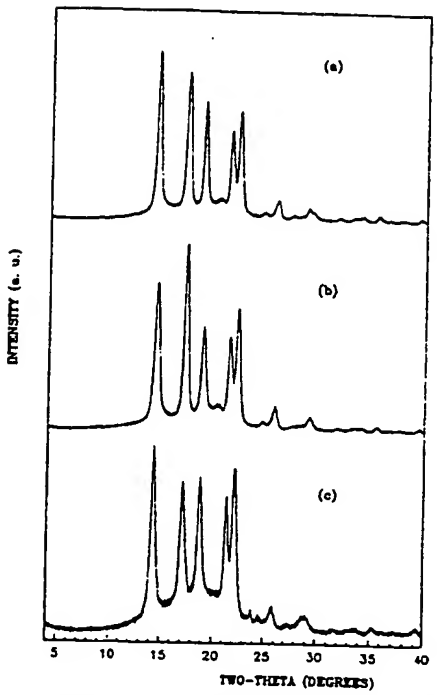

Figure 5. WAXS diffractograms of sample M102 K0.42 crystallized at three different temperatures: (a) $T_c = 145$ °C, 5% γ; (b) $T_c = 155$ °C, 8% γ; (c) $T_c = 160$ °C, 0%. Note the absence of γ reflection in the sample crystallized at 160 °C.

quenching peaks are also similar. However, the WAXS measurements at room temperature indicate that the γ fraction of the sample crystallized at 140 °C is 0.43 while it is 0.60 for the one crystallized at 135 °C. Therefore, the decrease in γ content with increasing crystallization temperature (above the maximum in Figure 2) cannot be attributed to incomplete crystallization. Further support of the validity of the maximum in Figure 2 comes from studies of isothermal crystallization kinetics that will be discussed shortly.

The formation of the γ polymorph as a function of the crystallization temperature was also studied for all the polymers listed in Table 2. In this series the concentration of defects is constant and very small, about 0.4 mol %. They are mainly of the 1, 2 head-to-head type, with only a minor stereoisomer content. The molecular weight in this group vary from 102 500 to 439 000 g/mol. Only α crystals are formed after relatively rapid crystallization of the polymers in this group. For crystallization temperatures between 140 and 155 °C, the samples display a weak reflection at $2\theta = 20.05°$, which is characteristic of the γ crystals. X-ray diffractograms are shown in Figure 5 for the polymer M102 K0.42 that was crystallized at 145, 155, and 160 °C. The γ fraction is very small in this series, relative to the values found with the polymers from Table 1. It is about 5% after crystallization at 145 °C and increases to about 8% for crystallization at 155 °C. The γ content is negligible, or zero, after crystallization at 160 °C. The transformation at each of these temperatures was complete. Hence, the variations of the γ content with crystallization temperature cannot be attributed to any effect of the crystals formed during quenching. Thus, a small, but significant, amount of the γ form can even be developed at atmospheric pressure in these highly regularly structured isotactic poly(propylenes), when the crystallization is conducted at sufficiently high temperatures. A small, but discernible, maximum in the fraction of γ form with crystallization temperature is also observed.

Effect of Varying Defect Concentration. The above results give an indication that the optimum γ content that can be achieved after isothermal crystallization of homopolymers increases with defect concentration. To examine this effect on a quantitative basis, a series of polymers whose defect content ranged from 0.3% to 2.35%, stereo and regio defects included, were also studied. The polymers in this series are those listed in Table 3. These polymers are not of strictly uniform molecular weight. However, in this range of high molecular weight the effect of chain length on the formation of the γ polymorph is, as noted in the previous section, negligible. The pair of samples M346K 1.00 and M236 K1.17 is of particular interest because they have about the same fractional content of defects but of the reverse type; i.e., M346 K1.00 contains 0.84 mol % stereo defects and 0.16 mol % of 2,1 additions while M236 K1.17 has 0.22 mol % stereo and 0.95 mol % of 2,1 additions. A comparison of the results for this pair will ascertain whether the formation of the γ form is enhanced by a specific defect type. Rapid crystallizations of all of these polymers, such as crystallization in ice water or at 25 °C, led to the formation of only α crystals.[43]

The results with this series follow the trends that have already been described. For a given polymer the γ form is favored at high crystallization temperatures below the maximum. The temperature at which γ crystals are first observed increases with decreasing concentration of defects. For example, the polymer with the lowest defect concentration, 0.30%, does not show any γ crystals over the whole temperature interval studied. Even after crystallization at temperatures as high as 164 °C, the diffractogram was characteristic of the α form. If a very small amount of γ was formed, it

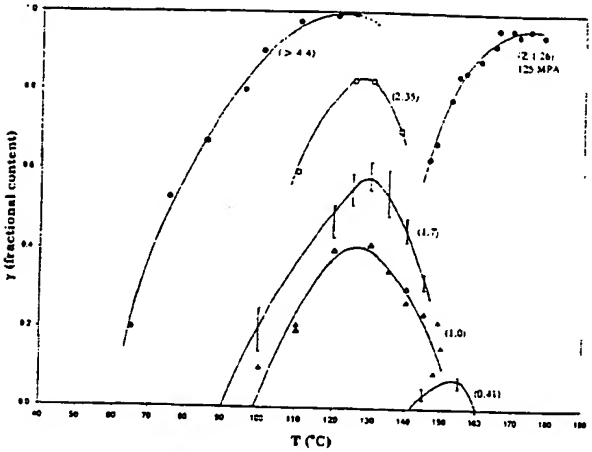

Figure 6. Variation of the fraction of the γ polymorph in isotactic poly(propylenes) as a function of percentage of chain defects and crystallization temperature. This work: ○, I, △, ▲ (the ranges of values indicated as I includes the values of percent γ obtained with different molecular weights (see Figure 3). Literature data: ●, low molecular weight iPP from ref 28; ○, Ziegler–Natta iPP crystallized at high pressure from ref 12.

was not resolved. We have found in the previous series that a small γ content can be observed with defect concentrations of about 0.40%. In contrast, the polymer in this series with the highest defect content (2.35%) shows no, or a very small, concentration of γ form at the low crystallization temperatures and very high values, >82%, when crystallized at 124.5 °C. Prolonged crystallization of this sample at 138 °C led to smaller values of the concentration of the γ form (70%) and also confirms the existence of the maximum in this polymer.

Figure 6 is a compilation of the fractional content of γ that forms as a function of the crystallization temperature for the polymers listed in Table 3, as well as the available literature data. Each curve represents the data for a different defect content. The bars in the curves for the polymers with 1.7 and 0.4 mol % defects indicate the range of values obtained with the different molecular weights (Tables 1 and 2). The literature data are those of Thomann et al.[28] for a metallocene isotactic poly(propylene) having a defect concentration greater than 4.4 mol % and that of Phillips et al.[44] for an unfractionated Ziegler-type isotactic poly(propylene), 1.2 mol % defects, crystallized under a pressure of 125 MPa. The quantitative aspects of the figure demonstrate in a dramatic fashion the role of crystallization temperature and defect concentration on the development of the γ form. As an example for crystallization at 100 °C, the γ content is ~0% for polymers with 1 mol % defects; 20% for polymers in Table 1, defect content 1.7 mol %; approximately 45% for polymer M355 K2.35 that has 2.35 mol % defects; and 90% for the low molecular weight polymer studied by Thomann et al.[28] that has a defect content greater than 4.4 mol %. The maximum percentage of γ that is developed follows a similar pattern being 40%, 60%, 83%, and 100% for the respective polymers and only about 8% for the polymer containing 0.40% defects. To develop a γ concentration of 50% at the left side of the maximum requires crystallization at 120 °C for polymers listed in Table 1 (1.70 mol % defects). The polymer having greater than 4.4 mol % defect only requires a 75 °C crystallization temperature to achieve the same value for the γ concentration. This difference in crystallization temperature also shifts the formation of equivalent γ concentrations to higher undercoolings with increasing defect content. These temperatures correspond to undercoolings of 63 and 102 °C when 186 °C is taken as the equilibrium melting temperature, T_m^o, of the γ form.[45] The undercooling differences would be qualitatively similar if a higher value was taken for T_m^o.[46,47] This effect of temperature is even more marked at low γ concentrations. For example, a γ content of 5% is achieved at 60 °C for the polymer with greater than 4.4 mol % of defects, while 145 °C is required for the 0.4% sample. This is a dramatic change for forming just a small amount of γ. Thus, the defect content and the crystallization temperature are the key variables that govern the fraction of γ that is formed. Although the role of these two variables has been discussed qualitatively previously,[28] we find in Figure 6 a comprehensive set of detailed quantitative data covering a wide range in defect concentration and crystallization temperatures.

Interestingly, the two polymers with essentially the same total defect content, M346 K1.00 and M236 K1.17, but inversely distributed between stereo and regio develop identical values of the fractional content of the γ form at all crystallization temperatures. The results for this pair are represented in Figure 6 by the open and closed triangles. We can conclude from these results that the two types of defects have the same influence in the formation of the γ polymorph.

The Ziegler–Natta catalyzed polymer that contains 1.26% stereo defects, and no regio ones, behaves in a similar manner when crystallized under pressure. Under atmospheric pressure the γ form cannot be developed over the accessible temperature range for crystallization.[11] However, when crystallized under 125 MPa about 65% of the γ polymorph develops at 145 °C. There is, initially, a continuous increase in the γ content as the crystallization temperature is increased. A maximum, or leveling off, is then reached at the highest temperatures studied. Much higher γ concentration levels are observed than would be expected from the atmospheric pressure studies that have been described. A major consequence of applying hydrostatic pressure is that it enables the crystallization to be conducted at higher temperatures. Thus, for this reason alone higher γ concentrations are expected relative to those obtained at atmospheric pressure. There may also be an influence of the applied pressure on the crystallization kinetics. This in turn could influence the development of the γ form.[48]

The maximum fraction of γ that was obtained for each of the polymers listed in Table 3, as well as one from Table 2 with just regio defects (M182 K0.40), is plotted against the total defect concentration in Figure 7. The bars represent the range of experimental values obtained at temperatures in the vicinity of the maximum. Also indicated with each data point are the regio and stereo fractions of the polymer, the stereo ones preceding the regios. The solid straight line that is drawn is an approximate representation of the data. This straight line extrapolates to 2.8 ± 0.1 as the minimum percentage of defects that will allow 100% crystallization of the γ form at the optimum crystallization temperature. This conclusion is based on the molecular weight range studied. Very low molecular weight polymers may behave in a somewhat different manner for reasons that will be discussed shortly.

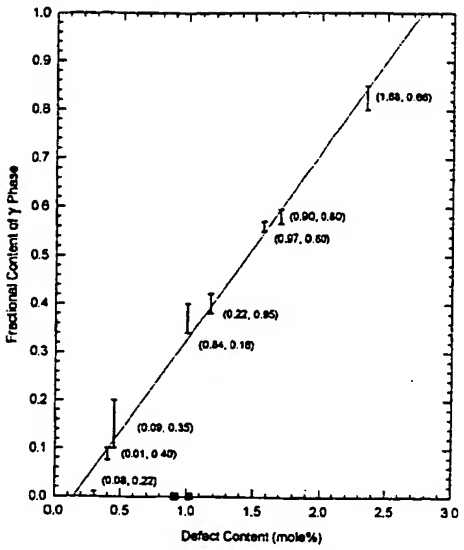

Figure 7. Maximum value of the fractional content of γ polymorph as a function of the concentration of chain defects for metallocene poly(propylenes) (I) and commercial Ziegler–Natta type (■). The range of values in I are from samples with different molecular weights as well as from different crystallizations at temperatures in the region of the maximum of Figure 6.

The two Ziegler–Natta catalyzed samples that were studied, which only contain stereo defects, are also included in Figure 7. Sample A, with 0.86% stereo defects, was isothermally crystallized at six different temperatures over the range between 26 and 164 °C. The γ phase was not found under any of these crystallization conditions. Sample B, with 1.02% stereo defects, was crystallized at 26 and 145 °C. As was found with sample A, only the α polymorph was formed. The polymer studied by Mezghani and Phillips, which contained 1.26 mol % of stereo defects, also did not form the γ polymorph when crystallized at atmospheric pressure.[11] If these Ziegler–Natta type polymers followed the pattern of the metallocenes, then between 25% and 40% of γ form would be expected. It should be noted that the Ziegler–Natta polymers studied by Fischer and Mülhaupt[29] developed about 20% of the γ form. However, the defect concentration of these polymers was not given so that a comparison with the metallocene type isotactic poly(propylenes) cannot be made. Other literature reports indicate only small concentrations of the γ phase in Ziegler–Natta isotactic poly(propylenes).[49] The difference in behavior between the two types of isotactic poly(propylenes) with respect to γ formation must be related to the broad distribution of the defect content of commercial Ziegler type polypropylenes. Thus, although the overall concentration of defects is about 1 mol %, a relatively large number of these defects may be concentrated in a small fraction of poorly crystallizable molecules, which will have a minor contribution to the crystalline properties.[50]

Fischer and Mülhaupt[29] have suggested that the average isotactic segment length n_{iso}, also termed average meso run length,[50] is an important factor in determining the γ fraction that can be achieved. This postulate is in accord with the observation that higher defect content favors γ formation. Accordingly, the average isotactic segment length, calculated according to eq 1, is plotted in Figure 8 against the maximum percentage of the γ form that was obtained. It is clear

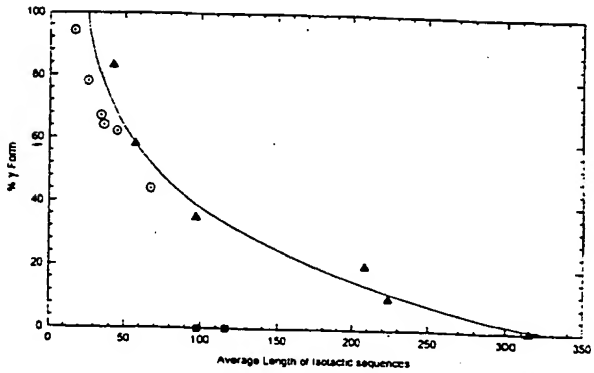

Figure 8. Maximum value of the fractional content of the γ polymorph as a function of the average length of isotactic sequences (n_{iso}): ▲, metallocenes iPP from this work; ■, Ziegler–Natta iPP from this work; ⊙, slowly cooled metallocene iPP from ref 29.

that the maximum γ content that can be achieved decreases continuously with average isotactic sequence length. We can estimate from the present work that polymers with n_{iso} of about 300 units would only produce α type crystals. In contrast, average sequence lengths of about 35 would yield only the γ form. The values reported by Fischer and Mulhaupt for the γ form of slowly cooled samples (not necessarily the optimum value) are also plotted in Figure 8. To make a comparison with the present work, the reported n_{iso} values were recalculated according to eq 1. Their results are in good agreement with those obtained in this work, particularly in consideration of the different crystallization methods used. The important conclusion from Figure 8 is that very small sequences of isotactic poly(propylene) can crystallize in the 3/1 helical form and do so as the γ polymorph. On the other hand, with very long sequences, only the α polymorph forms, while the same ordered conformation is maintained.

The work reported here has been for high molecular weight polymers so that the results are essentially independent of chain length. However, for very low molecular weights that have the same level of defect content, the n_{iso} values, calculated by eq 1, will be reduced significantly. This explains in a quantitative manner why low molecular weights crystallize predominantly in the γ form.[14–17,28] The crystallization of a low molecular weight of isotactic poly(propylene) allowed for the determination of the crystal structure of the γ polymorph.[6,7]

Melting. With the establishment of the conditions for γ formation in terms of the chain microstructure and crystallization temperature, we next examine the fusion behavior. Thermograms of four polymers from Table 1, that were crystallized at four different temperatures, are given in Figure 9. All of the thermograms show multiple endothermic peaks. The thermograms for crystallization at 60 °C are given in Figure 9A. Under these crystallization conditions the WAXS patterns have shown that only the α polymorph is formed. Two endothermic peaks are observed that have been identified with the two different lamellae types that are associated with the α form.[3] A mesh, crosshatched type lamellar morphology is observed with these crystals. The low-temperature endotherm represents the melting of thinner transversal lamellae while the higher-temperature endotherm is due to the melting of the radial (usually thicker) lamellae.[3] For relatively low crystal-

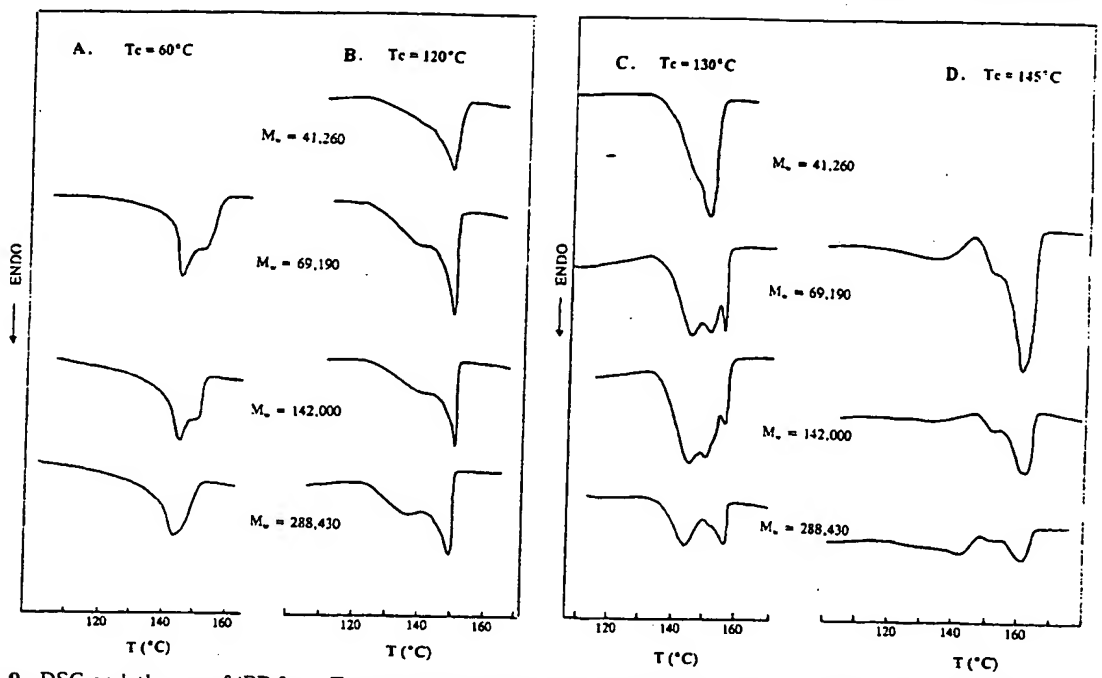

Figure 9. DSC endotherms of iPP from Table 1 crystallized at the indicated temperatures. See text for discussion of multiple endotherms.

lization temperatures there could also be a contribution from a melting–recrystallization process.

After crystallization at 120 °C (Figure 9B), a major endothermic peak is observed at 149.5 °C along with a low-temperature shoulder. The shoulder becomes better defined with the higher molecular weight samples. The relative areas of the two peaks are qualitatively similar to the ratio of the γ to α contents of these samples. It is, therefore, tempting to postulate that the two peaks represent the melting of the α and γ forms, respectively. This postulate will be addressed after the thermograms for the higher crystallization temperature and the diffractograms obtained during melting are analyzed.

The thermograms in Figure 9C for crystallization at 130 °C, which corresponds to the temperature of the maximum in Figure 2, display some unique features. For polymers with molecular weights between 68 000 and 169 800 g/mol, three separate endothermic peaks are resolved. The central endotherm of the highest molecular weight studied is less intense and overlaps with the high-temperature endotherm. These peaks are not a consequence of a melting followed by recrystallization process because varying the heating rate does not change the number or relative intensity of these peaks. All three peaks develop simultaneously during the initial stages of the crystallization. They could be associated with melting of different morphological or crystallographic entities. Qualitatively similar results are obtained for crystallization temperatures between 125 and 140 °C. No quenching peaks are observed in the thermograms for crystallization temperatures up to 130 °C. The absence of such peaks indicates that at crystallization temperatures equal to, or less than, 130 °C the transformation is complete.

After crystallization at 145 °C for 6 days (Figure 9D), a low-temperature endotherm at about 137 °C is found that is due to the crystallites formed on quenching. Besides this broad quenching peak, the thermograms of the samples show two melting peaks. Thus, it appears that at the high crystallization temperatures the middle endotherm shifts to higher melting temperatures and overlaps with the high melting peak. The intensity of the low melting peak at $T_c = 145$ °C decreases considerably with respect to the intensity of the same peak for $T_c = 130$ °C. As will be demonstrated shortly, the low-temperature peak corresponds to melting of γ type crystals; therefore, the variation of the intensity of this peak with T_c in Figure 9B–D parallels the variation of the fractional content of γ form shown previously (see Figure 2). The resolution of the three different structures into separate melting endotherms appears to depend on the molecular weight of the polymer. Inspecting Figure 9C, $T_c = 130$ °C, the lowest molecular weight only gives a broad melting peak, and the central endotherm of the highest molecular weight polymer is only resolved as a broad shoulder. The intermediate molecular weights clearly show the three melting endotherms. The variation of the melting behavior with molecular weight seems to reflect variations of the average crystallite thickness of both polymorphs with molecular weight.

To investigate the origin of the three melting endotherms observed for crystallization temperatures between 125 and 140 °C for the samples listed in Table 1, of which Figure 9C is an example, WAXS and birefringence studies were carried out with sample M142 K1.70 that was isothermally crystallized at 135 °C. A DSC melting thermogram was obtained under the same crystallization conditions. This thermogram serves as a reference to identify the temperatures of interest in the diffractograms and is given as an insert to Figure 10. Wide-angle X-ray scattering patterns were obtained at a series of temperatures that were dictated by the main features of the thermogram. These patterns comprise the main portion of Figure 10. The uppermost diffractogram was taken at 137 °C, which represents a temperature below the melting range. Thus, the fractions of the α and γ form obtained at this temperature

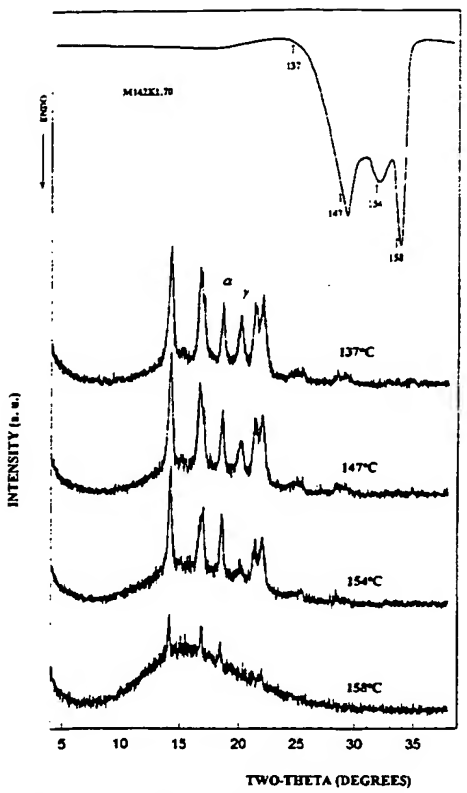

Figure 10. Top: DSC melting thermogram of sample M142K1.70 crystallized at 135 °C. Lower: WAXS diffractograms of the same sample obtained at the temperatures indicated by arrows in the thermogram. The relative variations of the α or γ reflections with temperature are discussed in the text.

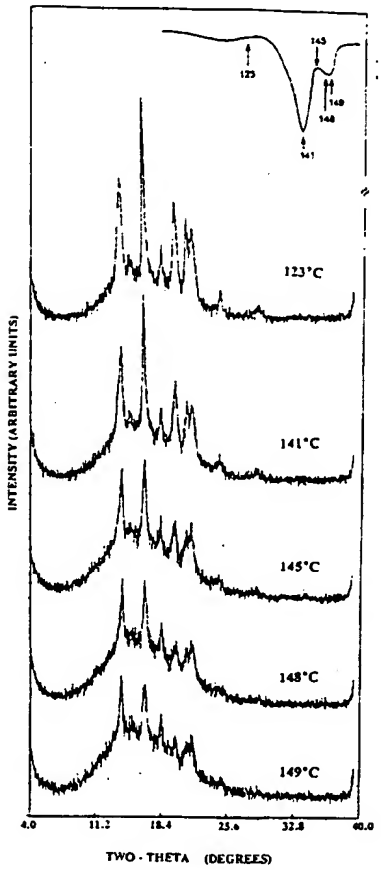

Figure 11. DSC melting and WAXS diffractograms at different temperatures during melting for sample M335K2.35 crystallized at 124.5 °C. The temperatures at which WAXS were obtained are indicated by arrows in the thermogram.

are the same as those at room temperature. As the temperature is raised to 147 °C, close to the peak of the lowest endotherm, the 117 reflection, characteristic of the γ polymorph, decreases significantly. However, the intensity and width of the characteristic α reflection remain constant. It is clear, therefore, that the γ polymorph begins to melt at a temperature lower than that for the α form. At 154 °C, the temperature which corresponds to the peak of the central endotherm, the γ polymorph is still observed in the diffractogram, although its content has decreased to less than 10%. In contrast, at this temperature the intensity and width of the α reflection remained constant. Thus, the diffractogram recorded in the temperature region of the two lowest endotherms shows that the γ polymorph has preferentially melted. There is no contribution from the α crystal to these two endotherms. Only in the temperature region of 158 °C, which corresponds to the sharp, highest temperature endotherm, does the characteristic 130 reflection of the α form decrease and eventually vanish. The two melting endotherms attributed to the γ polymorph could be caused by either two crystallite populations with different average thicknesses or two sets of crystallites with similar thicknesses but having different morphologies. The possible γ structures will be discussed shortly.

Unusual lamellar morphologies were observed for γ isotactic poly(propylene) spherulites formed at elevated pressure.[12] Radial lamellar patches, postulated to be either the α or γ phase, were reported to melt at temperatures ~10 °C lower than featherlike structures grown epitaxially. In our studies of crystallization at atmospheric pressure the α phase has never shown to have a lower melting temperature than the γ phase. Thus, if thin lamellae are part of the morphology of γ crystals formed at high pressure, by analogy with our studies, they most probably are of the γ form. We have investigated this hypothesis further by studying the crystallization and melting of both crystallographic forms in our poly(propylene) sample that had the highest γ content. The WAXS studies were again correlated with thermal measurements. Figure 11 depicts the DSC thermograms and WAXS patterns of polymer M335 K2.35 that was crystallized at 124.5 °C for 4 days. The γ content of this sample is 82.5%. The WAXS patterns were obtained at room temperature and at the temperatures indicated by the arrows in the thermogram. Paralleling the results shown in Figure 10, for a polymer that contained a lower defect content, the intensity of the 130 reflection ($2\theta = 18.8°$), which identifies the α crystals, remains constant until the final stages of melting. At temperatures that correspond to the intense high-temperature endotherm and its vicinity, 148 and 149 °C, the intensity of the γ peak at $2\theta = 20.05°$ decreases significantly, but it does not completely vanish. The two last diffractograms show that a small percentage of γ crystals remain even at temperatures close to complete melting. Thus, the association of the low-temperature peak with the complete melting of the γ crystals, and the high-temperature one with the melting of α, is not completely supported by the results

shown in Figures 10 and 11. Although only γ crystallites contribute to the low melting endotherm and the melting of all of α is reflected in the high-temperature endotherm, a small concentration of γ crystals, a few percent, melt in the temperature region of the high melting peak. The melting of this second population of γ crystals was resolved as a distinct endotherm in Figure 10 for a sample with fewer defects. However, it does not show as a third endotherm in Figure 11 when a higher content of γ phase is involved. This middle endotherm is most probably buried within the high-temperature endotherm.

The results shown in Figures 10 and 11 indicate that the γ reflection is observed within both the low -and high-temperature endotherms, albeit with quite different intensities. On the basis of these results, two different morphological γ structures can be postulated to coexist with the α form. It has also been concluded, on the basis of microscopic observations, that the γ crystals exist in two different morphological forms.[12,28] The atomic force microscopic studies of Thomann et al.[28] clearly distinguished bundlelike entities of the γ phase growing as triangular slices arranged in rows in an angle of 80° to each other on α structures. These entities exist along with structures of pure γ entities. The present thermodynamic and WAXS results strongly support the conclusion drawn from the microscopic studies. An explanation for the existence of three different lamellar entities, with distinctly different melting behavior, can be given on the basis of crystallographic modes of lamellar packing for the α and γ polymorphs.[1,51] These models favor epitaxial crystallization of α from α and of γ from α forms and, thus, support the common observation of the $\alpha-\alpha$ and $\alpha-\gamma$ branching. However, they do not allow for $\gamma-\gamma$ branching. Although speculative at this stage, it is not unreasonable to associate the low-temperature peak with unbranched γ crystals and the middle peak with melting of γ crystals that grew epitaxially on a preexisting α surface. The relative percentage of the latter crystals that are formed is conditional to the percentage of α crystals formed in the high-temperature region in which the γ phase develops. This explains the lack of resolution of a distinct middle endotherm in Figure 11 since the percentage of crystals of the α polymorph in this sample is only 17%. The validity and details of these possibilities representing the two different γ morphologies still need to be elucidated.

The relation between the polymorphic form developed at a given temperature and its melting behavior was also studied by optical microscopy. As an example, it was found that the sign of the birefingence of the spherulites of sample M142K1.70, crystallized at 135 °C whose melting was depicted in Figure 10, is preferentially positive. This positive birefingence is due primarily to the ~55% of γ crystals present and perhaps also by some daughter, transversal, α type lamellae. The sign changes to a mixed-type birefringence at a temperature corresponding to the lowest temperature endotherm (148 °C). This change is in agreement with partial melting of the γ crystals. At 154 °C, the temperature corresponding to the peak of the middle endotherm shown in Figure 10, the WAXS diffractogram indicates that a small fraction of γ crystals still remain together with all of the α ones. However, the sign of the birefringence changes to negative at this temperature. This change confirms that the α type lamellar crystals

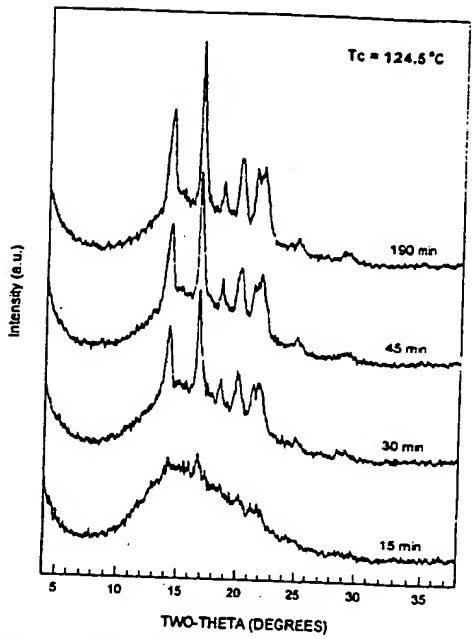

Figure 12. WAXS diffractograms of sample M335K2.35 crystallized at 124.5 °C as a function of crystallization time. Both polymorphs form from the early stages of the crystallization.

are relatively long and radially oriented, conferring this negative character to the global birefringence of the spherulites. These crystallites melt sharply at about 160 °C, in agreement with the highest temperature peak in the thermogram.

Kinetics. Studies of the crystallization kinetics from the melt of the two polymorphs should contribute to our understanding of the mechanisms involved in their formation. Consequently, we undertook such studies using WAXS and DSC techniques. The total fusion process is characterized by a low-melting endotherm that is characteristic of the melting of the γ crystallites and a high-temperature one that corresponds primarily to the α form. Thus, by monitoring the development of each of the endothermic peaks as a function of time, and converting them to heats of fusion, a quantitative kinetic analysis can be made that complements the WAXS studies.

Wide-angle X-ray scattering patterns were obtained in situ of the crystallization of M335K2.35 at 124.5 °C as a function of time. This polymer has the highest defect content among the isotactic poly(propylenes) that were studied here. The results are given in Figure 12 for the indicated crystallization times. Both polymorphs are observed at the very onset of the crystallization as is indicated by the pattern obtained after crystallization for 15 min. In the early steps of the crystallization the relative intensities of the two reflections, characteristic of each polymorph, remain essentially constant. However, after 45 min the reflection characteristic of the γ form increases continuously, while that of the α does not change.

The thermograms for the same polymer, crystallized at the same temperature, 124.5 °C, without further cooling, are shown in Figure 13. Two endotherms are observed at the very early stages of the crystallization, and they increase in parallel up to a crystallization time of 65 min. At longer times the intensity of the higher temperature peak remains constant while that of the

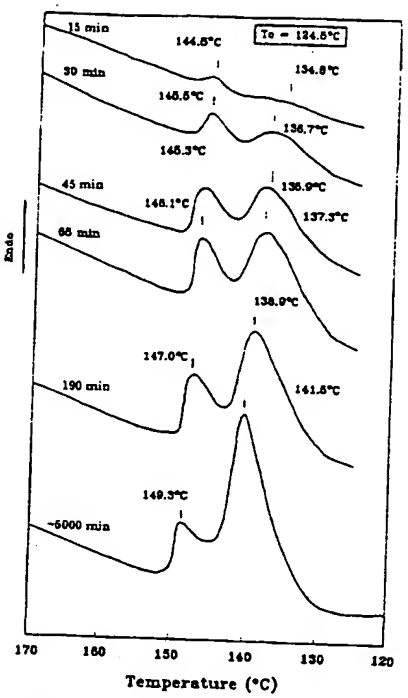

Figure 13. DSC melting endotherms of sample M335K2.35 crystallized at 124.5 °C as a function of crystallization time. Melting after crystallization up to 190 min was started from the crystallization temperature, without previous cooling. The lowest endotherm was obtained in a sample crystallized in an oil bath. Thus, the melting process was started at 37 °C. (Note that in this plot the melting peaks are displayed facing upward, opposite to meltings shown in Figures 2 and 9.)

low-melting peak continues to increase. From the thermograms about 80% of the γ form develops at this crystallization temperature as compared to 83% after complete transformation as determined by WAXS. A comparison of the diffractograms with the thermograms (Figures 12 and 13) demonstrates that as the crystallization progresses, the relative intensities of the reflections that correspond to each of the polymorphs correlate very well with the enthalpies of fusion obtained from the two endotherms, and thus the two crystalline forms.

The crystallization kinetics of this polymer were also studied at temperatures between 117 and 138 °C. The results are summarized in Figure 14. Here the degrees of crystallinity of each of the forms, $(1 - \lambda)_{\Delta H}$, obtained from the enthalpies of fusion, are plotted against log time for each crystallization temperature.[52] Sigmoidal-type isotherms, which are typical of crystallizing polymers, are obtained for both polymorphs. The time scale that ranges from several minutes to several thousand minutes is indicative of a nucleation-controlled process.[53] A major conclusion from these results, made quite clear in Figure 14, is that the crystallization of both polymorphs begins at the same time, at any given temperature. At the very initial stages of the crystallization, the crystallization rates are the same for both polymorphs. A similar conclusion was reached from analysis of the WAXS patterns. However, as the crystallization progresses at constant temperature, the α crystallinity becomes constant. Eventually, the concentrations of γ crystals given in Figure 6 for the crystalline region are reached. The crystallization kinetics of polymer M346 K1.00 (not shown), with 1 mol % of chain

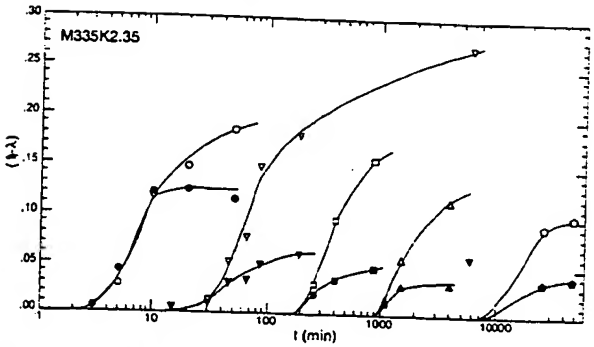

Figure 14. Sigmoidal variation of the development of α and γ crystallinities, $(1 - \lambda)$, with time for sample M335K2.35 crystallized at the following temperatures: (○, ●) 117 °C, (▽, ▼) 124.5 °C, (□, ■) 129 °C, (△, ▲) 133 °C, (◇, ◆) 138 °C. Open symbols, γ crystallinity; closed symbols, α crystallinity.

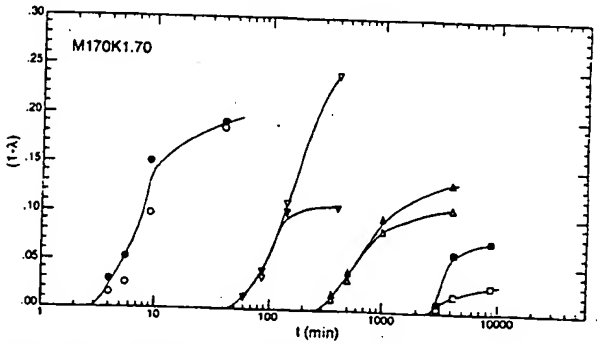

Figure 15. Sigmoidal variation of the development of α and γ crystallinities, $(1 - \lambda)$, with time for sample M170K1.70 crystallized at the indicated temperatures: (○, ●) 120 °C, (▽, ▼) 130 °C, (△, ▲) 136 °C, (□, ■) 140 °C. Open symbols, γ crystallinity; closed symbols, α crystallinity.

defects, shows some similar as well as some significantly different characteristics. The crystallization of both polymorphs is again initiated at the same time, and the initial crystallization rates are also the same. In contrast with the results in Figure 14, however, it is the γ content that now levels off and becomes constant, while the α content continues to increase with time to satisfy the higher fractional content of α formed at any temperature (Figure 6). Thus, this aspect of the crystallization process is just the opposite from that for the polymer that contains 2.35 mol % of defects. The reason for this behavior resides in the difference in defect concentrations between the two polymers and, thus, the final relative γ content (~40% of the crystals) that this polymer develops.

The crystallization kinetics of polymer M107 K1.70 were also studied at temperatures between 120 and 140 °C. The results are given in Figure 15 for four different crystallization temperatures: $T_c = 120$ °C, below the maximum; $T_c = 130$ °C, the maximum temperature; and $T_c = 136$ and 140 °C, above the maximum. The defect concentration of this polymer is intermediate between that of the two polymers just discussed. The initial crystallization times and rates of the two polymorphs are again found to be the same at each crystallization temperature. This behavior thus appears to be universal for the crystallization of the polymorphs in isotactic poly(propylene). At 120 °C, both polymorphs crystallize very rapidly and at about the same rate over the entire transformation. At 130 °C, although the crystallization rates for both forms are virtually identical at the early

stages of the crystallization, the concentration of the α crystals formed from the melt levels off at relative early times, while the γ continue to crystallize. Thus, increasing the temperature enhances the material transformed to γ. However, at the right side of the maximum, 136 and 140 °C, the situation is reversed. The γ content levels off to a relatively low concentration, while the α crystallizes to a significantly higher level. The kinetic data of Figure 15 give further and direct substantiation of the maximum observed in Figure 6 for the polymers of Table 1. We can also conclude from these kinetic studies that the initial crystallization rate from the melt is the same for both polymorphs.

The heat of fusion for each of the polymorphs, as well as the total, is plotted in parts a and c of Figure 16 for M107 K1.70 and M335 K2.35, respectively. The total degree of crystallinity ranges from about 0.40 at 120 °C to about 0.14 at 140 °C. The fractional content obtained for each polymorph at a given temperature can be calculated from these data. The heat of fusion at any given temperature is taken as the value corresponding to 1 decade of time in the flat portion of the isotherm. The independent variation of the heat of fusion at the final stages of the transformation for the α and the γ polymorphs gives the variation with temperature of the contents of α and γ crystals formed from the original melt, i.e., the variation of the α crystallinity and γ crystallinity. While the variation of the α crystallinity follows the expected trend that has been observed with other random copolymers,[54,55] the variation of the γ crystallinity with temperature goes through a maximum, reflecting again that two competing mechanisms are involved in the formation of this polymorph. The ultimate fraction of γ crystals that is obtained at each crystallization temperature is plotted in Figure 16b,d for each polymer. Very good agreement is obtained between the WAXS and DSC data for the fractional content of the γ polymorph in the crystalline region. Consistent with the WAXS results shown in Figure 6, the fractional content of γ calculated from heat of fusion also shows a maximum in the same temperature region (Figure 16b,d). These data indicate that, in the interval of molecular weights studied here, the relative contents of the α and γ polymorphs in isotactic poly(propylenes) can be estimated from the analysis of the heat of fusion of the respective melting peaks.

Summary and Discussion

The crystal structure (unit cell) of the γ polymorph and the condition for its formation bring some special features to the study of polymer crystallization. The unit cell of this form is unique among polymer crystal structures in that the chains are not parallel to one another.[6,7] The conditions for forming this polymorph are also unusual as it depends in a very specific way on both the chain microstructure and the crystallization temperature. A full understanding of the formation of γ and its structure involves correlating these apparently diverse facts.

Central to all considerations is the role of the chain microstructure. Figure 6 makes clear that as the defect (regio and stereo) concentration increases, the propensity for γ formation is enhanced. One only needs to compare the results for the polymer studied by Thomann et al.[28] with the one studied here, which contains 0.40% regio defects. In the former case, the polymer has a defect concentration greater than 4.4%, and 100% of the γ structure could be developed. In the latter case, the maximum γ concentration that can be formed is 10% at best. Extrapolation of these results indicates that only very small amounts, if any, of the γ form would develop in the pure polymer devoid of any defects. In fact, Thomann et al.[28] report that only the α polymorph could be formed in a sample of isotactic poly(propylene) of M = 16 000 g/mol that was devoid of any type of irregularities in the chain.

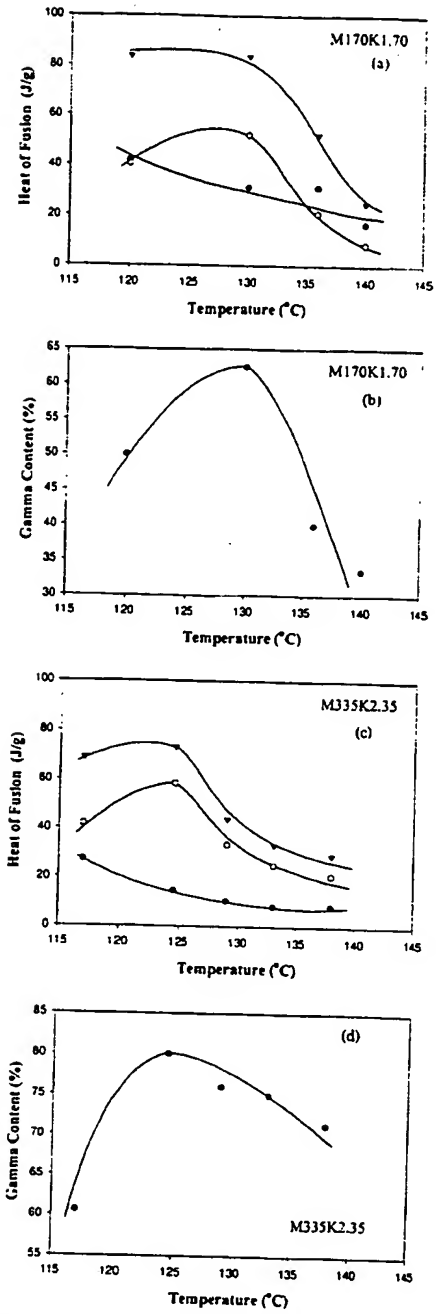

Figure 16. (a, c) Variation of the independent heat of fusion of α type crystals (●) and γ crystals (○) as well as the combined heat of fusion as a function of crystallization temperature. The heats of fusion at a given temperature were taken as the value corresponding to 1 decade of time in the flat portion of the isotherm. (a) Sample M170K1.70, (c) sample M335K2.35. (b, d) Variation with crystallization temperature of the calculated percentage of γ form from the data in (a) and (c).

The experimental requirement for a significant concentration of chain defects, with the concomitant small average isotactic sequence length between defects, to form an appreciable amount of γ results in crystallites whose dimensions in the chain direction (thickness) will by necessity be small. Thus, only a relatively *small* number of chain units participate in a given γ crystallite. Thomann et al.[28] have estimated that approximately 20 monomer units arranged in a 3_1 helix participate in a 40 Å thick lamellae. The development of lamellar crystallites is thermodynamically favored. Electron microscopy studies clearly indicate that one of the γ morphological forms is lamellar-like.[28] However, for a lamellar structure to evolve, the large flux of chains that emanates from the very small crystallite needs to be dissipated.[56] Chain folding, of one type or another, is one common method by which flux in many crystalline chain molecules is dissipated, including the α form of isotactic poly(propylene). However, this is not a tenable option with extended chains of small isotactic sequences. The very long sequence length of the attached noncrystallizable units precludes any significant folding with adjacent reentry and probably any significant chain folding at all. However, there is another way by which the chain flux can be dissipated, so that crystallization can proceed with the development of lamellar crystallites. This involves tilting of the ordered sequences within the crystallite. For example, in polyethylene the chain flux is reduced by folding (with only a small amount of regular folding randomly distributed along the basal plane) and a modest amount of chain tilting.[57,58] In the situation under consideration here chain tilting is highly favored since the γ crystalline form, with a particular set of tilted chains in the unit cell, represents a low-energy structure.[1,7] The fact that it is crystalline indicates that it represents a low-energy form. Thus, the formation of the ordered γ structure, with the antiparallel tilted chains, is a natural consequence of reducing the flux of chains that emanate from the 001 plane and accommodating chain defects outside the crystal. It has been postulated, without detail, that the features of the crystal–liquid interphase play a significant role in the formation of γ.[59] Other copolymers that have similar sequence distribution, i.e., random ethylene copolymers with a relatively high comonomer content, do not have the advantage of the accessibility of a low-energy three-dimensional ordered structure by chain tilting. Hence, in these cases after a relatively low comonomer content, 3–4%, is added, the crystallites are not longer lamellar, although crystallization occurs.[60,61] There is, therefore, a fundamental reason that the formation of the γ polymorph is so highly favored by isotactic poly(propylene) chains with high concentrations of structural and chemical irregularities, regio units, stereoisomers, and comonomers. These structural irregularities generate short crystallizable sequences, and associated long sequences of noncrystalline units, that are required to form γ. From these considerations it is concluded that the thickness of γ crystals will be restricted and relatively small when compared to the other crystal structures of isotactic poly(propylene), as well as those in other polymers.

Another unique situation exists when one wants to compare the true thermodynamic stability of the γ form with other structures, such as the α. Conventionally, the thermodynamic properties, particularly the melting temperatures, of very large crystals that are devoid of surface effects are compared for the different structures. Since large, thick γ crystals cannot be obtained, one is presented with a serious dilemma. Since the properties of only very small γ crystallites can be measured, and even then over a very small and restricted thickness range, extrapolation of melting temperatures, enthalpy, and entropy of fusion to large sizes, including an infinitely thick crystallite, involves very large errors. Pragmatically, therefore, a comparison of the thermodynamic stability of the α and γ forms can only be made with crystallites that have the same, small thickness. Such samples have not as yet been prepared. Even if this procedure could be followed, there is concern for the contribution of the interfacial free energies associated with the basal planes of each polymorph to the free energies of fusion. With respect to the interphase, chain folding will be minimal with the γ crystallite while the folding that is required in order to propagate an α type lamellar crystallite will involve an expenditure of free energy.[62,63]

An estimate can be made, however, of the relative stability of the α and γ forms. For polymers, in general, the major contribution to the entropy of fusion is the conformational change that occurs on melting.[64] Since the ordered chain conformation is the same for both the α and γ crystals, and the same melt is involved, the entropy of fusion of the two polymorphs should be close to one another. Calculations of the packing energies indicate that the γ form would be slightly more stable than the α.[1,65] On the basis of these considerations, one can hypothesize that, for the relatively thin crystallites of interest, the γ form will be slightly more stable than the α one. In the fusion processes that have been described here the low-temperature endotherm was identified with the melting of the γ form. This is a consequence of the very small thickness of the γ as compared to the α.

A qualitative explanation of the fraction γ that is formed as a function of temperature, as is illustrated in Figure 6, can now be offered. It is based on the chain microstructure requirements with temperature. The salient features that need to be explained are the increase in the relative γ concentration as the crystallization temperature is raised initially, the attainment of a temperature where the maximum γ content is reached, and its subsequent decrease with a further increase in temperature. The presence of the maximum requires that at least two competing mechanisms are involved, each with a different temperature coefficient. The temperatures are considered to be relative to the equilibrium melting temperature and thus to the defect concentration. Treating the defected chain as a random copolymer establishes the sequence distribution. It is also important to recognize the broad melting range typical of random copolymers.[55]

Central to the problem is the question of how the concentration of crystallizable sequences, i.e., those of length that equal or exceed the requirement for a nucleus of critical size, will change with temperature.[54,66] Attention is focused on the dimensions of the critical nucleus since nucleation is the primary step in the crystallization. This quantity can be calculated for the coherent unimolecular deposition on a preexisting substrate.[54] The result of such a calculation is illustrated in Figure 17. Here, ξ^*, the critical number of repeating units in a chain direction, is plotted against the mole percent of structural irregularities for different

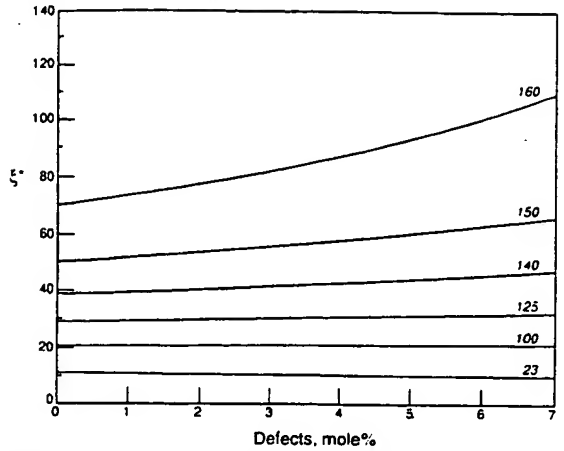

Figure 17. Variation of the calculated critical nucleus thickness[54] as a function of the concentration of chain defects of iPP for the indicated crystallization temperatures. In the calculation of ξ^* a coherent Gibbs type nucleus was adapted with the following parameters: $\sigma_e = 81.5$ erg/cm^2, $\Delta H_u = 19.76 \times 10^8$ erg/cm^3, $T_m^\circ = 458$ K and infinite molecular weight chain.

crystallization temperatures. This particular calculation was performed with $\sigma_{en} = 4000$ cal/mol (81.5 erg/cm^2) and $T_m^\circ = 185$ °C.[67] However, the most important factor is the change in ξ^* with temperature and composition. From the data in Figure 17 we take as an example the 2.3 mol % defected polymer (M335 K2.35). For this polymer, crystallized at 80 °C, isotactic sequences of 16 repeating units and greater are allowed to participate in the crystallization. With such a small lower limit for ξ^*, the smaller sequences can crystallize in extended form and the larger ones can fold. Consequently, close to the optimum level of crystallinity is attained. Under these circumstances there is not a sufficient concentration of long noncrystallizable sequences to serve as the "triggering" mechanism to cause formation of γ crystals. Thus, only α type crystals will be observed. As the crystallization temperature is raised, the ξ^* requirement increases so that the very short sequences can no longer crystallize. In the remaining grouping of crystallizable sequences the shorter ones can still not crystallize by folding because the associated noncrystallizable sequences have become too long. Thus, in order for a lamellar crystallite to evolve in extended form, from this sequence, tilting and γ formation will occur. As is indicated in Figure 6, as the crystallization temperature is initially increased, the concentration of γ does in fact increase. However, by the same token, as temperature increases, the availability of short sequences for crystallization is being continuously reduced. Thus, there are two competing mechanisms that eventually lead to the maximum in Figure 6. At sufficiently high temperatures, above the maximum, only a small amount, if any, of γ will form due to the higher requirement. Under these circumstances, the noncrystallizability of the shorter sequences that are required will prevent its formation. However, since the α form only crystallizes from the longer sequences and the lamellar crystallites are propagated by some type of chain folding, they will dominate at the higher crystallization temperature. A similar description can be given to the data plotted in Figure 6 for the other polymers. These arguments are consistent with the kinetic studies that were given in Figures 14–16 and with the details of the lamellar structure. Electron micrographs of sample M335 K2.35 crystallized at 124.5 °C are also in agreement with this discussion.[68] The crystals developed in this sample are 83% γ and 17% α. The thin section electron micrographs show an asymmetric bimodal population of crystallite thickness with relative contents similar to the fractional content of γ and α crystals obtained by WAXS. The lamellar thickness of the major population of crystals is 60 Å. This value agrees closely with the calculated value from the average length of isotactic sequences in this sample, 69 Å. In calculating this value, the length of the repeating unit in the c axis (2.17 Å) and the 40° tilt in γ type crystals of the chain axis with the crystal surface are considered. The thickness of the minor population of lamellae averages 110 Å.

In summary, in a consistent, but qualitative, manner the unique features of the γ polymorph of isotactic poly(propylene) can be explained. The explanation is based on the confluence of some basic principles. The key factors are the requirement of chains whose microstructure leads to thin crystallites and the structure of the interfacial region that requires tilted ordered chains in order for a lamellar crystallite habit to develop.

Acknowledgment. This work was supported by the National Science Foundation Polymer Program (DMR-94-19508) whose aid is gratefully acknowledged. R.G.A. acknowledges support from the Exxon Education Foundation, and M.J.G. acknowledges support from the National Research Council of Argentina (CONICET). We also thank Dr. Eric Lochner of the Materials Research and Technology Center of Florida State University (MARTECH) for helpful discussions.

References and Notes

(1) Brückner, S.; Meille, S. V.; Petraccone, V.; Pirozzi, B. *Prog. Polym. Sci.* **1991**, *16*, 361.
(2) Padden, F. J.; Keith, H. D. *J. Appl. Phys.* **1959**, *30*, 1479.
(3) Alamo, R. G.; Brown, G.; Mandelkern, L. *Polymer*, in press.
(4) Addink, E. J.; Beintema, J. *Polymer* **1961**, *2*, 185.
(5) Turner-Jones, A.; Aizlewood, J. M.; Beckett, D. R. *Makromol. Chem.* **1964**, *75*, 134.
(6) Bruckner, S.; Meille, S. V. *Nature* **1989**, *340*, 455.
(7) Meille, S. V.; Brückner, S.; Porzio, W. *Macromolecules* **1990**, *23*, 4114.
(8) Lotz, B.; Graff, S.; Straupé, S.; Wittmann, J. C. *Polymer* **1991**, *32*, 2902.
(9) Kardos, J. L.; Christiansen, A. W.; Baer, E. *J. Polym. Sci. (A-2)* **1966**, *4*, 777.
(10) Pae, K. D.; Sauer, J. A.; Morrow, D. R. *Nature* **1966**, *211*, 514.
(11) Campbell, R. A.; Phillips, P. J.; Lin, J. S. *Polymer* **1993**, *34*, 4809.
(12) Mezghani, K.; Phillips, P. J. *Polymer* **1997**, *38*, 5725.
(13) Brückner, S.; Phillips, P. J.; Mezghani, K.; Meille, S. V. *Macromol. Rapid Commun.* **1997**, *18*, 1.
(14) Lotz, B.; Graff, S.; Wittman, J. C. *J. Polym. Sci., Polym. Phys. Ed.* **1986**, *24*, 2017.
(15) Morrow, D. R.; Newman, B. A. *J. Appl. Phys.* **1968**, *39*, 4944.
(16) Kojima, M. *J. Polym. Sci. (B)* **1967**, *5*, 245.
(17) Kojima, M. *J. Polym. Sci. (A-2)* **1968**, *6*, 1255.
(18) Turner-Jones, A. *Polymer* **1971**, *12*, 487.
(19) Mezghani, K.; Phillips, P. J. *Polymer* **1995**, *36*, 2407.
(20) Cham, P. M.; Marand, H. *ACS Polym. Mater. Sci. Eng.* **1992**, *67*, 365.
(21) Giuidetti, G. P.; Busi, P.; Ginlianelli, I.; Zannetti, R. *Eur. Polym. J.* **1983**, *19*, 757.
(22) Horton, A. D. *Trends Polym. Sci.* **1994**, *2*, 158.
(23) Paukkeri, R.; Väänänen, T.; Lehtinen, A. *Polymer* **1993**, *34*, 2488.
(24) Lehtiner, A.; Paukkeri, R. *Macromol. Chem. Phys.* **1994**, *195*, 1539.
(25) Paukkeri, R.; Lehtinen, A. *Polymer* **1994**, *35*, 1673.
(26) Rieger, B.; Chien, J. C. W. *Polym. Bull.* **1989**, *21*, 159.
(27) Rieger, B.; Mu, X.; Mallin, D. T.; Ransch, M. D.; Chien, J. C. W. *Macromolecules* **1990**, *23*, 3559.

(28) Thomann, R.; Wang, C.; Kressler, J.; Mülhaupt, R. *Macromolecules* **1996**, *29*, 8425.
(29) (a) Fischer, D.; Mülhaupt, R. *Macromol. Chem. Phys.* **1994**, *195*, 1433. (b) Pérez, E.; Zucchi, D.; Sacchi, M. C.; Forlini, F.; Bello, A. *Polymer* **1998**, *40*, 675.
(30) Marigo, A.; Marega, C.; Zannetti, R.; Paganetto, G.; Canossa, E.; Coletta, F.; Gottardi, F. *Makromol. Chem.* **1989**, *190*, 2805.
(31) Randall, J. C. *J. Polym. Sci., Polym. Phys. Ed.* **1976**, *14*, 2083.
(32) Zambelli, A.; Zetta, L.; Sacchi, C.; Wolfsgruber, C. *Macromolecules* **1972**, *5*, 440.
(33) Grassi, A.; Zambelli, A.; Resconi, L.; Albizzati, E.; Mazzochi, R. *Macromolecules* **1988**, *21*, 617.
(34) Tsutsui, T.; Mizuno, A.; Kashiwa, N. *Makromol. Chem.* **1989**, *190*, 1177.
(35) Toyota, A.; Tsutsui, T.; Kashiwa, N. *J. Mol. Catal.* **1989**, *56*, 237.
(36) Cheng, H. N.; Ewen, J. A. *Makromol. Chem.* **1989**, *190*, 1931.
(37) Collins, S.; Gauthier, W. J.; Holden, D. A.; Kuntz, B. A.; Taylor, N. J.; Wardt, D. G. *Organometallics* **1991**, *10*, 2061.
(38) Mizuno, A.; Tsutsui, T.; Kashiwa, N. *Polymer* **1992**, *33*, 254.
(39) Randall, J. C. In *Polymer Sequence Determination: Carbon 13 NMR Method*; Academic Press: New York, 1977.
(40) Krigbaum, W. R.; Uematsu, I. *J. Polym. Sci., Polym. Chem. Ed., Part A* **1965**, *3*, 767.
(41) Galante, M. J.; Mandelkern, L.; Alamo, R. G.; Lehtinen, A.; Paukkeri, R. *J. Therm. Anal.* **1996**, *47*, 913.
(42) In ref 28 only the fraction of stereo defects is explicitly given. However, it is stated that regio defects are also present. Hence, the 4.4 mol % defects serves as a lower limit to the total defect concentration.
(43) We should note parenthetically that, after quenching thin films of all the poly(propylenes) from the melt to temperatures as high as about 60 °C, the so-called "smectic" form can develop.[69] However, we have also noted that the formation of this structure at the low crystallization temperatures depends on the film thickness. It can develop under rapid quenching conditions in films whose thicknesses are less than about 20 μm. The thickness of the films used to obtain the X-ray diffractograms are about 0.5 mm, so that a slower heat transfer throughout the film allows the formation of well-defined α type crystals.
(44) Mezghani, K.; Phillips, P. J. *Polymer* **1998**, *39*, 3735.
(45) Mezghani, K.; Campbell, R. A.; Phillips, P. J. *Macromolecules* **1994**, *27*, 997.
(46) Fatou, J. G. *Eur. Polym. J.* **1971**, *7*, 1057.
(47) Monasse, B.; Haudin, J. M. *Colloid Polym. Sci.* **1985**, *263*, 822.
(48) Utilizing the equilibrium melting temperature that has been given for the γ form as a function of pressure,[44] the crystallizations at 125 MPa of the 1.26% polymer and the 1.7% polymer at atmospheric pressure are carried out at approximately the same undercooling.
(49) Kalay, T.; Zhong, Z.; Allan, P.; Bevis, M. J. *Polymer* **1996**, *37*, 2077.
(50) Randall, J. C. *Macromolecules* **1997**, *30*, 803.
(51) Lotz, B.; Wittmann, J. C.; Lovinger, A. J. *Polymer* **1996**, *37*, 4979.
(52) The degrees of crystallinity were calculated using the same heat of fusion for the α and the γ forms. They have been reported to be similar.[44]
(53) Mandelkern, L. *Crystallization of Polymers*; McGraw-Hill: New York, 1964.
(54) Alamo, R. G.; Mandelkern, L. *Macromolecules* **1991**, *24*, 6480.
(55) Flory, P. J. *Trans. Faraday Soc.* **1955**, *51*, 848.
(56) Flory, P. J. *J. Am. Chem. Soc.* **1962**, *84*, 2857.
(57) Voigt-Martin, I. G.; Mandelkern, L. *J. Polym. Sci., Polym. Phys. Ed.* **1981**, *19*, 1769.
(58) Voigt-Martin, I. G.; Mandelkern, L. *J. Polym. Sci., Polym. Phys. Ed.* **1984**, *22*, 1901.
(59) Meille, S. V.; Ferro, D. R.; Brückner, S. *Macromol. Symp.* **1995**, *89*, 499.
(60) Voigt-Martin, I. G.; Alamo, R.; Mandelkern, L. *J. Polym. Sci., Polym. Phys. Ed.* **1986**, *24*, 1283.
(61) Michler, G. H.; Brauer, E. *Acta Polym.* **1983**, *34*, 533.
(62) Flory, P. J.; Yoon, D. Y.; Dill, K. A. *Macromolecules* **1984**, *17*, 862.
(63) Yoon, D. Y.; Flory, P. J. *Macromolecules* **1984**, *17*, 868.
(64) Flory, P. J. In *Principles of Polymer Chemistry*; Cornell University Press: Ithaca, NY, 1953.
(65) Corradini, P.; Petraccone, V.; Pirozzi, B. *Eur. Polym. J.* **1983**, *19*, 299.
(66) Mandelkern, L.; Fatou, J. G.; Howard, C. *J. Phys. Chem.* **1965**, *69*, 956.
(67) The calculation can be carried out for other types of nucleation and different parameters. Although the values of ξ^* change, the trends with defect concentration and temperature remain essentially the same.
(68) Brown, G. M.; Alamo, R. G.; Mandelkern, L., to be published.
(69) McAllister, P. B.; Carter, T. J.; Hinde, R. M. *J. Polym. Sci., Polym. Phys. Ed.* **1978**, *16*, 49.

MA981849R

EXHIBIT 4

Polymer Journal, Vol. 34, No. 9, pp 700—708 (2002)

Fractionation and Characterization for a Propylene–Ethylene Random Copolymer

Yu-Dong ZHANG,† Chang-Jiang WU, and San-Nong ZHU*

National Engineering Research Center for Polyolefin, Beijing Research Institute of Chemistry Industry, SINOPEC, Beijing 100013, China

**Institute of Chemistry, Chinese Academy of Sciences, Beijing 100080, China*

(Received May 7, 2002; Accepted August 9, 2002)

ABSTRACT: A random copolymer of propylene with 3.5 mol% ethylene comonomer is firstly fractionated by temperature rising elution fractionation (TREF). Techniques including ^{13}C nuclear magnetic resonance (NMR) spectroscopy, Fourier transform infrared spectroscopy (FT-IR), gel-permeation chromatography (GPC), crystallization analysis fractionation (Crystaf) and differential scanning calorimetry (DSC) are used to characterize the obtained fraction polymers. The results show that each fraction polymer is composed mainly of isotactic propylene sequence plus a small amount of ethylene comonomer and has uniform molecular weight and ethylene content. The PPP, PPE, and PEP are main part of triad sequence unit. As the elution temperature increasing, ethylene content of the fraction polymers decreases, number average molecular weight increases, and meanwhile number average sequence length of propylene, $\bar{n}_P$, increases, while that of ethylene, $\bar{n}_E$, decreases, close to 1. The results show that ethylene content affects linearly the melting temperature (T_m) in a range of ethylene content being as low as less than 10.23 mol%; there is a linear relationship between the reciprocal melting temperature ($1000/T_m$, K^{-1}) and reciprocal number average molecular weight (M_n^{-1}) in a range of number average molecular weight as low as less than 1.7×10^5.

KEY WORDS Elution Temperature / Ethylene Content 1/K / Melting Temperature / Number Average Molecular Weight / Sequence Length / Tacticity / Temperature Rising Elution Fractionation (TREF) /

Polypropylene is a common semi-crystalline synthetic polymer, and its macromolecular chain structure is an important factor to affect such properties of propylene polymers as crystallization behavior, morphologies, melting temperature, degree of crystallization, toughness, and rheological and optical properties. By the way of introducing some comonomers (*e.g.*, ethylene) into its macromolecular chain, the performance of propylene polymers can be improved purposefully and effectively. Because propylene tacticity and ethylene comonomer complicate the macromolecular chain structure, and can farther lead to complex crystallization behaviors and morphologies, it is very important to firstly characterize the macromolecular chain structure well. In order to investigate thoroughly the relationship between performance and macromolecular chain structure, it is necessary to make samples uniform. Temperature rising elution fractionation (TREF)[1–15] has been shown to be a powerful technique to make crystal polyolefins uniform on the basis of their crystallizability and molecular weight. Through TREF experiments, a set of fraction polymers with uniform molecular weight and content of ethylene comonomer can be obtained; hereafter crystallization analysis fractionation (Crystaf) will be used to check the effect of fractionation by analyzing such parameters as σ and R,[16] which can define the broadness of the crystallization temperature distribution of the fraction polymers.[16–22] Up to now most samples of propylene copolymers on investigation are the impact propylene–ethylene copolymers, a very complex blend. Even though after they have been fractionated by TREF,[3–11] each fraction polymer also consists of PE, PP, propylene–ethylene copolymer and so on, so it is difficult to make sure the relationship among performance, macromolecular chain structure and elution temperature. However the corresponding random copolymers of propylene are not blends, but has received much less attention, and our knowledge of the topic is very limited.[23,24] Brull *et al.*[23] ever made a study on propylene–ethylene random copolymers, in which the samples, with comonomer content as low as less than 3.5 mol%, are obtained by polymerization. The comonomers are considered as defects in propylene long chains, so relationships between melting temperature and content of the comonomers are determined, but the effect of molecular weight on melting temperature is ignored,

The aim of the present study is to first characterize the macromolecular chain structure of uniform propylene polymers, including ethylene content, number average molecular weight, number average sequence length, tacticity and so on, then to study a relation-

†To whom correspondence should be addressed (E-mail: YD-Zhang@brici.ac.cn, Fax: +86-10-64273136).

Table I. Quality specifications of the samples

	$\frac{T_m}{°C}$	$\frac{T_c}{°C}$	$\frac{M_n}{g\ mol^{-1}}$	M_w/M_n	$\frac{T_w}{°C}$	$\frac{T_n}{°C}$	R	σ	$\frac{[E]}{mol\%}$
PERC	144.0	98.3	56703	4.76	65.5	63.1	3.8	9.9	3.5
PHP	163.4	114.0	70662	3.67	80.6	79.4	1.4	6.4	0

ship between melting temperature (elution temperature considered as melting temperature in solution) and macromolecular chain structure. In a typical experiment, a copolymer of propylene with 3.5 mol% of ethylene comonomer is first fractionated by using a preparative TREF. Then the fraction polymers are characterized by ^{13}C nuclear magnetic resonance (NMR) spectroscopy, Fourier transform infrared spectroscopy (FT-IR), gel-permeation chromatography (GPC), crystallization analysis fractionation (Crystaf) and differential scanning calorimetry (DSC). Finally, the relationships between melting temperature and ethylene content & number average molecular weight will be discussed.

EXPERIMENTAL

Materials

The samples used in this study are a commercial copolymer of propylene with a small amount of ethylene comonomer (PERC) and a commercial propylene homopolymer (PHP) initiated with Z-N Ti-catalyst by a liquid phase bulk polymerization process. The product quality specifications are listed in Table I. Before being used, the polypropylene homopolymer is treated with *n*-heptane for more than 10 h to extract and remove the low stereoregular and small molecular weight polymer. The propylene–ethylene random copolymer is fractionated by TREF to obtain a set of fraction polymers. In the Table I, T_w is the weight average crystallization temperature; T_n is the number average crystallization temperature; σ and R are parameters defining the broadness of the crystallization temperature distribution of the fraction polymers.[16]

Preparative TREF

A preparative TREF is used to carry out fractionation of the propylene–ethylene random copolymer sample. The preparative TREF system consists of a jacketed column thermo-stated to ±0.1°C by circulating heated oil and a fractionation column with free volume of 1240 mL made of a large double-walled glass condenser and packed with fine glass beads. About 15 g of sample is first dissolved in 400 cm^3 of 1,2,4-trimethylbenzene at 140°C, and stabilized with the antioxidant 2,6-di-*t*-butyl-*p*-cresol (3 g/1000 mL). Then the solution is transferred into the fractionation column from the top end of the column at 140°C. In order to make polymer deposit around the glass beads in layers step by step on the basis of the crystallizability, it takes more than 70 h for the column to be cooled to room temperature. With this process, the most easily crystallizable polymers precipitate first and deposits on the glass beads in the innermost layer. On the contrary, the polymers with the least crystallinity precipitate last and deposit on the outermost layer. As the column is heated, and the elution temperature increases, the polymers on the outermost layer is first eluted with 1,2,4-trimethyl benzene, and subsequent polymers are collected. While increasing the elution temperature stepwise from room temperature to 140°C, a set of fraction polymer will be obtained. The fraction polymers obtained from TREF are precipitated into a large excess of acetone at room temperature, then filtered and dried in vacuum at 60°C to constant weight.

Crystaf

Commercial Crystaf equipment, Model 200, manufactured by Polymer Char S.A., is used to check the effect of TREF experiment to obtain such parameters as σ, R, T_w, and T_n.[16] Concentrations of 0.1% (w/v) are used in this experiment, with 30 mg of samples in 30 mL of 1,2,4-trichlorobenzene solvent. The crystallization process is carried out in stirred stainless steel reactors of 60 mL volume where dissolution and filtration takes place automatically. The whole process of temperature changes during the experiments is as follows: from room temperature to 160°C at rate of 30°C m^{-1}, after staying for 60 min at 160°C, the temperature decreases to 95°C at rate of 30°C m^{-1}, staying 45 min, then the experiments begin from 95°C to 25°C at rate of 0.1°C m^{-1}. In order to monitor the concentration for the samples in solution *in situ*, an infrared detector with a fixed wavelength of 3.5 μm is used to detect the intensity of the C–H stretching frequencies of methylene and methyl group. As temperature decreases according to the temperature program, the samples experience the stepwise crystallization. By monitoring on-line intensity of absorbance peak of the fraction polymers, the polymer concentration in solution is measured in time, which can reveal the crystalline process.

^{13}C NMR Analysis

^{13}C NMR spectra are measured on a Bruker

Table II. Fractionation of the propylene–ethylene random copolymer

Fraction No.	T_e(°C)	W_i (mg)	$W_i/\Delta T_i$ (mg °C^{-1})	W_i (%)	ΣW_i (%)
F1	26.98	553.5		3.57	3.57
F2	52	583.7	23.33	3.91	7.48
F3	65	608.7	46.82	4.08	11.56
F4	75	670.9	67.01	4.49	16.05
F5	85	1296	129.6	8.68	24.73
F6	90	924.2	184.8	6.19	30.92
F7	95	1781.9	356.38	11.94	42.86
F8	100	3350.1	670	22.44	65.3
F9	102	569.4	284.7	3.81	69.11
F10	105	1506	502.1	10.09	79.2
F11	107	1227.1	613.55	8.22	87.42
F12	110	1780.5	593.5	11.93	99.35
F13	112	46.9	23.45	0.31	99.66
F14	115	8.8	2.67	0.06	99.72
F15	117	3.7	1.85	0.02	99.74
F16	120	3.8	1.27	0.03	99.79
F17	123	1.1	0.3	0.01	99.80
F18	140	10.7	1.53	0.07	99.87
F19	>140	20.6			

Weight of sample used: 14996.8 mg. Total recovery: 14898.9 mg (99.35%, ≦110°).

400 MHz FT NMR spectrometer operating at 100 MHz on polymer solutions (< 20 wt%) in *o*-dichlorobenzene at 110°C, the highest single peak of which is considered as the reference (132.9 ppm). A program with pulse angle of 90° is used, matching with 2 s acquisition time and 10 s relaxation delay, so as to attain conditions far from any saturation but close enough to the maximum signal-to-noise ratio. In order to eliminate the NOE, an inverse-gate decoupling pulse program is selected, and meanwhile proton broad-band decoupling is achieved with the walth 16 sequence. Due to the high resonance, 5000–15000 scans are collected with 64 k points/scan. The nomenclature and assignments of the different carbon atoms along the molecular chain adopted for the absorption bands in the NMR spectra are those of Carman & Wilkes, Randall and Cheng.[25–28]

FT-IR

FT-IR spectra are measured with a Nicolet Fourier transform infrared spectrophotometer (MAGNA-IR 760). The samples are first compression-molded into films in 10–100 μm thick. Then the absorption bands are observed and analyzed.

GPC

A gel-permeation chromatography (GPC, waters, Alliance GPCV 2000), equipped with a polystyrene column in the GPC-viscometer module, is used for the characterization of the molecular weight and molecular weight distribution of the fraction polymers at 140°C. The molecular weight obtained is calculated by a standard procedure based on the universal calibration curve of polystyrene.

DSC

DSC measurement is carried out on a DSC-7 from Perkin–Elmer. In order to ensure an identical thermal history, the sample is heated from 0°C to 190°C at a rate of 10°C min^{-1} and subsequently cooled down from 190°C to 0°C at same rate. The maximum of the exotherm in the cooling cycle is utilized to determine the crystallization temperature, T_c. The melting endothermic changes are recorded while heating the sample from 0°C to 190°C at a heating rate of 10°C min^{-1}, and the peak maximum of the second heating cycle is used to determine the melting temperature, T_m.

RESULT AND DISCUSSION

Fractionation and Characterization

TREF. A copolymer of propylene with a small amount of ethylene comonomer is fractionated by using a preparative TREF as described above, and 18 fraction polymers are collected from room temperature (about 26°C) to 140°C. Important data of the fractionation experiment are summarized in Table II, including elution temperature (T_e, °C), the weight of fraction polymers (W_i for the ith fraction), the differential weight to temperature ($W_i/\Delta T_i$), the accumulative weight (ΣW_i) and so on. Figure 1 shows the curves of the accu-

Table III. Characteristics of Fraction Polymers

Fraction No.	T_m °C	T_c °C	M_n g mol^{-1}	M_w/M_n	T_w °C	T_n °C	R	σ
F2	97.9	58.3	20989	3.5				
F3	114.0	75.6	30566	3.295	35.9	35.6	0.7	3.0
F4	123.4	84.6	44642	3.529	44.1	43.8	0.7	3.2
F5	132.2	92.6	52243	3.705	52.1	51.7	0.8	4.4
F6	136.9	95.5	60542	3.273	56.8	56.3	0.9	5.1
F7	141.9	100.0	87164	2.850	59.1	58.4	1.1	6.0
F8	146.2	102.5	105040	2.795	63.2	62.5	1.0	5.8
F9	147.7	105.6	101123	2.928	67.6	67.4	0.4	3.5
F10	150.5	105.5	126632	2.705	69.6	69.1	0.7	4.4
F11	150.5	107.1	151702	2.643	71.8	71.7	0.1	2.8
F12	152.7	107.3	169953	2.645	73.8	74.1	−0.4	2.0

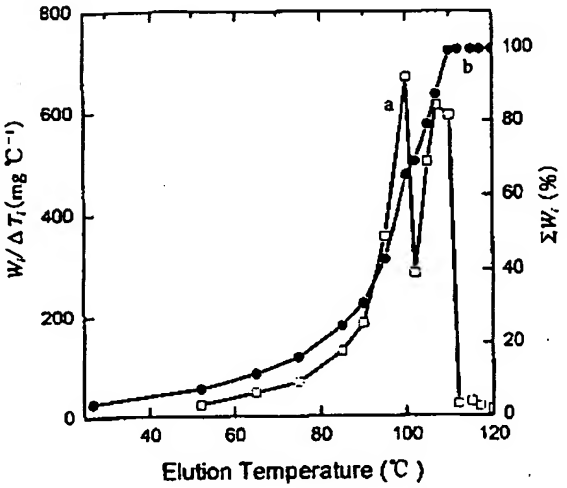

Figure 1. The curves of temperature rising elution fractionation for the propylene–ethylene random copolymer. The weight of the fraction polymers as a function of the elution temperature (°C) (a) the differential weight to temperature, $W_i/\Delta T_i$ (mg °C^{-1}), (b) accumulative weight, $\sum W_i$ (%).

mulative weight and the differential weight to temperature against elution temperature. From the curve of the differential weight to temperature, $W_i/\Delta T_i$, against temperature, we can observe two peaks at 95–100°C and 105–107°C, respectively, implying the fractionation process is complicated. The curve of accumulative weight indicates that at elution temperatures below 85°C or above 110°C, the weight of each fraction polymer is low, though most fractions occur over a narrow temperature region, 85–110°C, suggesting that macromolecular chain structure of the copolymer is uniform. The curves of accumulative weight appears nearly a straight line in a range from 85°C to 110°C.

Crystaf

Through Crystaf experiment, the effect of fractionation by TREF can be checked up. Table III summarizes the characteristics of the fraction polymers. Figure 2

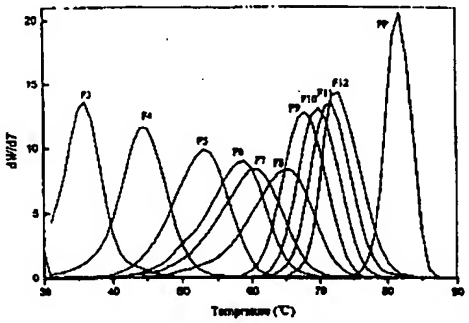

Figure 2. The concentration in solition determined by Crystaf of the fraction polymers as a function of the temperature.

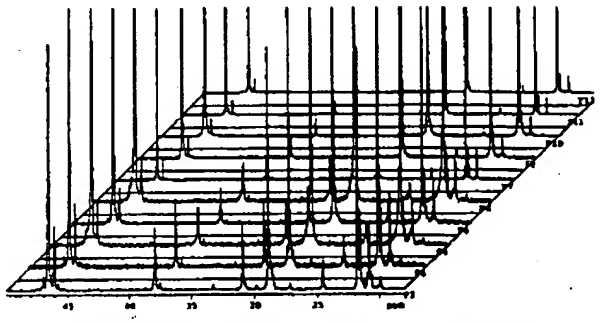

Figure 3. ^{13}C NMR spectra of fraction polymers.

shows the curves of the crystallization temperature distribution from the Crystaf experiment. In the experiment, the concentration of the corresponding fraction polymers in solution is determined as a function of temperature. By analyzing such parameters put forward by B. Monrabal as T_w, T_n, R, and σ,[16] the uniform of crystallization temperature distribution of the fraction polymers can be characterized. The results indicate that the broadness of the crystallization temperature distribution of the fraction polymers becomes narrower than that of rude samples, and the fraction polymers at low or high elution temperature have narrower distribution than at middle area of elution temperature, showing that the effect of fractionation is good.

Table IV. Chemical shifts and intensities for the carbon atom in propylene–ethylene copolymer in ^{13}C NMR

Chemical shift		Peak intensity(%)									
	ppm	F2	F3	F4	F5	F6	F7	F8	F10	F11	F12
$S_{\alpha\alpha}$	46.5	1000	1000	1000	1000	1000	1000	1000	1000	1000	1000
$S_{\alpha\gamma}$	37.9	207.3	148.8	123.8	97.3	85	68.4	59.5	44.2	42.2	35.7
$S_{\alpha\delta}$	37.5	23.5	12.0	5.9	3.4	1.1					
$S_{\beta\delta}$	27.2	23.5	12.0	5.9	3.4	1.1					
$S_{\gamma\delta}$	30.4	2.4	0.9								
$S_{\delta\delta}$	30.0	0.4									
$T_{\beta\beta}$	28.98	918.7	931.8	958.3	957.7	978.7	988.2	988.1	992.6	995.5	1010.6
$T_{\beta\delta}$	30.99	217.8	164.2	136.4	102.1	90.6	72.3	61.1	45.3	44.0	37.2
$T_{\delta\delta}$	33.27	11.4	4.5								

Table V. Sequence distributions of the fraction polymers

	F2	F3	F4	F5	F6	F7	F8	F10	F11	F12
PPP	71.91	78.49	82.43	86.14	88.03	90.27	91.58	93.64	93.86	94.83
PPE	17.05	13.83	11.73	9.18	8.15	6.60	5.66	4.27	4.15	3.49
EPE	0.89	0.38	0	0	0	0	0	0	0	0
PEP	8.11	6.27	5.32	4.38	3.82	3.12	2.76	2.08	1.99	1.68
EEP	1.84	1.03	0.51	0.31	0	0	0	0	0	0
EEE	0.19	0	0	0	0	0	0	0	0	0
PP	80.48	85.70	88.29	90.71	92.17	93.60	94.35	95.77	95.95	96.55
PE	18.57	13.78	11.45	9.14	7.83	6.40	5.65	4.23	4.05	3.45
EE	0.95	0.51	0.26	0.15	0	0	0	0	0	0
P	89.76	92.59	94.01	95.28	96.08	96.80	97.17	97.88	97.98	98.28
E	10.23	7.41	5.99	4.72	3.92	3.20	2.83	2.12	2.02	1.72

^{13}C NMR

Figure 3 is the ^{13}C NMR spectra of fraction polymers. Here each spectrum relates to the fraction polymer with certain ethylene content, and they are positioned from F2–F12 according to ethylene content. The peaks of ^{13}C NMR spectra are assigned according to the methods of Carman & Wilkes,[25] Randall[26,27] and Cheng,[28] and Table IV lists the assignment of the important peaks, chemical shifts and intensity of each carbon atom in the ^{13}C NMR spectra of the fraction polymers. In ^{13}C NMR spectrum, $S_{\alpha\gamma}$ (37.9 ppm), $S_{\alpha\delta}$ (37.5 ppm), and $S_{\gamma\delta}$ (30.4 ppm) are thought to relate to the following sequence structure, (1) only an ethylene monomer, PEP; (2) more than two-linked ethylene monomers, P(E)nP, $n \geqq 2$; (3) more than three ethylene monomers, P(E)mP, $m \geqq 3$, respectively. The results show that with elution temperature increasing, peaks of $S_{\alpha\gamma}$, $S_{\alpha\delta}$ and $S_{\gamma\delta}$ decreases, implying the ethylene content decreases. As elution temperature increases beyond 75°C and 90°C, the $S_{\gamma\delta}$ and $S_{\alpha\delta}$ peak vanish one by one, suggesting that the sequence structure of P(E)nP, $n \geqq 2$ begin not to exist in the macromolecular chains at higher elution temperature. In addition, as seen from the experiment, $S_{\alpha\delta}$ is much more than and $S_{\gamma\delta}$, suggesting PEEP is majority in P(E)nP. The dyad sequence distribution of the copolymers is determined from the methylene peaks by using the following relationships:[26,27]

$$PP = S_{\alpha\alpha} \tag{1}$$

$$EP = S_{\alpha\gamma} + S_{\alpha\delta} \tag{2}$$

$$EE = (S_{\alpha\delta} + S_{\delta\delta})/2 + S_{\gamma\delta}/4 \tag{3}$$

The triad sequence distribution will be analyzed from both methine and methylene absorptions peaks, using:

$$PPP = T_{\beta\beta} \tag{4}$$

$$PPE = T_{\beta\delta} \tag{5}$$

$$EPE = T_{\delta\delta} \tag{6}$$

$$PEP = S_{\beta\beta} = S_{\alpha\gamma}/2 \tag{7}$$

$$EEP = S_{\alpha\delta} = S_{\beta\delta} \tag{8}$$

$$EEE = S_{\delta\delta}/2 + S_{\gamma\delta}/4 \tag{9}$$

From the dyad sequence distributions, the ethylene content can be calculated as follows:

$$P = PP + PE/2 \tag{10}$$

$$E = EE + PE/2 \tag{11}$$

Table V summarizes sequence distribution of the fraction polymers. As can be seen from Table V, in macromolecular chains, PPP holds the majority of the sequence units, varying from 71.9 to 94.8 mol%. The number average sequence length of the fraction polymers is derived from the following relationship:[26,27]

Table VI. Number average sequence length of the fraction polymers

	F2	F3	F4	F5	F6	F7	F8	F10	F11	F12
$\bar{n}_P$	9.7	13.4	16.4	20.8	24.6	30.3	34.7	46.3	48.4	57.0
$\bar{n}_E$	1.10	1.07	1.04	1.03	1	1	1	1	1	1

$$\bar{n}_P = \frac{[PP] + \frac{1}{2}[PE]}{\frac{1}{2}[PE]} \quad (12)$$

$$\bar{n}_E = \frac{[EE] + \frac{1}{2}[PE]}{\frac{1}{2}[PE]} \quad (13)$$

where $\bar{n}_P$ and $\bar{n}_E$ are the number average sequence lengths of monomer P and E, respectively. The number average sequences length, $\bar{n}_P$ and $\bar{n}_E$, are tabulated in Table VI. As shown in Figure 3, Table V, and Table VI, during TREF process, with elution temperature increasing from 52°C to 110°C, ethylene content in fraction polymers is gradually reduced, and number average sequence length of propylene, $\bar{n}_P$, becomes longer and longer, however that of ethylene, $\bar{n}_E$, decreases. When elution temperature in the range from 52°C to 85°C, the ethylene content are more than 4.72 mol%, the n_E is more than 1 and the small peak of $S_{\alpha\delta}$ can appear at 37.5 ppm, implying that a very small amount of more than one ethylene units, like EE, exist in macromolecular chains (F2, F3, F4, and F5). For example, when elution temperature is as low as 52°C, *i.e.*, ethylene content (F2) in about 10.23 mol%, number average sequence length of propylene polymer, $\bar{n}_P$, is only 9.7, however that of ethylene, $\bar{n}_E$, is 1.1, in addition, the intensity of the $S_{\delta\delta}$ peak at 30.0 ppm is 0.4, implying that in F2 fraction polymers there exists a very small amount of three or more ethylene monomers-linked units, like short block ethylene units EEE. The weight of the partial fractions from F2 to F5 is as low as less than 25 wt%. As elution temperature increases from 90°C to 110°C, *i.e.*, ethylene content decreases from 3.92 to 1.72 mol%, $\bar{n}_P$ becomes longer and longer, but $\bar{n}_E$ is close to 1, suggesting that it becomes almost improbable that two ethylene comonomers are successively inserted into a macromolecular chain simultaneously, namely, there is only single E in a macromolecular chain, not EE and EEE sequence. For example, $\bar{n}_P$ and $\bar{n}_E$ of F12 are 57 and 1, respectively, and the peak of $S_{\alpha\delta}$ at 37.5 ppm no longer appears. At elution temperature above 110°C, the weight of fraction polymers with ethylene content as low as less than 1.72 mol% is less than 1 wt%. From above-mentioned analysis, a conclusion can be drawn that most (more than 75 wt%) of the random copolymer can been fractionated in a range of ethylene content from 1.72 to 3.92 mol%; and the triad of PPP, PPE, and PEP are predominately preserved.

Since propylene tacticity complicates the molecular microstructure, it is necessary to assign and scrutinize some peaks that can reflect information on tacticity of propylene segment. Figure 4 indicates fine assignment of some peaks of the fraction polymers, including $S_{\alpha\gamma}$, $S_{\alpha\delta}$. According to Randall and Cheng,[26–28] the $S_{\alpha\gamma}$ reflects sequence structure of the PEP, namely, only an ethylene monomer between two propylene monomers, and the experiment suggests that this kind of sequence structure occupies the majority of the macromolecular chains; $S_{\alpha\delta}$ reflects sequence structure of the P(E)nP, $n \geq 2$, namely, more than two-linked ethylene monomers between two propylene monomers. Figure 4 shows $S_{\alpha\gamma}$ consists of two main peaks: 1a and 1b, which can be assigned to molecular sequence structure of the PPPEP(m_1r_2) and PPPEP (m_1m_2), respectively. The spectrum reveals that the PPPEP (m_1m_2) occupies most part of the PEP, more than 90 wt%, implying that isotacticity sequence of propylene segment is very high, and the distribution of ethylene comonomer in macromolecular chains is almost uniform too. The 1c and 1d included in $S_{\alpha\delta}$ can be assigned to EPEEP and PPEEP, respectively. The results indicate that PPEEP (m) is most sequence unit. From Figures 3 and 4, we can find that with elution temperature increasing, isotacticity of propylene segment becomes higher and higher, and the distribution of ethylene comonomer in macromolecular chains becomes more and more uniform.

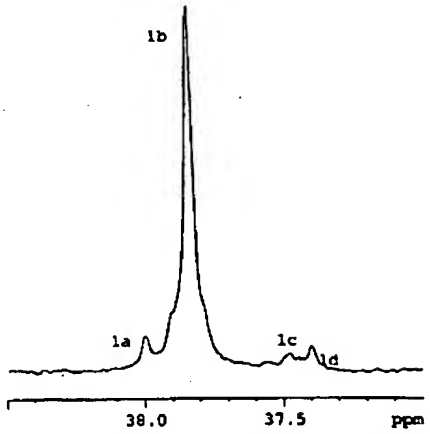

Figure 4. Expanded plots of the $S_{\alpha\gamma}$ and $S_{\alpha\delta}$ region.

If the ethylene comonomer and racemic structure of propylene sequence are thought to be the attribution to the destruction of tacticity of propylene polymer, the peaks of methyl from 18 to 23 ppm in Figure 5 must be considered. According to Randall and Cheng,[26–28] the peaks of 2a, 2b, 2c, and 2d are assigned

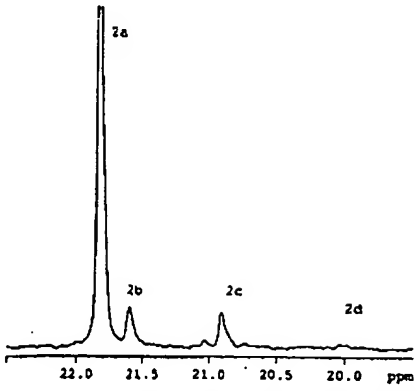

Figure 5. Expanded plots of the methyl region.

to PPPPP (mmmm), PPPPE (mmm) + PPPPP (mmmr), PPE (m) + PPP(mr), EPE + PPP(rr), respectively. As seen from Figures 3 and 5, the PPPPP (mmmm) is the most probable sequence unit of fraction polymers, suggesting that the fraction polymer is a copolymer with high isotactic propylene sequence plus a small amount of ethylene comonomer. So we can conclude that with elution temperature increasing, the tacticity of propylene sequence becomes higher and higher.

FT-IR

The above-mentioned conclusion is also supported by FT-IR experiments. According to Rudin and Bucci,[29–31] the absorption peak at 733 cm^{-1} in Figure 6 can be assigned to the $-(CH_2)_n-$, $n = 3$, but the absorption peak at 722 cm^{-1}, which can reflect the structure of $-(CH_2)_n-$, $n > 3$, do not appear, implying that the amount of the long chain ethylene is too small to be detected distinctly. In other words, the ethylene comonomer incorporated in macromolecular chains is mainly isolated, and there is hardly a group of two or more ethylene monomers in the propylene macromolecular chains. The conclusion from FT-IR is identical to that by NMR. In addition, the experiment also reveals that with eluting temperature increasing from environment temperature to 110°C, the intensity of absorption peak at 733 cm^{-1} of IR spectra of fraction polymers becomes smaller and narrower, showing that the ethylene content in fraction polymers gradually decreases.

Melting and Crystallization Behavior

For copolymers of propylene with a small amount of ethylene comonomer, the macromolecular chain length and the ethylene content are considered to be the important factors to affect the melting and crystallization behavior of copolymers. The melting temperature of the fraction polymers from solution can be obtained from TREF, $T_{m\,(sol)}$, and the melting temperature of fraction

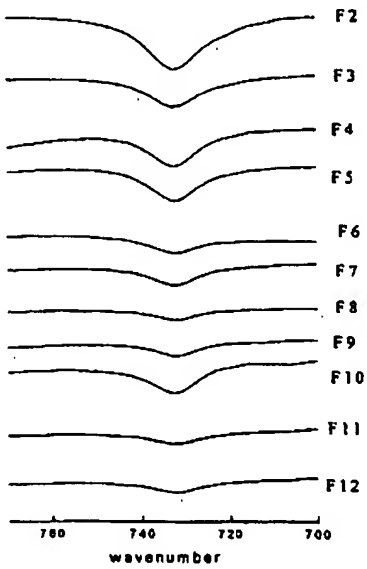

Figure 6. FT-IR spectra of the fraction polymers of the Propylene–ethylene random copolymers.

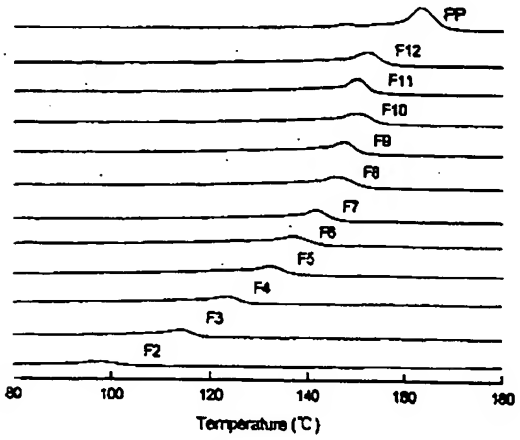

Figure 7. DSC endothermal curves (2nd heating cycle) of the fraction polymers of the propylene–ethylene random copolymer. Heating rate at 10°C min^{-1}.

polymers & the propylene homopolymer from bulk will be recorded from DSC experiments. All DSC endothermic curves are put in Figure 7. Here DSC curves are positioned according to ethylene content. The maximum of the endothermic peak is recorded as the melting temperature, T_m. In order to ensure an identical thermal history of the investigated fraction polymers, only the melting temperatures obtained during a second heating cycle are considered.

On the basis of Flory's theory, in the propylene–ethylene random copolymer, propylene chains is considered as a long crystallizable chain, however ethylene as no crystallizable comonomer, *i.e.*, they will be excluded from the polypropylene crystal lattice as de-

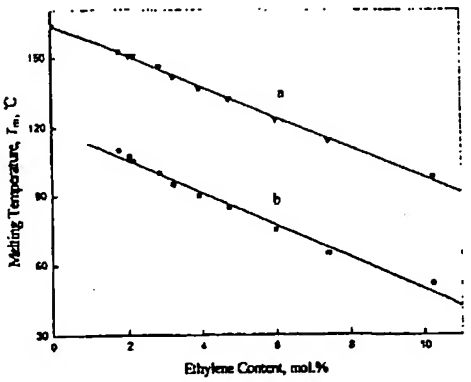

Figure 8. Melting temperature of the propylene–ethylene random copolymer, as a function of ethylene content (mol%). a: Melting Temperature in bulk (T_m, °C) determined by DSC. b: Melting Temperature in solution ($T_{m\,(sol)}$, °C) determined by TREF.

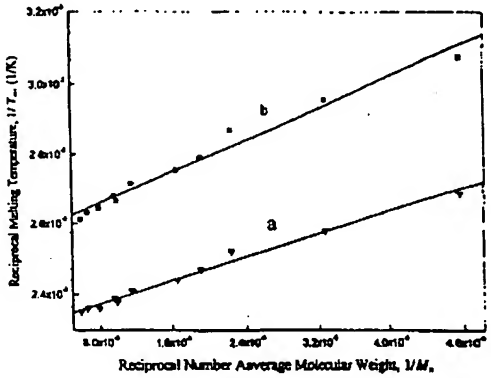

Figure 9. Reciprocal melting temperature, $1/T_m$, (1/K) *vs.* reciprocal number average molecular weight of the fraction polymers ($1/M_n$). a: Melting Temperature in bulk (T_m, K) determined by DSC. b: Melting Temperature in solution ($T_{m\,(sol)}$, K) determined by TREF.

fects.[23] According to Benjamin Monrabal[16] and Robert Brull,[23] the Flory eq 14[32] can be simplified to eq 15, which reveals a relationship between melting temperature and content of comonomer, by assuming that the melting temperature of the copolymer, T_m, is close to that of the propylene homopolymer, T_m^0, hence, $T_m \times T_m^0 \approx (T_m^0)^2$, and also that ΔH_u is constant in the considered crystallization temperature range. A straight-line relationship between T_m and comonomer content is obtained, which is good fit in a range of content of comonomer less than 3.5 mol%.[23] Figure 8 shows the curves of the melting temperature of copolymer as a function of ethylene content according to eq 15. In Figure 5, line a is for the melting temperature from bulk by DSC, and line b is for melting temperature from solution by TREF.

$$\frac{1}{T_m} - \frac{1}{T_m^\circ} = \frac{-R}{\Delta H_u} Lnp \tag{14}$$

$$T_m \cong T_m^0 - \frac{R(T_m^0)^2}{\Delta H_u} X_E \tag{15}$$

On the other hand, macromolecular chain length is also an important factor to affect the melting and crystallization behavior of polymer. For copolymer of propylene plus a small amount of ethylene comonomer, when ethylene content is less than 10.23 mol%, the macromolecular chain of the copolymer is considered identical to that of propylene homopolymer. Therefore, another application of Flory's theory is shown as eq 16,[33] which relates to melting temperature, T_m, with number average molecular weight. In eq 16, i is the number average degree of polymerization. When number average degree of polymerization, i, is transformed to number average molecular weight, M_n, the eq 16 will be replaced by eq 17.

$$\frac{1}{T_m} - \frac{1}{T_m^\circ} = \frac{2R}{\Delta H_u} \times \frac{1}{i} \tag{16}$$

$$\frac{1}{T_m} - \frac{1}{T_m^\circ} = \frac{2R_m}{\Delta H_u} \times \frac{1}{M_n} \tag{17}$$

Figure 9 indicates the effect of number average molecular weight on melting temperature. A linear relationship exists between the reciprocal melting temperature ($1000/T$, K^{-1}) and reciprocal number average molecular weight (M_n^{-1}) in a range of number average molecular weight of less than 1.7×10^5, which is in good agreement with the Flory's theory.[33] According to the experiment, with the number average molecular weight (M_n) increasing, the melting temperatures, from both solution, $T_{m\,(sol)}$ and from bulk, T_m, decreases. Within the range of ethylene content less than 10.23 mol%, the melting temperature, T_m, is dependant on the molecular chain length, even though the number average molecular weight is very large nearly to 1.7×10^5. In Figure 9, the line a and line b have same meaning to that in Figure 8.

As seen from Tables III, Figures 8 and 9, when number average molecular weight of the polymers increases, but the ethylene content and the poly-dispersity (M_w/M_n) of molecular weight decreases, the melting temperature increases. In other words, the larger the number average molecular weight, the smaller the ethylene content, and the narrower the poly-dispersity, the higher the melting temperature of polymer is. When polymer has higher ethylene content, the regularization of macromolecular chains is poor, so it is easy to melt at lower temperature (F2, F3, F4, and F5), even though those polymers with higher molecular weight. Therefore, at least two kinds of macromolecular chains have lower melting temperature, that is, the macromolecular chains with low molecular weight and those with high ethylene content. As number average molecular weight of the polymers becomes larger, and ethylene content and poly-dispersity (M_w/M_n) of fraction poly-

mers decreases, regularization of the macromolecular chains becomes higher, so the melting temperature of polymer is higher. Therefore we may conclude that only the macromolecular chains with both high molecular weight and low ethylene content have high melting temperature, that is, the better the regulation of macromolecule, the higher the melting temperature. For example, ethylene content and M_w/M_n of F11 with high melting temperature are only 2 mol% and 2.6, respectively, and its number average molecular weight is also beyond 1.5×10^5. The broadness of crystalline temperature distribution of fraction polymers is also important parameter charactering for crystalline polymers. As shown in Table III, in the range from 85 to 100°C, the fraction polymers has large σ, this is because the crystalline mechanism and morphologies are complicated enough to widen the distribution of crystalline temperature of fraction polymers. With regularization of the macromolecular chain increasing, σ of the fraction polymers decreases, for example, that of F12 is even unexpectedly negative, suggesting that the fraction polymer is uniform very much.

CONCLUSIONS

A set of fraction polymers with uniform molecular weight and ethylene content can be obtained by using a preparative TREF. Each fraction polymer is composed of mainly isotactic propylene sequence plus a small amount of ethylene comonomer. Macromolecular chains with high ethylene content or that of low molecular weight have low melting temperature, however the macromolecular chains with both high molecular weight and low ethylene content have high melting temperature. Distribution of ethylene monomers in a macromolecular chain is uniform, and the propylene sequence had high tacticity. Ethylene content affects linearly the melting temperature in a range of ethylene content as low as less than 10.23 mol%; and there is a linear relationship between the reciprocal melting temperature ($1000/T_m$, K^{-1}) and reciprocal number average molecular weight in a range of number average molecular weight (M_n^{-1}) less than 1.7×10^5.

Acknowledgment. Supported by the Special Funds for Major State Basic Research Projects of P. R. China (G1999064807). Supported by the Basic Research Funds of SINOPEC (X501016).

REFERENCES

1. J. B. P. Soares and A. E. Hamielec, *Polymer*, 36, 1639 (1995).
2. J. Xu and L. Feng, *Eur. Polym. J.*, 36, 867 (2000).
3. P. W. O. Wijga, J. V. Schooten, and J. Boerma, *Macromol. Chem.*, 36, 115 (1960).
4. F. M. Mirabella, Jr., *J. Appl. Polym. Sci., Appl. Polym. Symp.*, 51, 117 (1992).
5. T. Usami, Y. Gotoh, H. Umemoto, and S. Takayama, *J. Appl. Polym. Sci., Appl. Polym. Symp.*, 52, 145 (1993).
6. T. Abiru, A. Mizuno, and F. Weigand, *J. Appl. Polym. Sci.*, 68, 1493 (1988).
7. Y. Feng and J. N. Hay, *Polymer*, 39, 6723 (1998).
8. J. Xu, L. Feng, S. Yang, and Y. Wu, *Polymer*, 38, 4381 (1997).
9. R. Zacur, G. Goizueta, and N. Capital, *Polym. Eng. Sci.*, 39, 921 (1999).
10. H. Mori, H. Kono, and M. Terano, *Macromol. Chem. Phys.*, 201, 543 (2000).
11. J. Xu, Y. Deng, and L. Feng, *Polym. J.*, 30, 824 (1998).
12. V. Desreux and M. C. Spiegels, *Bull. Soc. Chim. Belg.* 59, 476 (1950).
13. S. W. Hawkins and H. J. Smith, *J. Polym. Sci.*, 28, 341 (1958).
14. E. Karbashewski, A. Rudin, L. Kale, and W. J. Tchir, *Polym. Eng. Sci.*, 32, 1370 (1999).
15. G. Elicabe, J. Carella, and J. Borrajo, *J. Polym. Sci., Part B: Polym. Phys.*, 34, 527 (1996).
16. B. Monrabal, J. Blanco, J. Nieto, and J. B. P. Soares, *J. Polym. Sci., Part A: Polym. Chem.*, 37, 89 (1999).
17. L. D. Britto, J. B. P. Soares, A. Penlidis, and B. Monrabal, *J. Polym. Sci., Part B: Polym. Phys.*, 37, 539 (1999).
18. J. Nieto, T. Oswald, F. Blanco, Joao B. P. Soares, and B. Monrabal, *J. Polym. Sci., Part B: Polym. Phys.*, 39, 1616 (2001).
19. L. J. D. Britto, J. B. P. Soares, and A. Penlidis, *Polym. React. Eng.*, 8, 159 (2000).
20. P. Starck, P. Lehmus, and J. V. Seppala, *Polym. Eng. Sci.*, 39, 1444 (1999).
21. W. J. Wang, E. Kolodka, S. Zhu, A. E. Hamielec, and L. K. Kostanski, *Macromol. Chem. Phys.*, 200, 2146 (1999).
22. F. M. Mirabella, *J. Liq. Chromatogr.*, 17, 3201 (1994).
23. R. Brüll, H. Pasch, H. G. Raubenheimer, R. Sanderson, A. J. van Reenen, and U. M. Wahner, *Macromol. Chem. Phys.*, 202, 1281 (2001).
24. Y. Feng and J. N. Hay, *Polymer*, 39, 6589 (1998).
25. C. J. Carman and C. E. Wikes, *Rubber Chem. Technol.*, 44, 781 (1971).
26. J. C. Randall, "Polymer Sequence Determination", Academic Press, Inc., New York, N.Y., 1977.
27. J. C. Randall, *JMS-Rev Macromol. Chem. Phys.*, C29, 201 (1989).
28. H. N. Cheng, *Macromolecules*, 17, 1950 (1984).
29. G. Bucci and T. Simonazzi, *J. Polym. Sci., C, Polym. Lett.*, 7, 203 (1964).
30. F. Ciampelli and A. Valvassori, *J. Polym. Sci., C, Polym. Lett.*, 16, 337 (1967).
31. G. P. Michael and A. Rudin, *J. Appl. Polym. Sci.*, 51, 303 (1994).
32. P. J. Flory, *Trans. Faraday Soc.*, 51, 848 (1955).
33. P. J. Flory, *J. Chem. Phys.*, 17, 225 (1949).

EXHIBIT 5

ELSEVIER

Polymer 42 (2001) 4597–4603

polymer

www.elsevier.nl/locate/polymer

Influence of stereoirregularities on the formation of the γ-phase in isotactic polypropene

R. Thomann[a,*], H. Semke[a], R.-D. Maier[a], Y. Thomann[a], J. Scherble[a], R. Mülhaupt[a], J. Kressler[b]

[a]*Freiburger Materialforschungszentrum und Institut für Makromolekulare Chemie, Albert-Ludwigs-Universität Freiburg, Stefan-Meier-Str. 21, D-79104 Freiburg i. Br., Germany*

[b]*Martin-Luther-Universität Halle–Wittenberg, Fachbereich Ingenieurwissenschaften, D-06009 Halle (Saale), Germany*

Received 28 March 2000; received in revised form 28 August 2000; accepted 11 September 2000

Abstract

Medium to high molar mass isotactic polypropenes with different amounts of stereoirregularities were characterised with respect to their crystallisation behaviour and for comparison a random copolymer of ethene and propene with 5.8 wt% ethene is used. The influence of stereoregularity and crystallisation temperature on the γ-content of the crystallised samples is studied by means of wide angle X-ray scattering, atomic force microscopy and light microscopy. The paper deals also with the temperature rising elution fractionation of an i-PP with large amounts of stereoirregularities and the influence of a nucleation agent on the γ-content. It is shown that effects which render the chainfolding in lamellae more difficult, enhance the formation of the γ-modification. The necessity of chainfolding in isotactic polypropene is discussed in terms of a model that is based on the number of chains that emerge from the lamellae surfaces of the α- and the γ-modification, respectively.

Keywords: Isotactic polypropene; Gamma phase; Crystallisation

1. Introduction

The crystallisation behaviour of isotactic polypropene (i-PP) is very complex. Different crystal modifications are known (α, β, γ and smectic) [1–7]. Calculations of the packing energies of γ- and α-modifications suggest that the γ-modification is slightly more stable than the α-modification [8,9]. The orthorhombic unit cell of the γ-modification is formed by bilayers composed of two parallel helices [10,11]. The direction of the chain-axis in adjacent bilayers is tilted at an angle of 80° [10–12]. At atmospheric pressure the γ-modification is observed as a minor constituent [2,13]. Its content is enhanced when i-PP is crystallised at elevated pressures [14,15], or in low molar mass samples (between 1000 and 3000 g/mol) [16–19]. Also random copolymers of propene with 2.5–20 wt% of other 1-olefins may crystallise preferably in the γ-modification [20–25]. In a previous paper we were able to show that i-PP with stereoirregularities tends to crystallise in the γ-modification [26]. Recently Almao et al. published a detailed work about structural and kinetic factors governing the formation of the γ-modification [27].

In this paper i-PPs with different amounts of stereoirregularities are compared. The influence of stereoirregularities and crystallisation temperature on the γ-content is studied by means of wide angle X-ray scattering (WAXS), atomic force microscopy (AFM), and light microscopy. One sample is fractionated using a temperature rising elution fractionation (TREF) apparatus. The influence of a nucleation agent (NA) on the γ-content is studied for a random copolymer of propene and ethene with 5.8 wt% ethene (P(P-*co*-E)). A model based on the differences in the number of chains that emerge from the lamellae of α- and γ-modification is used for the explanation of the competition during the crystal growth of the two modifications.

2. Experimental

2.1. Materials

The i-PP samples under investigation were synthesised using catalyst systems $Me_2Si(Benz[e]Ind)_2$–$ZrCl_2$/MAO (PP1/PP3) and SiO_2/MAO/$Me_2Si(2\text{-Me-Benz[e]Ind})_2$–$ZrCl_2$ (PP2/PP4), respectively. All characteristic polymer data are given in Table 1. The molar mass data were obtained by size exclusion chromatography (SEC) of the

* Corresponding author. Fax: +49-761-203-5016.
E-mail address: thomannr@fmf.uni-freiburg.de (R. Thomann).

0032-3861/01/$ - see front matter
PII: S0032-3861(00)00675-3

Table 1
Polymer data

Polymer	M_n (g/mol)	M_w/M_n	2,1-Insertion (%)	Mrrm-pentads (%)	∑Defects (%)	n_{iso}[a]	Catalyst[b]
PP1	51 000	2.1	0.4	0.7	1.18	84.6	BI
PP2	117 000	2.7	0.6	1.1	1.74	57.6	Si–BI
PP3	22 000	1.9	0.9	1.4	2.49	40.2	BI
PP4	117 000	2.2	1.0	1.2	2.24	44.7	Si–BI
P(P-*co*-E)	54 000	4.3	Comonomer content: 5.8 wt%				

[a] Catalyst: BI = $Me_2Si(Benz[e]Ind)_2$–$ZrCl_2$/MAO; Si-BI: SiO_2/MAO/Me_2Si(2-Me-Benz[e]Ind)$_2$–$ZrCl_2$.
[b] $n_{iso} = P_n/(1 + P_n(W_{mrrm} + W_{2,1}))$.

i-PP samples or P(P-*co*-E) dissolved in 1,2,4-trichlorobenzene at 140°C. An IR detector is used and the calibration is done with narrow molar mass i-PP samples characterised by light scattering. P(P-*co*-E) is a technical propene/ethene copolymer (Novolen MC 3300/BASG AG) with an ethene content of 5.8 wt%.

As a NA, bis(*p*-ethylbenzylidene)sorbitol (commercial name: NC-4) was used. It was kindly supplied by Mitsui Toatsu Chemicals, Japan. The melting point of bis(*p*-ethylbenzylidene)sorbitol is 235°C.

2.2. Sample preparation

The samples used to study the crystalline morphology by light microscopy were produced by melting the powder of the as-prepared and dried polymer between two cover glasses. The layer thickness between the glasses was about 30–50 μm. The samples were held for 10 min at 180°C and then quenched to the crystallisation temperature. The samples used to study the influence of the NA were prepared by extrusion of P(P-*co*-E) and 1 wt% NA using the twin-screw extruder ZSK25 (Werner and Pfleiderer) at processing temperatures between 190 and 230°C. Tensile test specimens were injection moulded using a Ferromatic Milacron K40-DE. From these specimens, pieces were cut and prepared for crystallisation experiments.

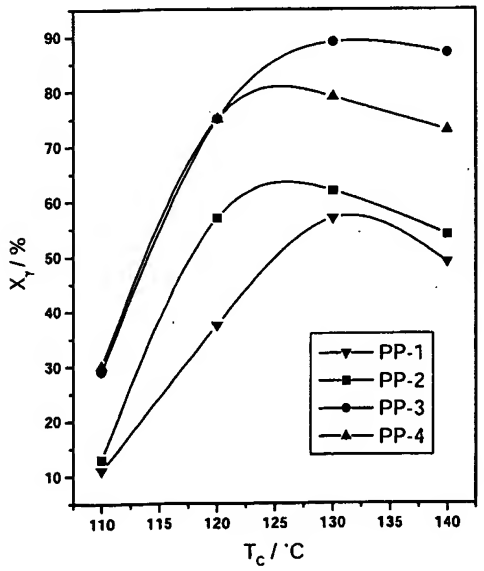

Fig. 1. Content of the γ-modification as a function of the crystallisation temperature for PP1, PP2, PP3 and PP4.

2.3. Light microscopy

The light microscopic investigations were carried out with an Olympus-Vanox AH2 microscope and a Linkam TMS 90 hot stage that allows observation during isothermal crystallisation.

2.4. Atomic force microscopy

The prepared films were etched to remove amorphous material from the surface. The etching reagent was prepared by stirring 0.02 g potassium permanganate in a mixture of 4 ml sulphuric acid (95–97%) and 10 g orthophosphoric acid. The 30–50 μm thick films were immersed in the fresh etching reagent at room temperature and held there for 1 h. In the beginning the samples were held in an ultrasonic bath for 30 min. For subsequent washings, a mixture of 2 parts by volume of concentrated sulphuric acid and 7 parts of water was prepared and cooled to near the freezing point with dry ice in isopropanol. The samples were washed successively with 30% aqueous hydrogen peroxide (to remove any manganese dioxide present). Then the samples were washed with distilled water. Each washing was supported with an ultrasonic bath. The AFM experiments were carried out with a 'Nanoscope III' scanning probe microscope (Digital Instruments) at ambient conditions in the height- and amplitude- mode.

2.5. Wide angle X-ray scattering

Samples for WAXS measurements were isothermally crystallised at various temperatures. The measurements were carried out with a Siemens D500 apparatus. For the measurements CuK_α radiation of a wavelength of $\lambda = 0.154$ nm was used.

2.6. Temperature rising elution fractionation

TREF was carried out using a preparative TREF apparatus. 4 g of PP4 were dissolved in 400 ml xylene under N_2 at 100°C and then very slowly and steadily

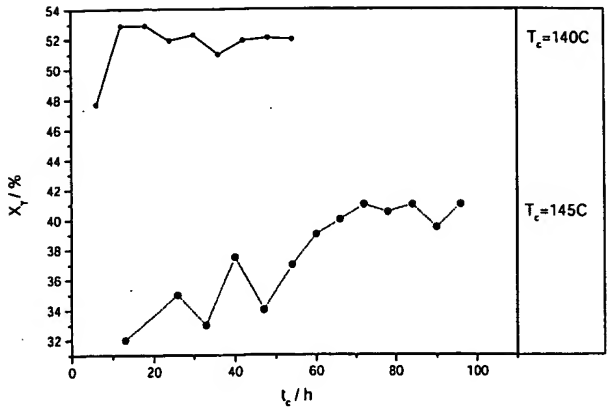

Fig. 2. Content of the γ-modification as a function of the crystallisation time for PP4 taken at $T_c = 140°C$ (·) and $T_c = 145°C$ (●).

cooled at a rate of 1.8°C/h to 25.9°C. At this temperature the sample is precipitated. The precipitate was then dissolved by gradually adding fresh solvent and a stepwise increase of temperature in intervals of about 12°C. For each dissolution step, 400 ml solvent were added. After each temperature increase, the solutions were collected and taken as further fractions. Six fractions were collected.

3. Results and discussion

3.1. X-ray measurements

Fig. 1 shows the amount of the γ-modification in PP1, PP2, PP3 and PP4 as a function of the crystallisation temperature. All measurements are taken at room temperature after isothermal crystallisation and subsequent quenching to room temperature. The γ-content X_γ is calculated

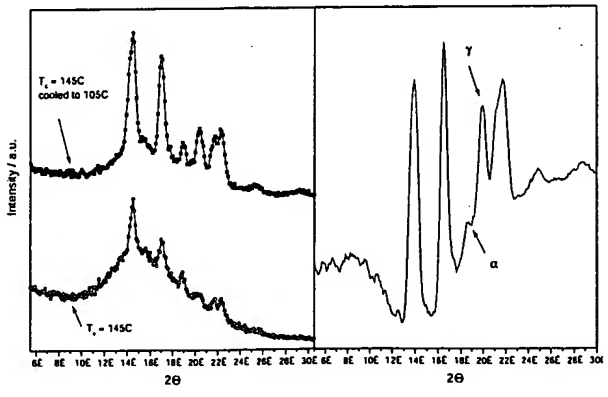

Fig. 3. Left: WAXS traces of PP4 isothermally crystallised at 145°C for 100 h taken at 145°C and after additional cooling to 105°C. Right: WAXS trace calculated by subtracting the WAXS traces given on the left. This WAXS trace represents the crystallisation behaviour of material that crystallises during the cooling process.

according to Turner Jones [13] from the ratio of the heights of the peaks at $2\Theta = 18.8°$ (130 peak of the α-modification) and at $2\Theta = 20.2°$ (117 peak of γ-modification). It can be seen that the γ-content increases with increasing crystallisation temperatures. Only at very high crystallisation temperatures the γ-content decreases. The γ-content also depends strongly on the amount of stereoirregularities. This behaviour is similar to that of samples published in Ref. [27]. For the samples under investigation the γ-content decreases with decreasing amount of stereoirregularities.

Fig. 2 depicts the content of the γ-modification in the PP4 sample as a function of crystallisation time taken at crystallisation temperatures of $T_c = 140°C$ (·) and $T_c = 145°C$ (●), respectively. The γ-content is relatively constant, a small increase with crystallisation time can be observed. The γ-content of the sample crystallised at 145°C is lower than the γ-content of the sample crystallised at 140°C. The sample crystallised at 140°C reaches a constant γ-content and a constant degree of crystallinity after 10 h; the sample crystallised at 145°C arrives at a constant γ-content and a constant degree of crystallinity after 70 h. The γ-content is significantly lower than the values measured after rapid cooling of the samples to room temperature as shown in Fig. 1.

WAXS traces of PP4 measured at 145°C after isothermal crystallisation at 145°C for 100 h (i.e. after reaching a constant degree of crystallinity and a constant content of the γ-modification), and the WAXS trace of the same sample after additional slow cooling to 105°C can be seen in Fig. 3 (left). Upon cooling, the γ-content and the crystallinity increases. Fig. 3 (right) shows a WAXS trace calculated by subtracting the WAXS data taken at 145°C from the WAXS trace taken at 105°C. The resulting WAXS trace shows the crystallisation behaviour of a portion of the sample that was unable to crystallise at 145°C. The peak at $2\Theta = 20.2°$ is very intense. The amount of PP4 that crystallises during this slow cooling process shows about 90% of the γ-modification. This indicates that the decrease of the γ-content at high crystallisation temperatures is caused by a fractionation process. Fractions with high contents of stereoirregularities show lower melting temperatures than highly stereoregular fractions. These fractions are able to form high contents of the γ-modification at relatively high crystallisation temperatures above 100°C but they are unable to crystallise at 145°C. This fractionation appears at temperatures above 125°C. With increasing crystallisation temperatures the amount of this non-crystallisable fraction increases. Quenched to room temperature, the non-crystallisable fraction stays amorphous or crystallises in a temperature range where the α-modification is preferably formed. This leads to a decrease of the γ-content compared to samples crystallised at temperatures in the range of 120°C. Very slow cooling of samples that were isothermally crystallised at very high temperatures leads to significant higher amounts of the γ-modification compared to quenched samples. In these samples, the portion that was

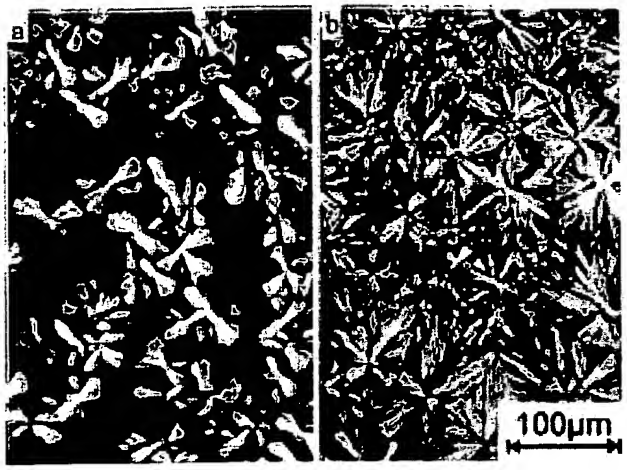

Fig. 4. Light micrographs of TREF fractions 1 (left) and 6 (right) isothermally crystallised at 135°C.

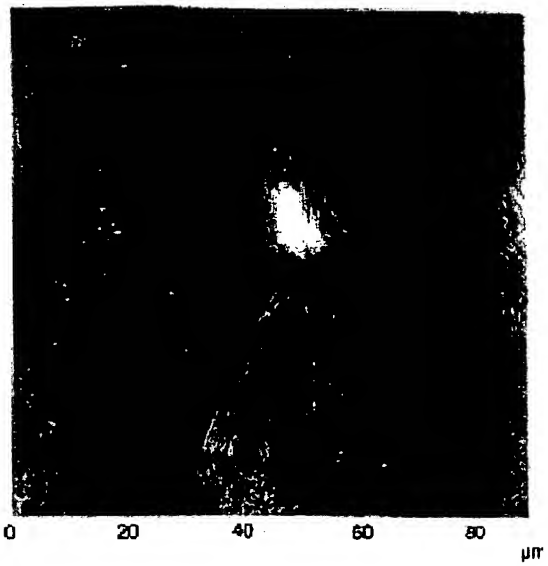

Fig. 5. AFM micrograph of a bundle like morphology formed during isothermal crystallisation of PP4 at 130°C.

unable to crystallise during the isothermal annealing crystallises in a temperature range where it is able to form the γ-modification. Under these conditions a decrease of the γ-content at high crystallisation temperatures is not observed.

3.2. Temperature rising elution fractionation

To support the results discussed above, TREF was used for the fractionation of PP4. TREF is a special fractionation technique, developed to characterise semicrystalline polymers with respect to their crystallisability. It is especially effective to fractionate copolymers according to their comonomer distribution, because of its direct relation to the crystallisability. The influence of the molar mass on the fractionation is usually negligible for molar masses >10 000 g/mol [28,29]. As shown above PP4 is composed of fractions of different crystallisability. Our TREF experiments resulted in 6 fractions with different stereoregularities determined by ^{13}C NMR spectroscopy according to Ref. [30]. The number of mmmm-pentads differ from 91% (fraction 1) to 96% (fraction 6). Thus TREF can be used to fractionate i-PP according to a distribution of macromolecules with differences in their stereoregularity. Therefore, it is not surprising that the crystallisation behaviour of the fractions is different. Isothermally crystallised at 135°C and then slowly cooled to room temperature, fraction 1 yields a γ-content of about 90%, the more stereoregular fraction 6 forms under identical conditions only 60% of the γ-modification. The behaviour of fraction 1 is hence very similar to the portion of PP4 that is found to be non-crystallisable at high crystallisation temperatures (e.g. 145°C). The influence of the stereoregularity on the supermolecular appearance is shown in the light micrographs of Fig. 4. The less stereoregular fraction 1 forms bundle like structures at a crystallisation temperature of 135°C shown in Fig. 4a (γ-content: 90%). The fraction 6 with the highest stereoregularity crystallised under identical conditions forms spherulites well-known from the crystallisation of i-PP in the α-phase (γ-content: 60%).

3.3. Morphology

Fig. 5 depicts an AFM micrograph of PP4 isothermally crystallised at 130°C. The morphology is different from the spherulites formed by the α-modification. PP4 forms at elevated temperatures, bundle like morphologies known from mixed superstructures of the α- and γ-modification in i-PP of relatively low molar mass [26].

Fig. 6 shows an AFM micrograph of PP3 isothermally crystallised at 125°C. At this magnification the typical triangular morphology of γ-phase single crystal like entities is visible. These single crystal like structures are arranged at an angle of 50° to the completely covered underlying lamellae of the α-modification, forming the superstructure. This angle is exactly the angle of the epitaxial ongrowth of the γ-modification on lamellae of the α-modifiaction that is shown schematically on top of the photograph of Fig. 6.

These morphologies composed of α-lamellae and epitaxial ongrowth of the γ-modification are also observed in PP4 cooled from the melt at 10°C/min (Fig. 7). The bundle like morphology (lower right part of the photograph, marked as γ) is surrounded by the typical cross-hatched structure formed by the α-modification of i-PP (indicated by an arrow as α). This is a clear indication that non-isothermally crystallised samples of i-PP with large amounts of stereoirregularities show a heterogeneous superstructure built up by bundle like structures with high contents of the γ-modification, and of areas formed by the pure α-modification. This heterogeneity might have a influence on the optical and mechanical properties of such samples.

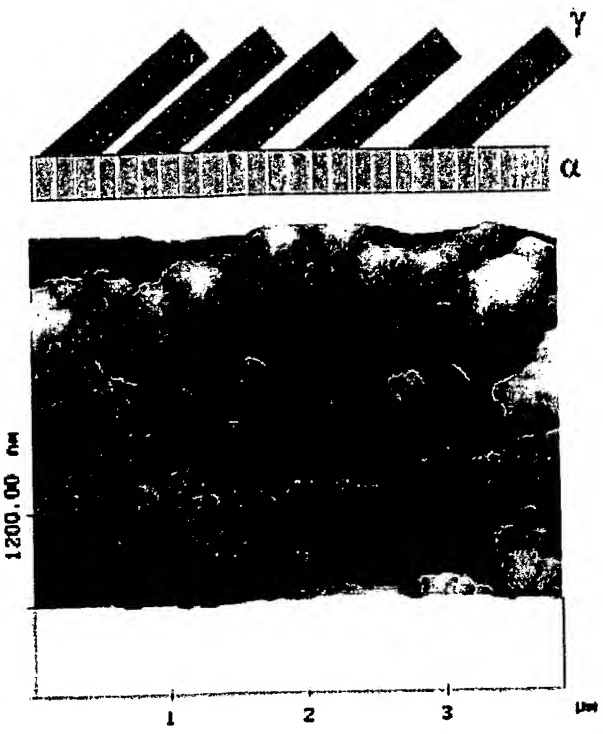

Fig. 6. AFM micrograph of the epitaxial ongrowth of the γ-modification on α-lamellae in PP3 isothermally crystallised at 125°C (bottom); scheme of the epitaxial ongrowth (top).

3.4. Nucleation

It is mentioned above that the amount of the γ-modification depends on the crystallisation temperature. It is well known that NAs are able to raise the crystallisation temperature of i-PP during the cooling regime from the melt. Therefore, nucleation should have a significant influence on the amount of the γ-modification formed during non-isothermal crystallisation. The content of the γ-modification as a function of the cooling rate for P(P-*co*-E) and P(P-*co*-E) + 1 wt% of NA is shown in Fig. 8. For the very slow cooling rate of 0.2°C/min only differences of about 20% in the γ-contents between the copolymer with and without NA, respectively, are found. For higher cooling rates the γ-content stays relatively high for the nucleated sample but decreases rapidly for the non-nucleated sample.

Under isothermal crystallisation conditions no significant difference in the γ-content is found between the nucleated and the non-nucleated sample (Fig. 9, top). Hence the observed higher γ-content is caused by an increase of the crystallisation temperature in the nucleated sample and not by preferential growth of the γ-modification on the NA. The bottom part of Fig. 9 shows DSC traces of P(P-*co*-E) and P(P-*co*-E) + 1 wt% of NA cooled from the melt at 10°C/min. It is demonstrated that the nucleation is effective in order to shift the crystallisation temperatures in a temperature range where large amounts of the γ-modification are formed. Therefore, it can be concluded that the increase of the γ-modification in nucleated samples, crystallised under non-isothermal conditions, is only caused by an increase of the crystallisation temperature and not by a special nucleation of the γ-phase.

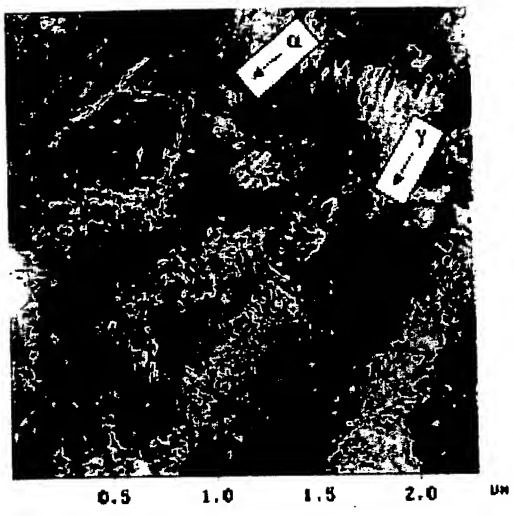

Fig. 7. AFM micrograph of the heterogeneous morphology found in a PP4 sample that was cooled from the melt with 10°C/min. Areas are marked as α and γ with respect to the dominating modification.

4. Model

It was shown by Almao et al. [27] that kinetic requirements are important for the formation of the γ-modification. They discussed the fact that the flux of chains that emanate from the 001 plane is reduced in the γ-modification due to the arrangement of antiparallel tilted chains, and that therefore

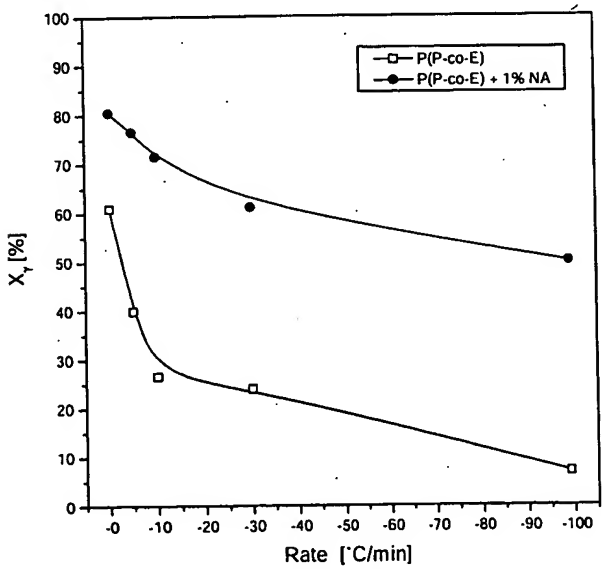

Fig. 8. Content of the γ-modification as a function of the cool rate for P(P-*co*-E) and P(P-*co*-E) + 1% of NA.

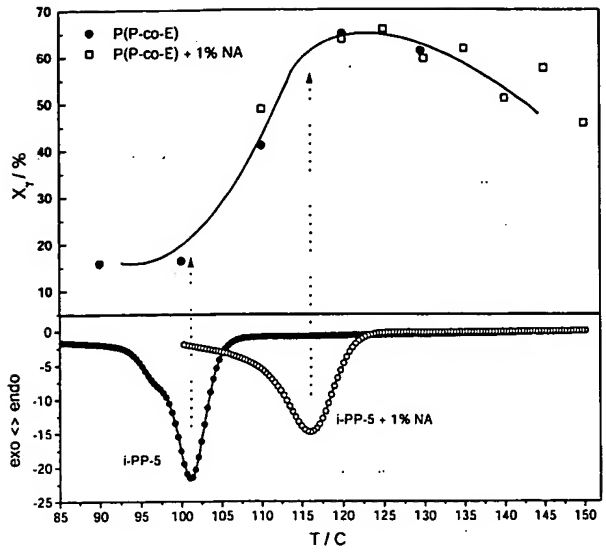

Fig. 9. Content of the γ-modification as a function of the crystallisation temperature for P(P-*co*-E) and P(P-*co*-E) + 1% of NA (top), DSC crystallisation traces of P(P-*co*-E) and P(P-*co*-E) + 1% NA taken upon cooling with a rate of 10°C/min.

the formation of the γ-phase is a natural consequence of accommodating chain defects outside the crystal.

Fig. 10 schemes the different arrangements of helices in the α- and the γ-modification. In the α-modification (Fig. 10a) the helices are arranged perpendicular to the lamellae surface. The distance between the chains at the lamella surface (d_α) is identical with the chain distance in the lamellae themselves (d_h). Fig. 10b shows the arrangement of helices in the γ-modification. The helices have an angle of 50° to the lamella surface. In this case the distance of the chains at the lamella surface (d_γ) is significantly higher than the chain distance in the lamellae (d_h), and also higher than d_α for an identical d_h. This reduces the number of chains that emerge from the lamellae surface [5.73 chains per nm^2 for the α-modification and 4.39 chains per nm^2 for the γ-modification].

This difference has a remarkable effect on the amorphous phase. Fig. 11 shows two chains of the same length emerging from a lamella: (a) chains in an elongated helical conformation; (b) chains in random coil conformation. In the case that all chains of an α-lamella emerge in the elongated 3_1-helical conformation (similar to Fig. 11a), the density of the 'amorphous' phase would be 26.46 propene units per nm^3. This density is identical with that of the crystalline lamella. If all chains adopt random coil conformation (similar to Fig. 11b), the density would be significantly higher than that of the crystalline lamella. A realistic density, lower than that of the crystalline material, cannot be achieved when all chains emerge from the lamella surface. This calculation is one of the main arguments for a chain folding in melt crystallised polymers [31,30]. Therefore, a large amount of chains that emerge from lamellae of the α-modification must fold back (Fig. 11c). For polyethylene it was calculated that 50% of the chains must fold back [32].

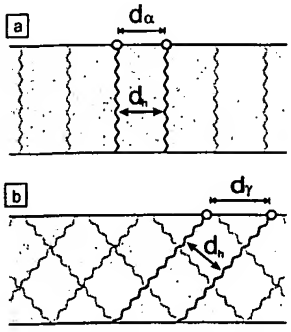

Fig. 10. The arrangement of helices in lamellae: (a) α-modification; (b) γ-modification.

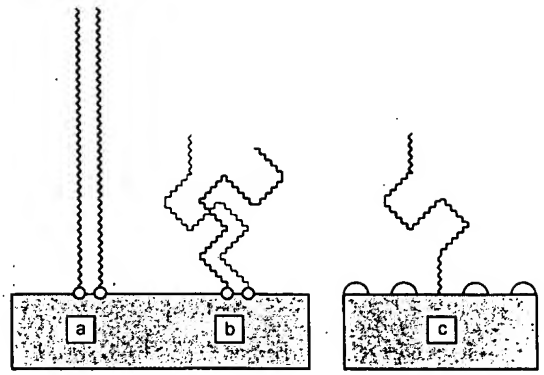

Fig. 11. Helices that emerge from the lamella surface: (a) helical conformation; (b) random walk conformation; (c) lamellae surface with chainfolding.

The situation is totally different for the γ-modification. As described above the number of chains per unit lamella surface is reduced. If all chains emerge from the lamella in an elongated helical conformation (similar to Fig. 11a), the density of the 'amorphous' phase would be 20.27 propene units per nm^3. This value is significantly lower than that of the crystalline core, and even lower than that of amorphous i-PP. The density at the lamella surface is thus relatively small so that even a high degree of conformational disorder can appear without the necessity of chain folding. This means, that any factor which suppresses chainfolding makes the formation of α-modification difficult, but promotes the formation of the γ-modification.

Crystallised random copolymers of propene with ethene, 1-butene, 3-methylbutene, 1-octene and other comonomers are known to crystallise in significant amounts in the γ-modification [20–25]. Depending on its size and structure, the comonomer units can be excluded from, or included into the crystal lattice. In general, the exclusion from the crystal lattice is energetically favoured and even if an inclusion is possible the majority of comonmer units are excluded [33]. Because the comonomers are distributed randomly in the chain, it can only happen coincidentally that a comonomer unit is in the right position to be part of a sharp chain folding

connected with adjacent re-entering. In general, the exclusion of comonomers leads to the formation of long loops, or the chainfolding is totally suppressed. As discussed above a large amount of sharp chain folds is necessary to form α-lamellae. For that reason it is easy to understand that the exclusion of comonomer units increases the amount of γ-modification. A very similar effect is caused by stereoirregularities, that leads to imperfections in the 3_1 helices which must be excluded. Similar to comonomer units, the exclusion of stereoirregular units renders the formation of sharp adjacent chain folds difficult and promotes the formation of γ-modification. The smaller lamella thickness of the γ-modification compared to that of the α-modification [26] amplifies this effect, due to an easier collecting of i-PP segments of fitting length to form lamellae [34]. In low molar mass i-PP samples tapered ends and chemically different end-groups might have a similar influence.

5. Conclusions

Isotactic polypropenes with different amounts of stereoirregularity were compared. It is shown that the γ-content depends on the stereoregularity and on the crystallisation temperature. At high crystallisation temperatures the samples are fractionated in a non-crystallisable fraction with a large number of stereoirregularities and a crystallisable fraction with higher stereoregularity. Upon cooling also, the more stereoirregular fraction is crystallisable. Slowly cooled to room temperature, it forms mainly the γ-modification. TREF on a metallocene i-PP sample leads to fractions of different stereoregularity that form different amounts of the γ-modification. These fractions show different types of superstructures, spherulites for low contents of stereoirregularities, bundle like structures for high contents of stereoirregularities. Nucleation increases the crystallisation temperature of P(P-*co*-E). Therefore, nucleation with bis(*p*-ethylbenzylidene)sorbitol is able to increase the γ-content in P(P-*co*-E) significantly during the cooling regime from the melt.

A remarkable difference between the α- and the γ-modification of i-PP is the necessity of chain folding in melt crystallised lamellae. Similar to polyethene a large number of chains that emerge from the surface of α-lamellae of i-PP must fold back in order to guaranty that the amorphous has a lower density compared to the crystalline regions. There is no necessity to fold back for chains that emerge from γ-lamellae of i-PP. This difference becomes important when the chemical structure of the polypropene chain suppresses the formation of sharp chain folds. In that case the formation of the α-modification is more difficult, and the amount of γ-modification increases. Typical examples are random copolymers of polypropene, polypropenes with regio- and stereoirregularities, and low molar mass samples.

Acknowledgements

Financial support was provided by the Deutsche Forschungsgemeinschaft (Sonderforschungsbereich 428 and Innovationskolleg 'Neue Polymermaterialien').

References

[1] Khoury H. J Res Natl Bur Stand 1966;70A:29.
[2] Padden FJ, Keith HD. J Appl Phys 1966;37:4013.
[3] Padden FJ, Keith HD. J Appl Phys 1973;44:1217.
[4] Bassett DC, Olley RH. Polymer 1984;25:935.
[5] Norton DR, Keller A. Polymer 1985;26:704.
[6] Brückner S, Meille SV, Petraccone V, Pirozzi B. Prog Polym Sci 1991;16:361.
[7] Lotz B, Wittmann JC. Prog Colloid Polym Sci 1992;87:3.
[8] Ferro DR, Brückner S, Meille SV, Ragazzi M. Macromolecules 1992;25:5231.
[9] Meille SV, Ferro DR, Brückner S. Polym Prepr (Am Chem Soc, Div Polym Chem) 1992;33(1):268.
[10] Brückner S, Meille SV. Nature 1989;340:455.
[11] Meille S, Brückner S, Porzio W. Macromolecules 1990;23:4114.
[12] Brückner S, Meille S, Sozzani P, Torri G. Makromol Chem, Rapid Commun 1990;11:55.
[13] Turner Jones A, Aizlewood JM, Beckett DR. Makromol Chem 1964;75:134.
[14] Kardos JL, Christiansen E, Baer E. J Polym Sci 1966;A2(4):777.
[15] Pae KD, Morrow DR, Sauer JA. Nature 1966;21:514.
[16] Lotz B, Graff S, Wittmann JC. J Polym Sci 1986;B(24):2017.
[17] Morrow DR, Newman BA. J Appl Phys 1968;39:4944.
[18] Kojima M. J Polym Sci 1967;B(5):245.
[19] Kojima M. J Polym Sci 1968;A2(6):1255.
[20] Turner Jones A. Polymer 1971;12:487.
[21] Guidetti GP, Busi P, Giulianetti I, Zanetti R. Eur Polym J 1983;19:757.
[22] Busico V, Corradini P, De Rosa C, Di Benedetto E. Eur Polym J 1985;21:239.
[23] Avella M, Martuscelli E, Della Volpe G, Segre A, Rossi E, Simonazzi T. Makromol Chem 1986;187:1927.
[24] Marigo A, Marega C, Zanetti R, Paganetto E, Canossa E, Coleta F, Gottardi V. Makromol Chem 1989;190:2805.
[25] Mezghani K, Phillips PJ. Polymer 1995;35:2407.
[26] Thomann R, Wang C, Kressler J, Mülhaupt R. Macromolecules 1996;29:8425.
[27] Alamo RG, Kim M-H, Galante MJ, Isasi JR, Mandelkern L. Macromolecules 1999;32:4050.
[28] Thomann Y, Sernetz FG, Thomann R, Kressler J, Mülhaupt R. Macromol Chem Phys 1997;198:739.
[29] Penning AJ. J Polym Sci, Part C 1967;16:1799.
[30] Jüngling S. PhD thesis, Freiburg, 1995.
[31] Frank FC. Faraday Discuss R Soc Chem 1980;68:7.
[32] Barham PJ. In: Chan RW, editor. Crystallisation and morphology of semicrystalline polymers in materials science and technology, vol. 12. Weinheim: VCH, 1993.
[33] Wunderlich B. Macromolecular physics, vol. 1. New York: Academic Press, 1980.
[34] Anderson R, Phillips PJ, Lin JS. Polymer 1993;34:23.

EXHIBIT 6

ELSEVIER

Polymer 40 (1999) 675–681

polymer

Obtaining the γ phase in isotactic polypropylene: effect of catalyst system and crystallization conditions

Ernesto Pérez[a,*], Debora Zucchi[b], Maria Carmela Sacchi[b], Fabricio Forlini[b], Antonio Bello[a]

[a]Instituto de Ciencia y Tecnología de Polímeros del CSIC, Juan de la Cierva 3, 28006 Madrid, Spain
[b]Istituto di Chimica delle Macromolecole del CNR, Via E. Bassini 15, 20133 Milan, Italy

Received 17 February 1998; revised 6 April 1998

Abstract

Five samples of isotactic polypropylene, iPP, and two copolymers of iPP with 1-hexene, synthesized with different catalyst systems, both heterogeneous and homogeneous, have been studied in order to analyse the effect of the catalyst system, the presence of comonomer units and the crystallization conditions on the phase structure of iPP and, in particular, on the amount of γ modification obtained. Minor amounts, if any, of γ modification are present in iPP samples synthesized with highly isospecific Ziegler–Natta catalysts and crystallized from the melt at different cooling rates, ranging from 100 to 3°C/min. On the contrary, considerable amounts of the γ form have been obtained both in samples prepared with catalysts of very low isospecificity or in those prepared with homogeneous metallocene catalysts. It has been shown that the relative proportion of the α and γ modifications can be controlled just by changing the crystallization conditions. A clear influence of the presence of comonomer units on favouring the formation of the γ phase has not been ascertained. Moreover, attempts to deduce the γ content from the d.s.c. melting patterns have been unsuccessful, since the two modifications exhibit very similar melting temperatures.

Keywords: Isotactic polypropylene; Copolymers with 1-hexene; α and γ modifications

1. Introduction

The polymorphic behaviour of isotactic polypropylene (iPP) is well documented [1–3]. The monoclinic α form is by far the most common [1–4], being found in all kinds of solution-crystallized iPP samples and also in most melt-crystallized specimens. The hexagonal β modification appears only under special crystallization conditions or in the presence of selective β nucleating agents [1–3,5–8]. The triclinic γ form has been found in the case of low-molecular weight iPP, crystallization under high pressure, in copolymers or in those samples prepared with homogeneous metallocene catalysts [1–3,9–15]. The γ form seems to be favoured by the presence of defects in the iPP chain. In addition, fast quenching of iPP leads to a phase of intermediate order, whose structure is still under controversy [1–3,16–20].

Since conventional supported Ziegler–Natta (ZN) catalysts usually lead to high molecular weights and high stereoregularities, only traces of the γ form are obtained in such cases under normal crystallization conditions. It has been shown [1,10] that the diffractograms corresponding to the α and γ modifications are very similar and only the region around $2\theta = 18–21°$ is appropriate for the differentiation between the two phases. Thus, the α form presents a diffraction at 18.6°, while the γ one shows a peak at $2\theta = 20.1°$. The rest of the diffractogram is very similar for the two modifications.

We are presently carrying out a comparative study of the properties of iPP-based samples synthesized with different catalyst systems, including heterogeneous ZN catalysts of different generations and homogeneous metallocene systems.

The purpose of this work is to analyse the effect of the catalyst system, the presence of comonomer units and the crystallization conditions on the phase structure of iPP and, in particular, on the amount of γ modification obtained.

2. Experimental

Five different types of catalysts have been used in obtaining the samples. Types A, B and C are heterogeneous ZN catalysts based on the system $MgCl_2/TiCl_4$, activated by $AlEt_3$. The difference is that type A does not have any

* Corresponding author.

0032-3861/98/$ - see front matter
PII S0032-3861(98)00291-2

Table 1
Results of the characterization of the different polymer samples

Sample	Catalyst	1-Hexene (mol%)	$[\eta]_v$	M_n	M_w/M_n	II	[mmmm]	T_m^a (°C)
PPML83	A	0	—	—	—	0.42	0.65	134
PPF08	B	0	—	47900	6.5	0.93	0.85	159
PHF24	B	4.7	—	—	—	—	0.77	147
PP1901	C	0	0.75	29900	6.1	0.92	0.82	156
PPZ02	D	0	0.58	35160	1.8	—	0.94	143
PPZ19	E	0	0.64	38600	1.9	—	0.93	145
PHZ431	E	2.6	0.52	31480	1.9	—	0.91	121

[a]Peak melting temperature after crystallization from the melt at 100°C/min

kind of donor while type B includes diisobutyl phthalate as internal donor and phenyltriethoxysilane as external donor, and type C includes 2,2-dicyclopentyl-1,3-dimethoxy propane as internal donor [21] and without external donor. Type D is an homogeneous metallocene catalyst of *rac*-ethylene-bisindenyl-zirconium dichloride, $Et(Ind)_2ZrCl_2$, activated by methylaluminoxane, MAO. Finally, type E consists also of $Et(Ind)_2ZrCl_2$ activated with a suitable Al*i*-But$_3$/MAO mixture [22].

These types of catalysts have been used to prepare the iPP homopolymers and the iPP–1-hexene copolymers indicated in Table 1. The comonomer compositions and the isotactic pentad fractions, [mmmm], were determined from the n.m.r. spectra in solutions of $C_2D_2Cl_4$. The isotactic content, II, corresponds to the weight fraction of the insoluble part of the polymer in boiling heptane. Intrinsic viscosities, $[\eta]_v$, were determined in 1,2-dichlorobenzene, DCB, at 135°C. Molecular weights were measured by g.p.c. in solutions of DCB at 135°C. Table 1 shows the results for the different samples. Some of them were not fractionated for II measurement because they have been prepared by using the above-mentioned single-site catalyst $Et(Ind)_2ZrCl_2$.

Wide-angle x-ray diffraction, WAXD, patterns were recorded at room temperature using a Philips diffractometer with a Geiger counter, connected to a computer. Ni-filtered Cu Kα radiation was used. The diffraction scans were collected over a period of 15 min between 2θ values of about 5 and 35° using a sampling rate of 1 Hz. The initial films for WAXD were prepared in a Collin press by cooling from the melt under a little pressure. The cooling process was carried out by quenching to room temperature (cooling rate of about 100°C/min) or by slow cooling at the inherent rate of the press (approximately at 3°C/min). Selected specimens were also crystallized by cooling from the melt at controlled rates in a Mettler FP82HT hot stage.

Calorimetric analyses were carried out in a Perkin-Elmer DSC7 calorimeter, connected to a cooling system and calibrated with different standards. About 7 mg of sample were used, and the heating rate was 10°C/min. The peak melting temperatures of the different samples after crystallization from the melt at 100°C/min are shown in the last column of Table 1.

3. Results and discussion

Since the diffractograms corresponding to the α and γ forms of iPP are rather similar, the determination of the relative proportion of both phases is not straightforward, and several methods have been proposed [10,23]. We have used a deconvolution procedure, after subtraction of the amorphous component. For that purpose, we acquired the diffraction pattern of an elastomeric polypropylene sample, obtained with an unbridged 'oscillating' metallocene catalyst [24,25]. No crystallinity has been detected in this sample by d.s.c., or by x-ray diffraction, as observed in the middle diffractogram of Fig. 1. A certain proportion of this amorphous pattern has been subtracted from the profiles

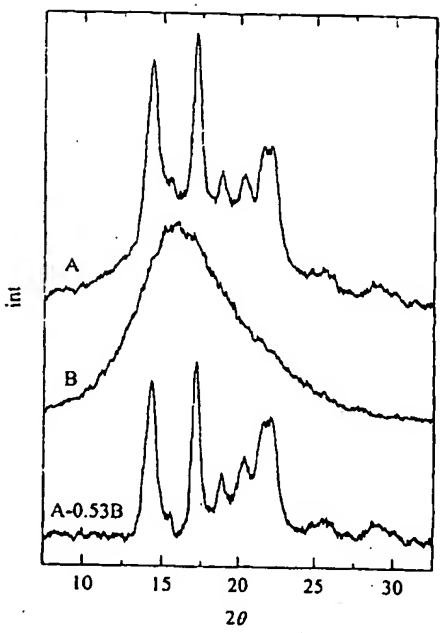

Fig. 1. X-ray diffraction profiles showing the procedure for obtaining the 'pure crystalline' diffractogram. (A) Actual sample (PPML83-d); (B) totally amorphous sample (elastomeric polypropylene), and difference A–0.53B, representing the 'pure crystalline' profile. A and B are normalized to the same total area, so that the x-ray degree of crystallinity of A is 0.47.

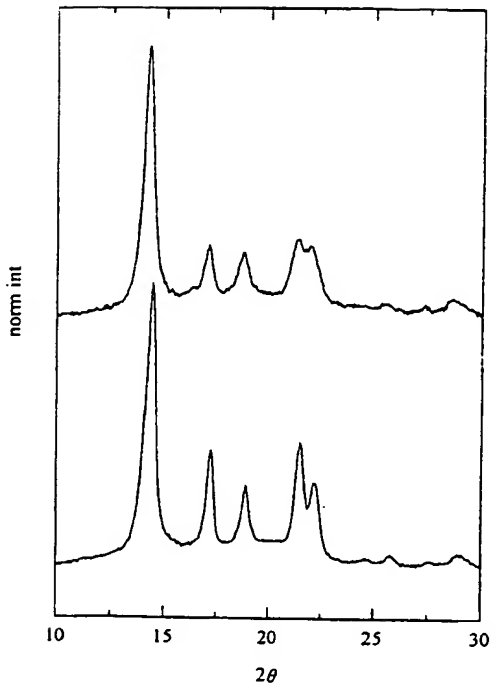

Fig. 2. X-ray diffractograms corresponding to homopolymer PP1901 crystallized from the melt at different cooling rates: 100°C/min (upper) and 3°C/min (lower).

of the different sample preparations and, assuming a simple two-phase model, the corresponding 'pure crystalline' diffractogram can be deduced when a flat background is obtained, as depicted in Fig. 1. Since all the original diffractograms were normalized to the same total intensity, the estimation of the x-ray crystallinity is straightforward.

Subsequently, the crystalline diffractograms were deconvoluted by using Pearson VII profiles for the crystalline diffractions. The proportion of the two modifications is obtained from the relative areas of the diffractions at $2\theta =$ 18.7 and 20.2°. Evidently, the results will change slightly if a different method or different profiles for the fitting are applied, since the diffractions overlap. Moreover, we are assuming with this procedure that, in the samples with 100% of α or γ modification, the relative areas of the diffractions at 18.7 and 20.2°, respectively, in relation to the total crystalline area, are the same in both cases (we were unable to prove this point since we have not got pure modifications of both in any sample).

It is known that obtaining significant amounts of γ modification is rather difficult in the case of iPP samples of high isotacticity obtained with heterogeneous catalysts. Thus, Fig. 2 shows the diffractograms of two specimens of sample PP1901, obtained with catalyst C. These diffractograms show the diffractions corresponding to the α form of iPP. The presence of a peak at 20.1°, arising from the γ phase, cannot be totally disregarded, but it is inside the noise level (an upper limit of 15% of γ content is deduced, as indicated in Table 2). The total crystallinity of these specimens is rather high (see also Table 2) and the crystallites for specimen PP1901-b seem to be large, as expected, judging from the width of the reflections. Similar arguments apply for sample PPF08 (see Table 2), obtained with catalyst B, which displays a slightly higher isotacticity than polymer PP1901.

The presence of comonomer units have been reported to favour the formation of the γ modification. We have studied, in a previous paper [26], several copolymers of iPP and 1-hexene obtained with a catalyst of type B. The reported diffractograms of the quenched samples did not show any clear indication of the γ modification, although the crystallinity levels obtained for high comonomer contents preclude any precise conclusion. We have focused our attention, therefore, on the copolymer with the smaller comonomer content: 4.7 mol% of 1-hexene. The diffractograms for a quenched and a slowly crystallized specimen of this copolymer, named PHF24, are shown in Fig. 3. No clear indication of the γ modification can be deduced from these diffractograms. A peak at 20.1° may be present, although in a minor proportion. We also studied, in a previous paper [27], several fractions of copolymer PHF24, obtained by extracting with octane at different temperatures. The diffractograms of these fractions, with varying comonomer contents, stereoregularity and molecular weight, and crystallized from the melt, did not show a clear indication of the presence of γ form.

The situation is much different for the iPP sample obtained with catalyst A. This sample, PPML83, has a rather small isotactic content (see Table 1). Fig. 4 shows the

Table 2
X-ray crystallinity, f_c, and γ phase content, f_γ, for the iPP samples crystallized from the melt at different cooling rates

Specimen	Cooling rate (°C/min)	f_c^a	f_γ^b
PPML83-a	100	0.52	0.25
PPML83-b	10	0.47	0.44
PPML83-c	5	0.52	0.57
PPML83-d	1.5	0.47	0.67
PPF08-a	100	0.67	< 0.10
PPF08-b	3	0.70	< 0.20
PHF24-a	100	0.29	< 0.20
PHF24-b	3	0.42	< 0.30
PP1901-a	100	0.72	< 0.10
PP1901-b	3	0.74	< 0.15
PPZ02-a	100	0.60	~0.15
PPZ02-b	10	0.59	0.39
PPZ02-c	5	0.60	0.50
PPZ02-d	1.5	0.58	0.57
PPZ19-a	100	0.55	~0.15
PPZ19-b	16	0.57	0.36
PPZ19-c	8	0.56	0.41
PPZ19-d	4	0.55	0.48
PPZ19-e	1.5	0.51	0.58
PHZ431-a	100	0.50	< 0.3
PHZ431-b	3	0.50	~0.7

[a] Estimated error, ± 0.05
[b] Estimated error, ± 0.10

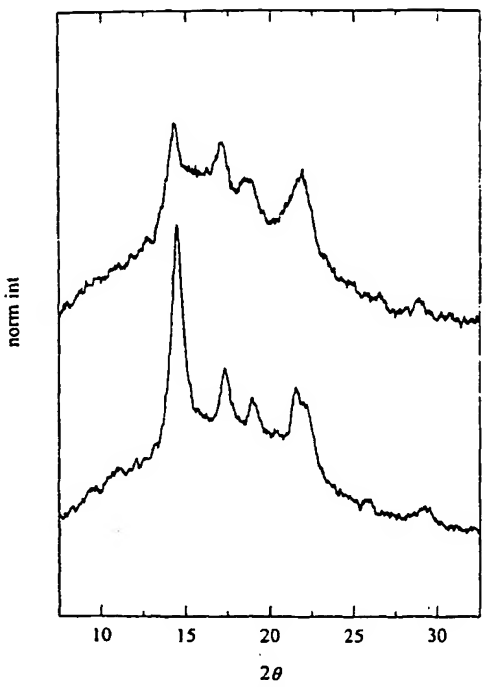

Fig. 3. X-ray diffractograms corresponding to copolymer PHF24 crystallized from the melt at different cooling rates: 100°C/min (upper) and 3°C/min (lower).

WAXD patterns corresponding to specimens of sample PPML83 prepared at different cooling rates. A clear peak of varying intensity can be observed at around 20.2°, indicating that the γ content increases as the cooling rate decreases, since this diffraction increases in intensity while the one at $2\theta = 18.7°$, arising from the α phase, diminishes. Thus, only a minor amount of the γ modification is present in the quenched sample, while it represents the major proportion for the specimen crystallized at the smallest rate.

The results of Table 2 indicate that the estimated content of the γ modification for sample PPML83 increases markedly as the cooling rate decreases, and the proportion between the two modifications can be controlled, therefore, by the crystallization conditions.

The remaining three samples have been synthesized with metallocene-based catalysts. Homopolymer PPZ02 was obtained with catalyst D. The corresponding results for the crystallinity and the γ content are also presented in Table 2. It is observed that the fractions of γ form for this polymer are slightly smaller than those for sample PPML83, for the same cooling rate.

We have also analysed a sample, PPZ19, synthesized with catalyst E, similar to catalyst D, but activated with Al*i*But$_3$, thus exhibiting a significantly higher activity (2.3 times higher). Fig. 5 shows the diffractograms of different specimens of this sample. The results of crystallinity and γ content (see Table 2) are practically identical to those for sample PPZ02, i.e. a higher yield of polymer is obtained

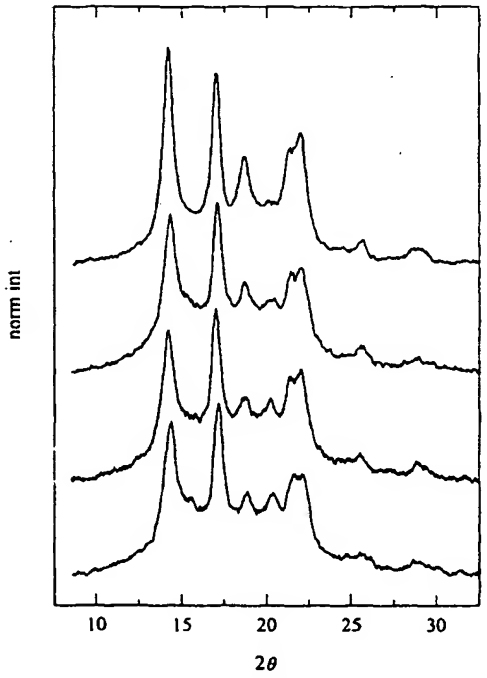

Fig. 4. X-ray diffractograms corresponding to homopolymer PPML83 crystallized from the melt at different cooling rates. From top to bottom: 100, 10, 5 and 1.5°C/min.

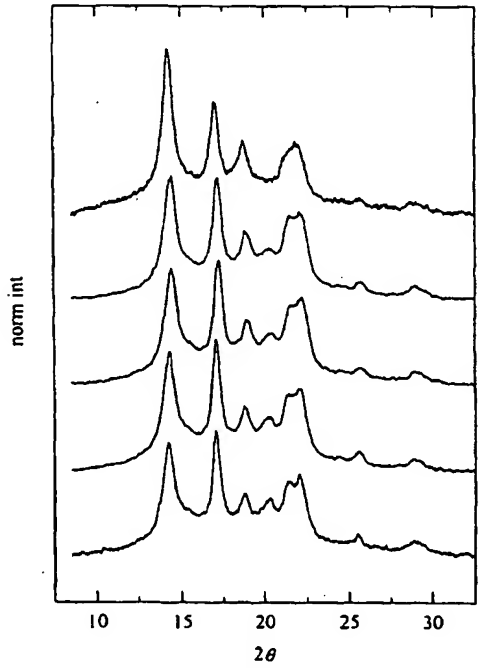

Fig. 5. X-ray diffractograms corresponding to homopolymer PPZ19 crystallized from the melt at different cooling rates. From top to bottom: 100, 16, 8, 4 and 1.5°C/min.

with catalyst E without a change in the properties analysed in this paper.

The last sample, PHF431, is a copolymer of iPP and 1-hexene, also prepared with the metallocene-based catalyst E. The diffractograms of two specimens of this copolymer are shown in Fig. 6. The noise level is rather high, due to the limited amount of sample. Nevertheless, the diagram for the slowly crystallized specimen shows a prominent peak around 20.2°, i.e. the γ form is predominant in this specimen. Regarding the quenched specimen, the amount of γ modification does not appear to be significantly different than the corresponding amount for homopolymer PPZ19, even though the molecular weight of the copolymer is slightly smaller. It seems, therefore, that the presence of comonomer units has not increased the ability to produce the γ phase by very much.

The influence of the cooling rate on the total crystallinity seems to be rather small, since the values for any particular sample are within the experimental error (see Table 2), and only in the case of copolymer PHF24 was a significantly smaller crystallinity obtained for the quenched specimen.

The effect of the cooling rate on the proportion of γ modification can be observed in Fig. 7, where the γ contents have been plotted against the logarithm of the cooling rate for three of the samples. Since the number of data points is very limited, and considering the experimental uncertainty, any conclusion from these results is rather speculative. A single line has been drawn through all the data points in Fig. 7, but it seems that different lines are obtained, the

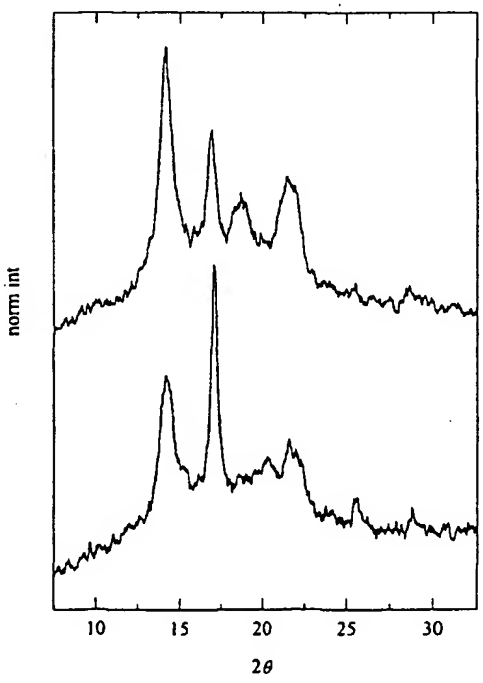

Fig. 6. X-ray diffractograms corresponding to copolymer PHZ431 crystallized from the melt at different cooling rates: 100°C/min (upper) and 3°C/min (lower).

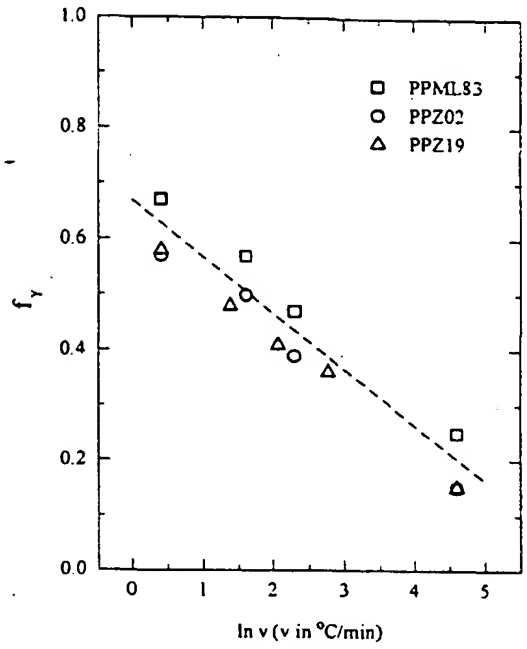

Fig. 7. Plot of the γ phase content as a function of the logarithm of the cooling rate for the indicated samples.

ordinate depending on the kind of sample, showing its higher or lower tendency to produce the γ phase. Of course, the molecular weight of the sample will also play an important role on the ability to produce the γ modification. In fact, a metallocene iPP sample with $M_w = 18000$ has been reported [28] to produce 100% γ form when isothermally crystallized at high temperatures (in that paper, progressively lower proportions of γ form were obtained when lowering the crystallization temperature).

The right-hand side of Fig. 7, corresponding to very high cooling rates, may present a discontinuity due to the formation of the disordered phase obtained by fast quenching of iPP. We have not found any indication of this phase in this study (the highest cooling rate has been around 100°C/min).

We plan to extend these investigations to other iPP samples, trying to get a better picture of the ability to produce the γ modification. It seems from Fig. 7 that any iPP sample will be able to give this modification: it is just a matter of diminishing the cooling rate (or the molecular weight), and the more steric defects present in a given sample, the less we need to diminish the cooling rate. This is the case of iPP samples of very low isotactic content or those synthesized with metallocene catalysts, where the errors, although not very numerous, are evenly distributed, and considerable amounts of γ phase are obtained at moderate cooling rates. On the contrary, iPP samples of high stereoregularity from heterogeneous catalysts need extremely low cooling rates. We plan to carry out such experiments, keeping the samples under vacuum or in inert atmosphere to prevent the degradation of the samples in the very long times required. Moreover, isothermal

experiments are also planned, since the isothermal crystallization at progressively higher temperatures will also give higher amounts of γ form.

We have also analysed these samples by d.s.c., trying to get another estimation of the γ content from the melting patterns. Fig. 8 shows the melting curves corresponding to sample PPZ02 crystallized from the melt at three different cooling rates. It is evident from these patterns that the melting temperatures of both the α and γ modifications are very similar and their relative content cannot be determined by d.s.c. The peak melting temperature of the slowly crystallized specimen (with more γ form) is slightly higher than the one for the quenched sample. It has been reported [28] that the α form is the one that melts at higher temperature. However, a slower crystallization will produce thicker crystals, with higher melting temperatures, which could explain the d.s.c. results. Moreover, recrystallization phenomena may be present in the d.s.c. experiments. We plan to analyse these aspects by real-time synchrotron experiments.

The peak melting temperatures of the different samples, quenched from the melt, are shown in the last column of Table 1. Besides the molecular weight, three other variables influence the melting temperatures: [mmmm] content, comonomer content and kind of catalyst (distribution of errors). Regarding the heterogeneous catalysts, a decrease of 25°C is found when comparing homopolymer samples PPF08 and PPML83, mainly due to their very different [mmmm] content. However, the decrease of the peak melting temperature caused by the presence of comonomer (sample PHF24) is rather small, since, for heterogeneous catalysts, the comonomer units (and any kind of error, including tacticity errors) are concentrated in the lower molecular weights, and the higher molecular weight chains have a content smaller than average, thus leading to longer sequences free of defects.

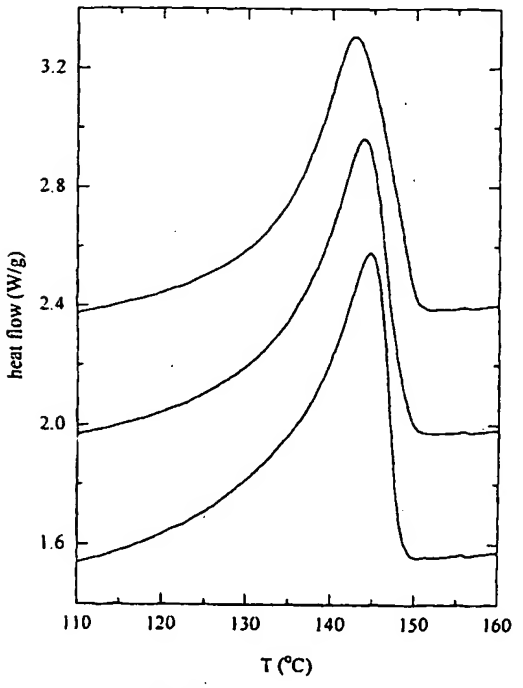

Fig. 8. D.s.c. melting curves corresponding to sample PPZ02 crystallized from the melt at different cooling rates. From top to bottom: 100, 20 and 3°C/min.

The errors are much more evenly distributed in the samples synthesized with homogeneous catalysts, in such a way that samples PPZ02 and PPZ19 display lower melting temperatures than PPF08 or PP1901, even though those have a higher [mmmm] content. For the same reason, a considerable decrease of the melting temperature is found for copolymer PHZ431, with only a 2.6 mol% comonomer content, but with a distribution presumably more random than that for copolymer PHF24. A similar behaviour is found in ethylene copolymers, when comparing samples prepared with heterogeneous and homogeneous catalysts [29,30].

4. Conclusions

Minor amounts, if any, of γ modification are present in iPP samples synthesized with highly isospecific ZN catalysts and crystallized from the melt at different cooling rates, ranging from 100 to 3°C/min. On the contrary, considerable amounts of the γ form have been obtained both in samples prepared with catalysts of very low isospecificity or in those prepared with homogeneous metallocene catalysts. It has been shown that the relative proportion of the α and γ modifications can be controlled just by changing the crystallization conditions.

A clear influence of the presence of comonomer units on favouring the formation of the γ phase has not been ascertained. Moreover, attempts to deduce the γ content from the d.s.c. melting patterns have been unsuccessful, since the two modifications exhibit very similar melting temperatures.

Acknowledgements

The financial support of the EEC (Network ERBCHRXCT930158) and of the Comisión Interministerial de Ciencia y Tecnología (project no. MAT96-2310) is gratefully acknowledged.

References

[1] Turner-Jones A, Aizlewood JM, Beckett DR. Makromol Chem 1964;75:134.
[2] Brückner S, Meille SV, Petraccone V, Pirozzi B. Prog Polym Sci 1991;16:361.
[3] Varga J. J Mater Sci 1992;27:2557.
[4] Natta G, Corradini P. Nuovo Cimento Suppl 1960;15:40.

[5] Meille SV, Ferro DR, Brückner S. Macromol Symp 1995;89:499.
[6] Crissman JM. J Polym Sci 1969;A2:389.
[7] Lovinger AJ, Chua JO, Gryte CC. J Polym Sci, Polym Phys Ed 1977;15:641.
[8] Zhou G, He Z, Yu J, Han Z, Shi G. Makromol Chem 1986;187:633.
[9] Addink EJ, Beintema J. Polymer 1961;2:185.
[10] Turner-Jones A. Polymer 1971;12:487.
[11] Marigo A, Marega C, Zannetti R, Paganetto G, Canossa E, Coletta F, Gottardi F. Makromol Chem 1989;190:2805.
[12] Kardos JL, Christiansen AW, Baer EJ. Polym Sci 1966;4 (A2):777.
[13] Fischer D, Mülhaupt R. Macromol Chem Phys 1994;195:1433.
[14] Alamo RG, Lucas JC, Mandelkern L. Polym Prepr 1994;35:406.
[15] Brückner S, Meille SV. Nature 1989;340:455.
[16] Slichter WP, Mandell ER. J Appl Phys 1958;29:1438.
[17] McAllister PB, Carter TJ, Hinde RM. J Polym Sci, Polym Phys Ed 1978;16:49.
[18] Corradini P, Petracone V, De Rosa C, Guerra C. Macromolecules 1986;19:2699.
[19] O'Kane WJ, Young RJ, Ryan AJ, Bras W, Derbyshire GE, Mant GR. Polymer 1994;35:1352.
[20] Alberola N, Fugier M, Petit D, Fillon B. J Mater Sci 1995;30:1187.
[21] Sacchi MC, Forlini F, Tritto I, Locatelli P, Morini G, Noristi L, Albizzati E. Macromolecules 1996;29:3341.
[22] Sacchi MC, Forlini F, Tritto I, Locatelli P, Morini G, Noristi L, Albizzati E. Macromol Chem Phys 1997;198:2397.
[23] Rieger B, Mu X, Mallin DT, Rausch MD, Chien JCW. Macromolecules 1990;23:3559.
[24] Coates GW, Waymouth RM. Science 1995;267:217.
[25] Mansel S, Pérez E, Brintzinger HH, submitted.
[26] Benavente R, Pereña JM, Bello A, Pérez E, Locatelli P, Fan Z-Q, Zucchi D. Polym Bull 1996;36:249.
[27] Pérez E, Benavente R, Bello A, Pereña JM, Zucchi D, Sacchi MC. Polymer 1997;38:5411.
[28] Thomann R, Wang C, Kressler J, Mülhaupt R. Macromolecules 1996;29:8425.
[29] Pérez E, Benavente R, Bello A, Pereña JM, Aguilar C, Martínez MC. Polym Eng Sci 1991;31:1189.
[30] Clas SD, McFaddin DC, Russell KE, Scammell-Bullock MV. J Polym Sci, Polym Chem Ed 1987;25:3105.

EXHIBIT 7

ELSEVIER

Polymer 42 (2001) 1167–1176

polymer

www.elsevier.nl/locate/polymer

Competition between α and γ phases in isotactic polypropylene: effects of ethylene content and nucleating agents at different cooling rates

T. Foresta[a], S. Piccarolo[a,*], G. Goldbeck-Wood[b]

[a]Dipartimento di Ingegneria Chimica dei Processi e dei Materiali, Viale delle Scienze, 90128 Palermo, Italy
[b]Department of Materials Science and Metallurgy, University of Cambridge, Pembroke Street, Cambridge CB2 3QZ, UK

Received 11 October 1999; received in revised form 7 March 2000; accepted 4 May 2000

Abstract

The influence of ethylene content, nucleating agents and cooling rate upon the formation of γ phase in isotactic polypropylene is investigated. Detailed analysis of wide angle X-ray diffraction shows that some γ phase can appear even in copolymers of very low ethylene content (0.5 mol.%). Differential scanning calorimetry shows a double melting peak. Nucleating agents of different types are found to enhance γ phase crystallization, even in high molecular weight homopolymers. In any of the materials studied the amount of γ phase decreases with increasing cooling rate, going to zero at a cooling rate of about 10°C s^{-1}. We interpret the observations in terms of the kinetics of growth and the phase stability, which shows that: (a) there is a region in which the γ phase has a lower free energy than the α phase; and (b) this region reaches lower temperatures with increasing comonomer content.

Keywords: Isotactic polypropylene; α and γ phases; Ethylene content

1. Introduction

Isotactic polypropylene (iPP) is on the one hand an 'ordinary' commodity polymer with a very simple chemical structure. On the other hand despite its chemical simplicity it shows a remarkable complexity of crystal structures, and self-assembly behavior [1,2]. Control of the growth of the different polymorphs as a function of material grade and crystallization conditions is of great technological importance.

Many studies have therefore been carried out with the aim of understanding the complex crystallization scenario. Concerning the crystal structures themselves, this work is concerned with the α and γ modifications. The monoclinic α phase is the most prevalent. It is generally the majority phase observed both in melt and solution-crystallized samples prepared at atmospheric pressure. For the γ phase, initially indexed as triclinic [3,4], studies of a form generated at atmospheric pressure from low molecular weight polymer led to a reassignment of the structure as orthorhombic [5] with a unique crossed arrangement of the chains in subsequent growth layers. It has an epitaxial relationship with the α phase such that either can grow onto lamellae of the other phase [6,7]. In general, however, the α phase is observed to grow first, followed by epitaxial growth of the γ phase, rather than the other way round [8]. The amount of γ phase generated is known to be enhanced by (i) crystallization under high pressure [9,10], (ii) low molecular weight [4,11] (iii) the presence of chain defects or chemical heterogeneity caused by atacticity [12,13], and (iv) ethylene comonomer units in the chain [4,14–16].

The latter effect was first noticed by Turner-Jones et al. [4]. Zimmermann [14] investigated random polypropylene–ethylene copolymers with ethylene contents from 4.3 to 11 mol.%. From the wide angle X-ray diffraction (WAXD) patterns the author determined the amount of γ-phase formed. Although he concluded that γ-phase can first be detected for an ethylene content of 5 mol.%, close inspection of the WAXD pattern of the 4.3 mol.% sample shows a clear sign of the γ phase, namely a small peak at just above $2\theta = 20°$ (as will be explained in Section 3).

More recently, detailed studies on the γ phase have been carried out by Laihonen et al. [16] and Mezghani et al. [15,17]. They confirmed the earlier findings that the amount of γ phase is proportional to the ethylene content, and show that more material crystallizes in the γ phase at low supercoolings and a smaller cooling rate. A maximum in the fractional content of the γ phase reported by Mezghani et al. [15] has recently also been found in an investigation of metallocene catalyzed polypropylenes with different defect concentrations [13]. For homopolymers [17] the amount of

* Corresponding author. Fax: +39-091-6567280.
E-mail address: piccarol@dicpm.unipa.it (S. Piccarolo).

0032-3861/01/$ - see front matter
PII: S0032-3861(00)00404-3

Table 1
Materials studied and their molecular weight (*Mw*), molecular weight distribution (*Mwd*), xylene solubility (*Xs*), comonomer content and nucleating agent

Material	*Mw*	*Mwd*	*Xs*	% ethylene	Nucleating agent
M7	377 000	4.8	2.3	0.0	–
M7N	379 000	5.3	3.4	0.0	Talc 1000 ppm
M4	268 000	5.0	3.8	0.0	–
M4N	277 000	5.1	4.1	0.0	DBS 2000 ppm
M3	213 000	4.3	2.8	0.0	–
M9	380 000	3.8	5.0	0.5	–
M16	293 000	7.3		3.1	–
M14	293 000	7.3		3.1	DBS

γ phase formed increases with pressure and crystallization temperature, so that it becomes possible at e.g. 125 MPa to grow pure γ phase material. Based on their extensive data, Mezghani and Phillips [17] were able to derive equilibrium melting point data and construct a temperature–pressure phase diagram for the α and γ forms.

This study presents recent results on the influence of ethylene content, nucleating agents and cooling rate upon the γ phase formation. The novelty of this work arises from two factors. Firstly, crystallization was carried out under a wide range of controlled cooling conditions, emulating non-isothermal solidification conditions usually experienced in polymer processing. Secondly, we analyze our observations of the phase behavior, as well as those of previous studies, in terms of the kinetics and size dependent stability of the phases.

2. Materials

The present study encompasses a wide range of iPP, kindly provided by Borealis AS, Norway, within the Brite project BRPR.CT92.0331. The main material characteristics are listed in Table 1.

Considering the data in Table 1, the influence of ethylene content was studied comparing M3, M9 and M16, while that

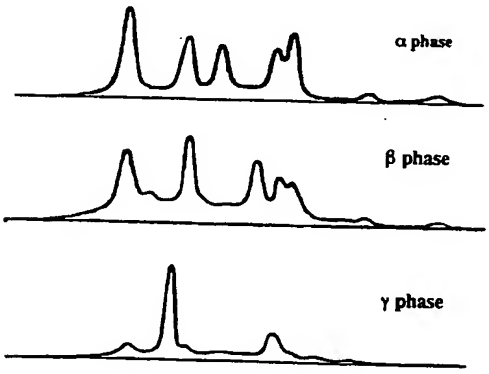

Fig. 1. Templates of typical WAXS patterns of pure α, β and γ crystalline forms of iPP.

Table 2
Assignment of WAXD peaks of the α, β and γ crystalline phases of iPP. For each phase the number at the top is the angle 2θ, and the index (*hkl*) is given below

	I	II	III	IV	V	VI	VII
α	14.08	16.95	18.5	21.2	21.85	25.5	28.45
	(110)	(040)	(120)	(131)	(041)	(060)	
β	16.1	16.6	21.3	24.7	28.07		
		(008)					
γ	13.84	15.05	16.72	20.07	21.2	21.88	
	(111)	(113)	(008)	(117)	(202)	(026)	

of different nucleating agents was studied comparing M7N and M4N with the respective nucleating agent free polymers (M7, M4). Finally, the effect of a simultaneous presence of ethylene and nucleating agents was studied by comparison of M14 and M16.

All the samples were solidified as thin films from the melt, controlling the cooling rate by an apparatus recently developed [19]. Prior to quenching, the polymer is kept in the melt at 250°C for a period of 30 min in order to erase memory effects. A nitrogen atmosphere prevents degradation [20]. The sample is quenched by spraying a suitable cooling fluid through two opposite spray nozzles onto the sample assembly, whereby the thin polymer film is sandwiched between two copper plates. One dimensional heat transfer is obtained in the thickness direction and, by control of sample thickness, homogeneous cooling conditions can be obtained. These, measured on the copper plates, can be controlled by changing their thickness and the cooling fluid used and its flow rate from 0.1 up to 1000°C s^{-1}. In the present work the cooling rates have been restricted to the range 0.04–30°C s^{-1} since outside this interval no γ phase is observed.

The advantage of our approach over standard methods of thermal analysis is that a wider range of cooling conditions can be explored. Characterization of the final structure can then be related to the thermal history recorded during cooling. While the full thermal history is available (and is used for the validation of models of crystallization kinetics examined elsewhere [19]), here only the cooling rate at 70°C is used as a single parameter characterizing the cooling conditions. The relevance of this parameter has been established elsewhere [19].

3. Characterization methods

Samples were characterized by means of Differential Scanning Calorimetry (DSC) using a Perkin-Elmer DSC7, and Wide Angle X-ray Diffraction (WAXD) on a Philips diffractometer with a Cu Kα tube and wavelength of $\lambda = 0.15418$ nm. DSC provides melting points, and WAXD was used to identify the phases and their respective amounts. Peak deconvolution was performed using the software program Peakfit, supplied by Jandel Sci.

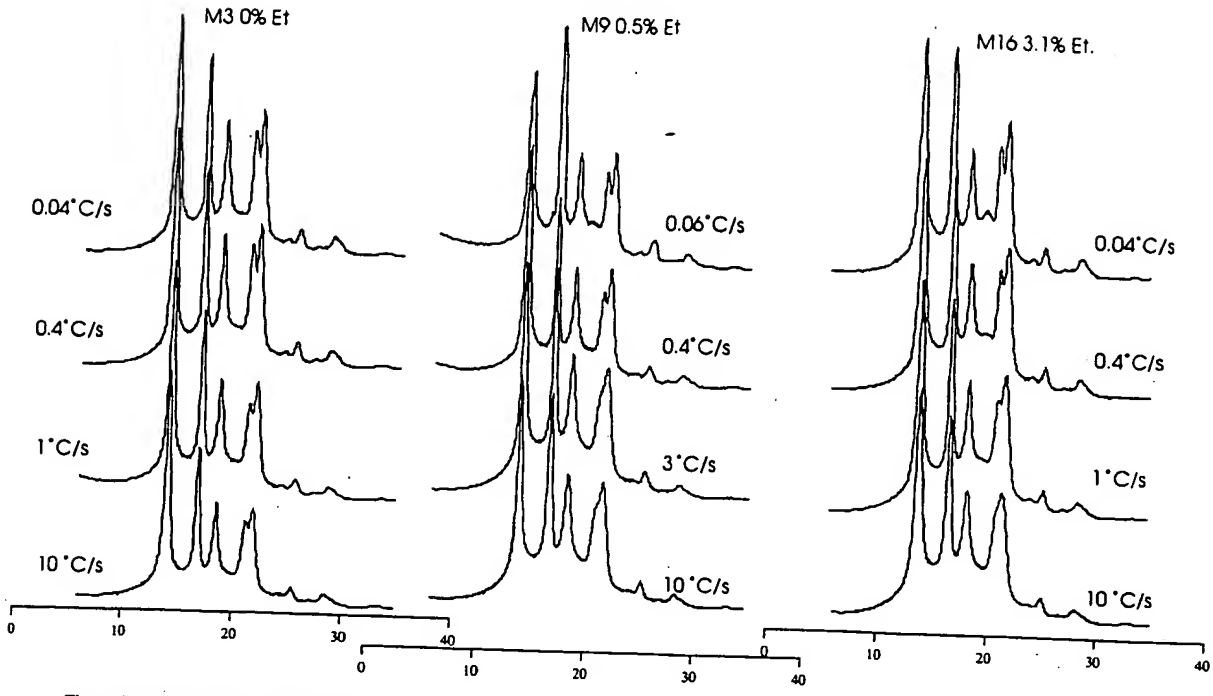

Fig. 2. WAXS patterns of M3, M9 and M16 with ethylene content of 0, 0.5 and 3.1%, respectively for different cooling rates at 70°C.

4. WAXD analysis methods

Each of the α, β and γ crystalline forms has its own distinctive peaks in the WAXD patterns, shown qualitatively in Fig. 1 and quantitatively in Table 2.

In a typical WAXD diffraction pattern of the α phase, the second peak is always smaller than the first one. However, this effect is not observed in samples containing the γ phase; their patterns are characterized by a second peak larger than the first one, which is not surprising considering the location of the strong peak II in the γ phase. Due to the closeness of the α and γ phase peaks in this region, peaks I, II and III are not ideal for an identification of the γ phase. Therefore, the identification of the presence of γ phase usually relies on the peak at $2\theta = 20.07°$. In previous studies [14,15], the γ to α ratio was calculated simply from the relative intensities of the unique γ and α peaks at 20.07 and 18.5°, respectively. Although this ratio provides the correct limits of zero γ and α phase in the absence of the respective peaks, it does not necessarily give the correct ratios in the intermediate regime. Therefore, in the present work the overall intensities in the angular range 10–23° of both phases are determined by means of a WAXD pattern deconvolution procedure. After subtraction of background scattering, for the γ phase the intensity of the unique peak IV is obtained directly from Peakfit. The intensities of all other peaks are then calculated on the basis of the relative intensities proposed by Brückner and Meille [5]. From their interpretation of the γ form, the peaks at $2\theta = 15.05°$ (113) and 20.07° (117) not overlapping with the α form ones, have a constant ratio of ca. 15/85. Moreover, the intensity of the (117) peak at 20.07° divided by the sum of the intensities of all peaks in the angular range between 10 and 23° is also constant. After subtracting the γ phase intensity so determined, the overall α phase intensity could be determined easily following the peak pattern of Table 2. The relative phase amounts were then given by the relative intensities. This rationale is adopted throughout this work to evaluate quantitatively the amount of γ phase.

The above method fails for very small amounts of γ phase when the (117) peak can no longer be distinguished from the amorphous background. Nevertheless, our observations indicate that the presence of γ phase can still be identified from the relative height of the peaks at $2\theta = 14°$ and $2\theta = 16.8°$. The former is the sum of the α peak at 14.08° and the γ peak at 13.84°, the latter the sum of the α peak at 16.95° and the γ peak at 16.72°. The latter being higher is the signature of the γ phase.

5. Results

5.1. Effect of ethylene content and cooling rate

The WAXD patterns obtained after cooling materials M3, M9 and M16 at increasing rates are shown in Fig. 2. By visual inspection we note that, at the lowest cooling rate, for the three materials, the second peak is either higher or comparable to the first one, and a little additional peak can be found at $2\theta = 20.07°$. This feature is more evident with increasing ethylene content. The same situation can be observed for cooling rates up to $1°C\,s^{-1}$, although less

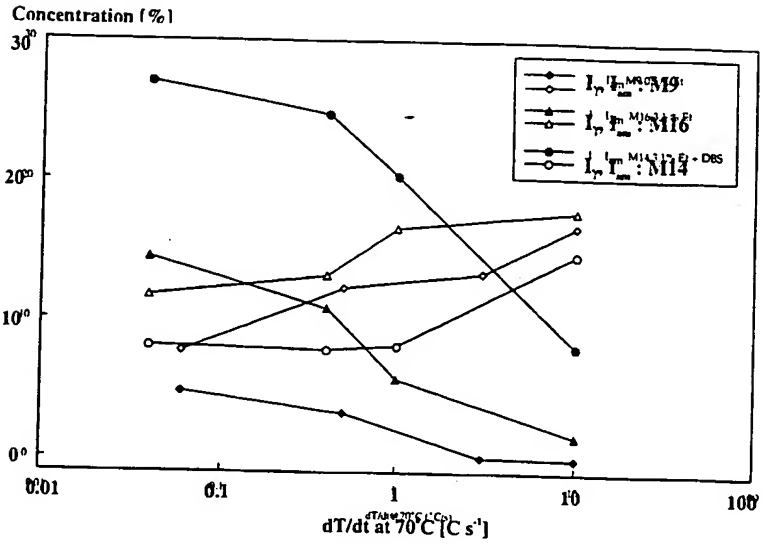

Fig. 3. The γ phase and amorphous content, respectively, as a function of cooling rate for the different copolymers.

evidently. The γ phase seems to have more or less disappeared at a cooling rate of 10°C s^{-1}.

Quantitatively, the amount of γ phase and of the amorphous halo calculated for the copolymers is shown in Fig. 3. For a given cooling rate the amount of γ phase as well as the amorphous halo increase with ethylene content. With increasing cooling rate the content of γ phase decreases, disappearing at higher cooling rate the larger the ethylene content.

The DSC traces of the copolymers M9 and M16, shown in Fig. 4, reveal a double peak over most of the range of crystallization conditions, in contrast to the single melting peak of the homopolymer M3.

There is disagreement about the assignment of the peaks in the literature. According to Mezghani and Phillips [17] the γ phase is preferred at lower cooling rates and lower supercoolings. It therefore is expected to form the first

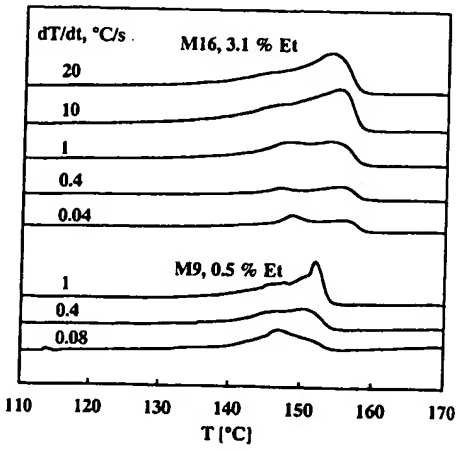

Fig. 4. DSC traces of the copolymers M9 and M16.

dominant lamellae onto which the α phase crystallizes epitaxially. Due to the tilt of the chains in the γ phase, the stem length of the epitaxial α phase crystals would be reduced by 24% [17]. Hence, on the basis of smaller crystal thickness Mezghani and Phillips assign the lower peak to the α phase. On the other hand, the DSC traces show the lower peak to decrease in strength relative to the higher temperature peak with increasing cooling rate. Melting and recrystallization phenomena will play a role especially for the larger cooling rates, and may result in a smearing out of the lower peak and strengthening of the final melting peak. Although this distortion makes it difficult to discern the effect of the initial phase content, the observed trend in relative peak heights is at least consistent with the WAXD results if we assign the lower peak to the γ phase. This would also be consistent with the γ phase growing onto the α phase [11], hence in our case at lower temperature. The recent work by Alamo et al. [13] corroborates the latter view. WAXD during melting shows a significant portion of the γ phase crystals disappear in the lower peak but some remain until the final melting. This observation is related to two populations of γ phase crystals: one that nucleates initially and independently and one that grows epitaxially onto the α phase. We shall come back to this point in our analysis.

5.2. Effect of nucleating agents and cooling rate

The WAXD patterns obtained for homopolymers with and without nucleating agents (M7,M7N and M4,M4N) are shown in Figs. 5 and 6. Visual inspection and quantitative analysis (Fig. 7) clearly show that the γ phase formation is enhanced by the presence of either nucleating agent, talc or DBS. M4N and M7N are mainly characterized by a second peak much larger than the first one for all cooling rates. In the case of M4N, in addition to the above

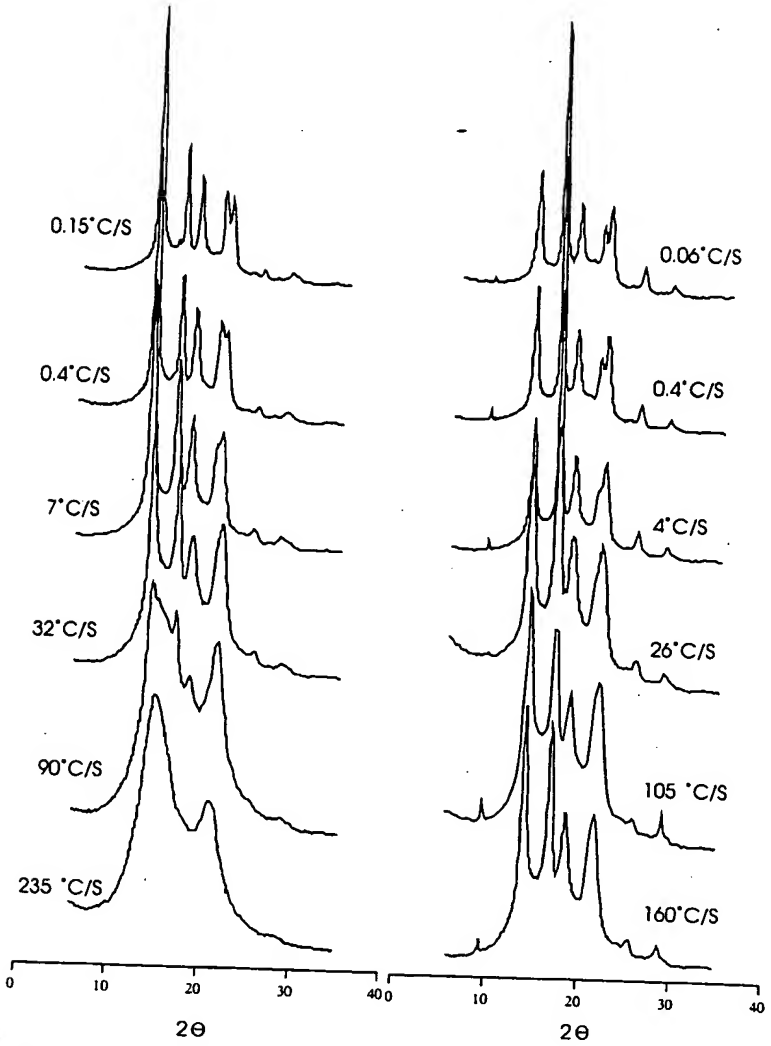

Fig. 5. WAXS patterns of M7 (left) and M7N (right) for different cooling rates at 70°C showing the influence of the nucleating agent talc on the γ phase content.

observation, the γ phase peak at 20.07° is also observed at low cooling rates. We cannot at present conclude whether this is an effect of the type of nucleating agent or is related to the lower molecular weight in comparison to the talc-filled polymer M7N. However, much lower molecular weights are usually needed to give rise to an increase of the γ phase content [4]. As above, increasing the cooling rate leads to a decreasing amount of γ phase and an increase of the amorphous halo (Fig. 7).

5.3. Combined effect of ethylene content, nucleating agents and cooling rate

We compared the two copolymers, M16 and M14, both with the same ethylene content (3.1%), and the latter including a nucleating agent. The first question to ask is whether the γ phase enhancing effects of the ethylene content and nucleating agents combine. The WAXD of the nucleated copolymer, Fig. 8, shows that this is indeed the case. Hence, for M14 the amount of γ phase is larger, and the cooling rate range in which the γ phase appears is wider, than for M16, as Fig. 3 shows.

The DSC traces of the M14 sample (Fig. 9) show an endothermic 'hump' followed by the main melting peak. The traces are similar to those reported by Mezghani and Phillips for isothermally crystallized samples with a considerable amount of γ phase. However, as noted above it is likely that different γ phase crystals are involved in the whole melting range.

6. Discussion and analysis of phase behavior

An analysis of the phase behavior of isotactic

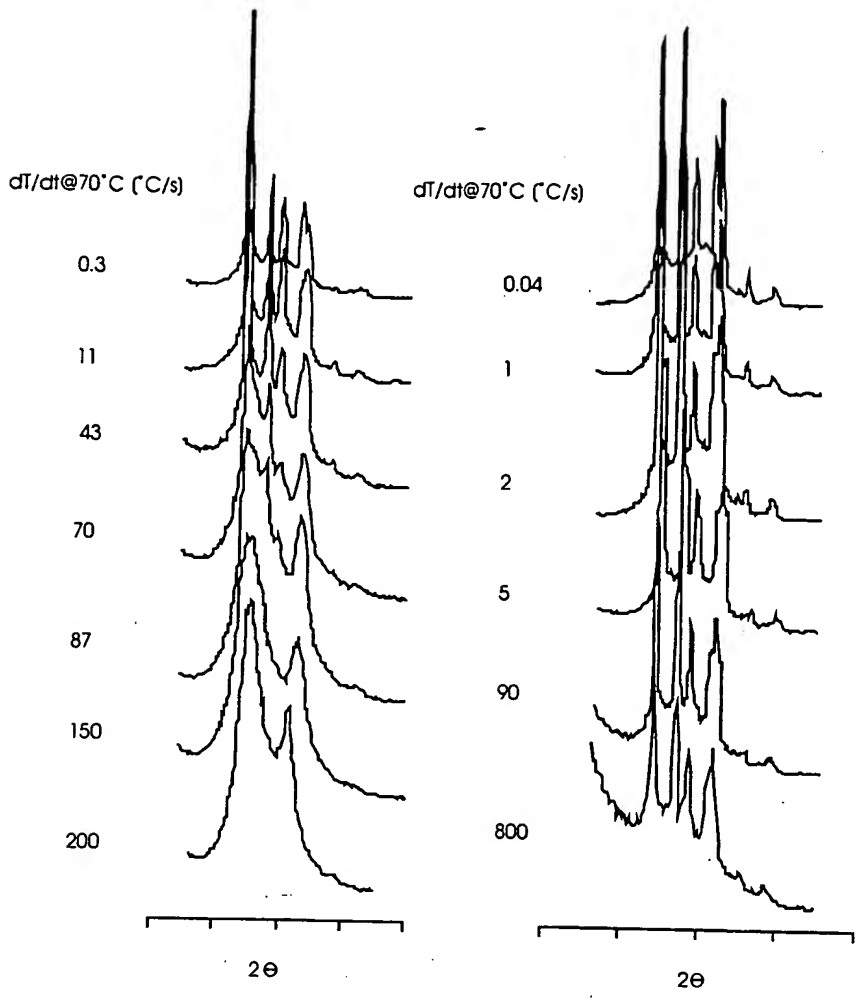

Fig. 6. WAXS patterns of M4 (left) and M4N (right) for different cooling rates at 70°C showing the influence of the nucleating agent DBS on the γ phase content.

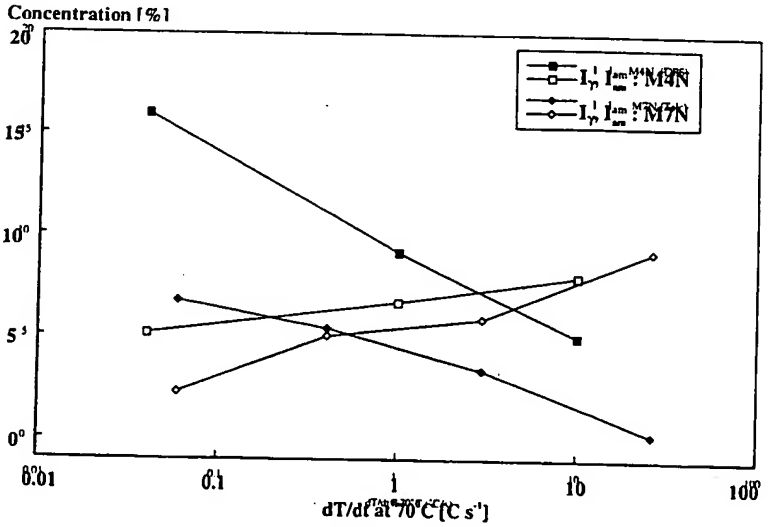

Fig. 7. γ phase and amorphous halo content based on Peakfit deconvolution vs cooling rate for the nucleated iPPs (M4N and M7N).

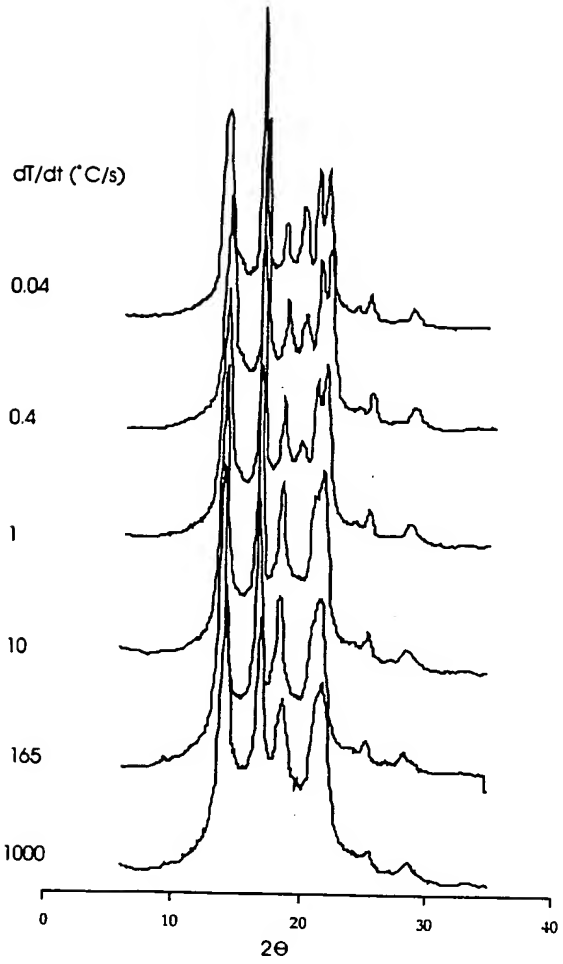

Fig. 8. WAXS patterns of M14 for different cooling rates at 70°C.

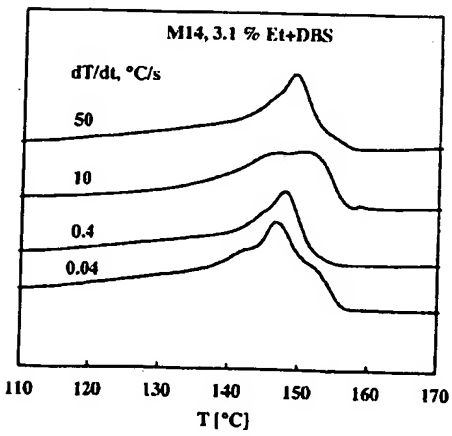

Fig. 9. DSC traces of the M14 sample.

polypropylene was recently carried out by Mezghani and Phillips [17]. They considered mainly the equilibrium melting points of the α and γ phases, and the effect of pressure on the phase behavior. Our concern is to put forward a possible explanation of the observation of phase behavior in copolymers, materials with nucleating agents and their dependence on cooling conditions.

The results above show that ethylene comonomer units, even in small amounts, lead to some γ phase crystallization. Higher cooling rates, hence higher supercoolings, are shown to be less favorable for γ phase growth. The question remains as to why this is so. There are basically two possible factors determining the likelihood of growth of a particular phase: kinetics and thermodynamics. In our discussion of these effects we follow broadly the considerations put forward by Keller et al. [21] in their discussion of the competition between the orthorhombic and hexagonal phases in polyethylene.

Kinetically, most of the evidence suggests that the α phase crystallizes faster than the γ phase. Experimentally it is generally found to crystallize first [11]. From a theoretical view point we would also conclude that the α phase is preferred in a homopolymer. To rationalize this we assume as in [21] that the rate of formation N is given by:

$$N = A \exp\left[-\frac{B}{T(\Delta T)^{n-1}}\right] \quad (1)$$

where the value of n is either 3 or 2 for primary nucleation or surface growth, respectively. The prefactor A contains, apart from transport terms, the frequency with which chain sections ready to crystallize present themselves. We expect this to be larger for the α phase due to its simpler structure. For phases with very similar melting points, the exponential term is mainly determined by the factor B, which is basically given by the ratio of surface free energy over heat of fusion [21]. A smaller ratio means faster growth, and this is indeed the case for the α phase, as follows from the thermodynamic data [17] shown in Table 3. For the copolymer we can argue that both factors change in favor of the γ phase. The increased flexibility in the chains should enhance the availability of segments to crystallize in the γ phase structure. Furthermore, the surface free energy will increase considerably more with comonomer content for the α phase structure than for the γ phase structure for the following reasons argued by Alamo et al. [13]. The presence of defects leads to shorter crystallizable sections, and many sections become too short for chain-folded crystallization. The chains will therefore proceed straight into the amorphous phase, which leads to an overcrowding and high surface free energy in the α phase structure, but can be accommodated in the γ phase structure because of the high tilt angle.

Thermodynamically, the relative stability of the different polymorphs may change as a result of growing phase size as well as changing temperature. For very small crystals, i.e. initially, a different phase may be stable to that which is the finally stable one at large size. This concept was discussed

Table 3
Thermodynamic parameters for the homopolymer [17]

Phase	T_m^0(°C)	ΔH (J g^{-1})	ρ (g cm^{-3})	σ_e (10^{-7}J cm^{-2})
α	186.1	209	0.936	52.2
γ	187.2	190	0.933	51.7

e.g. by Keller et al. [21] in the context of the competition between the orthorhombic and hexagonal phases in polyethylene, and we shall follow a similar analysis.

Since the β phase is absent in the materials and conditions we studied, we concentrate on the relative stability of the α, γ and melt phases. For this purpose we need to determine the melting lines of the two phases as a function of size, and a line which denotes the transition between the two crystalline phases.

The melting lines are defined by the Gibbs–Thomson relation:

$$T_m(\ell) = T_m^0\left(1 - \frac{2\sigma_e}{\ell\rho\Delta H}\right) \tag{2}$$

where T_m^0 is the equilibrium melting point, σ_e the fold surface free energy, ρ the density, and ΔH the heat of melting of the respective phase (α or γ). The transition line is defined in principle by a similar equation with the respective quantities in Eq. (1) relating to the transformation between the α and γ phases. As in Ref. [21] it is determined simply by a straight line through two points: (i) the triple point T_Q (at which the melting lines cross), and (ii) the transition temperature T_{tr}^0, which is given by equating the Gibbs free energies of the two phases [18]:

$$T_{tr}^0 = \frac{T_{m,\alpha}^0 T_{m,\gamma}^0(\Delta H_\alpha - \Delta H_\gamma)}{T_{m,\gamma}^0\Delta H_\alpha - T_{m,\alpha}^0\Delta H_\gamma} \tag{3}$$

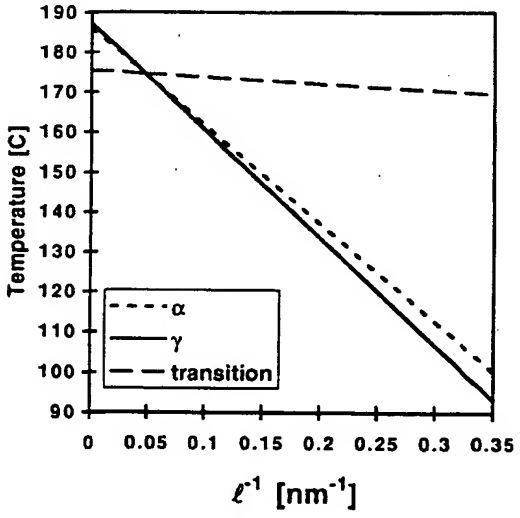

Fig. 10. Schematic phase stability diagram of an iPP homopolymer showing the melting lines of the α phase and γ phase, respectively, and the transition line between the two phases.

In combination with Eqs. (1) and (2) and inserting the data from Table 3 we obtain the homopolymer phase stability diagram shown in Fig. 10. We note in particular the transition lines between the two phases that divides the diagram into a region above it where the γ phase is more stable than α, and below it where the α phase is more stable.

Numerically, on the basis of the parameter values given by Mezghani and Phillips, the range of lower free energy of the γ phase in homopolymers is limited to temperatures close to the melting point. The equilibrium transition point is at $T_{tr}^0 = 175$°C, and the triple point is at a temperature $T_Q = 174$°C, and a lamellar thickness of 21.2 nm. Hence hardly any γ phase can be expected for a plain homopolymer. However, the higher the temperature of crystallization, the more likely it becomes that some γ phase is formed. This agrees with the observation of small amounts of γ phase in the nucleated materials (Figs. 5 and 6).

The question now arising is how this scenario changes in the case of copolymers. The melting points of copolymers of similar molecular weight and ethylene content were determined by Mezghani and Phillips [17]. However, their data refer to mixed phase crystals and hence only provide some average melting point of 180°C for a 0.5% copolymer and 166°C for a 3% copolymer. We assume that the melting point of the α phase is still slightly below that of the γ phase and set the melting points to 165 and 166°C, respectively. The density and heat of fusion are reduced due to an inclusion of some of the ethylene in the crystalline phase [18]. The data in Ref. [18] have a considerable uncertainty but suggest that for the 3% copolymer the heat of fusion is reduced by about 10 J g^{-1} and the density decreased by about 2%. As for the surface free energies we assume that σ_e increases somewhat more for the α than for the γ phase due to overcrowding of chains on the α phase fold surface but not on the γ phase crystals [13]. The resulting data set in Table 4 is hence our best estimate for the copolymer M16. In any case it should serve qualitatively to illustrate the expected behavior, and we shall comment on alternative scenarios below. The corresponding phase stability diagram is shown in Fig. 11. The melting lines are shifted downwards in temperature by about 20°C, and the (negative) slope of the α phase melting line is slightly increased. This scenario is in good agreement with experimental observations of the effect of co-units on the equilibrium melting behavior. As an example we quote the study by Cheng et al. [22] on the isotacticity effect on crystallization and melting of polypropylenes.

Fig. 11 shows that the region in which the γ phase has the lowest free energy is significantly larger than in the homopolymer. The melting and transition lines are almost parallel due to similar surface free energy to heat of fusion ratios.

Table 4
Estimated thermodynamic parameters for the copolymer M16

Phase	T_m^0(°C)	ΔH (J g^{-1})	ρ (g cm^{-3})	σ_e (10^{-7}J cm^{-2})
α	165	199	0.917	57
γ	166	180	0.914	52

The triple point has therefore shifted down to 95°C, and a thickness of about 4 nm. The diagram is an expression of the fact that (a) the thermodynamic driving force for the growth of γ phase crystals is very similar to that of the α phase, (b) some γ phase may form initially as its region of lower free energy is passed, and (c) this region becomes wider at higher temperatures. The phase stability diagram is consistent with our observations that faster cooling leads to less γ phase and with that of isothermal studies [15] showing that the formation of γ phase takes place at lower supercoolings only [17]. Although the material finally, when cooled down, ends up in the region in which the α phase is most stable, such a solid–solid transformation would not be expected to take place during cooling at the given rates nor at room temperature because of the small free energy difference and the large difference in crystallographic structure of the two phases.

The considerable enhancement of γ phase that we observed in the case of copolymer with nucleating agent (M14) can also be understood in the scenario of Fig. 11. We note first that the nucleating agent is expected to be active for both α and γ phases due to their epitaxial relationship. In the presence of nuclei crystallization sets in at higher temperatures, and therefore a much larger part of the transformation will take place in the γ phase 'stability region'.

Finally, we comment on alternative scenarios. The above interpretation relies on the two facts that the γ phase melting point is above that of the α phase, and the slope $S = 2T_m^0\sigma_e/\rho\Delta H$ is greater for the γ phase. If the order of the melting points is reversed, two alternative scenarios arise: (i) if the slope S remains in the same order for the two phases; then the α phase is the most stable phase under all conditions; and (ii) if at the same time the order of S is changed, then the whole picture is simply reversed and the γ phase is the most stable phase at lower temperatures.

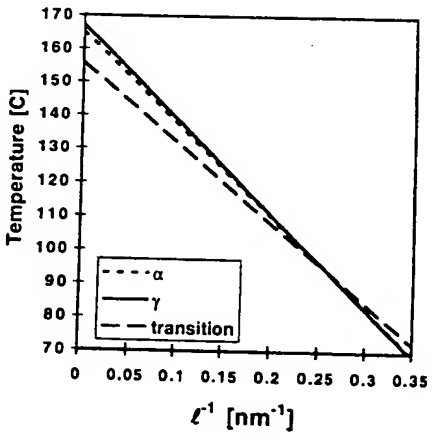

Fig. 11. Schematic phase stability diagram of an iPP copolymer with 3% ethylene. The melting lines of the α phase and γ phase, respectively, and the transition line between the two phases are shown.

7. Conclusions

We have observed the crystal structure of isotactic polypropylene homopolymer and ethylene copolymers with and without nucleating agents crystallized at different cooling rates. The results can be summarized as follows: As observed by previous studies, ethylene comonomers lead to the formation of some γ phase, the amount increasing with ethylene content, but decreasing with increasing cooling rate. Nucleating agents also lead to a small amount of γ phase and enhance the amount of γ phase formed in ethylene copolymers. We put forward an interpretation for all of these observation in terms of crystallization kinetics and phase stability diagrams. The phase stability diagram shows a small region where the γ phase has lower free energy than the α phase. It is limited to high temperatures for homopolymers but moves to lower temperatures and increases in size with increasing comonomer content. In addition, the kinetics acts in the same way, favoring the α phase for homopolymers but less so with increasing ethylene content. Therefore on both counts more γ phase is expected to form with increasing comonomer content. As the α phase remains the most stable one at lower temperatures, the amount of γ phase formed will decrease with increasing cooling rate or undercooling. Nucleating agents will hence lead to an increase in the amount of γ phase since crystallization will set in at higher temperatures.

Acknowledgements

This work has been performed with the financial support of EU Brite Contract BRE2.CT92.0331 and of Italian Ministry of University 40% quota. The characterization of the materials by Borealis AS, Norway, is gratefully acknowledged.

References

[1] Brückner S, Meille SV, Petraccone V, Pirozzi B. Prog Polym Sci 1991;16(2–3):361–404.
[2] Lotz B, Wittmann JC, Lovinger AJ. Polymer 1996;37:4979–92.
[3] Turner-Jones A, Aizlewood JM, Beckett DR. Makromol Chem 1964;75:134–58.
[4] Morrow DR, Newman BA. J Appl Phys 1968;39:4944–50.
[5] Brückner S, Meille SV. Nature 1989;340:455–7.
[6] Lotz B, Graff S, Wittmann JC. J Polym Sci, Polym Phys Ed 1986;24:2017–32.
[7] Lotz B, Graff S, Straupé C, Wittmann JC. Polymer 1991;32:2902–10.
[8] Lotz B. Private communication, 1999.

[9] Campbell RA, Phillips PJ, Lin JS. Polymer 1993;34(23):4809–16.
[10] Pae KD, Morrow DR, Sauer JA. Nature 1966;211:514.
[11] Addink EJ, Beintema J. Polymer 1961;2:185.
[12] Turner-Jones A. Polymer 1971;12:487.
[13] Alamo RG, Kim MH, Galante MJ, Isasi JR, Mandelkern L. Macromolecules 1999;32(12):4050–64.
[14] Zimmermann HJ. J Macromol Sci, Phys B 1993;32(2):141–61.
[15] Mezghani K, Phillips PJ. Polymer 1995;36:2407–11.
[16] Laihonen S, Gedde UW, Werner P-E, Martinez-Salazar J. Polymer 1997;38:361–9.
[17] Mezghani K, Phillips PJ. Polymer 1998;39:3735–44.
[18] Laihonen S, Gedde UW, Werner P-E, Westdahl M, Jaaskelainen P, Martinez-Salazar J. Polymer 1997;38:371–7.
[19] Brucato V, Crippa G, Piccarolo S, Titomanlio G. Polym Engng Sci 1991;31(19):1411–6.
[20] Piccarolo S. J Macromol Sci, Phys B 1992;31(4):501–11.
[21] Keller A, Hikosaka M, Rastogi S, Toda A, Barham PJ, Goldbeck-Wood G. J Mater Sci 1994;29:2579–604.
[22] Cheng SZD, Janimak JJ, Zhang A, Hsieh ET. Polymer 1991;32(4):648–55.

EXHIBIT 8

POLYMER

the science and technology of polymers and biopolymers

IPC Science and Technology Press Ltd

Development of the γ-crystal form in random copolymers of propylene and their analysis by DSC and X-ray methods

A. TURNER-JONES

Random copolymers of propylene with minor proportions of ethylene, butene and other comonomers develop γ-form crystallinity, mixed with α-form, on crystallisation from near the melting point. The proportion of γ-form increases with comonomer content. γ-form determinations, together with measurement of degrees of crystallinity by X-rays and melting point distributions by differential scanning calorimetry (DSC), after carefully controlled thermal treatment, can be used to characterize the chain distribution present. The effect of thermal history on the melt distribution observed by DSC and the α/γ ratio has been investigated in detail for one copolymer containing 6·5mol% ethylene, and the crystal morphology developed in this copolymer and fractions obtained by solvent extraction is discussed.

INTRODUCTION

IN AN EARLIER paper by the author[1] it was shown that stereoblock fractions obtained by solvent extraction of normal commercial polypropylene cooled from above their melting points gave γ-form crystallinity as well as normal α-form. The low temperature fractions, obtained over the approximate range 35–70°C using petroleum ether or xylene as solvents, were of high molecular weight and crystallized entirely in the γ-form. The development of γ-form was ascribed to discontinuities in the isotactic sequences in the chains. These discontinuities were caused either by short atactic sequences of propylene units or by simple switches (one heterotactic unit) from an isotactic sequence where the methyl groups are all on one side of the main C—C backbone (regarded as a linear zig-zag) to an isotactic sequence where they are all on the opposite side.

Since then highly isotactic polypropylene, as opposed to stereoblock polymer has been obtained in the γ-form free of α-form by crystallization under very high pressure by Kardos[2] and Pae[3] and also independently in these laboratories. Very low molecular weight isotactic polymer has also been shown to crystallize in the γ-form by melt crystallization[4] and from certain solvents[4–6].

In this paper it is shown that random copolymerization of small amounts of various comonomers with propylene using stereospecific catalysts, gives copolymers which, on slow cooling from the melt, yield mixed α/γ crystallinity with a high proportion in the γ-form. This supports the thesis that development of the γ-form is due to interruptions in the isotactic propylene sequences, in this case due to comonomer units. As with the stereoblock fractions the copolymers as originally made, before they are melted, show

α-form of relatively low crystallinity. The two comonomers showing this effect that have been investigated in most detail are ethylene and butene, but 3-methylbutene and octene and other randomly polymerized comonomers have also been shown to increase the proportion of γ on crystallization from the melt. Neither of these two comonomers co-crystallizes with polypropylene although low levels of randomly distributed butene units may enter the polypropylene lattice to a limited extent, reducing, but not disrupting crystallinity. This is shown by the expansion of the polypropylene crystal lattice[7,8]. Random copolymers of propylene and ethylene in roughly comparable proportions are, as is well known, amorphous.

This paper discusses the effect of the proportion of comonomer and the thermal history on the amount of γ-form produced in mixed α/γ crystallinity and on the melting point distribution observed by differential scanning calorimetry (DSC). It describes how these parameters can be used to analyse qualitatively the chain distribution in propylene copolymers containing small amounts of ethylene and butene distributed randomly, or as block copolymers, and mixtures of polypropylene with small amounts of polyethylene. The methods differ from those of Barrall *et al.*[9] previously reported.

One copolymer containing 6·5 mol% ethylene was selected for more detailed investigation and for fractionation studies.

EXPERIMENTAL

Preparation of copolymers

All the copolymers were made with $TiCl_3/AlEt_2Cl$ catalysts in a high boiling aliphatic hydrocarbon at 60°C. The rates of feeding propylene and ethylene (or butene) were adjusted so as to obtain random copolymers. The molecular weights were controlled by hydrogen modification to approximately $M_w = 300\,000$. The polymer was isolated by filtration at 60°C and the soluble portion discarded.

Five random copolymers were examined containing between 3 and 17 mol% butene (B_1–B_5, see *Table 1*) and two random copolymers E_1 and E_2 containing 3 mol% and 6·5 mol% ethylene respectively. Three other copolymers with ethylene were examined. These were made by first polymerizing propylene to homopolymer before introducing the ethylene to make random copolymer during the subsequent polymerization. The initial polypropylene portion amounted to 15% or 30% by weight of the final polymer. The data on the copolymers E_1–E_5 are also included in *Table 1*.

In the butene series of copolymers a very small amount of homopolymer (1·5% by weight of the total polymer) was polymerized before the butene was introduced. Four of these copolymers, all except B_4, contained a nucleating agent. None of the copolymers with ethylene contained a nucleating agent.

Unfortunately no directly comparable homopolymer was made at the same time under identical conditions but a typical commercial polypropylene (PP) has been included for comparison, and also a blend of the same propylene homopolymer with 4% of high density polyethylene (PP/E) made by mixing the homopolymers as powders and milling into a crêpe.

Determination of comonomer content

The proportion of comonomer present in the samples was determined by M. E. A. Cudby of these laboratories by infra-red methods which will be published separately. It was shown that the ethylene was present mainly as $-(CH_2)_n-$ sequences where $n = 5$ or 7. The average length of the butene sequences is not certain.

Table 1 Degrees of crystallinity and percent γ developed on slow cooling

Sample	*Comonomer*			*Cryst. %* (cooled from 160°C at 6C°/h)	*γ %** (cooled from 160°C at 6C°/h)	*Cryst. %* (cooled from 190°C at 6C°/h)	*γ %** (cooled from 190°C at 6C°/h)
		(Wt%)	(Mol%)				
PP		—	—	70	0	69	7
PP/E	ethylene blend	4	6	70	0	62·5	0
B_1	butene (random)	4	3	60·5	20		
B_2		7	5·5	58·5	32		
B_3		10	8	52·5	39		
B_4		12	10	50	48		
B_5		20·5	17	40	?		
E_1	ethylene (random)	2	3	60	22	59	33
E_2		4·5	6·5	57·5	46	53	52
E_3	(15% PP)†	3	4·5	57·5	24	55	37
E_4	(15% PP)†	4·5	7	53	34	52	38
E_5	(30% PP)†	5	7·5	57·5	31	50·5	27

* % of total crystallinity (α + γ) not of whole sample
† Proportion polymerized as propylene homopolymer before ethylene is fed to give random copolymer

Crystallinity determinations

These were carried out by methods basically similar to that of Natta[10]. X-ray diffraction scans were obtained with a Philips PW 1010 diffractometer with Cu-Kα radiation and pulse height discrimination and working in transmission. A straight background was drawn in between 4° and 16° of θ and the diffraction scans were then divided into areas attributable to diffuse scatter from the amorphous regions (A) and to sharp diffraction peaks from the crystalline regions (C) as shown by the dotted lines of *Figures 1a* and *1b*. The crystallinity was calculated as $C/(C + A)$ with no corrections. The object was to place samples in order of crystallinity and show trends in crystallinity. Naturally the method is not claimed to be absolute. No polymer in any case is a simple two phase system of crystalline and amorphous regions and the determinations are further complicated by the presence of two crystal forms. Close comparisons are not valid when different proportions of the two forms are present.

Determination of α- and γ-forms

The X-ray diffraction patterns of the α-and γ-forms were described in

reference 1. They are similar in many respects but the third strong reflection at d-spacing 4·77 Å (0·477 nm) of the α-form (α_3) is absent in the γ-form and is replaced by a line at 4·42 Å (γ_3). The relative proportions of α and γ of the total crystallinity (not of the total sample) which are quoted are based on the relative intensities of these two lines. The x-ray diffractometer scans of the two samples, one wholly α-form and the other wholly γ-form and both with overall crystallinity 60%, were normalized to constant area (crystalline + amorphous) above background between 4° and 16° of θ (see *Figures 1a* and *1e*

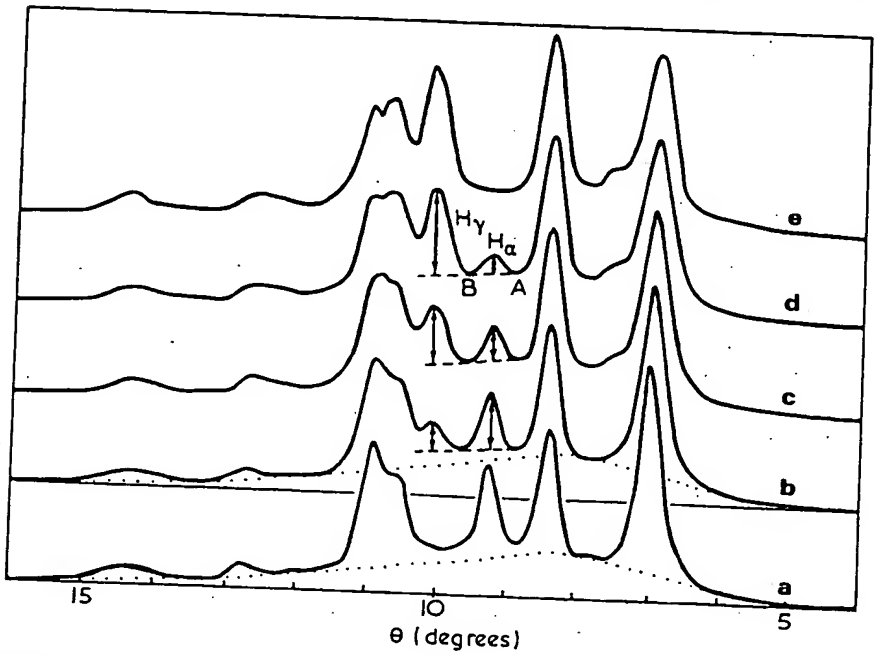

Figure 1 x-ray diffraction scans of propylene homopolymer: (a) α-form; (e) γ-form; (b), (c), (d) α/γ ratios of 75:25, 50:50, 25:75, respectively, derived graphically from (a) and (e)

respectively). The scan attributable to a polymer of 60% crystallinity with α/γ ratio 50:50 was obtained by adding graphically one half of the intensity above background of the γ-form scan to half of the intensity of the α-form scan at suitable intervals of θ. The resulting scan is shown in *Figure 1c*. Similar scans were obtained for α/γ ratios of 25:75 and 75:25 (see *Figures 1b* and *1d*). The heights H_α and H_γ of the α and γ peaks were measured as shown in *Figure 1* and the quantity $H_\gamma/(H_\alpha + H_\gamma)$ plotted against the percent γ crystallinity (*Figure 2*).

From the graph the proportion of γ-form could be obtained in experimental specimens by measuring H_γ and H_α in the same way. (The extrapolation of the line AB was used as a base line in determining H_γ because γ_3 is not always well resolved from the strong reflections at $\theta = 10{\cdot}5$–11°, particularly in poorly crystalline specimens.) Confirmation of the validity of the method

was obtained by mixing together the finely divided all-γ and all-α polymers in the proportions 50:50 and 40:60 and 60:40. γ-form determinations from the X-ray scans of these mixtures are marked with crosses in *Figure 2* and fall close to the line obtained graphically.

This method differs slightly from that used by K. D. Pae[11] who, in the investigation of γ to α conversion in high pressure crystallized polypropylene,

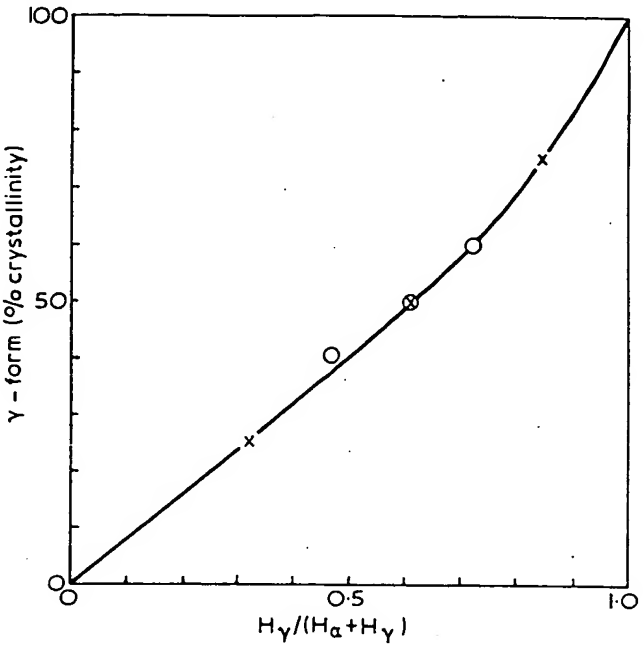

Figure 2 Percent of total crystallinity in γ-form vs. $H_\gamma/(H_\alpha + H_\gamma)$ (see *Figure 1*)

took the proportions of α and γ equal when the height of the α and γ peaks were equal and from that of Morrow and Newman[4] who regarded them as equal when the height of the γ peak was twice that of α.

Preparation of DSC and X-ray specimens

Specimens for DSC examination (10 mg) were cut from thin films to fit the standard aluminium pans (¼ in diameter). The films were obtained by pressing, at 210°C, the powders as originally made and cooling at a moderate rate.

In some of the experiments the specimens were first slowly cooled at 6C°/h from 160°C or 190°C. Specimens of the polymers to be compared were placed in their aluminium pans in cavities of suitable size cut in a brass block sealed by a thick brass lid. The whole was placed in an oil bath heated to the temperature from which cooling was to start. The mass of metal reduced the temperature of the bath and slow heating was continued until the desired

starting temperature was again reached as measured by a thermocouple placed inside the metal block. Cooling was then started immediately. The final heating process took some 15 min and the starting temperature was thus reached asymptotically, the last ten degrees taking about 10 min. This thermal history before cooling was started is important and, in comparing different batches of samples, it is necessary to carry out the procedure consistently and not to exceed the starting temperature for reasons which become clear later. The high thermal conductivity and heat capacity of the metal block ensured that all the samples at different parts of the block were given the same thermal treatment and helped to smooth out the temperature fluctuations of the oil bath. The block itself showed cyclic temperature fluctuation of $\pm$ 1°C. When required, extra specimens of each polymer were included for X-ray crystallinity determinations to ensure that DSC and X-ray specimens had received identical thermal treatment. These were subsequently chopped finely and placed in thin walled PANTAK glass tubes of 2 mm diameter for X-ray examination.

Differential scanning calorimetry

Differential scanning calorimetry was carried out with a Perkin-Elmer DSC-1 instrument using 10 mg samples. Calibration for heating runs was carried out by observing the onset of melting of standard indium samples. This takes account of both the temperature scale error and the lag in recording which arises from the relative positions of the temperature sensors and the base of the sample pan; this lag varies with heating rate. No correction has been made for thermal lag through the sample which only amounts to ~1°C. Owing to the particular characteristics of the Perkin-Elmer instrument the corrections to the temperature scale are not constant over the whole temperature range. All the DSC heating curves shown in the diagrams were obtained at a heating rate of 16C°/min. Investigations using slower and faster rates showed that no significant recrystallization occurred during scanning. The approximate correction was – 4°C at the melting point of indium (156·5°C) and the temperature scales shown are correct at this temperature. The main object has been to present an entirely consistent series of scans. To facilitate comparison between different DSC curves all the scans have been normalized to a horizontal background. The position of the background could not always be clearly determined, especially at low temperatures when melting started gradually. Hence too much reliance should not be placed on small differences in these low temperature regions.

RESULTS AND DISCUSSION

X-RAY AND DSC ANALYSIS OF COPOLYMERS OF PROPYLENE WITH ETHYLENE AND BUTENE

The degrees of crystallinity and the proportions of γ-form developed in the butene and ethylene copolymers after prior cooling at 6C°/h from 160°C or 190°C are given in *Table 1*. The DSC scans of samples similarly slow cooled are shown in *Figures 3* and *4*. The scans shown by dotted lines in these figures

were obtained after continuing heating to 230°C, holding for 5 min, cooling at 16C°/min to room temperature and then reheating. Details of the crystallization exotherms recorded during cooling are given in *Table 2*.

The similarity in crystallization and melting behaviour between these copolymers and the stereoblock fractions obtained from homopolymers by

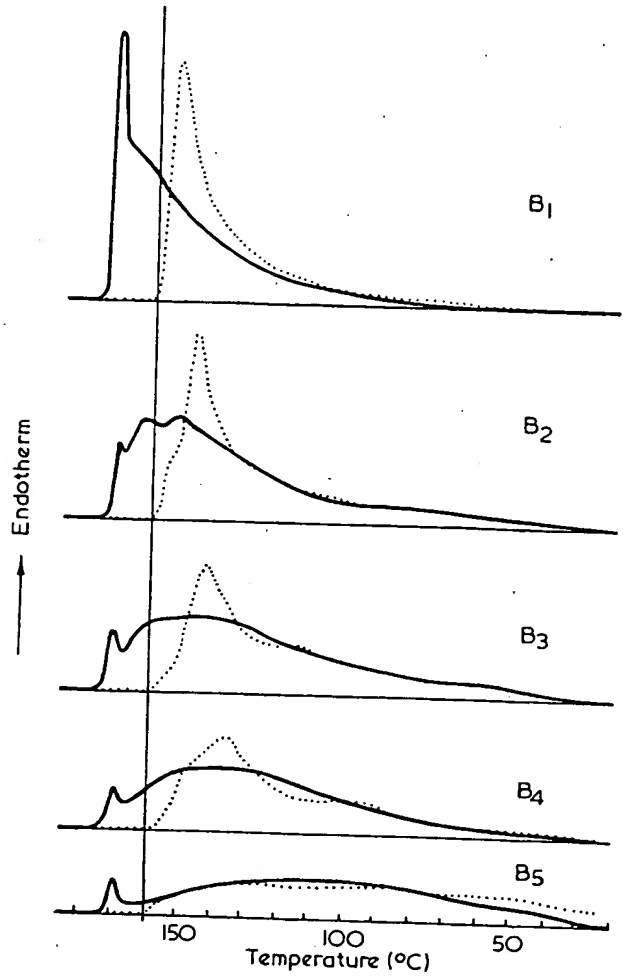

Figure 3 DSC reheat endotherms of random copolymers of propylene with butene (B_1–B_5, see *Table 1*) after cooling at 6C°/h from 160°C (thick lines); from 230°C at 16C°/min (dotted lines)

solvent fractionation[1] lends support to the hypothesis that the development of the γ-form is due to interruptions in the polypropylene isotactic sequences. In the copolymers these interruptions are now the comonomer units. When the interruptions are more frequent a higher proportion of γ-form is developed.

The wide melting ranges observed after slow cooling from 160°C show

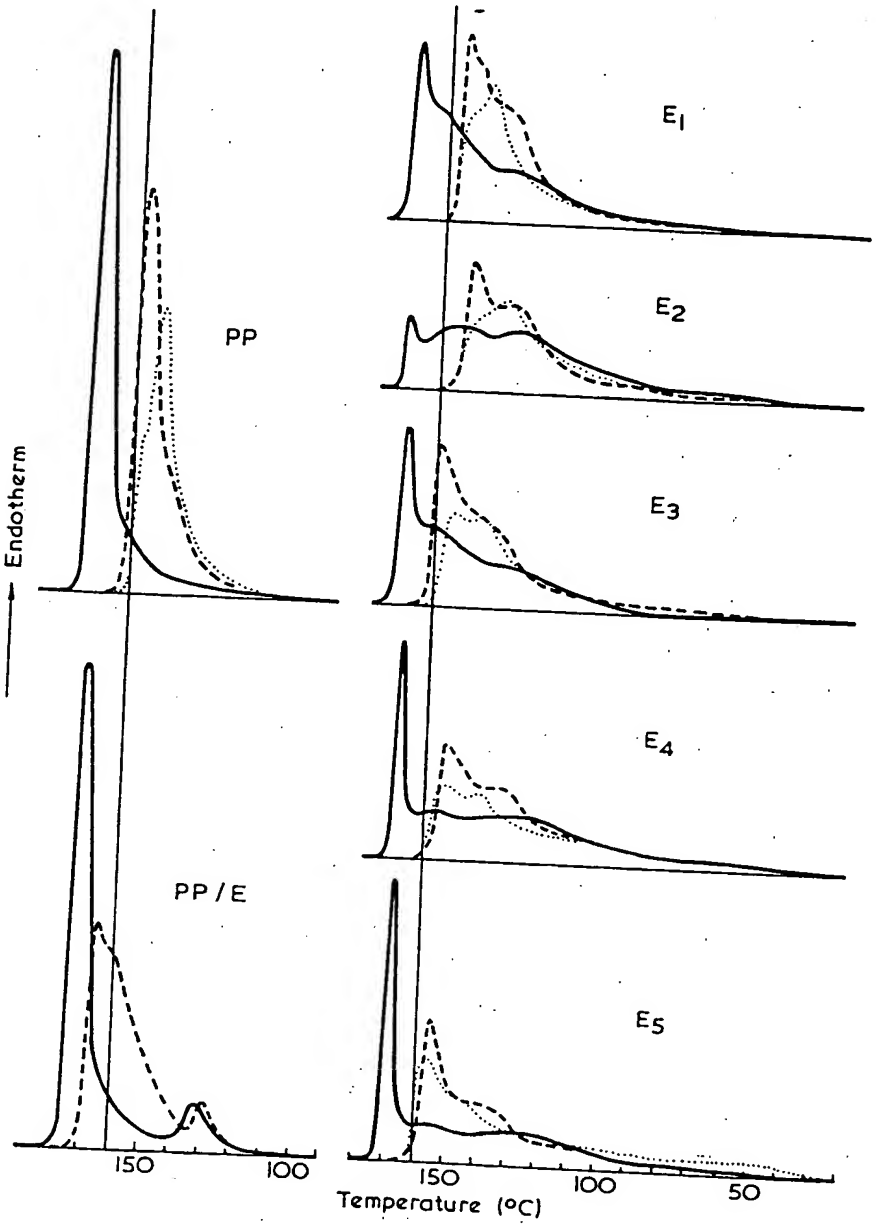

Figure 4 DSC reheat endotherms of propylene homopolymer (PP), blend with polyethylene (PP/E) and copolymers with ethylene (E_1–E_5, see *Table 1*), after first cooling at 6C°/h from 160°C (thick lines) and from 190°C (dashed lines); from 230°C at 16C°/min (dotted lines)

that the polymerization method adopted has resulted in copolymer chains with a wide distribution of isotactic polypropylene sequence lengths which, on slow cooling, crystallize at different temperatures to give crystallites of different thicknesses and perfection and hence different melting points. The high melting peaks at ~170°C show that some chains of very long isotactic sequences (either similar to those in normal propylene homopolymer or containing very few interruptions by comonomer units) are present in all

Table 2 DSC exotherms on cooling from 230°C at 16C°/min

Polymer	T_s(°C)	T_c(°C)	*Peak height*†	*Peak width*‡
PP	117	112	7·3	3·2
B_1*	120	113	6·3	4·0
B_2*	118	111	5·4	4·5
B_3*	115	107	4·2	4·6
B_4	103	85	2·8	7·7
B_5*	112	102	1·1	v. wide
E_1	108	96	3·6	7·5
E_2	106	90	2·6	10

T_s start of exotherm as defined by clear departure from base line; T_c peak of exotherm

* contains a nucleating agent
† in arbitrary units
‡ in °C on DSC trace, at half height

polymers but, as expected, are much fewer in the copolymers with the highest comonomer content. The very small peak at 168°C present in the most highly modified copolymer B_5 is due, at least in part, to the 1·5% of homopolymer present, as already mentioned.

As comonomer content increases the proportion of polymer melting at progressively lower temperatures increases. This is accompanied by increasing amounts of γ-form which must have developed from chains of progressively shorter, but still crystallizable, polypropylene sequences. The proportion of γ-form developed in B_5, the copolymer containing the highest proportion of butene (17 mol%), could not be determined because of the changes in the polypropylene x-ray spacings due to lattice expansion and to the presence of some polybutene type crystallinity. The development of polypropylene and polybutene phases during copolymerization with highly stereospecific catalysts when the butene content exceeds about 20% by weight has been described previously by the author[7] and also by Coover *et al*[8].

The object of starting the slow cooling process from 160°C, that is from below the maximum melting point of polypropylene, was to prevent complete melting and so leave some nuclei or crystallites on which crystallization could start immediately on cooling. The chains with the longest isotactic polypropylene sequences would then be expected to crystallize first, then, as the temperature drops, those with progressively shorter sequences thus effecting a fractionation on a chain structure basis which is reflected in the melt distribution on reheating.

Lower final melting points and therefore much narrower melt distributions are obtained by cooling from 190°C, even in the homopolymer and blend. At this time and temperature in the melt, nuclei are evidently effectively destroyed

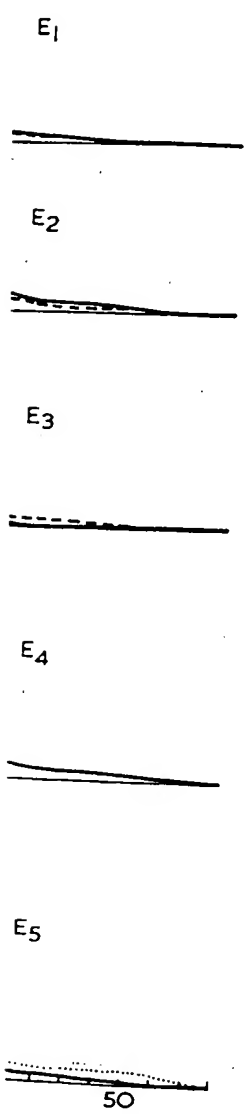

nd with polyethylene
:ooling at 6C°/h from
C°/min (dotted lines)

and crystallization starts after the considerable supercooling normally observed in unnucleated polypropylene[12]. As a result the final melting points are not much higher than those observed in the same samples cooled much faster at 16C°/min from 230°C, at which temperature nuclei are known to be destroyed[13]. It appears that both the long sequence chains and shorter sequence chains now crystallize simultaneously to give crystallites of similar melting point. Hence these conditions are much less effective in producing a melt distribution characteristic of the chain distribution present. The advantage

Table 3 Crystallinity and % γ developed in E_2 under various thermal treatments in DSC

Heating rate (C°/min)	*Holding temp.* (°C)	*Holding time*	*Cooling rate/ min*	T_s(°C)	T_c(°C)	*Cryst.* %	% γ	DSC *reheat figure no.*
16	160	0	0·5	immed.		54	55·5	*5b*
			16	123	110	49	44	*5b* (dashed)
			64	103	89	48	16	
		10 min	0·5			57	52·5	*5c*
			16			48	45	*5c* (dashed)
		16 h	0·5	immed.		55	31	*5d*
			16	121	104	50	19	*5d* (dashed)
	230	5 min	0·5	121	112	55	42	*5e*
			16	106	90	48	7	*5e* (dashed)
			64	90	74	45	0	
4	160	10 min	0·5	immed.				*6a*
0·5*	160	0	0·5	immed.		58	41	*6b*
		0	64	immed.				*6b* (*dotted*)
		1 h	0·5	immed.				*6c*
		16 h		immed.				*6d*
	162·5	0		immed.				*6e*
	165	0		immed.		57·5	63·5	*6f*
		16 h		immed.				*6f* (dashed)
	170	0		~135	124	55	45·5	*6g*

T_s start of exotherm as defined by clear departure from baseline; T_c peak of exotherm

*Heated 16C°/min to 140°C then at 0·5 C°/min

of cooling from 160°C instead of 190°C is evident from *Figure 4*. The melt distributions observed in copolymers E_2 and E_4 after cooling from 190°C would suggest that they had similar chain structure distributions. The differences are brought out by cooling from 160°C.

The usefulness of the method is further illustrated by the melt distributions of E_3, E_4 and E_5. The endotherms accurately reflect the composition of the copolymers. The size of the sharp endothermic peak at ~170°C characteristic of homopolymer is larger in E_5 which contained 30% homopolymer than in E_3 and E_4 (15% homopolymer). The size and melt distribution shown by the very broad low melting endotherms appropriately reflect the proportion and degree of modification of the random copolymer present. In making the comparison it must be noted that the ethylene contents of the random

copolymer portions are higher than the overall contents given in *Table 1*. The 7·5 mol% ethylene in E_5 is equivalent to about 9·5 mol% in the random copolymer portion.

Where high density polyethylene is present as a separate phase as in the blend PP/E it is shown as a distinct endothermic peak at ~130°C. Low density polyethylene is shown as a peak at ~110°C. Slow cooling from 160°C effects

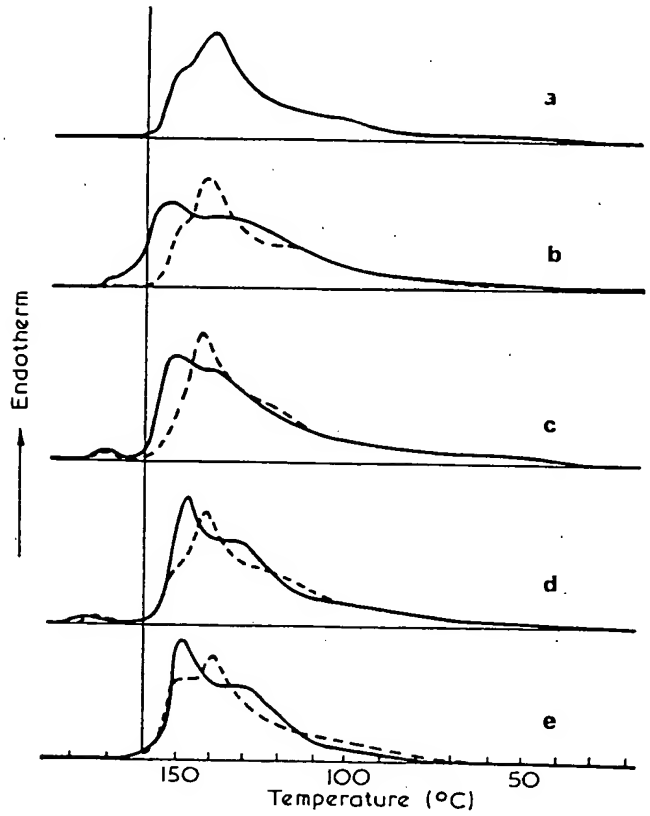

Figure 5 DSC heating curves of E_2 samples: (a) pressed sheet, no heat treatment; (b)–(e) prior thermal treatment as in *Table 3*, involving 16C°/min approach to maximum temperature and cooling rate 0·5C°/min (thick lines), 16C°/min (dashed lines)

the best resolution of the polypropylene and polyethylene melting peaks and hence facilitates quantitative estimation of the proportion of crystalline polyethylene present. This may most readily be carried out by comparing the areas of the polyethylene endotherms with those obtained from a series of calibration blends slow cooled under the same conditions.

EFFECT OF THERMAL HISTORY ON MELTING POINT DISTRIBUTION AND DEVELOPMENT OF γ-FORM

The results given in *Table 1* for the E series of copolymers show that the relative proportions of α- and γ-forms developed in each copolymer varied with the temperature from which slow cooling was started. Since the overall degrees of crystallinity are not very different it is clear that some chains can crystallize in either the α- or γ-forms. Copolymer E_2 was therefore selected for

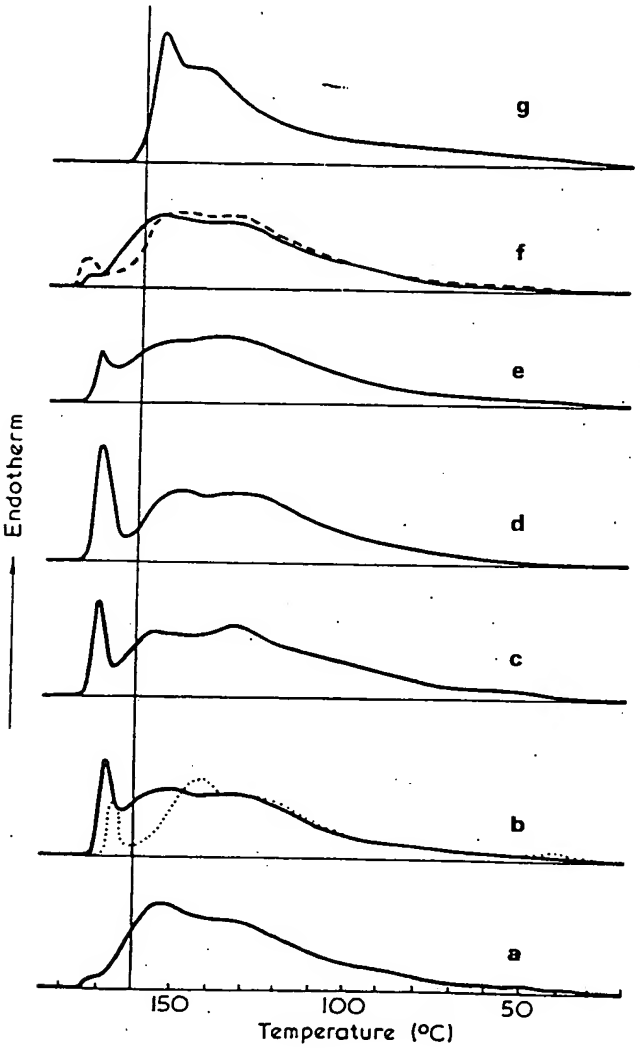

Figure 6 DSC heating curves of E_2 samples given prior thermal treatment as in *Table 3*, involving slow approach (4C°/min and 0·5C° min) to maximum temperature

a more detailed study of the effect of rate of heating to the holding temperature, the holding temperature itself, and the cooling rate, upon the overall crystallinity and amount of γ developed and on the melt distribution on reheating. *Figures 5* and *6* show DSC traces of E_2 copolymer film which had undergone different prior thermal treatments as indicated in *Table 3*. *Table 3* also gives data on the crystallization exotherms recorded during the cooling process.

Melting point distributions

It will be observed that, irrespective of holding time or cooling rate, the only samples displaying appreciable melting at ~170°C are those which had been heated fairly fast to a temperature where melting was not complete and then at the slowest possible rate available (0·5C°/min) to 160°C. This effect can be explained as follows. During heating, crystallites formed from chains of short isotactic polypropylene sequences will melt and those with longer sequences can recrystallize to form more perfect thick crystallites. The extent of this 'morphological rearrangement' will be very dependent upon the heating rate. Only at slow rates will there be enough time for crystallites to be developed which are sufficiently perfect to be stable at 160°C. These crystallites will act as nucleating agents during subsequent crystallization on cooling.

The rate of cooling also has an effect on the subsequent melting behaviour. As seen in *Figure 6b*, immediate cooling at the fast rate of 64C°/min gave a smaller peak at a slightly lower temperature than cooling at 0·5 C°/min. The latter gave a melt distribution resembling most closely that obtained after the standard slow cooling in the oil bath (*Figure 3*). Longer holding times, up to 16 h, increased the size of the upper peak slightly and increased its temperature. All chains potentially able to produce crystallinity with melting point > 170°C appear to now have done so.

The effect of higher holding temperature was also examined. E_2 was heated to 162·5, 165 and 170°C at 0·5C°/min and then cooled immediately at the same rate. The DSC curves are shown in *Figures 6e, f, g*. Up to 165°C the upper melting peak increases in temperature but decreases in size. After heating to 170°C it is no longer observable; crystallization has occurred with considerable supercooling as shown by the exothermic peak at 124°C. The DSC traces obtained while cooling from the lower temperatures show no such exotherm although the crystallinity developed is higher. This is consistent with crystallization starting immediately on cooling and continuing gradually. There is no sudden change in dH/dt to be recorded as a distinct exothermic process.

Nevertheless complete order cannot have been destroyed at 170°C because on cooling from 230°C at 0·5C°/min the peak temperature of crystallization is lower still at 112°C. This is reflected in the peak melting points on reheating of 155°C and 148°C respectively (*Figures 6g* and *5e*).

Figure 5 shows that, at the faster initial heating rate of 16C°/min, all but a very small amount of crystallinity in the E_2 copolymer film is melted at 160°C and only small peaks of melting point >170°C are recorded after subsequent cooling. It is also noticeable that more crystallites of higher melting point (i.e. in the approximate melting range 150–170°C) are developed on cooling immediately 0·5C°/min from 160°C than after holding for longer

times. In other words the balance between growth on nuclei present and their dispersion due to thermal motions is in favour of the latter, in spite of 160°C being well below the maximum melting point of an appreciable proportion of the polymer. The destruction of nuclei with increased holding time is also shown by the lower temperature of crystallization on cooling at 16C°/min.

The above results explain why the particular thermal pre-treatment we have adopted as our standard procedure involving slow approach to 160°C was effective as a chain structure fractionation procedure. *Figures 6b* and *6f* show that for E_2 the upper peak is related in temperature and size to the temperature from which slow cooling is started. For copolymers more highly modified than those discussed here, melting may be complete at 160°C and cooling would then have to be started from a lower temperature to prevent supercooling. We have found that 160°C is normally the best compromise when comparing different polymers.

In a later section it well be shown that annealing at a temperature below 160°C causes some recrystallization to polymer of higher melting point. Clearly a slower rate of cooling would produce a more perfect fractionation but for routine analysis we have found that the procedure described provides the best compromise.

Development of γ-form: morphology of mixed α- and γ-forms

The results given in *Table 3* show that after heating fast (16C°/min) to the holding temperature:

(a) The proportion of γ developed decreases as the rate of cooling increases: fast cooling from 230°C gave α-form only. This is consistent with earlier observations on the homopolymer stereoblock fractions[1] which gave α-form only on quenching from the melt.
(b) At corresponding cooling rates more γ is formed on cooling from 160°C than from 230°C.
(c) Longer holding times at 160°C decrease the amount of γ-form on cooling.

Development of γ-form is therefore favoured by slow cooling but more particularly when some crystallinity or order is left in the melt as discussed in the previous section.

Fractionation studies described in a later section show that the high melting peaks at ~170°C represent melting of α-form crystallites. On cooling at 0·5C°/min from 160°C a smaller proportion of γ-form is produced after approaching this temperature slowly (0·5C°/min) than at the faster rate (16C°/min). Comparison of the relevant DSC traces shows that this can be attributed to the development of the large α-form peak of *Figure 6b* which is not present in *Figure 5b*, i.e. to the preferential crystallization into the α-form and γ-form, respectively, of chains containing only a small proportion of ethylene units. Similarly more γ forms on cooling at 0·5C°/min from 165°C because no large α peak is developed, (*Figure 6f*). It appears that the maximum amount of γ is formed when a high proportion of crystallites melting in the range 150–170°C are present, as in *Figures 5b* and *6f* (thick lines), but no large α-form peak. The proportion of γ-form decreases again on cooling from

170°C because more order in the melt is destroyed and fewer crystallites in this melting range are developed (*Figure 6g*).

At this stage it is only possible to provide a speculative explanation for the above results. Crystal growth into α- or γ-form may occur by direct nucleation into either α- or γ-forms and by growth on to existing α-form crystallites, either in α-form or in the γ-form by epitaxial growth.

Evidence for epitaxial growth between the α- and γ-forms has been provided by Morrow[4] who showed that individual single crystals made from very low molecular weight propylene homopolymers by solution crystallization can consist of regions of α- and γ-forms. This is attributed to the close relationship between the packing of the left and right handed helices of the α- and γ-forms[1,2,4]. The crystal lamellae are formed from extended chains so that the question of chain folding does not arise.

Kardos[3] has shown that normal highly isotactic polypropylene crystallized in the γ-form under high pressure, converts to α-form on heating by a solid–solid crystal phase transition. As high pressure crystallized γ-form has been shown to consist of folded chains[3,14,15] and not extended chains as in polythene, it follows that the fold planes of the two forms must be closely related. Evidence has been provided that the fold plane of the α-form is the *ac* plane[16,17] so that the fold plane of the γ-form is likely to be the crystallographically closely related *ac* plane (see figure 10 of reference 1). Epitaxial growth of γ on α and vice versa is therefore extremely probable in high molecular weight polymers even where chain folding is involved.

In particular we have to explain why the maximum amount of γ-form is developed when a small proportion of α-form crystallites melting above 170°C are left in the melt before cooling, and when cooling is carried out under conditions which yield the maximum amount of crystallites melting in the range 150–170°C (see *Figures 5b* and *6f*).

On slow cooling from a melt in which a little α crystallinity is retained, crystallization can start immediately on these crystallites. As the temperature drops chains of progressively shorter sequence length can crystallize by lateral addition to the folded chain lamellae but with progressively shorter fold lengths. This type of overgrowth has been observed in single crystals grown from solution as the temperature is lowered[18]. These overgrowths are likely to be initially in the α-form from chains of the longest isotactic polypropylene sequence but may be epitaxial growths in the γ-form as more highly modified chains crystallize. Meanwhile more nuclei will form which will be more likely to be γ-nuclei as the chains forming the nuclei have progressively shorter average sequence lengths. It is known that stereoblock fractions with isotactic sequence lengths below a certain (unknown) average give γ-form only on slow cooling from the melt[1]. It is also possible that order remaining in the melt, as opposed to true α-form crystallites, may predispose to the formation of γ-nuclei by chains modified by copolymer units to only a low degree.

It seems possible that if all the most highly isotactic chains which will nucleate or grow on existing crystallites in the α-form only are first crystallized, and therefore removed from crystallizing phase, then further new nucleation may now occur preferentially in the γ-form. This might also favour γ-form epitaxial growth on existing α-crystallites. In this way the maximum amount

of γ-form can develop with the minimum interference from new α-form nuclei.

If, however, crystallization by slow cooling is carried out under conditions which ensure that nuclei or order are first destroyed, then crystallization develops from nuclei formed at a much higher degree of supercooling as discussed in the previous section. At this temperature both chains with the longest polypropylene sequences and the more modified chains nucleate and grow simultaneously. A large number of α-nuclei might then be formed from the former, favouring further overgrowths in the α-form and therefore decreasing the γ content, as observed.

As crystallization proceeds, and since the sequence lengths even within one chain are likely to vary, parts of chains with the shortest sequences may be excluded from the growing crystallites and be incorporated at lower temperatures into other crystals of shorter fold length and lower degree of perfection or as fringed micelle growth.

Fast cooling complicates the picture still more because development of α-form is now favoured even in the more highly modified chains. It is possible that there is a temperature above and below which direct nucleation occurs preferentially into γ and α respectively.

Crystallites of the same melting point may be formed from chains of different sequence length in either the α- or γ-forms depending whether growth occurs on existing crystallites or by direct nucleation. Hence we should not expect to find a clear temperature demarcation in the DSC remelt endotherms below and above which all the melting crystallites are γ or α respectively. At low temperatures γ-form melting predominates. We have attempted to follow the melting of the two forms by running X-ray diffractometer scans at different temperatures. In a sample of E_2 slow cooled from 160°C, γ-form started to melt first as expected but in the middle melting range recrystallization to polymer of higher melting point occurs because the rate of scanning is necessarily slow. This complicated the observations because some conversion of γ-form to α-form was also involved as described in the next section. The γ-form had completely disappeared by 145°C but the α-crystallinity increased slightly over this range. Conversion to α-form of γ-form made from homopolymer by high pressure crystallization has been discussed by several authors[2,11,14,19]. The mechanism of conversion will be discussed by the author in relation to these copolymers in a sequel to this paper.

FRACTIONATION OF PROPYLENE-ETHYLENE COPOLYMER E_2

None of the copolymers so far described has been crystallized entirely in the γ-form free of α-form. The solvent fractionation of propylene homopolymers[1] only yielded very small quantities of stereoblock polymer crystallizing entirely in the γ-form. Solvent fractionation of the copolymer E_2, the one yielding the highest proportion of γ-form, was undertaken with a view to obtaining larger quantities of polymer which could be crystallized in the γ-form only, to permit a more detailed investigation of the γ-form crystalline morphology and to provide material for attempts to grow single crystals which would help to confirm the unit cell postulated[1]. This work was carried

out before the publication of the electron diffraction photographs from γ-form single crystals obtained from very low molecular weight polymer[4]. These photographs did, in fact, confirm the originally proposed unit cell in *c*-axis projection except that doubling of the *b*-axis was proposed. The possibility that either *a* or *b* axes might be doubled had been suggested[1] but could not be established from X-ray photographs of unoriented polymer.

As γ-form is developed most readily in the chains with shorter polypropylene sequences, it was desirable to separate these from chains containing less comonomer which have been shown to crystallize either α or γ depending upon thermal treatment.

It was found that after applying the standard slow cooling procedure to E_2, further annealing at various temperatures below 160°C caused recrystallization of these less modified chains to crystallites of higher melting point and therefore lower solubility. Subsequent rapid cooling to room temperature crystallized the short sequence chains to a low degree and hence rendered them as soluble as possible, thus providing optimum conditions for their separation by solvent extraction. Annealing for one hour at 150°C, followed by rapid cooling, was found to give good separation as shown by the remelt distribution of *Figure 7*, curve B. A subsidiary upper melting peak has developed at 165°C while the broad low temperature endotherm, well separated from the upper peak, results from the short sequence chains which were melted at 150°C and recrystallized on cooling. The proportion of γ-form was reduced from 50% to 25% during this treatment.

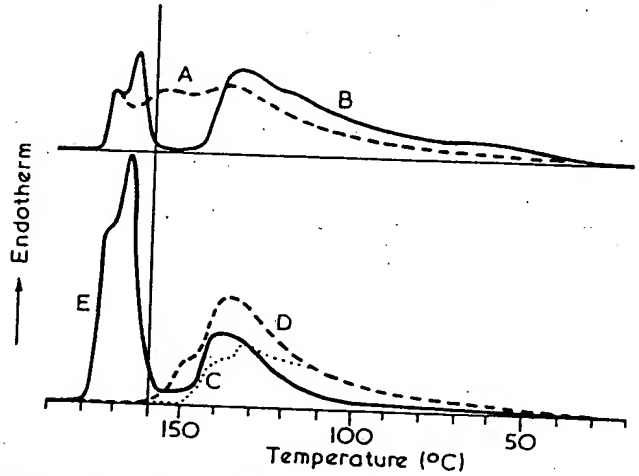

Figure 7 DSC reheat endotherms from copolymer E_2 and its fractions as described in *Table 4* (10 mg samples used for each scan)

The resulting polymer was first extracted with boiling hexane and then boiling heptane and the soluble polymer recovered. *Table 4* gives data on the soluble fractions and the residue. *Figure 7* shows the DSC heating curves of the two soluble extracts (C) and (D) after slow-cooling from 160°C and of the residue after extraction (E). It will be seen that the greater part of the lower melting crystallites of curve B had been extracted. The residue now showed

only a trace of γ-crystallinity while, as expected, the degree of crystallinity had been increased. The absence of γ-form from the residue shows that the melting peak at 172°C (curve A) which remained unchanged after annealing at 150°C was originally in the α-form.

The reduction in the proportion of γ-form during annealing is probably primarily due to conversion of γ to α of higher melting point but may partly be due to the subsequent fast cooling from 150°C which favours development

Table 4 Data on fractions from copolymer E_2

DSC Curve (Figure 7)	*Crystal-linity* (%)	*γ-form* (%)	*Weight* (mg)	*Ethylene* (wt %)	(mol %)
A, E_2 unextracted sc* from 160°C †	58·5	50	1000	4·5	6·5
B, A held at 150°C for 16h then rapidly cooled	53·5	25			
C, hexane sol. fract. from B — as recovered		0	166	~13	18·5
— sc from 160°C†	42·5	90			
D, heptane sol. fract. from B — as recovered		0	475	~4·2‡	6‡
— sc from 160°C†	51	92			
E, residue after heptane extraction	72·5	trace	355	~1·0	1·5
— sc from 160°C	68	25			

* sc—slow cooled † at 6 C°/h ‡ by difference

of α-form as previously discussed. Both the hexane and heptane soluble polymers were found to be in the α-form after recovery from solvent, but showed over 90% γ after slow cooling from 160°C. The heptane soluble fraction was still well crystalline (52·5%) so that the object of obtaining polymer capable of forming well crystalline γ-form only had been substantially achieved. The infra-red spectrum of this fraction was obscured by aromatic substances present in the heptane used, but by difference contained about 6 mol% ethylene compared with about 18·5 mol% in the hexane soluble fraction and 1·5% in the residue, both largely present as $-(CH_2)_n-$ sequences where $n = 5$ or 7. The heptane soluble fraction was of high molecular weight because highly oriented crystalline fibres in the α-form were obtained from it.

Twenty five percent of γ-form was developed in the residue after slow-cooling, again from 160°C, thus providing additional evidence that this fraction contained chains capable of crystallizing in either α- or γ-form.

ATTEMPTS TO GROW SINGLE CRYSTALS AND MORPHOLOGY OF BULK POLYMER

Attempts were made to grow single crystals in the γ-form from the hot heptane soluble fractions described in the last section and also from the

unfractionated copolymer E_2. With heptane as solvent α-form only was obtained on slow cooling and by isothermal crystallization. Similar experiments with 5% solutions in polyethylene wax[20] and an ester wax were also unsuccessful; even 50/50 mixtures developed no γ-form on slow cooling.

Five percent mixtures with a practically amorphous polypropylene wax made at 170°C and cooled at 6C°/h and 1C°/h yielded 40% γ and 50% γ, respectively, in the residue left after extraction with cold hexane. Isothermal crystallization at temperatures between 120°C and 130°C also yielded some 50–55% γ-form. The hexane insoluble residues were dispersed ultrasonically and then examined in the electron microscope. No evidence of single lamellar crystals was obtained although γ-form electron diffraction powder patterns were obtained from some fragments which were therefore aggregates of small crystals.

Specimens for examination of free surface and fracture surface morphology were made by isothermal crystallization of E_2 under the conditions given above. The best textural detail was obtained by crystallization at 125°C (51% γ). Replication of the free surface revealed a mat-like array of 'ropes', ~200 Å in width with a longitudinal periodicity of ~200 Å. Fractured surface replication indicated a 'pebbled' structure 500–1000 Å in diameter, possibly made up of smaller units ~200 Å in extent, but no clear lamellar structure was seen. Further heating of this specimen at 125°C for 5 h with a view to improving the lamellar structure resulted in no change in the fracture surface morphology.

The bulk crystallized specimen was disintegrated using the nitric acid selective oxidation procedure[21]. Electron diffraction studies of the debris again only gave γ-form powder patterns. For comparison, similar disintegration was carried out on a propylene homopolymer crystallized into α-form isothermally at 125°C under the same conditions. This gave sufficiently large fragments to enable well defined single crystal electron diffraction photographs to be obtained.

All evidence suggests that these propylene copolymers crystallized in the γ-form are composed of very small crystallites, the lateral dimensions of which are much less than 500Å.

As the heptane soluble fraction contains ~6 mol% ethylene present mainly as $-(CH_2)_5-$ and $(-CH_2)_7-$ sequences, then the propylene sequences will on average be 50 monomer units long, capable of forming ~17 helical turns in a 3_1 helix corresponding to 110 Å. Such short sequences are not likely to give well formed lamellae, even if of uniform length and the ethylene units are located at the folds. It also appears that the chains with longer polypropylene sequences present in E_2 (only 1·5 mol% ethylene was present in the residue after fractionation) are also unable to develop good lamellae even after annealing. It is not yet possible to say whether the crystal morphology involves chain folding or is of the fringe micelle type or a mixture of both.

SPHERULITIC TEXTURE

The spherulitic morphology developed in the various fractions after slow cooling from 160°C at 6C°/h is complicated. The texture varied considerably

in different regions of individual samples and sometimes spherulites were of mixed type and showed changes in birefringence during growth. Further investigations, which will be the subject of a later communication, are being undertaken to establish the distribution of α- and γ-crystallinity within the textural entities when both types are present simultaneously. The principal features are described below:

The heptane soluble fraction D showed well formed spherulites of positive birefringence which must be γ-form spherulites since 92% of the crystallinity is γ. The hexane soluble fraction C showed poorly formed sheaf spherulites of positive birefringence, varying in size considerably in different regions which must also be γ-form. The residue, after slow cooling from 160°C, showed well-formed positive and well-formed negative spherulites, both presumably α-form as described by Keith[22], together with some regions of poorly formed positive spherulites which might possibly be produced from the 25% γ-form present (*Table 4*), but may be α since it is not known how the γ-form is distributed. The γ-form may consist of very fine textural entities embedded in or between α-form spherulites. The whole copolymer A (50% γ) showed small areas of well-formed negative spherulites which are likely to be α-form corresponding to the high melting peak at ~170°C. The bulk of the material showed a very fine texture of small sheaf spherulites of positive birefringence, which by analogy with heptane and hexane soluble fractions are presumably mainly γ-form.

CONCLUSIONS

Random copolymers of propylene with minor amounts of ethylene and butene and other comonomers made with stereospecific catalysts develop mixed α and γ crystal forms on crystallization by slow cooling from temperatures near the melting point. The proportion of γ-form increases with increasing comonomer content; its development is ascribed to the interruptions in the isotactic polypropylene sequences caused by the comonomer units.

The observation by DSC of the melting point distributions produced after slow cooling from 160°C under carefully controlled conditions, together with measurements of the degrees of crystallinity and proportion of γ-form by X-ray diffraction on samples similarly prepared, offer a means at least qualitatively of characterizing the chain distribution present in these copolymers without fractionation. The two series of copolymers examined in this paper proved not to be truly random but to contain chains with widely varying comonomer contents.

The method of analysis is also applicable to mixtures of homopolymer and copolymer, to block polymers and blends of homopolymers with minor amounts of polyethylene, and also to homopolymers containing appreciable stereoblock polymer capable of forming γ-form on crystallization from the melt. These methods have been in use for many years in our laboratories for examining our own copolymers and those of unknown origin in conjunction with infra-red analysis.

The ratio of γ- to α-form developed in any one copolymer varies with

pretreatment and is a complicated balance of several factors — time and temperature in the melt and rate of approach to this temperature, which involves the proportion of crystallinity or 'order' retained before cooling, and the cooling rate itself.

No evidence of γ-form lamellar morphology has yet been found in the 6·5 mol% ethylene copolymer selected for special study, either in whole polymer or in lower melting (but still high molecular weight) fractions which crystallized almost entirely in the γ-form, and attempts to grow single crystals in the γ-form failed. The fractions have been shown to possess isotactic polypropylene sequences too short for regular chain folding and may contain crystallites primarily of the fringed micelle type. It is probable that in the whole polymer variation in sequence length, both between chains and within each chain, results in a complicated morphology involving very small crystals with chain folds of irregular length and fold surface, together with fringed micelle type growth.

The relative stabilities of the α- and γ-forms and the conversion of γ- to α-form in the copolymers in relation to their crystal structures will be discussed in a later paper.

ACKNOWLEDGEMENTS

The author's thanks are due to Dr T. G. Heggs and Dr C. N. Turton who made the copolymers, Messrs M. E. A. Cudby, D. A. Hemsley and A. J. Cobbold for infra-red, optical and electron microscope data, respectively, Dr P. J. Holdsworth for criticism of the manuscript, and to Mr D. R. Beckett and Mr A. B. Wootton for the experimental work.

ICI Plastics Division,
Welwyn Garden City, Herts, UK

(Received 4 January 1971)
(Revised 18 March 1971)

REFERENCES

1 Turner-Jones, A., Aizlewood, J. M. and Beckett, D. R. *Makromol. Chem.* 1964, **75**, 134
2 Kardos, J. L., Christiansen, A. W. and Baer, E. *J. Polym. Sci. (A-2)* 1966, **4**, 777
3 Pae, K. D., Morrow, D. R. and Sauer, J. A. *Nature* 1966, **211**, 514
4 Morrow, D. R. and Newman, B. A. *J. Appl. Phys.* 1968, **39**, 4944
5 Kojima, M. *J. Polym. Sci. (B)* 1967, **5**, 245
6 Kojima, M. *J. Polym. Sci. (A-2)* 1968, **6**, 1255
7 Turner-Jones, A. *Polymer, Lond.* 1966, **7**, 23
8 Coover, H. W., McConnell, R. L., Joyner, F. B., Slonaker, D. F. and Combs, R. L. *J. Polym. Sci. (A-1)* 1966, **4**, 2563
9 Barrall, E. M., Porter, R. G. and Johnson, J. F. *J. Appl. Polym. Sci.* 1965, **9**, 3061
10 Natta, G., Corradini, P. and Cesari, M. *Rend. Accad Naz. Lincei* 1957, **22**, 11
11 Pae, K. D. *J. Polym. Sci. (A-2)* 1968, **6**, 657
12 Ke, B. (Ed.) 'Newer methods of polymer characterisation,' Interscience, New York, 1964, Chap. IX
13 Beck, H. N. *J. Polym. Sci. (A-2)* 1966, **4**, 631
14 Sauer, J. A., Morrow, D. R. and Richardson, G. C. *J. Appl. Phys.* 1965, **36**, 3017
15 Kojima, M. *J. Polym. Sci. (A-2)* 1967, **5**, 597

16 Sauer, J. A. and Pae, K. D. *J. Appl. Phys.* 1968, 39, 4959
17 Kardos, J. L., Baer, E. and Morrow, D. *J. Polym. Sci.* (*B*) 1966, 4, 453
18 Bassett, D. C. and Keller, A. *Phil. Mag.* 1962, 7, 1553
19 Morrow, D. R. *J Macromol. Sci.* (*B*) 1969, 3, 53
20 Turner-Jones, A. and Cobbold, A. J. *J. Polym. Sci.* (*B*) 1968, 6, 539
21 Palmer, R. P. and Cobbold, A. J. *Macromol. Chem.* 1964, 74, 174
22 Keith, H. D. and Padden F. J. *J. Appl. Phys.* 1959, 30, 1485

EXHIBIT 9

Crystallization Rates of Matched Fractions of $MgCl_2$-Supported Ziegler Natta and Metallocene Isotactic Poly(Propylene)s. 1. The Role of Chain Microstructure†

Rufina G. Alamo* and Jose A. Blanco

Department of Chemical Engineering, Florida Agricultural and Mechanical University and Florida State University, Tallahassee, Florida 32310-6046

Pawan K. Agarwal

Exxon-Mobil Co., Baytown Polymers Center, Baytown, Texas 77522-5200

James C. Randall

2710 Ridge Road, Steamboat Springs, Colorado 80487

Received October 3, 2002; Revised Manuscript Received December 24, 2002

ABSTRACT: The microstructures of two poly(propylene)s with matched molar masses and overall defect concentrations are inferred from the crystallization behavior of their narrow molar mass fractions. One poly(propylene) was produced with a $MgCl_2$-supported Ziegler−Natta catalyst and the other with a metallocene catalyst. The fractions obtained from the metallocene isotactic poly(propylene) display a range in molar masses but each has the same defect concentration indicating a uniform intermolecular concentration of defects in the parent metallocene isotactic poly(propylene). These fractions provide direct evidence of the "single site" character of the metallocene catalyst. The variations of crystallization rates with molar mass reflect different chain diffusion/transport phenomena that are governed by the remnant entanglement state of the melt during crystallization. The molar mass fractions obtained from the ZN-iPP confirm that the interchain distribution of the nonisotactic content is broad in this polymer. The stereodefects are more concentrated in the low molar mass fractions. Furthermore, the invariance of the linear growth rates among the ZN fractions and the lack of formation of any significant content of the γ polymorph, even in the most defected fraction, is consistent with a nonrandom, blocky intramolecular distribution of defects in the ZN-iPP molecules. In contrast to the growth rates, the overall crystallization rates are a direct function of the primary nucleation density, which varies among the fractions and the unfractionated iPPs. Hence, the measured overall crystallization rates would be correlated with nucleation density and not necessarily with the microstructure of the iPP molecules. The crystallization data are also interpreted in light of results from pentad/heptad distributions predicted by two-state and three-state statistical models. Parameters from the models allow the prediction of sequence distribution curves that could be used to evaluate each of the models as to their consistency with the crystallization rate data.

Introduction

Isotactic poly(propylene)s prepared with "classical" heterogeneous Ziegler−Natta catalyst systems (ZN-iPP) are complex because a distribution of various types of catalyst sites leads to a mixture of poly(propylene) molecules having strongly differing intermolecular stereosequence distributions. In contrast, poly(propylene)s prepared with the single-sited metallocene family of isotactic poly(propylene) catalysts (M-iPP) should have uniform intermolecular stereosequence distributions.[1,2] The identification of types, concentrations and distributions of stereosequences found in various poly(propylene)s is customarily carried out by ^{13}C NMR. Such structural information is important, not only as a way to correlate with the physical properties of these materials but also as a means to extract information concerning the nature of the catalyst sites and the mechanisms of the polymerization processes.

The influence of catalyst type on the microstructure of various ZN-iPPs has often been reevaluated as higher field NMR spectrometers with higher resolution and sensitivity became available.[3−10] In most of these previous studies, ^{13}C NMR analyses of structural defects have relied upon analyses of either whole polymers,[2−4] poly(propylene)s where an atactic poly(propylene) component had been removed after crystallization from xylene[5−9] or fractions from a parent ZN-iPP.[11−14] Some level of fractionation is required in the microstructural analyses of ZN-iPP to ensure that the NMR characterization is performed on crystalline chains only without interfering contributions from atactic components. It was shown that valuable structural information can be obtained by studying different fractions from a parent poly(propylene) and analyzing the stereosequence distribution of each of the fractions utilizing ^{13}C NMR.[11−14]

The crystallization behaviors of ZN-iPPs and M-iPPs have been reported in separate publications[15−21] but a direct comparison of the physical properties and crystallization behavior of these two types of poly(propylene)s, matched by molar mass and defect concentrations, has yet to be presented. It is the objective of this work to fractionate such a matched pair of ZN-iPP and M-iPP and to compare the structural and crystallization characteristics of the individual fractions with that observed for the whole, parent polymers. This type of study is needed to document the nature of inter- and intramo-

* Corresponding author. E-mail: alamo@eng.fsu.edu.

† Dedicated to Prof. L. Mandelkern on the occasion of his 80th birthday.

10.1021/ma021549g CCC: $25.00
Published on Web 02/14/2003

lecular microstructures that leads to differences in crystallization properties. A highly isotactic M-iPP and a corresponding ZN-iPP of the industrial type were selected. From this study, it is possible to determine in detail how poly(propylene) microstructures, differing at inter- and intramolecular levels, can affect the crystallization behavior of isotactic poly(propylene)s.

The influence of the type of catalyst and polymerization process on microstructures of industrial ZN poly(propylene)s has been studied by different investigators.[11-14,22-23] TREF [14,22] and solvent gradient extraction[11-13] led to fractions of increasing isotacticity and increasing molar mass, a result that clearly indicated a nonuniform interchain composition of defects. They also observed that most of the fractions contained syndiotactic *rrrr* pentads and, as in other works,[7-13,24-26] it was proposed that some of the propagation errors were "blocky" in nature. Thus, the presence of stereoblocks in the ZN-iPP was inferred or suspected by most previous investigators and emphasized in Busico et al.'s latest work.[25]

Since it is important to identify the possibility of a nonrandom intramolecular distribution or blocky stereosequences in iPP chains, other types of physical evidence must be utilized in conjunction with ^{13}C NMR. This is the only approach that will satisfy the ultimate goal of correlating molecular microstructures with physical properties. For this purpose, indirect methods must be used to identify the intramolecular microstructure of the iPP molecule. One example is a recent publication in which a proposed blocky microstructure of highly defective iPPs was deduced by their crystallization properties.[27]

Different stereodefect distributions have been associated with quite different crystallization rates, even within a blocky microstructure. For example, in the crystallization process, short, isolated randomly distributed defected blocks will act as any other noncrystallizable single defect, retarding the crystallization rate and reducing the crystallinity and the melting temperature of the defected chain with respect to a defect free iPP chain. Moreover, noncrystallizable long defective blocks will have little or no effect upon the crystallization properties of long isotactic blocks of the chain. In the present work, we document the nature of the intermolecular defect distribution from GPC and NMR analyses of molecular fractions of ZN and metallocene types iPPs. Furthermore, indirect analyses are used to extract the intramolecular microstructure of the ZN poly(propylene)s. Focus is given to the analysis of the crystallization rates as a parameter that is a function of the defect microstructure.

Previous stereochemical analyses of the sequences of ZN fractions obtained by successive extractions with *n*-alkanes solvents were interpreted on the basis of two or three state models developed by Chûjô,[28] Doi,[29] and Busico et al.[25] to simulate a mixture of poly(propylene) chains produced by multisited Ziegler–Natta catalysts.[4,5,30] It is important to examine both the average microstructures and microstructural distributions of Ziegler–Natta poly(propylenes) in light of their crystallization behavior. Therefore, in a separate part of this work,[31] ^{13}C NMR data will be analyzed utilizing all of the current as well as some newly modified two state and three state statistical models. Each model was evaluated on how closely the predicted microstructural distributions conformed to the observed rates of crystallization.[31] The various models were also evaluated on the consistency of microstructural changes from fraction to fraction for the ZN-iPP where, from fractionation data, the average stereodefect level was observed to decrease with increasing molar mass. The results of a slight modification to the Busico three-state model,[25] utilizing first order Markovian statistics for the symmetric chain component instead of Bernoullian statistics, are discussed in the present paper. These results were found to be consistent with both the linear growth rates and fractionation data in addition to predicting the observed ^{13}C NMR pentad/heptad distributions and average sequence lengths.

The possibility of a nonrandom distribution of defects in the ZN-iPP will be discussed in the present paper from an analysis of the crystallization rates of the various molecular fractions. In addition, the crystallization rates of molecular fractions obtained from a M-iPP, will be compared to those from a ZN-iPP with a similar overall defect content. The value of comparisons with the M-iPP lies in the fact that we found the latter to have a random and uniform intra- and intermolecular distributions of stereodefects.

Experimental Section

Materials. The unfractionated poly(propylene)s were supplied by ExxonMobil. The ZN-iPP was obtained with one of the latest $MgCl_2$-supported industrial catalysts, and the metallocene iPP was obtained with an Exxpol Kaminsky type of catalyst.[32] The molecular characterization data, as per molar mass, molar mass distribution, and percentage of stereo- and regiodefects, are listed in Table 1. Only stereodefects were found in the ZN-iPP sample while both stereo- and 2,1-*erythro*-regiodefects were found in the metallocene iPP. These poly(propylene)s were chosen because they both comprise the same 0.51 mol % overall concentration of all types of defects. Table 1 also lists the peak melting temperatures of rapidly crystallized samples and the average isotactic sequence length calculated as the average *meso* run length (MRL).[10]

Both poly(propylene)s were fractionated via supercritical fluid extraction by the Phasex Co.[33,34] The fractionation was carried out isothermally by increasing pressure in supercritical *n*-propane at 150 °C. Seven fractions were obtained from the metallocene iPP and five fractions from the ZN-iPP. Data relevant to the molecular characterization of the fractions are also listed in Table 1. Sample designations encode, in consecutive order, the following items: catalyst ("M" for metallocene and "Z" for Ziegler–Natta), f for a fraction (no "f" for unfractionated parents), weight-average molar mass in kg/mol followed by "K", and the total number of defects per 100 monomeric units. For example, Mf86K0.56 stands for a fraction obtained from the metallocene iPP with a weight-average molar mass of 86 000 g/mol and with a 0.56 mol % total defect concentration.

Characterization Methods. The molar masses and their distributions were determined by standard gel permeation chromatography using polystyrenes as calibration standards. Melting temperatures and heats of fusion were obtained in a differential scanning calorimeter (Perkin-Elmer DSC-7) using ~4 mg of sample and a heating rate of 10 °C/min. Static temperature calibration of the instrument was carried out with indium.

The pentad/heptad sequence distributions and the concentration of 2,1 defects were obtained from solution ^{13}C NMR spectra carried out at 125 MHz on ^{13}C using 10 mm o.d. sample tubes. Only methyl resonances were employed in the determination of pentad/heptad sequence distributions. This avoids unwanted contributions from possible differences among nuclear Overhauser effects and relaxation times. Here 15% solutions in tetrachloroethane-1,2-d_2 were used at 125 °C. The pentad/heptad resonance chemical shifts were based on published assignments.[7,8,35-38] The stereodefect concentration was taken

Table 1. Characterization of Parent Polymers and Fractions from Metallocene and ZN-iPP

sample	M_w (g/mol)	M_w/M_n	defects (mol %) stereo	regio	total	T_m (°C)[a]	MRL[b]
M203K0.51 parent	203 900	2.00	0.11	0.40	0.51	155.0	194
Mf86K0.56	86 000	1.43	0.16	0.40	0.56	156.2	176
Mf121K0.50	121 000	1.32	0.11	0.39	0.50	156.3	199
Mf143K0.54	143 000	1.24	0.07	0.47	0.54	156.1	184
Mf200K0.46	200 000	1.23	0.08	0.38	0.46	155.8	216
Mf235K0.45	235 000	1.24	0.07	0.38	0.45	154.6	221
Mf358K0.41	358 000	1.34	0.07	0.34	0.41	154.0	243
Mf383K0.41	383 000	1.47	na[c]	na	na	na	
Z263K0.51parent	262 600	3.19	0.51		0.51	161.4	190
Zf97K1.03	97 000	1.31	1.03		1.03	159.0	91
Zf157Kxxx	157 000	1.27	na		na	na	
Zf163K0.60	163 000	1.97	0.60		0.60	161.3	161
Zf204K0.41	204 000	2.15	0.41		0.41	160.9	239
Zf328K0.36	328 000	1.77	0.36		0.36	162.3	270

[a] Rapidly quenched samples to 25 °C. [b] Average meso run length,[10,21] MRL = *mmmm*/[0.5(*mmmr* + *rmmm*) +(2.1 defects)]. [c] Data not available.

as half the fraction of *mmmr* pentads because any stereodefect sequence will always have two, and only two, associated *mmmr* (=*rmmm*) pentads located at the beginning and the end of each isotactic sequence. Thus, it is possible to determine the total stereodefect population independently of the structures of the various stereodefects.

The average *meso* run length (MRL),[10,21] which represents an average over contiguous *meso* sequences starting at $n = 4$ for $r(m)_n r$, was selected for the characterization of average sequence length of the isotactic components. This definition precludes contributions from short *meso* runs such as ~~~*mmmrmrmmm*~~~ and ~~~*mmmrmmmrmmm*~~~, which are most likely not crystallizable but are part of the overall stereodefect distribution. MRL values are listed in Table 1.

X-ray diffraction patterns were recorded in reflection mode at room temperature using a Philips X'Pert PW3040 MRD diffractometer operating at 45 mA and 40 kV. Ni-filtered Cu Kα radiation was used as the source.

Linear growth rates (G) were measured in an Olympus polarized optical microscope used in conjunction with a Linkam hot stage, TP-93. The temperature was controlled with a precision of ±0.1 °C, and the precision of the eyepiece used to measure the spherulitic growth was 0.15 μm. Photographs were also taken during isothermal growth using an Instant Polaroid camera. At any temperature the linearity of the plots of spherulite radius vs time and reproducibility of the measurements were highly satisfactory with regression coefficients higher than 0.99. The measured growth rates were also independent of the position of the spherulite in the specimen and the calculated uncertainty in the value of G was low (±0.01 × 10^{-6} cm/s).

Overall crystallization rates were taken as the inverse of the time required for 50% of the transformation to take place (similar to the half time rate concept).[39] The degree of transformation, at a fixed isothermal temperature, was followed by the variation of the heat-flow vs time in the DSC-7.

Sample Preparation and Crystallization Procedures. Films approximately 100 μm thick were prepared by compression molding the initial pellets or powders in a laboratory Carver press preset at 200 °C and were used for the microscopic and DSC measurements. Some of the ZN fractions were crystallized at temperatures > 120 °C in thermostated oil baths for analysis of crystallographic polymorphs by WAXS. For this purpose, plaques of 1 cm × 1 cm × 0.3 mm were molded, sandwiched between two metal plates covered with thin Al foil, and placed in a vacuum sealed tube to prevent degradation. The tube was immersed in a silicone oil bath at 210 °C for 15 min and then rapidly transferred to another oil bath preset at the required crystallization temperature.

Prior to crystallization in the hot stage or in the DSC, the films were melted at 200 °C for 5 min and cooled at 40 °C/min to the isothermal crystallization temperature. To maximize heat transfer, the DSC was operated in conjunction with an intracooler and under dry nitrogen flow.

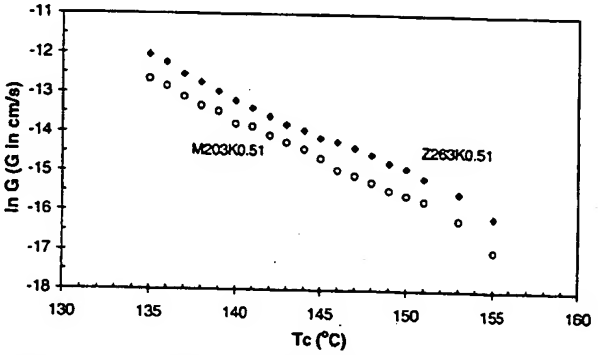

Figure 1. Linear growth rates as a function of crystallization temperature for parents metallocene iPP (O) and ZN-iPP (●) with matched overall concentration of defects, 0.51 mol %.

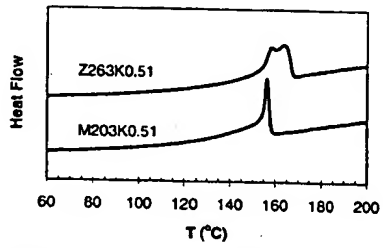

Figure 2. Melting temperatures of parents ZN-iPP (top) and metallocene iPP (bottom). Samples were crystallized at −10 °C/min and melted at +10 °C/min.

Results and Discussion

Comparison of Unfractionated Matched ZN and Metallocene Poly(propylene)s. Before results obtained from the fractions are analyzed in detail, it is also of interest to discuss the differences in melting and crystallization behavior of the unfractionated poly(propylene)s. Isothermal linear growth rates and DSC meltings of the metallocene and ZN parents iPPs are given in Figures 1 and 2, respectively. At any crystallization temperature, the spherulites of the unfractionated ZN-iPP grow at about twice the rate of the metallocene iPP. The DSC melting peak of the ZN-iPP is also considerably broader, multipeaked and shifted to a temperature about 8 °C higher than the melting behavior observed for the metallocene iPP crystallites.

Since the overall concentration of total defects in both poly(propylene)s is the same (0.51 mol %) and both chains are of similar molar mass, the differences in crystallization and melting behavior must reflect a significant difference in distributions of defects. The issue of stereodefects only in the ZN-iPP and stereo- + regiodefects in the M-iPP will be addressed shortly. Previous fractionations of similar industrial-type ZN-iPPs have revealed a nonuniform concentration of defects from chain to chain in these iPPs.[11-14,22-23] Racemic units were found to be more concentrated in the lower molar mass chains. However, the metallocene catalyst with its "single site" nature, leads to iPP chains of narrow molar mass distribution and a narrow distribution of defect concentrations among chains. One consequence of a broad intermolecular distribution of chain defects in the parent ZN-iPP is that it contains a fraction of highly defected molecules that do not participate in the crystallization process. This behavior leads to a lower effective overall defect concentration in the ZN than in the M-iPP. The ZN-iPP contains longer isotactic sequences that will be selected earlier in the crystallization and lead to thicker crystallites, in line with the observed higher growth rates and melting temperatures.

We should also consider if the observed differences in melting behavior between ZN-iPP and M-iPP might be a consequence of a different partitioning of regio vs stereodefects between the crystalline and noncrystalline regions. For example, if the stereodefects more easily enter the crystalline regions than do the regio-2,1-defects, the ZN-iPP chains, with defects only of the stereo-type, will be more crystallizable in line with the results of Figures 1 and 2. This issue has been previously addressed by analyzing the solid state ^{13}C NMR spectra of the crystalline regions of a series of M-iPPs with varied concentrations of stereo- and 2,1-regiodefects.[40,41] Both types of defects were found to enter the crystalline lattice at levels that do not differ significantly. In addition, the similarity of the slopes that characterize the variation of the growth rates with temperature in Figure 1, are indicative of the formation of crystallites with very similar interfacial free energies in both types of iPPs. Hence, we exclude any significant difference in the way stereo- (predominantly a single inversion in configuration shown by the presence of *mmrrmm*) and regio-2,1-defects affect the crystallization of the iPPs used in this investigation.

A confirmation of the predicted interchain microstructure, i.e., homogeneous for the metallocene iPP and inhomogeneous for the Z–N type, will be obtained from microstructural analyses of molecular fractions from both iPPs. The nature of the ZN-iPP inhomogeneous defect distribution as well as a possible nonrandom intrachain defect distribution will be discussed after a detailed analysis of the crystallization rates of the fractions presented in the next section.

Molecular Fractions from Metallocene iPP and Z–N iPP: Fractionation and Analysis of Growth Rates. The molecular characteristics of the fractions obtained from both iPPs by isothermal pressure profile are listed in Table 1. This technique allows solvent free recovery of the fractions in adequate quantities for NMR and physical studies.[33,34] With increasing pressure in the fractionation, a systematic increase of the molar mass of the fractions was also observed indicating that the fractionation took place preferentially by molar mass.[33,34] The parent metallocene iPP comprises chains of weight-average molar mass of 204 000 g/mol with the most probable molar mass distribution. From this polymer, seven fractions were isolated with a range in molar mass from 86 000 to 383 000 g/mol and with similar narrow molar mass distributions of 1.3 ± 0.1 in all these fractions. The data are listed in Table 1.[42] Of relevance are the very similar concentrations of defects found in all the metallocene fractions, as listed in the fourth and fifth columns of Table 1. A small variation in total defect concentration from 0.56 to ~0.40 mol % is observed with increasing molar mass. Even so, all of the M-iPP fractions have total defect levels that are very close to the 0.51 mol % observed for the parent M-iPP material. These results offer direct evidence that M-iPP chains have very small intermolecular variations among the concentration of defects and, thus, provide direct experimental basis to conclude that the interchain composition distribution is very narrow in the parent M-iPP. With such a narrow variation in the defect compositional distribution, the metallocene fractions offer an ideal series for analyzing the effects of molar mass on iPP crystallization, independent of the effects of defect content and defect distribution. This analysis will be reported in a subsequent publication.[43]

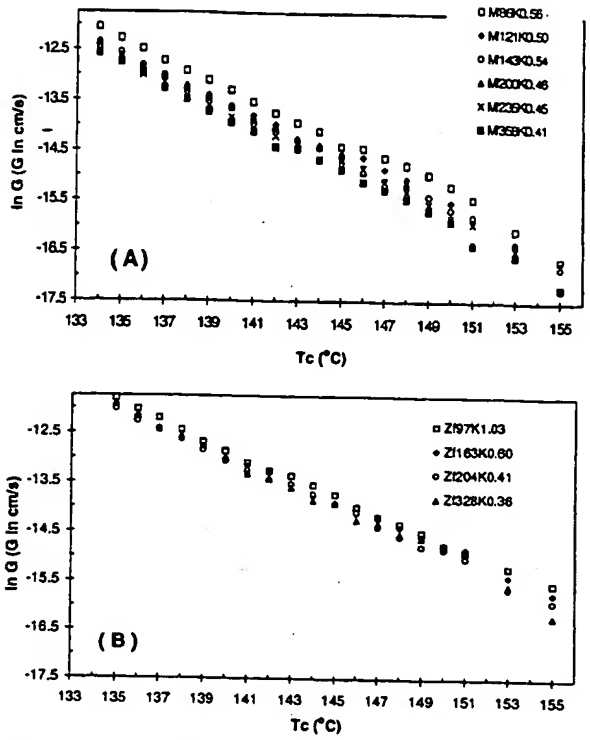

Figure 3. Linear growth rates of iPP molecular mass fractions as a function of crystallization temperature. (A) Fractions from metallocene iPP. (B) Fractions from ZN-iPP. Designation of the fractions follows that given in Table 1.

Well formed spherulites were observed under isothermal crystallization of all the metallocene fractions and the spherulitic linear growth rates, measured in a temperature range between 134 and 155 °C, are given in Figure 3A. Following the dictates of kinetics theories for nucleation and crystallization of polymers,[44,45] the growth rates of all the M-iPP fractions show a similar variation with undercooling, i.e., a decrease of the rate by about 100 times with increasing crystallization

Models for microstructure distribution in parent ZN iPP

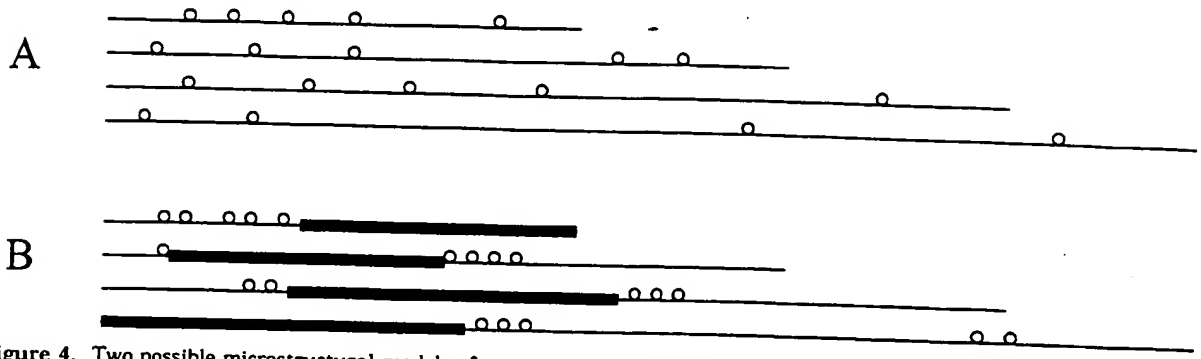

Figure 4. Two possible microstructural models of stereosequence distribution in the parent ZN-iPP. (A) The concentration of defects is nonuniform between the molecules and randomly distributed intramolecularly. Increasing concentration of defects is correlated with molar mass. Different lengths of crystallizable sequences are found. (B) The concentration of defects is also nonuniform between the molecules but the intramolecular distribution of defects is blocky. Long similar crystallizable sequences, highlighted for visual effect, are found in all the chains.

temperature in the range analyzed. In addition, the effect of molar mass is reflected by about a one-half decrease of the rate with increasing molar mass at any temperature. For example, at a crystallization temperature of 140 °C growth rates values (in cm/s) of 1.68×10^{-6}, 1.23×10^{-6}, 1.20×10^{-6}, 1.19×10^{-6}, 0.98×10^{-6}, and 0.89×10^{-6} were obtained for a molar mass change from 86 000 to 358 000 g/mol. This difference is not large, but it is, however, systematic and much larger than the estimated experimental error in the measurement of the growth rate.

A small molar mass dependence of the growth rate is qualitatively similar to that reported for linear polyethylene and for other homopolymers when crystallization takes place at high undercoolings.[45-52] For example, linear polyethylene displays a discrete maximum in the crystallization rate with molar mass for undercoolings lower than 30°. However, at higher undercoolings, the maximum is not observed, and the change of the rate with molar mass is less pronounced, becoming very small at the highest undercoolings. The crystallization of the metallocene iPP fractions takes place at undercoolings well above 30°. Hence, the small molar mass dependence of the growth rate, which is observed in Figure 3A, fits the pattern of other homopolymers and copolymers.[45-52] The linear growth rates of the metallocene fractions follow the expected variation for chains of different lengths with very similar contents of defects and the same random intramolecular distributions of defects.

The natural logarithm of the experimental linear growth rates (G) of the ZN-iPP fractions are given in Figure 3B for a range of crystallization temperatures between 135 and 155 °C. The x and y axes of this plot are identical to the axes in the plot of growth rates of the metallocene fractions (Figure 3A). This consistency facilitates a comparative study. In analyzing the data of Figure 3, parts A and B, we notice smaller but still significant differences in the growth rates of the ZN-iPP fractions, when compared to those of the metallocenes. No systematic variation of G with either molar mass or concentration of defects is found in the ZN-iPP fractions. In principle, this is an unusual result because a strong effect of the concentration of defects in lowering G was reported for metallocene iPPs of a fixed molar mass.[19] The same variation with defects was also found in other M-iPP fractions for which the details of the fractionation were not provided.[16] Therefore, in the range of defect concentrations of the ZN-iPP fractions, one would have expected a significantly lower G for the fraction with 1.03 mol % defects than for the fraction with 0.36 mol % defects. The data of Figure 3B show that this is not the case; in fact, there are only minor differences between the growth rates of the ZN-iPP fractions at a fixed crystallization temperature. The differences in crystallization behavior, when compared to the metallocene fractions, likely reflect significant differences in the distributions of defects.

The molar mass and concentration of defects of the fractions obtained from the ZN-iPP, also listed in Table 1, confirm the inhomogeneous interchain concentration of defects of the parent polymer. As the molar mass of the fractions increases from 97 000 to 328 000 g/mol, the total defect content decreases from 1.03 to 0.36 mol % respectively. This inverse relation between chain length and concentration of defects was also observed in ZN-iPP fractions obtained by a solvent–nonsolvent extraction fractionation procedure[11,12] and in fractions obtained by TREF.[14,22,23] Hence, quite different types of fractionation studies reveal an interchain variation of the concentration of defects in the ZN parent that decreases as the molar mass increases. Neither the fractionation nor characterization data reveal any details about the intramolecular distribution of defects. The molecular characteristics of a defect distribution are probably best addressed by indirect studies of properties that relate to an intramolecular defect distribution. In this context, different possible scenarios are viable and schematics for two of these models for the crystalline chains are given in Figure 4. A third composite model that results from applying a three-state statistical model to the observed NMR pentad/heptads stereosequences will be discussed in detail in the second part of this series.[31] The results of this model are summarized in the last section of the present paper.

In Figure 4A, a defect distribution is shown that is nonuniform on an intermolecular basis, but the intramolecular defect distribution is random. According

to this model, the defect concentrations increase continuously with decreasing molar mass. The crystallization behavior of fractions from this model is expected to be proportional to the average defect composition in the melt which changes among the fractions. Therefore, after fractionation, much lower crystallization rates are expected for the fractions of lower molar mass because, on average, they comprise a higher concentration of defects and shorter isotactic sequences than the less defected fractions.[16,17,19,40] The second possibility (depicted schematically in Figure 4B) is a microstructural model in which the intermolecular defect composition is also nonuniform with the shorter chains having a higher concentration of nonisotactic units. However, in this model the intramolecular distribution of defects is blocky (nonrandom) with long runs of crystallizable isotactic sequences being present in all chains. On average, the second model has similar types of long crystallizable sequences present in all of the chains. It is clear that the crystallization behavior of fractions from this second model will be quite different from the behavior of fractions in the first, which has a random intramolecular defect distribution. In the second model, the overall concentration of defects also changes from chain to chain but the crystallization is led by the long isotactic blocks. The concentration of short, less crystallizable isotactic sequences is minimal compared to the concentration of these sequences in the first model. The crystallization behavior of the fractions from the second iPP model should be similar to the crystallization of a diblock copolymer in which one of the blocks is noncrystallizable.

If the actual ZN defect distribution follows the microstructural model given in Figure 4A, one would expect, after fractionation, that a similar crystallization rate should be observed for both the metallocene and the narrow ZN fraction with matching defect concentrations. After fractionation, the overall defect concentration will be much closer to the single molecule concentration in both iPPs. A difference in crystallization behavior, however, is maintained as seen in Figure 3, parts A and B, where the growth rates of fractions Mf358K0.41 and Zf204K0.41 are compared. The spherulites of the Ziegler fraction grow more rapidly than those of the metallocene counterpart. This reaffirms the idea that, even after fractionation, the Ziegler fractions contain longer isotactic sequences; put in another way, the broad defect distribution of the parent ZN-iPP is sustained to some extent in the fractions. Moreover, the fact that the growth rates of all the Ziegler fractions are so similar also indicates that the intramolecular distribution of the defects in the ZN fractions is different from that of the metallocene fractions. The similarity of the rates in Figure 3B suggests that the same nonrandom intramolecular distribution is propagated along all the molecules of the parent ZN-iPP. In other words, the defect distribution of the ZN-iPP does not conform with the microstructure modeled in the scheme of Figure 4A.

The ZN fraction with the highest concentration of defects is also the fraction of the lowest molar mass. Thus, one could argue that the expected decrease of G with increasing defect content in the ZN fractions may be compensated by an opposite effect of molar mass on G, as demonstrated in the metallocene series. If this were the case, model 4A could still apply to describe the defect distribution of the ZN-iPP. To probe this possibility, the growth rate data of the lowest molar mass ZN fraction with 1.03 mol % defects were corrected to the values that this fraction would have if its molar mass is ~200 000 g/mol. To make this correction, data obtained for the metallocene fractions, shown in Figure 3A, are appropriate because they purely reflect the variation of G with molar mass independently from the effect on the rate of the defect concentration. Thus, the growth rate data of the fraction Zf97K1.03 were lowered by the difference in G given by the metallocene fractions in a range between 97 000 and 204 000 g/mol taken from Figure 3A. The corrected G data for the 1.03 mol % fraction (closed diamonds) and the uncorrected one for fraction Zf204K0.41 of low defect content (open circles) are plotted in Figure 5. The data are also compared with published growth rate data of a metallocene iPP with 1.0 mol % of defects,[19] given by the solid line in this figure. It is evident that the correction for molar mass has very little effect on the variation of G among the ZN fractions. The growth rates of the ZN fractions fall on the same line, which is positioned much higher than that expected had the defects been randomly distributed as is the case for the data of the metallocene iPP with the same 1.0 mol % defects of Figure 5.

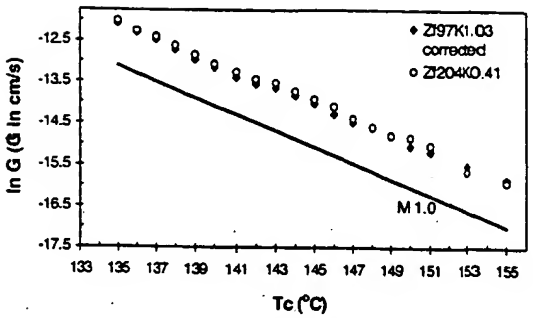

Figure 5. Linear growth rates of ZN fraction Zf97K1.03 corrected for the effect of molar mass on the rate (◆) compared with growth rates of ZN fraction Zf204K0.41 (O). The continuous line indicates the variation of growth rates with temperature of a metallocene-type iPP with 1.00 mol % of defects extracted from ref 19.

The similarity of the growth rates of all the ZN fractions, even after correction for different molar masses, provide evidence that suggests that the intramolecular defect microstructure of the parent ZN-iPP, as well as the fractions, could be blocky. Even after careful fractionation, the ZN-iPP growth rates are considerably higher than observed for the metallocene fractions. These observations offer additional evidence for the possible blocky nature of the ZN-iPP. As will be shown below in this work, the lack of formation of the γ polymorph, which requires short isotactic sequences, also rules against model 4A. Hence, the results of the growth rates favor the microstructural model shown in Figure 4B.

Additional evidence, which supports the stereoblock defect microstructure of the ZN-iPP chains, is found in the WAXS diffractograms obtained in the two most defected ZN fractions. We have previously reported that a metallocene iPP with a concentration of 1.0 mol % of homogeneously distributed defects, crystallized at 125 °C, develops about half of the crystallites in the γ polymorph and the other half in the α monoclinic form.[21] It was also observed in our previous work that the percentage of γ phase developed by two unfractionated

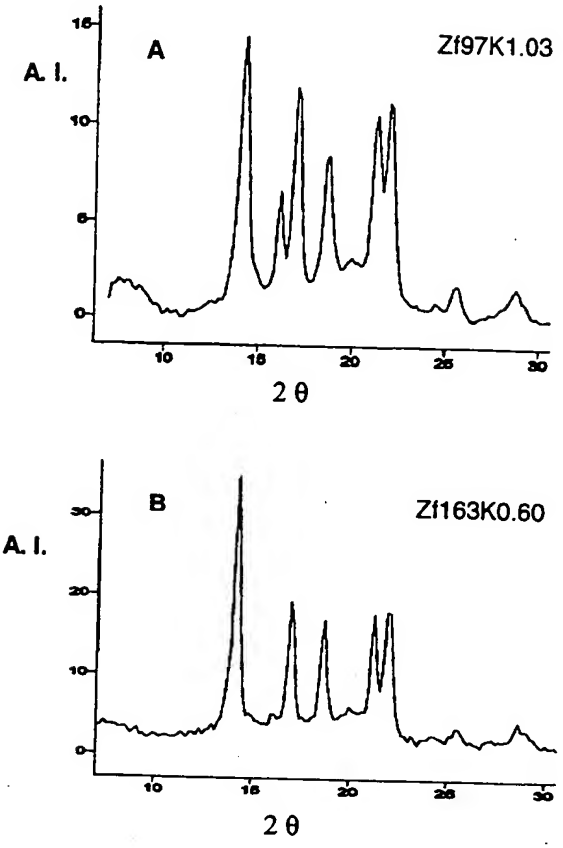

Figure 6. WAXS diffractograms of ZN-iPP fractions Zf97K1.03 and Zf163K0.60 collected at room temperature after 3 days of crystallization at 125 °C.

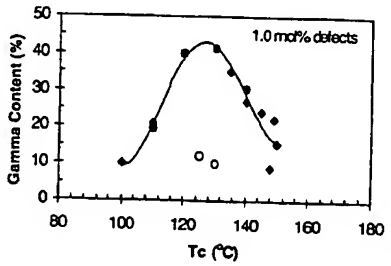

Figure 7. Variation of the concentration of the γ polymorph with crystallization temperature for different iPPs with matched 1.00 mol % overall defect concentration: (◆) metallocene type iPP (data from ref 21); (O) ZN-iPP fraction Zf97K1.03.

ZN-iPPs was, at any temperature, below the level of detection of this polymorph by WAXS. The low γ content was attributed to the broad defect distribution of the ZN-iPPs.[21] The WAXS diffractograms of the two most defected ZN fractions crystallized at 125 °C are shown in Figure 6A for Zf97K1.03 and in Figure 6B for Zf163K0.60. The intensity of the reflection at a 2θ of 20°, characteristic of the γ polymorph, is low and corresponds to less than 10% in both fractions. The peak at $2\theta = 16°$ is associated with the β polymorph, more abundant in the lower molar mass fraction. In Figure 7, the percentage of the γ phase obtained for the Zf97K1.03 fraction is compared to the γ form developed with increasing temperature by a metallocene iPP with matched concentration of defects. The content of γ phase developed by the ZN fraction is four times lower than the value of the metallocene iPP with its narrow defect distribution. It is basically constant in the range of temperatures studied. Hence, we find that at a matched overall concentration of defects of 1.0 mol %, the structural requirements for the formation of the γ polymorph are present in the metallocene iPP, but they are basically absent in the ZN fraction. These requirements were described in detail in our previous work[21] and are summarized in the following two major points: 1. Chains whose microstructure leads to thin crystallites must be present; i.e., there must be short crystallizable isotactic sequences available. 2. There must be a structure that prevents folding in the crystal amorphous interfacial region and requires tilted ordered chains to propagate a lamellar crystallite. The lamellar propagation is favored by a tilted antiparallel molecular arrangement of the γ crystallographic phase.[53,54] As seen in Figures 6 and 7, even after crystallization in a temperature range that is most favorable for the formation of the γ phase,[21] the content of γ phase obtained in the ZN fractions is much lower than that expected for a chain with a random defect distribution. The most characteristic reflection of the γ form, that at a 2θ of 20°, is almost absent from both diffractograms. This result is expected for a molecule where long isotactic sequences join blocks of poorly stereoregular sequences, such as those of the ZN stereoblocky type described schematically in Figure 4B.

From the relation between the maximum content of γ form and the concentration of defects in narrowly distributed metallocene iPPs, given in Figures 8 and 9 of ref 21, we find that 12% of the γ polymorph corresponds to an average *meso* run length (MRL) of 220 repeat units. This value is considerably larger than the average MRL of 91 units for the ZN-iPP fraction with 1.03 mol % defects and suggests that contiguous isotactic sequences of at least 220 units must be present in the Zf97K1.0 fraction in a relatively high concentration. As presented in next section, a modified Busico three-state model leads to a distribution of sequence lengths for this fraction consistent with these data. Long isotactic runs favor the formation of folded-chain crystallites in the ZN fractions and, hence, they crystallize preferentially in the α polymorph. In a recent publication,[27] the analysis of the polymorphic behavior was also taken as an indirect measure of the degree to which the defects in the iPP chain deviate from a random distribution.

Overall Crystallization Rates. Previous parallel or independent studies of the linear growth rates and the overall crystallization rates measured by dilatometry or by differential scanning calorimetry of linear polyethylene fractions and other types of homopolymers, have resulted in an identical temperature coefficient.[44,46,55,56] In addition, these methods of measurement give identical variation of the rates with molar mass or with concentration of defects. Hence, data from either growth rates or overall rates have been used to test for conformity with kinetic theories of polymer nucleation and growth.[44,46,51,52] We were also interested in testing if the overall crystallization rates measured by DSC follow the behavior observed by the growth rates of the parent iPPs and their fractions. Furthermore, the overall crystallization rates apply more directly to the solidification rates used in industrial processes because the data that characterize these rates are mass or volume-based quantities, and the measurements are not

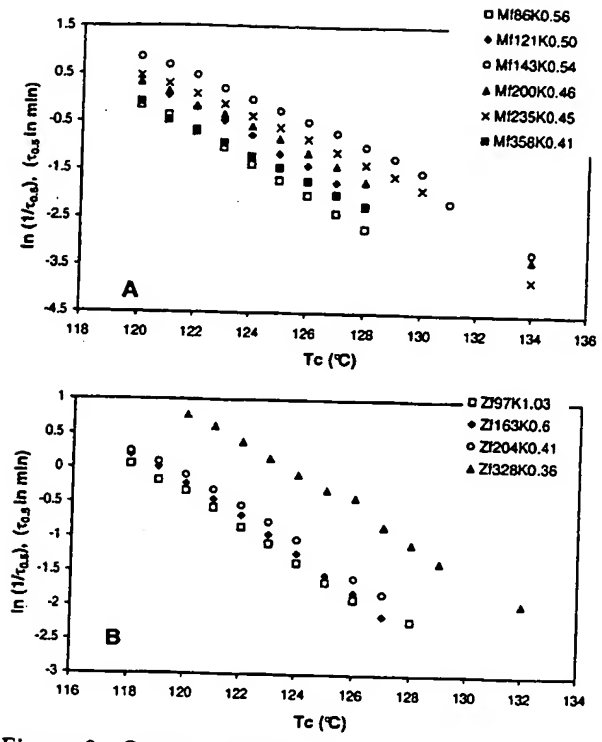

Figure 8. Overall crystallization rates of iPP molecular fractions as a function of crystallization temperature. (A) Fractions from metallocene iPP. (B) Fractions from ZN-iPP. Designation of the fractions follows that given in Table 1.

limited to having to observe a specific morphological feature as in microscopic methods.

The natural log of the inverse of the time required to obtain 50% of the total transformation ($\tau_{0.5}$), taken at the peak of the exotherms, is plotted vs crystallization temperature in Figure 8A for the metallocene fractions, and in Figure 8B for the ZN fractions. Different features are apparent from these plots. At a fixed crystallization temperature, the variation of the overall rate among the metallocene fractions is not systematic with molar mass as was observed with the growth rates. The variation of the overall rates of the ZN fractions is also different from the behavior observed for the growth rates in Figure 3B. At any temperature, the overall crystallization rate of the less defected ZN fraction (Zf328K0.36) is about three times faster than the rate of any of the ZN fractions. The difference in overall rates between the more defected ZN fractions, although small, is directly related to their concentration of defects. For example, it is the fraction with the highest concentration of defects (of the lowest molar mass) that shows the lowest overall rate.

These results can be explained by variations among the nucleation densities found in the fractions and parent iPPs. The number of spherulites that develop in each specimen were measured at selected crystallization temperatures. The data of the parent metallocene iPP and its fractions will be reported first. Figure 9 shows micrographs of the parent metallocene and selected fractions crystallized at 134 °C for approximately the same lengths of time. The spherulites are not uniformly distributed in most of the fractions and their rapid appearance and high numbers are indicative of a nucleation enhanced by some external agent. As seen in Figure 10, parts A and B, for five representative temperatures, the number of nuclei in a fixed volume follow the molar mass with the same random pattern as the overall crystallization rate. The latter is governed by the rate of nucleation, as demonstrated in the crystallization of many polymeric systems.[44,45,55,57,58] Consequently, the fractions with a higher nucleation density will yield a fixed level of crystallinity faster than fractions in which fewer nuclei are formed, regardless of the magnitude of the spherulitic linear growth rate. The solid lines in these figures follow the experimental data and are only intended as a guide to the eye. They do not represent any theoretical functionality.

Nucleants were not added to the parent metallocene or ZN polymer, inferring that what causes enhanced nucleation must be acquired either in the polymerization or the fractionation process. About 0.1% of the antioxidant Irganox 1010 was added to the *n*-propane before fractionation. However, as seen in Figure 10A, the parent metallocene iPP, free of this antioxidant, shows as high a nucleation density as the highest observed value among the fractions. From this, we conclude that the antioxidant, which could have been randomly distributed during fractionation is not nucleating the metallocene fractions. Since significant amounts of MAO are used as cocatalysts during polymerization, this agent or residues from the metallocene catalyst may enhance the nucleation rate of the metallocene iPP and its fractions.

Significant differences in the nucleation density of the ZN-iPP fractions are also observed. Representative micrographs of the lowest and highest molar mass ZN fractions are given in Figure 11. The nucleation density of the highest molar mass fraction is over 1 order of magnitude higher than any other ZN fraction. Nucleation densities and overall crystallization rates for the ZN fractions are shown in Figure 12, parts A and B, respectively, as a function of molar mass, for representative crystallization temperatures. Following the nucleation density pattern, the overall crystallization rates show a small increase with molar mass up to 200 000 g/mol and a large increase for the higher molar mass fraction. For example, at a crystallization temperature of 123 °C, the rate changed from 0.34 to 0.46 min^{-1} for defects changing from 1.03 to 0.41 mol % and to 1.16 min^{-1} for the less defected, highest molar mass fraction. Thus, as seen in Figure 12B, the variation of the logarithm of the rate is not linear with increasing molar mass or decreasing concentration of defects. The highest molar mass, low defected fraction shows a significantly higher rate. We ruled out that catalyst residues may be causing the high rates of the ZN fraction. Large contents of cocatalyst residues are not an issue in the polymerization with ZN catalysts. Moreover, statistical models[27] predict a fraction of very long, highly isotactic molecules in ZN-iPP, which naturally will be concentrated in the higher molar mass fraction. It is reasonable that these very long, highly isotactic molecules (absent in the metallocene iPP) may persist in the melt as aggregates and lead to a significant enhancement of the nucleation and crystallization rates. Melt memory effects have been observed previously in the crystallization of iPP[59] and were also tested in the ZN fraction Zf328K0.36. A small decrease of the overall crystallization rate at 124 °C was found by increasing the melt residence time at 200 °C from 5 to 30 min, but higher melt temperatures, such as 250 °C, could not be tested

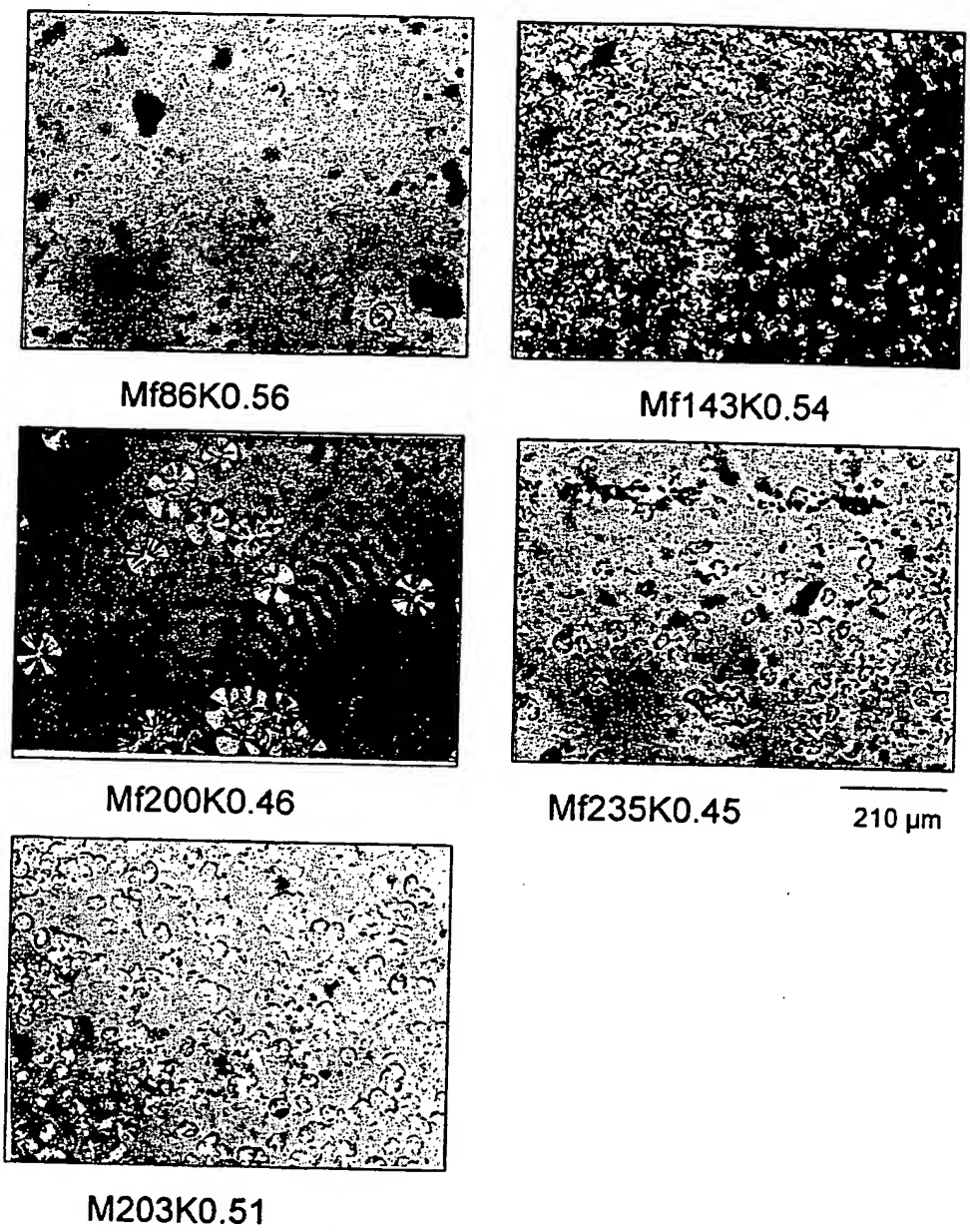

Figure 9. Polarized optical micrographs of the parent metallocene iPP and selected fractions isothermally crystallized at 134 °C for Mf86K0.56 (7 min), Mf143K0.54 (7 min), Mf200K0.46 (9 min), Mf235K0.45 (7 min), and M203K0.51 (7 min).

because the sample degraded. The concentration of very long, highly isotactic molecules is more diluted in the parent ZN-iPP and the lower molar mass fractions in agreement with their observed lower nucleation rates. Thus, the overall crystallization rate of the parent ZN-iPP and all the fractions, except the one with the higher molar mass, are very similar, in line with the similar growth rates observed in these fractions and in agreement with their blocky defect microstructure.

From the crystallization behavior of the two most general types of iPPs, we can postulate two different types of factors acting as "precursors" of the overall crystallization, i.e., catalyst residues and the very long chains present in the ZN-iPPs. These factors affect primary nucleation and, therefore, the overall crystallization rates characteristic of each fraction. Thus, it is not surprising that a correlation between the overall crystallization and microstructural variables is not found in the ZN-iPPs of this study. On the other hand, the linear growth rates which are independent of the primary nucleation rate and led by a process of secondary nucleation,[44] offer a better tool to correlate with the structural variables of the poly(propylene) chain. These results indicate that caution must be exercised when using overall crystallization rates to correlate physical properties with molecular microstructure. Any other mass or volume based measurement of the crystallization of iPP, such as optical or X-ray scattering may be subjected to the same type of enhanced nucleation described in this work.

Experimental NMR Stereosequences. Modified Busico Three-State Statistical Model. The defected pentads and heptads observed by ^{13}C NMR for the ZN-iPP fractions and the parent ZN-iPP are listed in

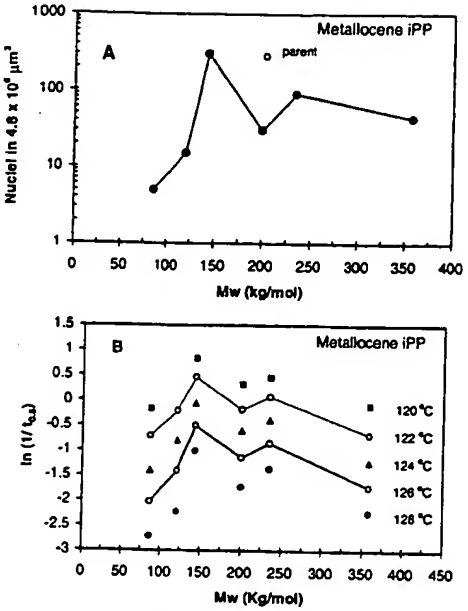

Figure 10. A. Variation of the nucleation density with molecular mass for fractions (●) and unfractionated metallocene iPP (○) crystallized at 134 °C for ~7 min. B. Overall crystallization rate as a function of molecular mass for metallocene iPP fractions crystallized at the indicated isothermal temperatures.

Table 2. In agreement with previous studies,[7-11,22-26] we notice a nonnegligible concentration of purely syndiotactic sequences (*rrrrrr*) in all the ZN fractions, including the fraction with the highest molar mass. In addition, stereoerrors of the type, *rmrrrm* or *rmrrrr* are also not detected.[25] The presence of the *mrrrmm* heptad indicates that isotactic blocks of opposite handedness are present. The most abundant defect consists of a single opposite configuration, ~0001000~, and is detected by the *mmrrmm* heptad. There are also more defective (*mmrrmr*) defects connecting isotactic blocks in all the ZN fractions as indicated by the normalized integrals corresponding to the steric pentads and heptads listed in Table 2.

The experimental pentad/heptads stereosequences were fit with two and three state statistical models. The predicted sequence length distributions will be discussed in detail for conformity to the observed fractionation and crystallization rates in the subsequent paper.[31] The value in fitting an observed pentad/heptad distribution with any statistical model is that the results can be used to identify the molecular component that gives rise to the various types of stereodefects. None of the models led to a defect distribution resembling the schematic microstructural model represented in Figure 4B, which most closely adheres to the experimental data. This blocky distribution of defects is difficult to propose with the classical two or three state statistical models because conceptually it would require switches between enantiomorphic (Es) and chain end control (CE) sites. The results obtained with the modified Busico three-state model are of relevance; therefore, they are also presented here. In the original work by Busico et al.[25] the ZN-iPP chains are modeled as a mixture of three types of molecules using a three-state statistical model. For a late generation, but weakly isotactic, Ziegler–Natta poly(propylene), the result was a mixture of very high isotactic molecules produced by an Es state, poorly isotactic or atactic molecules produced by a CE state and isotactic molecules produced by switching between two Es control sites (*C1*), each leading to different isotacticity levels.

As mentioned earlier, the only change made in Busico's original three-state model was to employ first-order Markovian statistics for the symmetric chain (termed CE in Busico's work, now referred to as CE1) component as opposed to the Bernoullian statistics used in the original Busico three-state model. The enantiomorphic Es and switching *C1* states were used exactly as represented by Busico and co-workers.[25] This modified model presents the unfractionated ZN-iPP as a composite of chains of different lengths in which molecules of the same length can have different concentrations of randomly distributed defects in two components (from Es and *C1* chains) and nonrandom defects in the third, CE1 chain component. The composite leads to a result where the defect concentration will decrease with increasing molar mass in agreement with the fractionation data. The most significant result obtained from fitting the modified Busico three-state model to the observed ZN-iPP pentad/heptad fraction data is that the three states are found to have similar compositions and similar sequence distribution curves in all four ZN-iPP fractions. It is only the relative amounts of each component that is predicted to change from fraction to fraction with increasing molar mass. The presence of very long isotactic sequences, predicted in the nonrandom CE1 component, is also important. This result may lead to similar growth rates as observed for the ZN-iPP fractions. During slow crystallization, highly isotactic Es molecules and long isotactic sequences from the CE1 component will be selected first and at about the same rate for all the fractions. This is inferred from the

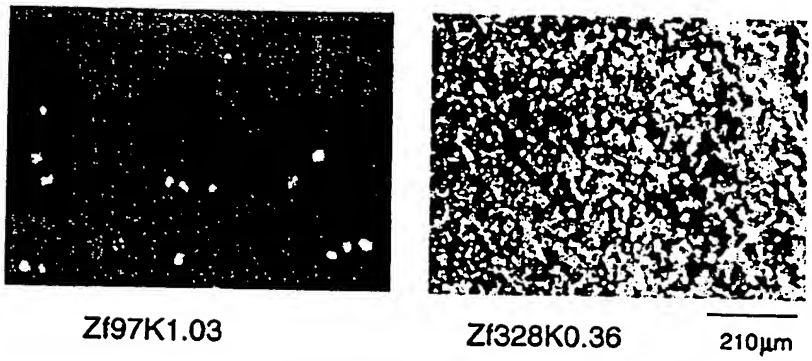

Figure 11. Polarized optical micrographs of fractions Zf97K1.03 and Zf328K0.36 isothermally crystallized at 134 °C (3 min)

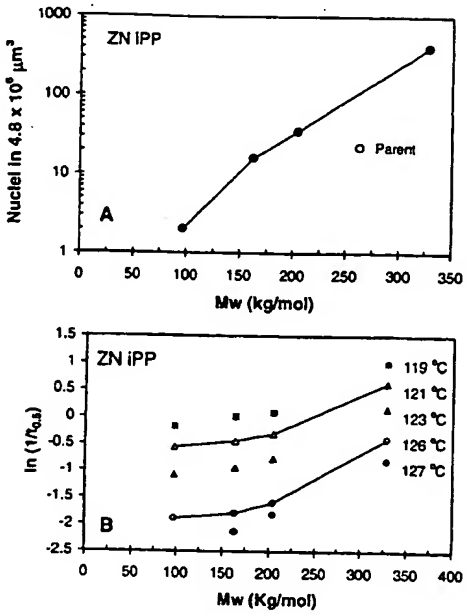

Figure 12. A. Variation of the nucleation density with molecular mass for fractions (●) and unfractionated ZN-iPP (○) crystallized at 134 °C for 3 min. B. Overall crystallization rate as a function of molecular mass for ZN-iPP fractions crystallized at the indicated isothermal temperatures.

>0.994 isotactic sequence probability of the Es component predicted for all the fractions.[31] The concentration of the less isotactic CE1 component was found to increase in the fractions of lower molar mass. However, the effect of this dilution on the crystallization of the Es component is predicted to be small and possibly compensated by differences in molar masses between the fractions. Therefore, the predicted crystallization behavior conforms to the experimental observations. In addition, most of the crystallizable sequence lengths predicted by the ES/*C1*/CE1 model are over 200 isotactic units in agreement with the small contents of the γ polymorph that are observed. Homogeneously distributed metallocene iPPs with average meso run lengths of ~200 units and higher, led to contents of the γ polymorph of less than 20%.[21] Thus, it is expected that a nonrandom, "stereoblocky", defect distribution of the most populated CE1 type molecules of the lowest molar mass fractions (Zf328K0.36 and Zf163K0.60), would crystallize with an even smaller content of this polymorph, in agreement with the experimental observations.

A similar pentad/heptad analysis of the stereosequences in the parent M-iPP and its fractions revealed only one principal stereodefect and that was *mmrrmm*, which is the defect that consists of a single opposite configuration. At the same level of NMR sensitivity used for the ZN-iPP fractions, the *rmmr*, *mmrm* + *rrmr*, and *rmrm* pentads and the various *rr* centered heptads, other than *mmrrmm*, were below the experimental NMR noise level in the metallocene iPPs. This result is predicted by a single state, enantiomorphic site control (Es) model[10] and is consistent with the behavior of a single sited catalyst. In addition to *mmmm*, the only other significant methyl resonances observed are *mmmr* + *rmmm*, *mmrr* + *rrmm*, and *mmrrmm*, which are expected in a 2:2:1 ratio, as observed for the M-iPP parent and its fractions. This stereodefect, which arises from a single configurational error, accounts for virtually all of the stereodefects in M-iPP and comprises about 20% of the total defect distribution. The stereodefect distribution is, therefore, Bernoullian[1] and consistent with the linear growth rate data obtained from the metallocene series, which does not support any significant grouping of regio- or stereodefects. In fact, iPP prepared with "single sited" metallocene catalysts have been shown in independent studies to display uniformly distributed stereo- and regiodefects.[1,60]

Concluding Remarks

The crystallization behavior of a metallocene and a ZN-iPP with the same molar mass and same overall concentration of defects was studied in relation to their defect microstructure. Conclusions with respect to inter- and intramolecular distribution of the defects in each type of iPP were possible from the analysis of the crystallization data of their molecular fractions, which were obtained by isothermal pressure profile in supercritical *n*-propane.

The fractions from the metallocene iPP provide direct, supporting evidence of the "single sited" nature of the catalyst. They display a range in molar mass but the same defect concentrations, which indicate the presence of uniform intermolecular defect concentrations in the parent metallocene iPP. The experimental linear growth rates of the fractions were those expected for chains with a random intramolecular distribution of defects. The variations of these rates with molar mass reflect their different number of entanglements per chain in the melt.

The overall crystallization rates of the parent metallocene iPP and its fractions are affected by an enhanced

Table 2. Stereosequence Distribution of Unfractionated ZN-iPP, and Its Fractions

sequence	assignment, ppm (TMS)	distribution				
		Z263K0.51 parent	Zf97K1.03	Zf163K0.60	Zf204K0.41	Zf328K0.36
mmmm	21.8	0.9632	0.9357	0.9683	0.9766	0.9802
rmmm	21.55	0.0102	0.0205	0.0120	0.0082	0.0073
rmmr	21.33	0.0029	0.0016	0.0016	0.0010	0.0008
mmrr	21.02	0.0113	0.0200	0.0099	0.0073	0.0057
mmrm + *rrmr*	20.79	0.0034	0.0036	0.0013	0.0014	0.0011
rmrm	20.55	0.0009	0.0008	0.0001	0.0005	0.0004
mrrrm	20.33	0.0006	0.0013	0.0003	0.0003	0.0003
mrrrr	20.3	0.0007	0.0016	0.0003	0.0002	0.0004
rrrrr	20.25	0.0014	0.0036	0.0007	0.0008	0.0012
rmrrm	20.17	0.0000	0.0000	0.0000	0.0000	0.0000
rrrrmr	20.13	0.0012	0.0016	0.0006	0.0005	0.0004
mmrrr + *mmrrrm*	20.06	0.0009	0.0023	0.0007	0.0005	0.0003
rmrrmr	20	0.0000	0.0000	0.0000	0.0000	0.0000
mmrrmr	19.93	0.0008	0.0014	0.0006	0.0004	0.0003
mmrrmm	19.85	0.0035	0.0062	0.0034	0.0026	0.0019

nucleation, probably caused by catalysts or cocatalyst residues. Thus, the rates follow the variation of nucleation density in each fraction, and a correlation between these measurements and the defect microstructure of the metallocene iPP, or its fractions, is not possible.

The molar fractions obtained from the ZN-iPP confirmed that the defect composition is broadly distributed on an intermolecular basis. Thus, while the molar mass of the fractions varied from 97 000 to 328 000 g/mol, the concentration of defects decreased from 1.03 to 0.36 mol %. In addition, the basically identical growth rates obtained in all the ZN fractions and the lack of formation of any significant content of the γ polymorph, even in the most defected fraction, is consistent with a blocky intramolecular nature of the defects in the ZN-iPP molecules. The data are also consistent with a microstructural model in which most of the crystalline chains comprise long runs of basically defect free isotactic units followed by runs of other less isotactic or atactic sequences.

Very similar overall crystallization rates were also found for most of the ZN fractions, which suggests a blocky microstructure. However, the highest molar mass fraction displayed much higher nucleation density and, thus, higher overall crystallization rates than the rest of the fractions. This could be attributed to the presence of aggregates in the melt from the higher concentration of molecules with very high molar mass in this fraction. These long, highly isotactic molecules are not found in the narrowly distributed metallocene iPP.

As a consequence of the enhanced nucleation caused either by foreign particles (possible catalyst residues) in the metallocene iPP, or by possible aggregates in the melt induced by the long chains of the ZN-iPP, a correlation between the overall crystallization and their microstructural variables may not be found. The linear growth rates, which do not depend on primary nucleation, were adequately correlated with molar mass in fractions from the metallocene iPP, with uniform distribution. The growth rates also served as a useful tool to infer an intramolecular, nonrandom distribution of defects in the ZN-iPP chain.

A multistate statistical model of the ZN-iPP microstructure predicts in all molar mass fractions the same three types of molecules, almost defect free isotactic chains, mainly isotactic molecules with non-Bernoullian defect distribution, and poorly isotactic molecules. The defect concentration and sequence distribution of the three types of molecules is the same in all ZN-iPP fractions, differing only in their relative amounts. This model was found to be consistent with the fractionation results and growth rates of the ZN fractions.

Acknowledgment. This work was supported by the National Science Foundation Polymer Program (DMR-0094485). The authors acknowledge useful comments on this work by Prof. L. Mandelkern. Eric Ritchson, a REU chemical engineering student, and Dongsheng Li are also acknowledged for helping with the DSC experiments and collecting the WAXS diffractograms. We are also grateful to Charles Ruff of the ExxonMobil Co. for NMR data. J.A.B. acknowledges partial support from the Fundacion Repsol YPF.

References and Notes

(1) Brintzinger, H. H.; Fischer, D.; Mülhaupt, R.; Rieger, B.; Waymouth, R. M. *Angew. Chem., Int. Ed. Engl.* **1995**, *34*, 1143.
(2) Fischer, D.; Mülhaupt, R. *Macromol. Chem. Phys.* **1994**, *195*, 1433.
(3) Zambelli, A.; Locatelli, P.; Bajo, G.; Bovey, F. A. *Macromolecules* **1975**, *8*, 687.
(4) Zambelli, A.; Locatelli, P.; Provasoli, A.; Ferro, D. R. *Macromolecules* **1980**, *13*, 267.
(5) Kawamura, H.; Hayashi, T.; Inoue, Y.; Chûjô, R. *Macromolecules* **1989**, *22*, 2181.
(6) Busico, V.; Corradini, P.; De Martino, L.; Graziano, F.; Iadicicco, A. M. *Makromol. Chem.* **1991**, *192*, 49.
(7) Busico, V.; Corradini, P.; De Biasio, R.; Landriani, L.; Segre, A. I. *Macromolecules* **1994**, *27*, 4521.
(8) Busico, V.; Cipullo, R.; Corradini, P.; Landriani, L.; Vacatello, M. *Macromolecules* **1995**, *28*, 1887.
(9) Busico, V.; Cipullo, R.; Talarico, G.; Segre, A. L.; Chadwick, J. C. *Macromolecules* **1997**, *30*, 4786.
(10) Randall, J. C. *Macromolecules* **1997**, *30*, 803.
(11) Paukkeri, R.; Vaananen, T.; Lehtinen, A. *Polymer* **1993**, *34*, 2488.
(12) Paukkeri, R.; Lehtinen, A. *Polymer* **1994**, *35*, 1673.
(13) Lehtinen, A.; Paukkeri, R. *Macromol. Chem. Phys.* **1994**, *195*, 1539.
(14) Morini, G.; Albizzati, E.; Balbontin, G.; Mingizzi, I.; Sacchi, M. C.; Forlini, F.; Tritto, I. *Macromolecules* **1996**, *29*, 5770.
(15) Cheng, S. Z. D.; Janimak, J. J.; Zhang, A.; Hsieh, E. T. *Polymer* **1991**, *32*, 648.
(16) Janimak, J. J.; Cheng, S. Z. D.; Giusti, P. A.; Hsieh, E. T. *Macromolecules* **1991**, *24*, 2253.
(17) Janimak, J. J.; Cheng, S. Z. D.; Zhang, A.; Hsieh, E. T. *Polymer* **1992**, *33*, 728.
(18) Monasse, B.; Haudin, J. M. *Colloid Polym. Sci.* **1985**, *263*, 822.
(19) Alamo, R. G.; Chi, C. Crystallization Behavior and Properties of Polyolefins. In *Molecular Interactions and Time-Space Organization in Macromoleculer Systems*; Morishima, Y., Norisuye, T., Tashiro, K., Eds.; Springer: Berlin, 1999; p 29.
(20) Alamo, R. G.; Galante, M. J.; Mandelkern, L.; Lehtinen, A.; Paukkeri, R. *J. Therm. Anal.* **1996**, *47*, 913.
(21) Alamo, R.; Kim, M.-H; Galante, M. J.; Isasi, J. R.; Mandelkern, L. *Macromolecules* **1999**, *32*, 4050.
(22) Viville, P.; Daoust, D.; Jonas, A. M.; Nysten., B.; Legras, R.; Dupire, M.; Michel, J.; Debras, G. *Polymer* **2001**, *42*, 1953.
(23) Xu, J.; Feng, L.; Yang, S.; Yang, Y.; Kong, X. *Eur. Polym. J.* **1998**, *34*, 431.
(24) Busico, V.; Cipullo, R.; Corradini, P.; De Biasio, R. *Macromol. Chem. Phys.* **1995**, *196*, 491.
(25) Busico, V.; Cipullo, R.; Monaco, G.; Talarico, G.; Vacatello, M.; Chadwick, J. C.; Segre, A. L.; Sudmeijer, O. *Macromolecules* **1999**, *32*, 4173.
(26) Chadwick, J. C.; Miedema, A.; Ruiseh, B. J.; Sudmeijer, O. *Makromol. Chem.* **1992** *193*, 1463.
(27) De Rosa, C.; Auriemma, F.; Circelli, T.; Waymouth, R. M. *Macromolecules* **2002**, *35*, 3622.
(28) Chûjô, R. *Kagaku* **1981**, *36*, 420.
(29) Doi, Y. *Makromol. Chem., Rapid Commun.* **1982**, *3*, 635.
(30) Hayashi, T.; Inoue, Y.; Chûjô, R.; Asakura, T. *Polymer* **1988**, *29*, 138.
(31) Randall, R. C.; Alamo, R. G.; Agarwal, P. K.; Ruff, C. J. Macromolecules **2003**, *36*, 1572.
(32) Kaminsky, W.; Hähnsen, H.; Külper, K.; Woldt, R. US Patent 4,542,199, 1985.
(33) Watkins, J. J.; Krukonis, V. J.; Condo, P. D., Jr.; Pradhan, D.; Ehrlich, P. *J. Supercrit. Fluids* **1991**, *4*, 24–31.
(34) Britto, L. J. D.; Soares, J. B. P.; Peulidis, A.; Krokonis, V. *J. Polym. Sci., Polym. Phys. Ed.* **1999** *37*, 553.
(35) Gassi, A.; Zambelli, A.; Resconi, L.; Albizzati, E.; Mazzocchi, R. *Macromolecules* **1988**, *21*, 617.
(36) Busico, V.; Cipullo, R.; Monaco, G.; Vacatello, M.; Segre, A. L. *Macromolecules* **1997**, *30*, 6251.
(37) Soga, K.; Shiono, T. *Makromol. Chem., Rapid Commun.* **1987**, *8*, 305.
(38) Busico, V.; Cipullo, R.; Monaco, G.; Vacatello, M.; Bella, J.; Segre, A. L. *Macromolecules* **1998**, *31*, 8713.
(39) This definition of the rate of crystallization ($1/t_{0.5} = d(X_c)/dt$) assumes constant volume during the transformation and a constant final degree of crystallinity, X_c, at any crystallization temperature.
(40) VanderHart, D. L.; Alamo, R. G.; Nyden, M. R.; Kim, M. H.; Mandelkern, L. *Macromolecules* **2000**, *22*, 6078.
(41) Nyden, M. R.; VanderHart, D. L.; Alamo, R. G. *J. Comput. Theor. Polym. Sci.* **2002**, *11*, 175.
(42) The last fraction, obtained at the highest pressure was not available for ^{13}CNMR analysis.

(43) Alamo, R. G.; Blanco, J. A.; Agarwal, P. Manuscript in preparation.
(44) Hoffman, J. D.; Frolen, L. J.; Ross, G. S.; Lauritzen, J. I. *J. Res. Natl. Bus. Standars* **1975**, *79A*, 671.
(45) Ergoz, E.; Fatou, J. G.; Mandelkern, L. *Macromolecules* **1972**, *5*, 147.
(46) Fatou, J. G.; Marco, C.; Mandelkern, L. *Polymer* **1990**, *31*, 1685.
(47) Magill, J. H.; Li, H. M. *Polymer* **1978**, *19*, 416.
(48) Hoffman, J. D. *Polymer* **1982**, *23*, 656.
(49) Lopez, L. C.; Wilkes, G. L. *Polymer* **1988**, *29*, 106.
(50) Alamo, R. G.; Fatou, J. G.; Guzman, J. *Polymer* **1982**, *23*, 379.
(51) Alamo, R. G.; Mandelkern, L. *Macromolecules* **1991**, *24*, 6480.
(52) Chen, H.-L.; Li, L.-J.; Ou-Yang, W.-C.; Hwang, J. C.; Wong, W.-Y. *Macromolecules* **1997**, *30*, 1718.
(53) Brückner, S.; Meille, S. U.; Petraccone, U.; Pirozzi, B. *Prog. Polym. Sci.* **1991**, *16*, 361.
(54) Lotz, B.; Graff, S.; Straupe, S.; Wittmann, J. C. *Polymer* **1991**, *32*, 2902.
(55) Fatou, J. G. *Encyclopedia of Polymer Science and Engineering*, 2nd ed.; John Wiley & Sons: New York, 1989; Suppl. -Vol., p 231.
(56) Allen, R. C.; Mandelkern, L. *Polym. Bull. (Berlin)* **1987**, *17*, 473.
(57) Alamo, R.; Fatou, J. C.; Guzman, J. *Polymer* **1982**, *23*, 374.
(58) Wagner, J.; Phillips, P. J. *Polymer* **2001**, *42*, 8999.
(59) Ziabicki, A.; Alfonso, G. C. *Colloid Polym. Sci.* **1995**, *273*, 317.
(60) Kaminsky, W. *Metal Organic Catalyst for Synthesis and Polymerization*; Springer: Berlin, 1999; p 601.

MA021549G